

2007

# Regulation of Histone Covalent Modifications During Yeast Apoptosis

Sung Hee Ahn-Upton

Follow this and additional works at: [http://digitalcommons.rockefeller.edu/student\\_theses\\_and\\_dissertations](http://digitalcommons.rockefeller.edu/student_theses_and_dissertations)



Part of the [Life Sciences Commons](#)

---

## Recommended Citation

Ahn-Upton, Sung Hee, "Regulation of Histone Covalent Modifications During Yeast Apoptosis" (2007). *Student Theses and Dissertations*. Paper 8.

This Thesis is brought to you for free and open access by Digital Commons @ RU. It has been accepted for inclusion in Student Theses and Dissertations by an authorized administrator of Digital Commons @ RU. For more information, please contact [mcsweej@mail.rockefeller.edu](mailto:mcsweej@mail.rockefeller.edu).



# REGULATION OF HISTONE COVALENT MODIFICATIONS DURING YEAST APOPTOSIS

A Thesis Presented to the Faculty of  
The Rockefeller University  
in Partial Fulfillment of the Requirements for  
the degree of Doctor of Philosophy

by  
Sung Hee Ahn-Upton  
June 2007





# REGULATION OF HISTONE COVALENT MODIFICATIONS DURING YEAST APOPTOSIS

Sung Hee Ahn-Upton, Ph.D.  
The Rockefeller University 2007

Chromatin compaction is a hallmark property of apoptosis, a highly coordinated suicide mechanism generally believed to be confined to vertebrates. However, invertebrates such as the budding yeast, *Saccharomyces cerevisiae*, display an apoptotic-like phenotypes including chromatin condensation, although its functions and mechanism are unclear. One mechanism that alters chromatin structure is the covalent modification of histones, which associates with DNA to form the nucleosome, the fundamental unit of chromatin. Phosphorylation of histone H2B at serine 14 (H2BS14ph), catalyzed by Mst1 kinase, has been linked to chromatin compaction during mammalian apoptosis. I extended these results to yeast by demonstrating that Ste20 kinase, a yeast orthologue of Mst1, directly phosphorylates H2B at serine 10 (H2BS10ph) in a hydrogen peroxide-induced cell death pathway. Unlike Mst1, Ste20 translocates into the nucleus in a caspase-independent fashion to mediate phosphorylation of H2B. H2BS10ph is dependent on the removal of acetylation mark on adjacent lysine residue, (H2BK11ac), which exists in growing yeast. During yeast apoptosis, the HDAC Hos3 deacetylates K11, which in turn, mediates H2BS10ph by Ste20 kinase. My studies underscore a concerted series of enzyme reactions governing histone modifications that promote a switch from cell proliferation to cell death. Moreover, the conservation of targeted H2B phosphorylation and the enzyme

system point to an ancient, late-stage chromatin remodeling event that likely governs cellular homeostasis in a wide range of organisms.

H2B phosphorylation may mediate apoptotic chromatin compaction by 1) directly affecting internucleosomal contacts and histone DNA interaction (“cis mechanism”), or 2) recruiting binding partners that then induce and direct downstream functions (“trans” mechanisms). Peptides corresponding to the phosphorylated form of yeast H2B and human H2B have the intrinsic ability to form “aggregates” in SDS polyacrylamide gel electrophoresis. In addition, nucleosome array containing yeast S10E or human S14E H2B fold into compacted conformation as measured by analytical ultracentrifugation. Moreover, an interaction between the forkhead homology-associated domain 1 (FHA1) of Rad53 and H2BS10ph was uncovered. This interaction inactivates the DNA damage checkpoint pathway and promotes apoptotic chromatin condensation. Thus, both mechanisms may contribute to chromatin remodeling event that govern apoptotic chromatin compaction in a pathway conserved from yeast to humans.

**To my parents and John**

## ACKNOWLEDGMENTS

The work here could not have been accomplished without contributions from the many scientists I have been associated with. I would like to thank Dr. Sydney Strickland and the Dean's office for accepting me as a transfer student to The Rockefeller University. I am grateful to The Rockefeller University and the Alexander Mauro Travel Fellowship for financial support. Members of the Dean's office have been very accommodating with all my needs and have made my life as a student very easy. In addition, I would like to thank my committee members, Dr. Hiro Funabiki, and Dr. Michael Rout for their guidance and helpful discussions during the course of this work. Many thanks also to Dr. Brehon Laurent for joining the committee as the outside examiner.

I would like to thank my thesis advisor, Dr. C. David Allis, for his constructive criticism, unwavering support, and for providing an intellectual environment in his lab that encouraged the flow of information, collaboration and the freedom to explore promising trails. I would also like to thank the Department of Molecular Biology, Biochemistry and Genetics at the University of Virginia for introducing me to David and his laboratory in the first place.

My years spent in the lab not only led to scientific progress, but also to the development of several friendships. I would like to thank the past and present members of the lab for their support and friendship. I couldn't have made it this far without all of you. I am grateful to my collaborators Dr. Fiona Tuner, Dr. Jer-Yuan Hsu, Robert Diaz, Dr. Andrew Xiao, as well as Dr. Wang Leung Cheung, who mentored me during my initial period in the lab. Great thanks to Beth Duncan, Shannon Anderson, Dr. Jason Tanny, Dr. David Shechter, Dr. Alexander Ruthenburg, and Dr. Ping Chi for their critical reading of this dissertation. It was a great pleasure to work with my fellow PhD students Holger Dormann,

Elizabeth Goneska, Eileen Woo, Amrita Basu, and Beth Duncan. I would to thank them for the spontaneous help I could always count on.

I would like to extend my most sincere thanks to Dr. Timothy Richmond for providing me with the opportunity to learn about *in vitro* nucleosome array systems and work in his lab in Zurich, Switzerland. Especially, many thanks to Dr. Thomas Schalch, Dr. Chrysoula Leontiou, Sylwia Duda, and Alexandra Kulangara for their technical expertise, as well as friendship while I was in Switzerland. I would also like to thank my collaborators, Dr. Mitch Smith, Dr. Scott Keeney and Dr. Michael Grunstein for their reagents and advice regarding this work, and Dr. Kiersten Henderson for her beautiful chromosome spreads. Also, Upstate Biotechnology Inc. (UBI; Lake Placid, NY) for generating the anti-H2BS10ph antibody. My immense gratitude goes out to Helen Shio for her expertise in electron microscopy and her patience with my constant visits and samples.

I could not have accomplished everything that I have without the incredible friendship and support of Soo-Kyun Choi, and Eleanor Burke-Daugherty. I am also grateful to Dr. Stephen J. Kron for helping me in every step of my career.

On a more personal note, my biggest thanks goes to my parents, whose love and moral support accompanied me all these years. Without my husband, John, I would not have attempted this seemingly impossible path. Thank you for loving me regardless of how crazy things got, reminding me of what really matters, and making commutes from Richmond, VA to NY every weekend with my dog for the first two years of my graduate studies. I am also grateful to my dogs, Casey and Prince, for brightening my life every day.

## TABLE OF CONTENTS

|  |            |
|--|------------|
| <b>DEDICATION.....</b>   | <b>iii</b> |
| <b>ACKNOWLEDGMENTS.....</b>  | <b>iv</b>  |
| <b>TABLE OF CONTENTS.....</b>                                      | <b>vi</b>  |
| <b>LIST OF FIGURES.....</b>  | <b>xi</b>  |
| <b>LIST OF TABLES.....</b>   | <b>xv</b>  |
| <b>ABBREVIATIONS.....</b>  | <b>xvi</b> |
| <b>CHAPTER 1: GENERAL INTRODUCTION.....</b>                        | <b>1</b>   |
| <b>Eukaryotic DNA is organized into chromatin.....</b>             | <b>2</b>   |
| <b>The nucleosome.....</b>   | <b>3</b>   |
| Histones.....  | 5          |
| Histone octamer.....   | 8          |
| Nucleosome core particle structure.....                            | 8          |
| Linker histone H1.....   | 9          |
| <b>The higher-order structure.....</b>                             | <b>10</b>  |
| Chromatin fiber dynamics.....                                      | 10         |
| <b>Histone variants.....</b>                                       | <b>12</b>  |
| <b>Post-translational modifications of histones.....</b>           | <b>15</b>  |
| Acetylation.....   | 17         |
| Methylation.....   | 21         |
| Ubiquitination.....  | 25         |
| Phosphorylation.....   | 26         |
| <b>Histone modification “cross-talk”.....</b>                      | <b>38</b>  |
| <b>Histone modification “cassette” .....</b>                       | <b>42</b>  |
| <b>Functional mechanism of histone covalent modifications.....</b> | <b>43</b>  |
| Cis mechanism.....   | 44         |
| Trans mechanism.....   | 46         |
| <b>Apoptosis.....</b>  | <b>52</b>  |

|   |    |
|---|----|
| Apoptotic pathways.....                 | 55 |
| Apoptotic chromatin condensation.....   | 61 |
| Yeast apoptosis.....                    | 63 |
| Histone modifications in apoptosis..... | 66 |

## CHAPTER 2: STERILE 20 KINASE PHOSPHORYLATES HISTONE H2B AT SERINE 10 DURING HYDROGEN PEROXIDE-INDUCED YEAST APOPTOSIS..... 69

|  |            |
|--|------------|
| <b>Introduction.....</b>   | <b>69</b>  |
| <b>Results.....</b>  | <b>73</b>  |
| Loss of the N-terminus of H2B, but no other histone N-terminal tails, abrogates hydrogen peroxide-induced cell death.....      | 73         |
| H2B S10A mutants abrogates hydrogen peroxide-induced yeast apoptosis.....  | 76         |
| Histone H2B is specifically phosphorylated at serine 10 in dying yeast cells.....  | 77         |
| Cells exhibiting phosphorylation of histone H2B at serine 10 display apoptotic DNA fragmentation.....                          | 84         |
| H2B S10E mutants induce apoptotic-like features including chromatin condensation.....  | 87         |
| Ste20 deletion mutants are resistant to hydrogen peroxide and abrogates H2B serine 10 phosphorylation.....                     | 89         |
| Hydrogen peroxide-induced H2B serine 10 phosphorylation is mediated by Ste20 <i>in vivo</i> .....                              | 93         |
| Ste20 kinase phosphorylates histone H2B at serine 10 <i>in vitro</i> ...   | 95         |
| MAPK cascade signaling during mating or osmotic process and Yca1 are not required for apoptotic H2B serine 10 phosphorylation. | 101        |
| Hydrogen peroxide treatment stimulates translocation of Ste20 from cytoplasm into nucleus.....                                 | 103        |
| <b>Discussion.....</b>   | <b>109</b> |
| <b>Materials and Methods.....</b>  | <b>116</b> |



### CHAPTER 3: REGULATED “PHOS/ACETYL CROSS-TALK” BETWEEN SERINE 10 AND LYSINE 11 IN HISTONE H2B DURING YEAST APOPTOSIS..... 132

Introduction..... 132

Results..... 135

H2B K11R mutants are resistant to hydrogen peroxide-induced yeast  
apoptosis..... 135

Characterization of anti-H2BK11ac antibody..... 137

Cells exhibiting deacetylation of histone H2B at lysine 11 display  
apoptotic phenotypes..... 143

H2B lysine 11 deacetylation is upstream of serine 10 phosphorylation  
during yeast cell death..... 144

Hos3p is the HDAC for histone H2B lysine 11 during yeast  
apoptosis..... 148

Hos3 deacetylates H2B lysine 11 *in vitro*..... 148

Discussion..... 154

Materials and Methods..... 159

### CHAPTER 4: THE ROLE OF THE H2B SERINE 10 PHOSPHORYLATION IN CHROMATIN FIBER FOLDING..... 163

Introduction..... 163

Results..... 167

H2BS10ph peptide displays an intrinsic “aggregation” property  
*in vitro*..... 167

H2B proline mutants are resistant to hydrogen peroxide  
treatment..... 171

Nucleosome arrays of yeast H2B S10E..... 173

Nucleosome array of *Xenopus* H2B S14E..... 180

Compaction of *Xenopus* H2B S11E and yeast H2B S10E are not  
dependent on linker histone H1..... 182

|  |            |
|--|------------|
| Yeast H2B+H2A chimera mutants display hydrogen peroxide-induced yeast apoptosis..... | 184        |
| Chromatin compaction of yeast H2A+B chimera mutant.....                              | 185        |
| <b>Discussion.....</b>   | <b>189</b> |
| <b>Materials and Methods.....</b>  | <b>198</b> |

## **CHAPTER 5: RAD53 ASSOCIATES WITH H2B SERINE 10 PHOSPHORYLATION DURING YEAST APOPTOSIS..... 206**

|  |            |
|--|------------|
| <b>Introduction.....</b>   | <b>206</b> |
| <b>Results.....</b>  | <b>211</b> |
| FHA1 of Rad53 specifically associates with phosphorylated serine 10 of H2B <i>in vitro</i> .....                   | 211        |
| In solution fluorescence polarization assay detects an interaction between FHA1 of Rad53 and H2BS10ph peptide..... | 212        |
| Rad53 associates with phosphorylated serine 10 H2B.....  | 216        |
| Rad53 is inactivated during hydrogen peroxide-induced yeast cell death pathway.....                                | 222        |
| Loss of FHA1 of Rad53 abrogates hydrogen peroxide-induced yeast apoptosis.....                                     | 224        |
| <b>Discussion.....</b>   | <b>226</b> |
| <b>Materials and Methods.....</b>  | <b>234</b> |

## **CHAPTER 6: H2B SERINE 10 PHOSPHORYLATION IS INDUCED DURING MEIOSIS..... 238**

|   |            |
|---|------------|
| <b>Introduction.....</b>  | <b>238</b> |
| <b>Results.....</b>   | <b>240</b> |
| Histone H2B is specifically phosphorylated at serine 10 during yeast meiosis..... | 240        |
| H2B serine 10 phosphorylation is enriched in condensed meiotic chromosomes.....   | 241        |

|  |         |
|--|---------|
| Discussion.....                        | 245     |
| Materials and Methods.....             | 248     |
| <br>CHAPTER 7: GENERAL DISCUSSION..... | <br>250 |
| APPENDIX.....                          | 267     |
| REFERENCES.....                        | 268     |

## LIST OF FIGURES

|            |   |           |
|------------|---|-----------|
| Figure 1.  | <b>Packaging of nucleosome.....</b>   | <b>4</b>  |
| Figure 2.  | <b>Crystal structure of the nucleosome core particle.....</b>   | <b>5</b>  |
| Figure 3.  | <b>Histone post-translational modifications.....</b>  | <b>7</b>  |
| Figure 4.  | <b>“Cross-talk” between histone modifications.....</b>  | <b>39</b> |
| Figure 5.  | <b>Putative “cassettes” in histone H3 and H4 N-terminal tail.</b>   | <b>42</b> |
| Figure 6.  | <b>Molecular mechanisms of covalent histone modifications.</b>  | <b>44</b> |
| Figure 7.  | <b>Examples of “trans” mechanism for the effect of histone modifications.....</b>   | <b>49</b> |
| Figure 8.  | <b>Apoptosis - the programmed death of a cell.....</b>  | <b>53</b> |
| Figure 9.  | <b>The intrinsic and extrinsic pathways leading to mammalian apoptosis.....</b>   | <b>56</b> |
| Figure 10. | <b>A four histone plasmid-shuffle strain in budding yeast.</b>  | <b>71</b> |
| Figure 11. | <b>N-termini of histone H2B, but no other core histone N-terminal tails, is required for hydrogen peroxide-induced cell death in yeast.....</b> | <b>74</b> |
| Figure 12. | <b>Hydrogen peroxide-treated yeast cells display intact membrane integrity and externalization of phosphatidylserine.....</b>                   | <b>75</b> |
| Figure 13. | <b>Sequence alignment of H2B N-terminal tails.....</b>  | <b>76</b> |
| Figure 14. | <b>H2B S10A mutants are resistant to yeast apoptosis elicited by hydrogen peroxide.....</b>   | <b>78</b> |
| Figure 15. | <b>ELISA of anti-H2BS10ph.....</b>  | <b>79</b> |
| Figure 16. | <b>Histone H2B is specifically phosphorylated at serine 10 in dying yeast cells.....</b>  | <b>81</b> |

|   |     |
|---|-----|
| Figure 17. Antibodies to H2B serine 10 phosphorylation selectively stain TUNEL positive yeast apoptotic cells.....                                | 82  |
| Figure 18. Apoptotic DNA fragmentation via TUNEL precisely coincides with the phosphorylation of H2B at serine 10.....                            | 85  |
| Figure 19. H2B is phosphorylated at serine 10 during acetic acid or $\square$ -factor- induced cell death.....                                    | 86  |
| Figure 20. Substitution of H2B serine 10 with glutamic acid induces apoptosis.....  | 88  |
| Figure 21. H2B S10E mutant constitutively induces apoptotic chromatin condensation.....   | 90  |
| Figure 22. Ste20 deletion mutants are resistant to hydrogen peroxide-induced yeast apoptosis.....   | 92  |
| Figure 23. Ste20 mediates hydrogen peroxide-induced H2B serine 10 phosphorylation <i>in vivo</i> .....  | 94  |
| Figure 24. An in-gel kinase assay identifies 100 kDa H2B phosphoserine 10 kinase as Ste20.....  | 96  |
| Figure 25. Recombinant Ste20 kinase preferentially phosphorylates unmodified H2B peptide containing amino acid residue 4-14 <i>in vitro</i> ..... | 98  |
| Figure 26. Nucleosomal H2B is the substrate for Ste20 kinase <i>in vitro</i> .....  | 100 |
| Figure 27. The MAPK cascade from mating or osmotic pathways are not required for hydrogen peroxide-induced H2B serine 10 phosphorylation.....     | 101 |
| Figure 28. Yca1 and H2B serine 10 phosphorylation act in independent pathways modulating yeast cell death.....                                    | 103 |
| Figure 29. Nuclear localization of GST-Ste20 upon hydrogen peroxide treatment.....  | 104 |
| Figure 30. Model for the Ste20 mediated H2B serine 10 phosphorylation in hydrogen peroxide-induced yeast apoptosis.....                           | 110 |

|   |     |
|---|-----|
| Figure 31. Histone H2B is specifically deacetylated at lysine 11 in dying yeast cells.....                                | 136 |
| Figure 32. Characterization of anti-H2BK11ac antibody.....  | 139 |
| Figure 33. Cells exhibiting “deacetylation” of histone H2B at K11 display TUNEL-positive DNA fragmentation.....           | 141 |
| Figure 34. Deacetylation of H2B lysine 11 precedes H2B serine 10 phosphorylation.....                                     | 144 |
| Figure 35. H2B lysine 11 deacetylation is upstream of H2B serine 10 phosphorylation during yeast apoptosis.....           | 145 |
| Figure 36. Hos3 deacetylates H2B lysine 11 during hydrogen peroxide induced yeast apoptosis.....                          | 149 |
| Figure 37. Hos3 deacetylates H2B lysine 11 and promotes H2B serine 10 phosphorylation by Ste20 <i>in vitro</i> .....      | 151 |
| Figure 38. Model for histone H2B “phos/acetyl cross-talk” (S10/K11) during hydrogen peroxide-induced yeast apoptosis..... | 155 |
| Figure 39. “Death”-inducing phospho-peptides contain an intrinsic self-aggregation property <i>in vitro</i> .....         | 168 |
| Figure 40. Prolines in the yeast H2B “death motif”.....   | 172 |
| Figure 41. Outline of the <i>in vitro</i> nucleosome array system.....  | 174 |
| Figure 42. Schematic delineation of chromatin higher-order structure system.....  | 175 |
| Figure 43. Purification and stoichiometry of the <i>in vitro</i> assembled nucleosome arrays.....                         | 176 |
| Figure 44. Folding of nucleosome arrays containing yeast H2B mutants.....   | 178 |
| Figure 45. Folding of nucleosome arrays containing <i>Xenopus</i> H2B mutants.....  | 181 |
| Figure 46. The influence of H1 on folding of <i>Xenopus</i> nucleosome array.....   | 183 |

|  |     |
|--|-----|
| Figure 47. Movable “death-cassette” in H2B.....  | 186 |
| Figure 48. Folding of nucleosome arrays containing yeast H2A+B mutants.....                                      | 188 |
| Figure 49. Activation of Rad53 during DNA damage pathway.....  | 209 |
| Figure 50. FHA1 of Rad53 is a potential binding effector for H2B serine 10 phosphorylation <i>in vitro</i> ..... | 213 |
| Figure 51. Binding studies of H2B tail peptides to FHA1 of Rad53..   | 217 |
| Figure 52. Rad53 is H2B-serine10-Phos-associated protein.....  | 219 |
| Figure 53. <i>In vivo</i> interaction between Rad53 and nucleosome carrying H2B serine 10 phosphorylation.....   | 221 |
| Figure 54. Rad53 is dephosphorylated during hydrogen peroxide-induced yeast apoptosis.....                       | 223 |
| Figure 55. FHA1 of Rad53 is required for hydrogen peroxide-induced yeast apoptosis.....                          | 225 |
| Figure 56. Model for Rad53’s role in yeast apoptosis.....  | 227 |
| Figure 57. H2B serine 10 phosphorylation is induced during meiotic prophase.....                                 | 241 |
| Figure 58. Anti-H2BS10ph antibody stains pachytene stage of meiotic prophase.....                                | 243 |
| Figure 59. Model for regulation of Histone H2B in yeast apoptosis  | 251 |

## LIST OF TABLES

|          |  |            |
|----------|--|------------|
| Table 1. | <b>Genotypes of yeast strains.....</b> | <b>121</b> |
|----------|--|------------|



## LIST OF ABBREVIATIONS

|                               |  |
|-------------------------------|--|
| A                             | alanine                                    |
| APAGE                         | agarose-Polyacrylamide gel electrophoresis |
| ac                            | acetylation                                |
| ATP                           | adenosine triphosphate                     |
| bp                            | base pair                                  |
| CH <sub>3</sub> COOH          | acetic acid                                |
| Da                            | Dalton                                     |
| DNA                           | deoxyribonucleic acid                      |
| E                             | glutamic acid                              |
| FHA                           | fork head domain                           |
| GST                           | glutathione sepharose-tagged               |
| HAT                           | histone acetyl transferase                 |
| HDAC                          | histone deacetylase                        |
| HOS                           | higher-order structure                     |
| H2A.XS139ph                   | H2A.X serine 139 phosphorylation           |
| H2BK11ac                      | H2B lysine 11 acetylation                  |
| H2BS10ph                      | H2B serine 10 phosphorylation              |
| H2BS14ph                      | H2B serine 14 phosphorylation              |
| H3S10ph                       | H3 serine 10 phosphorylation               |
| H3S28ph                       | H3 serine 28 phosphorylation               |
| H3T3ph                        | H3 threonine 3 phosphorylation             |
| H3T11ph                       | H3 threonine 11 phosphorylation            |
| H4S1ph                        | H4 serine 1 phosphorylation                |
| H <sub>2</sub> O <sub>2</sub> | hydrogen peroxide                          |
| K                             | lysine                                     |
| kD                            | kilodalton                                 |
| me                            | methylation                                |
| me1                           | mono-methylation                           |
| me2                           | di-methylation                             |
| me3                           | tri-methylation                            |

|          |   |
|----------|---|
| MNase    | micrococcal nuclease  |
| MMS      | methyl methanesulfonate   |
| MMTV     | mouse mammary tumor virus                                       |
| MW       | molecular weight  |
| NCP      | nucleosome core particle  |
| P        | proline   |
| PB       | phloxin B   |
| PCD      | programmed cell death   |
| ph       | phosphorylation   |
| R        | arginine  |
| rpm      | revolutions per minute  |
| S        | serine  |
| SDS-PAGE | sodium dodecyl sulfate-polyacrylamide gel electrophoresis       |
| TUNEL    | terminal deoxynucleotidyl transferase dUTP nick end<br>labeling |
| ub       | ubiquitination  |
| WT       | wild-type   |

# CHAPTER 1

## GENERAL INTRODUCTION

The faithful packaging of chromatin, the repeating polymer of DNA and associated histone proteins (H2A, H2B, H3 and H4), is an essential step in the accurate execution of proliferation, differentiation and apoptosis in eukaryotic cells. Each of these biological processes is characterized by elaborate mechanisms that involve different, but poorly understood, levels of chromatin compaction. Thus far, there are three well-documented molecular mechanisms that introduce meaningful variations into chromatin fiber: 1) by altering DNA-histone contacts within a nucleosome through the enzymatic activities of ATP-dependent chromatin-remodeling complexes, 2) by specific incorporation of histone variants, 3) by the addition and subtraction of covalent post-translational modification of the histones (reviewed in Felsenfeld and Groudine, 2003; Iizuka and Smith, 2003; Peterson and Laniel, 2004). Together, these variations may form a “histone code” (Strahl and Allis, 2000; Turner, 2000; de la Cruz et al., 2005), a signaling platform to specify unique downstream biological functions particularly for specialized forms of chromatin that include apoptotic and damaged DNA (Redon et al., 2002; Cheung et al., 2000).

Histones are subject to a large number of covalent modifications (van Holde, 1988). One of these modifications, phosphorylation, where a phosphate moiety is added onto serine/threonine residues in histones by an appropriate kinase, is the focus of my thesis. However, to understand how histone

phosphorylation can regulate chromatin structure, the general aspects of DNA organization in eukaryotic cells including chromatin and nucleosome, and their structures will be discussed in this Chapter. I will also address the role and functional mechanism of histone variants and histone modifications both of which introduce variation into the repetitive nucleosomal array. Since the majority of my work involves studying chromatin changes during apoptosis, I will also summarize the fundamental implications of chromosome dynamics during apoptosis and comment upon how yeast is emerging as a new model system for studying the apoptosis-induced signaling cascade. Finally, I will describe the functional roles for histone modifications in apoptosis.

### **Eukaryotic DNA is organized into chromatin**

First described by Robert Brown in 1831, the cell nucleus is one of the best known but least understood of cellular organelles. Around 1900, it was recognized that heredity was based on the transmission of nuclear material from one cell to its descendants. At that time, intensive studies involving chromosomes were started. Only in 1944 was it realized that the heredity information was encoded into DNA (Avery et al., 1944), and in 1953, the structure of DNA was postulated by Watson and Crick (Watson and Crick, 1953).

Eukaryotic cells contain from  $10^7$ - $10^{11}$  DNA base pairs (bp) in a nucleus just 5-7  $\mu\text{m}$  in diameter (van Holde, 1988). The DNA molecules that comprise the human genome span about 2 meters in length if they are laid end to end (van Holde, 1988). This vast quantity of DNA is packaged by the histone proteins into a hierarchical structure called chromatin (reviewed in Kornberg and Lorch, 1999). DNA in chromatin is compacted over 10,000-fold (Luger et al., 1997;

Davey et al., 2002). The nucleosome is the universal repeating-element of chromatin, and it accounts for the first level of DNA organization in the cell nucleus (Felsenfeld and Groudine, 2003). This level is also referred to as the “beads-on-a-string” because of its resemblance under the electron microscope (Bram and Ris, 1971; Olins and Olins, 1974; Figure 1). The “30-nm” chromatin fiber consists of nucleosome arrays in their most compact form, and is typically posited as the secondary structural level of DNA organization (Richmond and Widom, 2000; Felsenfeld and Groudine, 2003; Figure 1). The hierarchy continues with increasing DNA packing density until the metaphase chromosome is ultimately attained (Belmont et al., 1999; Strukov et al., 2003; Figure 1).

The total genetic information stored in the chromosomes of an organism constitutes its genome. The chromosome structure and activities in the cell change according to the stage of the cell-division cycle (reviewed in Ahmad and Henikoff, 2002). In mitosis, or M phase, they are highly condensed and transcriptionally inactive. Whereas in the other, much longer part of the division cycle, called interphase, they are less condensed and transcriptionally active (reviewed in Horvath et al., 2001). Replication of the genome occurs during a specific part of interphase, called S phase. After replication, chromatin structure is reassembled by the addition of new histones to the old histones, which are deposited on both parental and daughter DNA molecules (reviewed in Mello and Almouzni, 2001; Gunjan et al., 2005).

### **The nucleosome**

The nucleosome is the fundamental repeating unit of chromatin, occurring generally every 156-240 base pairs (Kornberg, 1974). The nucleosome core

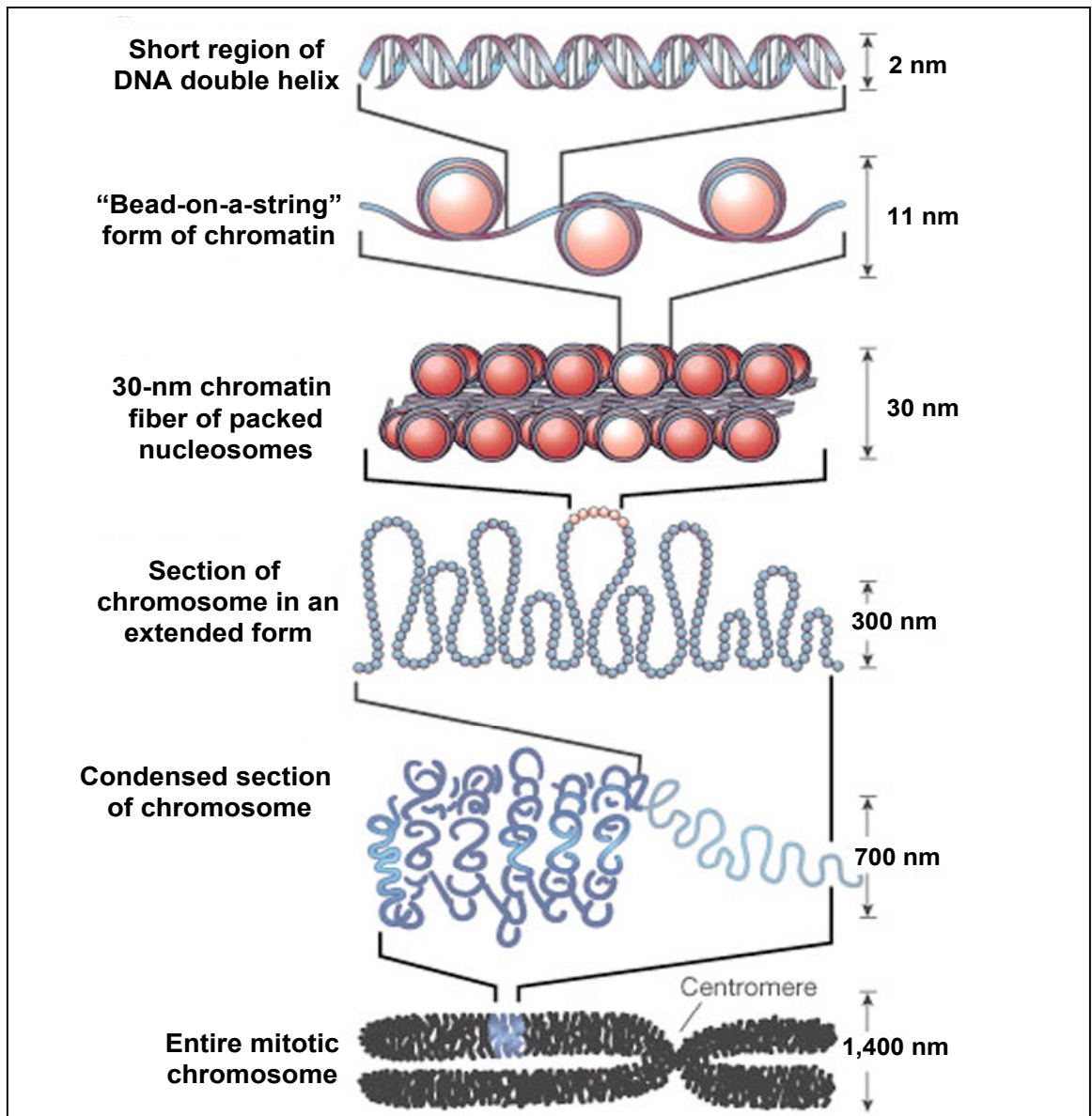
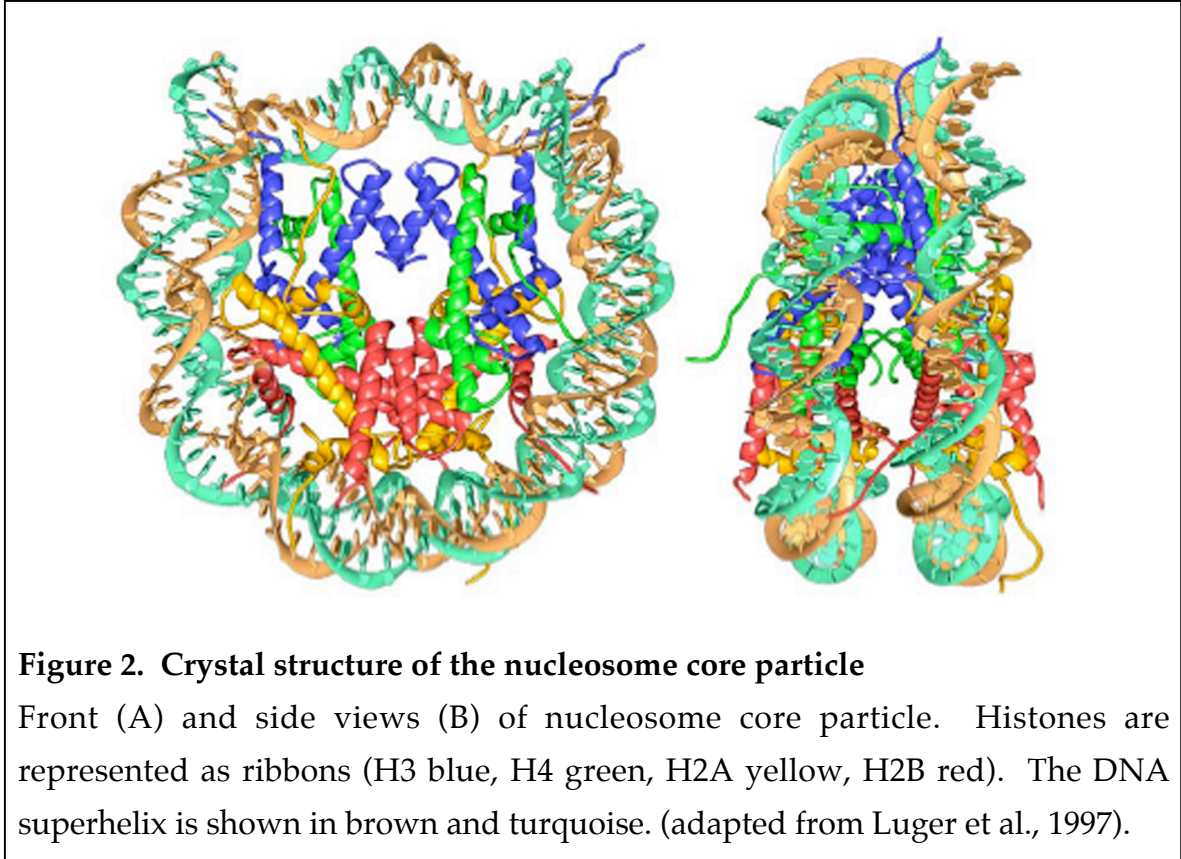


**Figure 1. Packaging of nucleosome**

The most fundamental level of DNA packaging is the nucleosome, in which two superhelical turns of DNA are wound around the outside of a histone octamer. Nucleosomes are connected to one another by short stretches of linker DNA. In the next level of organization, the string of nucleosomes ("bead-on-a-string") is folded into a fiber about 30 nm in diameter and these fibers are then further folded into higher-order structures. At levels of structure beyond the nucleosome, the details of folding are still uncertain (adapted from Felsenfeld and Groudine, 2003).

comprises 147 base pairs of DNA, a histone octamer containing a pair of each of the core histone proteins H2A, H2B, H3 and H4, and a linker histone H1 (Luger et al., 1997). The structure of the nucleosome core particle (NCP) has been solved by X-ray crystallography at high resolution (Davey et al., 2002; Luger et al., 1997; Figure 2).



### *Histones*

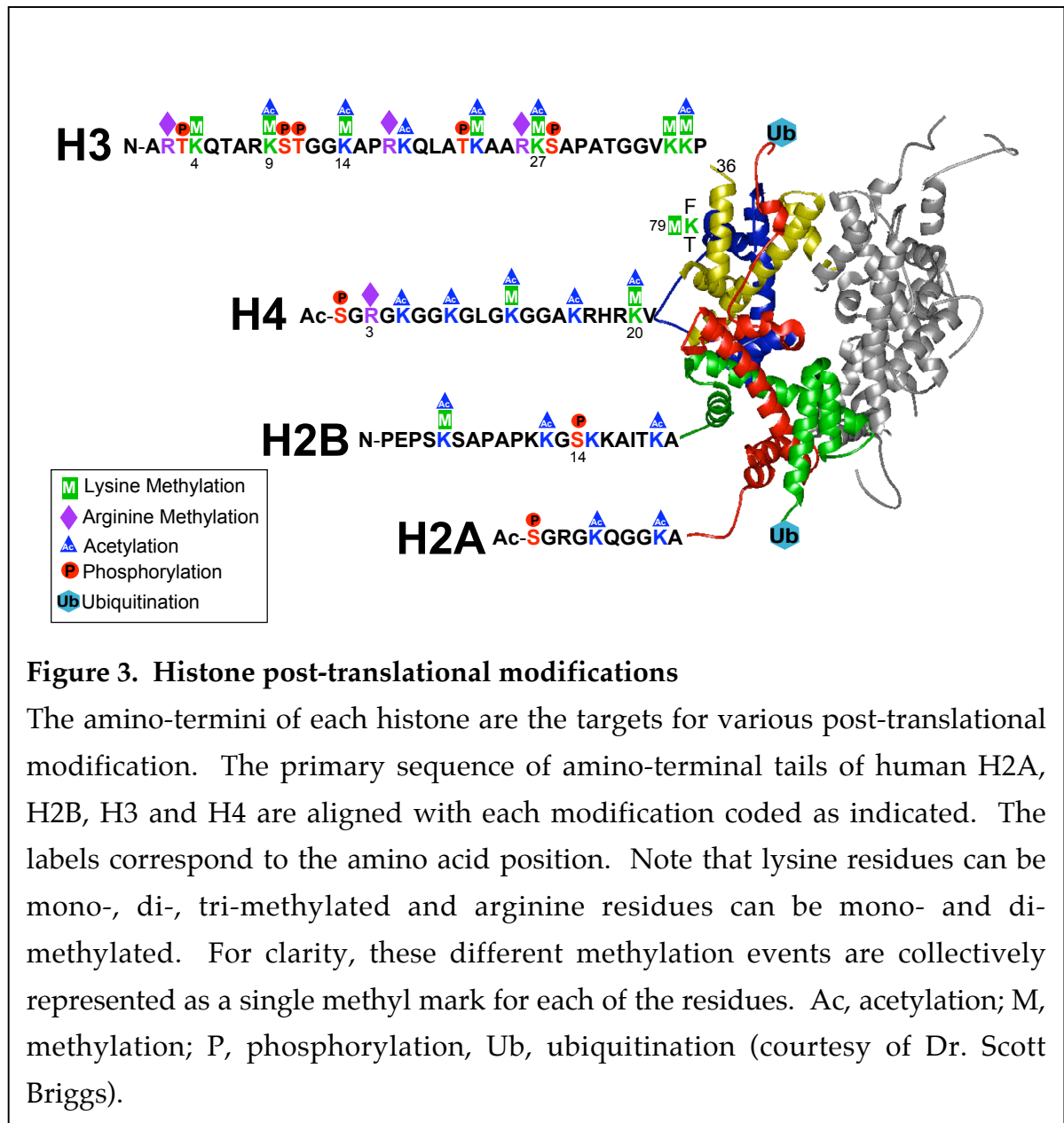
Histone proteins were first isolated from erythrocytes of geese by Kossel in 1884 (Kossel, 1884). Histones are small basic proteins and fall into five classes- H1, H2A, H2B, H3 and H4 – derived from their amino acid composition and sequence (Johns, 1967). Each histone class includes some gene variants or subtypes which are likely to provide tissue-specific and developmental-stage-

dependent variation of chromatin structure (Franklin and Zweidler, 1977; reviewed in Sarma and Reinberg, 2005). The histones H2A, H2B, H3, and H4 have molecular masses of 10–16 kDa and are known as the “core histones”, since DNA wraps around histones to form the nucleosome core of chromatin (van Holde, 1988; Luger et al., 1997; see Figure 1). The interactions between the DNA and histones are mainly due to electrostatic forces since histones can be extracted from chromatin with a high concentration of salt (Kornberg, 1974). The complete set of core histone proteins is essential for cell viability, as shown by genetic experiments using yeast (Kim et al., 1988). The core histone proteins are found in the same equal molar stoichiometry, with histone H1 in half this amount, in all eukaryotic organisms (Hayashi et al., 1978).

Histones are remarkably well conserved throughout evolution in both primary sequences and length. For example, histone H4 of human and pea differ in only two conservative amino acid replacements. H2A and H2B are conserved to a lesser extent especially in the non-structural tail domains (78% and 71% overall identity between human and yeast H2A and H2B, respectively). The higher degree of conservation of H3 and H4 is probably a reflection of their central role in keeping nucleosome structure and the biological processes in which they are involved. Structurally, each of the core histones contain an amino (N-) terminal tail and a histone fold domain containing three  $\alpha$ -helixes separated by short loops (Arents et al., 1991; Ramakrishnan et al., 1993; Cerf et al., 1994). Since histone fold domains are important for mediating histone-histone and histone-DNA interactions, they are indispensable in the formation of the nucleosome (Arents et al., 1991) and the conservation between the histone-fold domains between organisms is very high. Enriched with charged residues, the



N-terminal tails are targets for various post-translational modifications (Figure 3). It is now well appreciated that these chemical marks on the histone tails function by either directly affecting accessibility of DNA or serving as modules to recruit structural or nuclear proteins that alter chromatin conformation for particular cellular functions (Hecht et al., 1995; Strahl and Allis, 2000; Bannister et al., 2001; Roth et al., 2001).



### *Histone octamer*

Histones H2A and H2B form a heterodimer as do histones H3 and H4 (Camerini-Otero et al., 1976; Hayes et al., 1991; Arents and Moudrianakis, 1993). All histones are  $\alpha$ -helical proteins and the dimers are formed through a histone-specific interaction, the histone-fold domains (Arents et al., 1991). Two H3/H4 dimers associate into a tetramer that forms the core of the histone octamer (Luger et al., 1997). The H2A/H2B dimers are added symmetrically on each side of the tetramer, thereby giving the histone octamer a shape that resembles a helical spool onto which the DNA is wound (Klug et al., 1980; Richmond et al., 1984; Arents et al., 1991).

### *Nucleosome core particle structure*

The structure of the nucleosome core particle (NCP) has been determined to near atomic resolution (Luger et al., 1997; Davey et al., 2002; Figure 2). It shows how the histone octamer interacts with the 147 bp of DNA to form 1.67 turns of a superhelix. The H3/H4 tetramer organizes the central 60 bp of the nucleosome whereas the H2A/H2B dimer binds to the 30 bp adjacent to the central region. DNA binding occurs mainly over short stretches of the sugar-phosphate backbone whenever it is facing the octamer. The interactions are predominantly nonspecific and include extensive salt bridges, hydrogen bonds and non-polar contacts to the DNA sugar. The linker DNA that connects the nucleosome core is associated with H1. Thus, the nucleosome core, linker DNA and histone H1 make up the complete nucleosome.

The flexible tails of the histones reach out between and around the gyres of the DNA superhelix (Luger et al., 1997) and seems to be required for higher-

order folding of the chromatin fibers (Allan et al., 1982). The fact that tandem nucleosomal arrays were not able to adapt to a higher-order structure without the tails of core histones *in vitro* further support this notion (Garcia-Ramirez et al., 1992). Alternatively, tail to tail interactions between different nucleosomes were observed in the crystal studies (Luger et al., 1997; White et al., 2001). For instance, a “basic patch” from lysine 16 (K16) to asparagine 25 (R25) in H4 N-terminal tail makes extensive contact with an acidic region on an H2A/H2B dimer of an adjacent nucleosome (Luger et al., 1997). This interaction is important for crystallization of the *Xenopus* nucleosome (Luger et al., 1997). Consistently, this basic patch is important for maintaining silent chromatin in yeast suggesting that this tail might be critical in forming a higher-order condensed structure to silent gene expression (Megee et al., 1990; Johnson et al., 1990).

The structures of nucleosomes composed of *Xenopus* histone (Luger et al. 1997), yeast histones (White et al., 2001), and even one with a histone variant H2A.Z (Suto et al., 2000) are all super-imposable on one another, despite some sequence variation between species. Therefore, the fundamental structural information is well preserved throughout evolution.

### ***Linker histone H1***

Histone H1 is called the “linker histone” because it associates with the DNA connecting the nucleosome cores (Allan et al., 1980). Only one copy of H1 is found per nucleosome, and H1 is less strongly incorporated into chromatin than core histones (reviewed in Luger, 2003). Furthermore nucleosome core particles can be reconstituted without H1, whereas all four core histones are absolutely

required (Thomas, 1984). Biochemical results demonstrate that the H1 fold domain binds near the center of the nucleosomal DNA in the vicinity of DNA entry and exit, while the C-terminal domain is most likely associated with 10-20 bp of linker DNA (Zhou et al., 1998). However, other experiments suggest that H1 binds in the inside of only one DNA gyre (reviewed in Thomas, 1999). Therefore, the location of H1 in the nucleosome is still controversial.

### **The higher-order structure**

The higher-order structure, also referred to as 30-nm chromatin fiber, is the next packaging level of DNA after the nucleosome (Figure 1). In a non-dividing cell, chromosomes are decondensed and appear as a diffuse mass in the nucleus, separated into heterochromatin and euchromatin (reviewed in Pardue and Henning, 1990; van Holde, 1988). Most of the interphase chromosomes exist largely in the form of the 30-nm chromatin fibers (reviewed in Lamond and Earnshaw, 1998). This means that the chromatin fiber is the natural substrate for processes such as transcription, DNA repair and replication (during S phase). Hence it is of great interest to gain detailed insight into the dynamics and structure of this fiber.

### ***Chromatin fiber dynamics***

The chromatin fiber is a dynamic macromolecular entity that is intimately involved in nuclear function. In the last three decades, many attempts have been made in examining the structural properties of the chromatin fiber, or its subunit, the nucleosome. Despite this intense effort, many aspects of chromatin structure remain poorly understood. One such area is the conformational dynamics of the

chromatin fiber. Multiple, independent mechanisms are involved in the control of chromatin fiber formation and stability (reviewed in Hansen, 2002). The molecular determinants and mechanisms responsible for chromatin fiber dynamics remain elusive and are the subject of continued debate.

The folding of nucleosome arrays from 10 nm into the condensed 30 nm diameter chromatin fiber in solution is complex. Early electron microscopic studies of isolated chromatin fragments *in vitro* revealed that chromatin fibers would undergo a reversible cation-dependent compaction in response to changes in solution conditions (Thoma et al., 1979). In the presence of monovalent salt (10-200 mM NaCl), nucleosome arrays appear to equilibrate between the extended beads-on-a-string conformation (see Figure 1) exclusively present in low salt, and a partially folded zigzag-like conformation (Garcia-Ramirez et al., 1992; Hansen et al., 1989). Upon addition of low amounts of divalent cations (1-2 mM  $MgCl_2$ ), regularly spaced nucleosome arrays fold into a compacted conformation that is equivalent to a 30-nm chromatin fiber in its extent of compaction (Schwarz and Hansen, 1994). Analytical ultracentrifugation experiments show that defined nucleosome arrays exhibit continuous increases in their average sedimentation coefficient with increasing divalent cation concentration (Hansen, 2002). If the divalent cation concentration is increased further, the equilibrium is shifted toward oligomerization (Schwartz et al., 1996). However, oligomerization is not obligatorily coupled to intramolecular folding *in vitro*, since it can occur in extended or only moderately folded nucleosome arrays (Schwarz et al., 1996). Importantly, removal of salt leads to reestablishment of a single 10 nm fiber, indicating that all the transitions in the folding and self-association pathway are reversible (Hansen, 2002). The contribution of the

highly-basic core histone tail domains to the folding and dynamics of the chromatin fiber has been determined by sedimentation analysis (Garcia-Ramirez et al., 1992; Fletcher and Hansen, 1995; Schwarz et al., 1996; Tse and Hansen, 1997; Dorigo et al., 2004; Shogren-Knaak et al., 2006). To date, the N-terminal tail of H4 is uniquely associated with the formation of the chromatin fiber (Luger et al., 1997; Dorigo et al., 2004; Shogren-Knaak et al., 2006; see “cis mechanism”).

Although for many years it was thought that formation of the chromatin fiber depended on the presence of H1, sedimentation analysis of defined nucleosome arrays in  $\text{MgCl}_2$  has shown that compact fibers can form in the absence of H1 (Carruthers et al., 1998). Rather, H1 seems to play a significant role in the stabilization of the chromatin fiber. The linker histones stabilize the folded and oligomeric states of chromatin fibers *in vitro*; less  $\text{MgCl}_2$  when compared to H1-less nucleosome arrays is required to induce folding (Carruthers et al., 1998). In addition, studies of endogenous nucleosome arrays reassembled with linker histone indicate that the highly basic C-terminus provides localized charge neutralization for the chromatin fiber stabilization (Allan et al., 1986). These observations suggest that the formation of highly folded chromatin structure is mainly directed by the core histones rather than by H1.

### **Histone Variants**

Changing the constituent of the nucleosome at specialized chromatin domains can also introduce variations into the chromatin fiber and consequently, affect the DNA dependent processes occurring there (Falsenfeld and Groudine, 2003). This can be established by having core histones (H2A, H2B, H3 and H4) specifically substituted by histone variants. Their incorporation into the

nucleosome provides a means of specifying and inheriting an alternative chromatin state. Histone variants are also referred to as replacement histones because some variants exchange with the pre-existing histones during development and differentiation (Brandt et al. 1979; Wunsch et al. 1991; Bosch and Suau 1995). Therefore, histone variants have specialized functions regulating chromatin dynamics that have high impact on cell cycle and developmental growth (Felsenfeld and Groudine, 2003).

All the histones are encoded by several different genes. The histone H2A family is the most diverse and has the largest number variants including H2A.X (reviewed in Ausio and Abbott, 2002; Redon et al. 2002; Fernandez-Capetillo et al. 2004b). Histone H3 has major variants including CENP-A, H3.3 and hv2 (Kurokawa and MacLeod, 1985; Earnshaw et al., 1985; Marvin et al., 1990; Palmer et al., 1991). While no variants are known for H4, a few variants of H2B are known, which play important roles in spermatogenesis (reviewed in Poccia and Green 1992; Green et al. 1995). In this section, I will describe H2A.X and testis-specific H2B variant and how they are specifically correlated with different biological processes.

### ***H2A.X***

H2A.X is a histone variant in higher eukaryotes, which is the “normal” histone H2A in budding yeast (Downs et al., 2000). The yeast H2A and the higher eukaryote H2A.X histones contain an extension at the C-terminus, which includes the conserved amino-acid sequence SQ(E/D)□, where □ denotes a hydrophobic residue. H2A.X is phosphorylated (ph) on the serine (S) in this

unique C-terminal region (S139 in higher eukaryotes, S129 in yeast; see “H2A.X phosphorylation”) in response to DNA double-strand breaks (DSBs) (Rogakou et al., 1998). This phosphorylation at the site of DSBs then spreads rapidly to other H2A.X along the chromosome and recruits repair machinery (Rogakou et al., 1998; reviewed in Fernandez-Capetillo et al., 2004b). In addition, the phosphorylation of H2A.X is essential for the formation of efficient repair foci in cells (Celeste et al., 2002; Celeste et al. 2003). Therefore, H2A.X has become a marker for DNA damage.

### ***TSH2B***

Histone H2B is markedly deficient in variants. The few that have been documented completely replace the core histone H2B and appear to have very specialized functions in chromatin compaction and transcriptional repression, particularly during spermatogenesis (Poccia and Green 1992; Green et al., 1995). Spermatogenesis is a complex process in which diploid stem cells divide, differentiate and mature into haploid, highly specialized spermatozoa (Poccia and Green 1992). During meiotic phase of spermatogenesis, testis-specific histone H2B (TH2B) is synthesized in testis and replace core H2B, which is expressed in somatic cells (Meistrich et al., 1985; Kim et al., 1987; Schumperli, 1988). The first TH2B was cloned from rat (rTH2B) (Kim et al., 1987). There is extensive sequence divergence in the N-terminus of the rTH2B and core H2B, but the rest is highly conserved (Kim et al., 1987). The N-terminus of rTH2B interacts with DNA and their interaction increases DNase I sensitivity of the nucleosomes perhaps to loosen the structure for meiotic recombination and



facilitate replacement of histones with more basic, transitional proteins and protamines later during spermatogenesis (Rao and Rao, 1987).

TH2B is also found in human, except it is found in both testis and sperm, hence, this protein is referred as a human testis/sperm-specific H2B (hTSH2B; Zalensky et al., 2002). Protein sequence comparison reveals a strong (95%) homology of hTSH2B with testis-specific H2B from rat and mouse and a weaker homology with somatic histone H2B (85%) (Zalensky et al., 2002). The most pronounced differences between somatic and spermatogenic cell-specific H2Bs are found in their N-terminal regions (Zalensky et al., 2002), suggesting that the divergent N-terminus might provide a means of specifying and inheriting an alternative chromatin state. Immunofluorescence studies show that hTSH2B is localized in basal nuclear area of sperm cells (van Rooijen et al., 1998; Zalensky et al., 2002). Since the basal nuclei of sperm cells is where chromatin decondensation occurs first after fertilization (Terada et al., 2000), hTSH2B may associate with active chromatin.

### **Post-translational modifications of histones**

Besides changing nucleosomes by replacing the core histones with variants, post-translational modifications of the core histones can also modify the nucleosome to enhance or inhibit access of DNA by nuclear factors (reviewed in Henikoff et al., 2004; Kamakaka and Biggins, 2005). Histones are subject to vast array of post-translational modifications such as acetylation and methylation (me) of lysines (K) and arginines (R), phosphorylation (ph) of serines (S) and threonines (T), ubiquitination (ub) and sumoylation (su) of lysines (K), as well as ribosylation (ar) (reviewed in Fischle et al., 2003a; de la Cruz et al., 2005).

Adding to the complexity is the fact that each lysine residue can accept one (me1), two (me2) or even three methyl groups (me3), and an arginine can be either mono- (me1) or di-methylated symmetric (me2s) or asymmetric (me2a) (de la Cruz et al., 2005). In most cases, these modifications are found in the N-terminal tails, but recently modifications in the histone-fold domain have been found as well (reviewed in van Leeuwen et al., 2002; Fuchs et al., 2006). Given the number of new modification sites that are identified each year, it seems likely that nearly every histone residue that is accessible to solvent is a likely target for post-translational modification (Figure 3).

Since chromatin is the physiological template for all DNA-mediated processes, histone modifications are thought to affect the function of the chromatin fiber through two distinct mechanisms. First, nearly all modifications alter the electrostatic charge of the histone and this, in principle, could change the structural properties of the histone or its binding to the DNA. Indeed, recent studies have shown that site-specific combinations of histone modifications correlate well with particular biological functions. For instances, the combination of H4K8 acetylation (H4K8ac), H3K14 acetylation (H3K14ac), and H3S10 phosphorylation (H3S10ph) is often associated with transcription (Mahadevan et al., 1991; Kuo et al., 1996; Lo et al., 2000; Agalioti et al., 2002). Conversely, tri-methylation of H3K9 (H3K9me3) and the lack of H3 and H4 acetylation correlate with transcriptional repression in higher eukaryotes (reviewed in Fuks, 2005; Fuchs et al., 2006;). Particular patterns of histone modifications also correlate with global chromatin dynamics, as deacetylation of histone H4 at K5 and K12 is associated with histone deposition at S phase (Jasencakova et al., 2001), and phosphorylation of histone H2A (at S1 and T119)

and H3 (at T3, S10 and S28) appears to be a hallmark of condensed mitotic chromatin (Wei et al., 1998; Goto et al., 1999; Hsu et al., 2000; Aihara et al., 2004; Polioudaki et al., 2004; Barber et al., 2004). Second, modifications could create binding surfaces for protein recognition modules and thus recruit specific functional complexes to their proper sites of action (see “Functional mechanisms of histone covalent modification”).

Some of the best-known histone modifications (acetylation, methylation and ubiquitination) that have been characterized will be discussed below, and then a more detailed description of histone phosphorylation will follow. In addition, I will describe specific histone modification, the DNA process often associated with it, and the enzyme(s) responsible for bringing it about, where known. Finally, the potential mechanism of each modification and how that impacts on the nuclear process will be discussed.

### *Acetylation*

An acetyl group neutralizes a positive charge on the basic residues such as lysine or arginine of histones and thus is expected to weaken histone-DNA interactions. Acetylation of the  $\epsilon$ -amino group of lysine residues on histones was first described by Allfrey and colleagues (Allfrey et al., 1964). In the same report, they indicated that acetylated histones were less repressive for RNA synthesis, leading to the idea that histone acetylation may prime chromatin for active transcription. The discovery that acetylated histones correlate with transcriptionally active regions such as the macronucleus of *Tetrahymena*, the majority of the yeast genome, the X-chromosomes in male *Drosophila*, and the  $\epsilon$ -

globin gene in chicken erythrocytes has firmly established the link between histone acetylation and transcriptional activation (Vavra et al., 1982; Hebbes et al., 1992; Clarke et al., 1993; Bone et al., 1994; Hebbes et al., 1994). Conversely, histone deacetylation has been correlated with transcriptionally inactive regions such as the micronucleus of *Tetrahymena*, silent regions of the yeast genome, and the inactive X chromosome in female mammalian cells (Vavra et al., 1982; Braunstein et al., 1993; Braunstein et al., 1996; Jeppesen and Turner, 1993).

The functional link between acetylation and transcription was greatly reinforced when many transcriptional activators and repressor complexes were found to possess histone acetyltransferase (HAT) and deacetylase (HDAC) activity, respectively (Brownell et al., 1996; Taunton et al., 1996; Grunstein, 1997; Struhl, 1998; Berger, 1999; Roth et al., 2001). For example, yeast Gcn5, a positive transcriptional regulator of many genes, has HAT activity and stimulates the acetylation of histone H3 at K14, H4 at K8, and K16 (Kuo et al., 1996; Sterner and Berger, 2000). In contrast, the yeast HDAC, Rpd3, deacetylates lysine residues including H3K14, H4K8 and H4K16, and facilitates transcriptional repression (Suka et al., 2001; see "Deacetylation"). One possible mechanism of acetylated histone tails in regulating transcription is that acetylated histone tails can decrease the interaction between tails and nucleosomal DNA allowing transcription factors and co-activators to gain access to the DNA (Lee and Hayes, 1997; Cary et al., 1982). Consistent with this notion, acetylated histone tails were shown to directly bind to bromodomain-containing transcriptional co-activators (Dhalluin et al., 1999; Jacobson et al., 2000; Zeng and Zhou, 2002; see "Bromodomain"). This suggests that histone modifications (e.g. acetylation) might be a signal/code for factors to bind and perform specific nuclear functions,

including transcription (Strahl and Allis, 2000; Turner, 2000; Jenuwein and Allis, 2001).

Acetylation of H2A and H2B in yeast has been implicated in aspects of heterochromatin and euchromatin formation for some time. Recently, antibodies developed to selectively recognize the specific sites of acetylation of H2A and H2B demonstrated that Gcn5 is responsible for acetylating both K11 and K16 in H2B, whereas Esa1 is responsible for H2AK7 and H2BK16 and functions in transcriptional activation (Suka et al., 2001). Acetylation of both H2BK11 (H2BK11ac) and K16 (H2BK16ac) are also observed in exponentially growing yeast cells (Suka et al., 2001), suggesting that they might play a role in cell growth. Whether H2B tail acetylation is required for the cell viability is unknown.

### *Deacetylation*

The dynamic process of histone acetylation is reversed by histone deacetylases (HDACs). They remove the acetyl moiety from the  $\epsilon$ -amino groups of lysine residues. Yeast cells contain a group of related HDACs that include Rpd3, Hda1, Hos1, Hos2, Hos3, and Sir2 (Rundlett et al., 1996; Taunton et al., 1996; Denu, 2005). In the latter case, Sir2 has NAD<sup>+</sup> dependent histone deacetylase activity towards H3K14, H3K9 and H4K16 (Imai et al., 2000). All of the known deacetylases, except for Hos3, occur in multiprotein complexes with important functional consequences. First, the HDAC complexes are able to deacetylate histones in nucleosomes, whereas the isolated deacetylase subunits cannot; second, the complexes contain other proteins previously implicated in transcriptional repression and chromosome transactions; and finally, the

deacetylase complexes interact with DNA-binding proteins, bringing the deacetylases to promoters (reviewed in Grunstein, 1997; Struhl, 1998; de Ruijter et al., 2003; Ekwall, 2005). Hos3, on the other hand, has intrinsic catalytic activity as a homodimer when expressed in *Escherichia coli* in the absence of other deacetylase components (Carmen et al., 1999). However, Hos3 is found in a large multi-complex, therefore, the factors that interact with Hos3 has been proposed to sequester the catalytic subunit at specific cellular sties (Carmen et al., 1999).

In general, increased levels of histone acetylation activity (hyperacetylation) are associated with increased transcriptional activity, whereas decreased levels of acetylation (hypoacetylation) are associated with repression of gene expression (reviewed in Kurdistani and Grunstein, 2003; Luo and Dean, 1999). As discussed earlier, the deacetylation-repression connection is clearly demonstrated by yeast Rpd3, which is a member of the class I HDACs, the mammalian orthologues of which include HDAC1, HDAC2, and HDAC3. In yeast, Rpd3 is a repressor of *INO1*, a gene involved in inositol biosynthesis (Kadosh and Struhl, 1997). The mechanism for this chain of event involves the recruitment of the Rpd3 to a specific DNA element (URS1) in the *INO1* promoter through Sin3, which is a part of the Rpd3 complex (Kadosh and Struhl, 1997). In fact, the Rpd3 complex is physically enriched at the *INO1* promoter (Kurdistani et al., 2002) where it deacetylates all sites of acetylation on histones H4, H3, H2A and H2B N-terminal tails (Rundlett et al., 1998; Kadosh and Struhl, 1998; Suka et al., 2001). This highly localized deacetylation of histones might repress transcription by destabilizing the binding of multi-protein chromatin remodeling complexes such as SWI/SNF, SAGA and the basal transcription factor TATA-binding protein (TBP) at the promoter (Deckert and Struhl, 2002).

Yeast Hda1, which is a member of the class II HDACs, is related to HDAC4, HDAC5, and HDAC6 in mammals (Rundlett et al., 1996). Hda1 is recruited to its target promoters through Tup1, a yeast repressor that is a part of Hda1 complex (Wu et al., 2001). Unlike the broad substrate specificity of Rpd3, the Hda1 complex only deacetylates lysine residues in histone H3 and H2B N-terminal tails (Wu et al., 2001).

Hos3, which is distantly related to both class I and II HDACs, has intrinsic HDAC activity and remarkable resistance against HDAC inhibitors like trichostatin A (TSA) when recombinantly expressed in an *E. coli* host system (Carmen et al., 1999; Trojer et al., 2003). Hos3 has a distinct specificity *in vitro* for histone H4 sites K5 and K8, H3 sites K14 and K23, H2A site K7, and H2B site K11 (Carmen et al., 1999). Although Hos3 is required primarily for deacetylation in the ribosomal DNA locus, it is not known whether it represses rDNA transcription or whether it affects promoters throughout the yeast genome, a role identified for Rpd3 and Hda1 (Robyr et al., 2002).

### ***Methylation***

Histone methylation was first described in 1964 (Murray, 1964). Histones can be methylated either on their arginine or lysine residues. Many recent discoveries of lysine- and arginine- directed histone methyltransferases (HMT), and now histone demethylases activities have increased our understanding of methylation in regulating chromatin structure and functions (reviewed in Zhang and Reinberg, 2001; Iizuka and Smith, 2003; Holbert and Marmorstein, 2005; Shilatifard, 2006).

### *Lysine methylation and demethylation*

Each  $\epsilon$ -amino group of lysine can be mono- (me1), di- (me2), or tri-methylated (me3) *in vivo* and these states of methylation are functionally different (Rice et al., 2003; Peters et al., 2003; reviewed in Martin and Zhang, 2005). Methylation of lysine does not alter the overall charge, but increases the basicity and hydrophobicity of the histone tail (Rice and Allis, 2001). This is chemically different from lysine acetylation which neutralizes a positive charge of the amino group (Rice and Allis, 2001). Although mutually exclusive, both acetylation and methylation can occur on lysines (e.g. H3K9) and the difference in chemistry could function as a “switch” for opposing cellular processes (Jenuwein and Allis, 2001). The founding member of H3K9-specific HMTs, human Suv39h1 HMTases (Rea et al., 2000), are homologues of *Drosophila* Su(var)3-9 and of *S. pombe* Clr4, both of which are encoded by genes that are important for the establishment of transcriptionally silent heterochromatin (reviewed in Grewal, 2000). Swi6, a homologue of HP1, is localized to heterochromatin depending upon the HMT activity of Clr4 (Nakayama et al., 2001). Independently, biochemical studies demonstrate that the chromodomains of HP1 and Swi6 preferentially associate with H3 peptides carrying a K9me3 (Lachner et al., 2001; Bannister et al., 2001; Jacobs et al., 2001). These results suggest that H3K9me3 bound to Swi6 plays a role in transcriptional repression.

Interestingly, H3 methylation at K4 functions distinctly from methylation at K9. In the transcriptionally active macronucleus of *Tetrahymena* and  $\beta$ -globin gene in erythrocytes, H3K4 was determined to be methylated and was proposed to be involved in active transcription (Strahl et al., 1999; Litt et al., 2001). Both



H3K4me2 and H3K4me3 are enriched at actively transcribed genes in variety of eukaryotes (Santos-Rosa et al., 2002; Bernstein et al., 2002; Ng et al., 2003; Bernstein et al., 2005). These different methylation states, however, do not overlap completely. While the H3K4me2 seems to be generally distributed across the body of active genes, H3K4me3 is strongly and preferentially associated with promoter and transcribed regions of active genes (Santos-Rosa et al., 2002; Schneider et al., 2004). In yeast, the K4 methylation is mediated by the Set1 complex, whose catalytic subunit, the SET domain protein Set1, is homologous to the *Drosophila* trithorax protein and to a family of related human proteins, hSet1, MLL1, and MLL2 (Roguev et al., 2001; Miller et al., 2001; Nagy et al., 2002; Milne et al., 2002; Nakamura et al., 2002; Wysocka et al., 2003; Hughes et al., 2004; Yokoyama et al., 2004). Human SET-1 like complexes such as MLL1 complex is structurally and functionally similar to the yeast Set1 complex and is capable of methylation H3 at K4 (Wysocka et al., 2003; Goo et al., 2003; Hughes et al., 2004; Yokoyama et al., 2004), suggesting that MLL1 mediated H3K4 methylation establishes and maintains transcription. Recently, two different proteins, Chd1 and Wdr5 have been shown to interact specifically and directly with methylated H3K4 to mediate transcription (Pary-Grant et al., 2005; Wysocka et al., 2005). Chd1 binds to H3K4me2 (Pary-Grant et al., 2005) and Wdr5 binds to both H3K4me2 and H3K4me3 (Wysocka et al., 2005).

The identification of enzymes that are responsible for demethylating lysine within histones has lagged behind the identification of the HMTs. In fact, the very existence of such an enzyme was questioned. For the lysine demethylase, the first breakthrough came with the identification of Lsd1. Lsd1 demethylates mono- and di-methylated H3K4 in an amine oxidase reaction,

thereby leading to transcriptional repression (Shi et al., 2004; Lee et al., 2005). Conversely, LSD1 can relieve repressive histone marks by demethylation of histone H3 at K9, thereby leading to de-repression of androgen receptor target genes (Metzger et al., 2005). These conflicting observations seem to be explained by the existence of interacting proteins that can modulate the substrate specificity of Lsd1. For example, an association with the androgen receptor was shown to be capable of conferring H3K9 demethylase activity to Lsd1 (Metzger et al., 2005). Further studies will be required to identify the mechanism underlying the switching of substrate specificity of Lsd1. Recently, two JmjC domain-containing proteins, JHDM1 and JHDM2, have been shown to specifically demethylase histone H3K36 and H3K9 (me1 and me2), respectively (Tsukada et al., 2006; Yamane et al., 2006).

### *Arginine methylation and demethylation/citrullination*

The arginine residue in histone proteins can only be mono- (me1) or dimethylated (me2s or me2a) by protein arginine methyltransferases, PRMT (reviewed in Wysocka et al., 2006; Bedford and Richard, 2005). It is now known that histones are substrates of CARM1, PRMT1 and PRMT5 (reviewed in McBride and Silver, 2001). The first PRMT found to have specificity toward histones is CARM1 (Chen et al., 1999), which catalyzes methylation of H3 at R2, R17, R26 *in vitro* (Schurter et al., 2001). CARM1 was identified as a coactivator-associated arginine methyltransferases for its ability to interact with a transcription co-activator and to stimulate transcription in a methylation-dependent manner (Chen et al., 1999). Similar to CARM1, PRMT1 also activates transcription by specifically methylating R3 of H4 (Wang et al., 2001a; Strahl et

al., 2001). Both CARM1 and PRMT1, when co-expressed with p160 coactivator, can synergistically activate transcription of a reporter gene in a nuclear receptor dependent manner (Bedford and Richard, 2005). These finding provide a positive link between histone arginine methylation and transcriptional activation.

A major group of deiminated proteins are the core histones H2A, H3, and H4 (Nakashima et al., 2002). The peptidyl arginine deiminase Pad4 can block methylation on an arginine residue by converting it to citrulline (Cuthbert et al., 2004; Wang et al., 2004). Pad4 catalyzes the deimination of both arginine and mono-methyl arginine, but not di-methyl arginine, to citrulline. Peptidyl arginine deiminases are not true “demethylases,” as they do not convert mono-methyl arginine back to arginine (Wang et al., 2004). However, these enzymes may prevent the proposed recruitment of binding proteins to H3R17 or H4R3 upon dimethylation by CARM1 and PRMT1, respectively (Wang et al., 2004).

### ***Ubiquitination and deubiquitination***

Ubiquitin, a 76 residue of amino acid polypeptide found in most living organisms, is conjugated to the  $\epsilon$ -amino group of specific lysine residues of H2A, H2B, H3, and H2A variant H2A.X and H2A.Z (Rechsteiner, 1988). Unlike for other proteins, ubiquitination (ub) of histones does not result in degradation of histones (Seale, 1981; Wu et al., 1981). In budding yeast, ubiquitination of H2B on K123 by the Rad6-Bre1 complex is found to be important in the cellular response to DNA damage (Robzyk et al., 2000; Sun and Allis, 2002; Giannattasio et al., 2005). In the presence of DNA damage, *rad6* $\Delta$  (Rad6 deletion), *bre1* $\Delta$  (Bre1

deletion), and H2BK123A (K123 mutated to alanine) mutants showed impaired activation of the central checkpoint kinase Rad53, probably due to defects in Rad9 phosphorylation (Giannattasio et al., 2005). In addition, H3K4 methylation is eliminated in a strain where K123 has been mutated to R, whereas H3K4 to R retains H2BK123 ubiquitination (Sun and Allis, 2002). Mutation of K123 also disrupted silencing at the telomere (Sun and Allis, 2002), providing a link between ubiquitination of H2BK123, H3K4 methylation and transcriptional silencing. Recently, H2B ubiquitination was shown to be required for the H3K4me2 and H3K4me3, but not H3K4me1 (Shahbazian et al., 2005; Dehe et al., 2005).

Ubiquitination is a reversible process and several studies have recently demonstrated deubiquitination by the enzyme Ubp8 (Henry et al., 2003; Daniel et al., 2004). Because Ubp8 is a component of the SAGA histone acetyltransferase complex (Daniel et al., 2004), it has been proposed that the Rad6-catalyzed mono-ubiquitination of histone H2B is followed by the recruitment of SAGA to the unubiquitinated nucleosomes and subsequent deubiquitination of histone H2B, which is required to initiate transcription. In support of this observation, mutations affecting Ubp8 lead to a rise in global histone H2B ubiquitination and decrease in the transcription of SAGA-regulated genes (Henry et al., 2003; Daniel et al., 2004).

### ***Phosphorylation***

Phosphorylation (ph) at serine and threonine residues of histones has been shown to occur on linker histone H1, H2A variant H2A.X and all the core histones *in vitro* and/or *in vivo* (van Holde, 1988). This long-appreciated histone

modification is often associated with chromosome/chromatin condensation that includes mitosis, meiosis, apoptosis, and DNA damage, events regulated by different histone kinases (Fuchs et al., 2006; Wurtele and Verreault, 2006; Peterson and Laniel, 2004). Phosphorylation also closely correlates with chromosome decondensation events (Cheung et al., 2000), suggesting a “split personality” for certain modifications that remains to be fully understood.

### *H1 phosphorylation*

Early studies on the cell cycle of the slime mold *Physarum* and mammalian cells show that H1 phosphorylation is highest during metaphase, suggesting a role for this modification in mitotic chromatin condensation (Gurley et al., 1973; Bradbury et al., 1974). However, other experiments suggest that H1 itself is not required for chromatin condensation (Ohsumi et al., 1993; Shen et al., 1995; reviewed in Roth and Allis, 1992). Since faithful cell division is essential to life, it is possible that additional phosphorylation events on other histones may provide a redundant role to H1 phosphorylation. In addition to H3S10ph, H3 is phosphorylated at S28 (Goto et al., 1999), T11 (Preuss et al., 2003), and T3 (Polioudaki et al., 2004) during mitosis. Recently, H4 and H2A phosphorylation at their respective S1 was linked to mitosis (Barber et al., 2004). These additional sites of phosphorylation may share redundant functions with H1 phosphorylation in the process of chromosome condensation during mitosis.

H1 phosphorylation has been linked to transcriptional regulation (Roghi et al., 1998); however, mechanisms underlying this process remain unclear. One of the effects of phosphorylation is the alteration of the electrostatic charge of the surrounding region (Roth and Allis, 1992). Given that there are many “basic

patches” that flank potential phosphorylation sites within histone tails (Cheung et al., 2000), these short stretches of basic amino acids may engage acidic residues on other histones. The reversible phosphorylation may disrupt these electrostatic interaction and thereby unfold the chromatin polymer. Indeed, the regulation of “charge patches” in H1 by reversible phosphorylation can regulate transcription, presumably through the alteration of higher-order chromatin structure (Dou and Gorovsky, 2000).

### *H2A.X phosphorylation*

As discussed earlier, the C-terminal domains of the mammalian histone variant H2A.X and the yeast core H2A are rapidly phosphorylated in response to DSBs (reviewed in Iizuka and Smith, 2003). This phosphorylation is also present at directed DNA DSB such as V(D)J recombination in lymphocytes, meiotic recombination in mice, and apoptotic DNA fragmentation (Rogakou et al., 2000; Mahadevaiah et al., 2001). The phosphorylation of H2A.X is mediated by members of the phosphoinositide-3-kinase-related protein kinase (PIKK) family (Rogakou et al., 1999). Of these PIKKs, ataxia telangiectasia mutated (ATM) and DNA-dependent protein kinase catalytic subunit (DNA-PKcs) phosphorylate H2A.X in response to DSBs in higher eukaryotes (Falck et al., 2005; Stiff et al., 2004). In yeast, the PIKK family members, Mec1 and Tel1 in budding yeast, phosphorylates H2A at S129 (Downs et al., 2000; Redon et al., 2003; Shroff et al., 2004). The phosphorylation by these kinases takes place very rapidly after DNA damage, within minutes of ionizing radiation (IR) (Celeste et al., 2003; Celeste et al., 2002; Pilch et al., 2003).

In mammalian cells, the phosphorylation is detected in the vicinity of the DNA lesions by immunofluorescence in combination with “laser scissors” (Paull et al., 2000; Rogakou et al., 1999), and is present in megabase chromatin domains (Rogakou et al., 1999). In addition, the phosphorylation of the budding yeast H2AS129 (H2AS129ph) occurs on the DNA extending from an induced double-strand break in both directions (Shroff et al., 2004; Downs et al., 2000) covering regions of 50-100 kb of chromatin (Unal et al., 2004), demonstrating a direct role of H2A.X phosphorylation in facilitating repair at the site of the break.

H2A.X phosphorylation is important for promoting efficient repair in both mice and yeast. H2A.X<sup>-/-</sup> knockout mice are viable yet sensitive to IR (Celeste et al., 2002). H2A.X<sup>-/-</sup> mouse embryonic fibroblasts (MEFs) have more spontaneous chromosomal aberrations than their wild-type counterparts and generate more breaks when exposed to IR. H2A.X<sup>-/-</sup> cells are also slower to repair IR-induced damage (Celeste et al., 2002). Similar phenotypes were observed in yeast carrying an H2AS129 to alanine (S129A) mutation, which prevents H2AS129 from being phosphorylated in response to damage. Studies examining *S. cerevisiae* and *S. pombe* H2A S129A mutants report increased sensitivity to several DNA damaging agents, such as MMS, camptothecin, and IR, all of which generate DSBs (Downs et al., 2000; Nakamura et al., 2004). This sensitivity is far less than that conferred by checkpoint and repair mutants, suggesting H2A.X phosphorylation may contribute to but is not essential for both processes.

One of the functions of H2A.X phosphorylation is to provide a unique binding site for interaction factors. Indeed, Mdc1/Nfbd1 has been shown to directly interact with phosphorylated H2A.X via its BRCT domain in mammalian cells (Stewart et al., 2003; Stucki et al., 2005). Their interaction then results in the

recruitment of 53BP1, Nbs1 and phosphorylated ATM at sites of damaged chromatin to mediate DNA repair signaling cascade (Stucki et al., 2005) (See below).

### ***Dephosphorylation of H2A.X***

H2A.X phosphorylation can be eliminated by multiple mechanisms including removal by histone exchange followed by degradation, or, alternatively, dephosphorylation. Recently, histone H2A phosphatase complex, HTP-C, has been found to regulate the phosphorylation status of H2A.X phosphorylation *in vivo* and efficiently dephosphorylates H2A.X *in vitro* (Keogh et al., 2006). Htp-C contains the phosphatase Pph3 and the deletion of Pph3 leads to increase in H2A.X phosphorylation in *S. cerevisiae* (Keogh et al., 2006). In addition, H2A.X phosphorylation is lost from chromatin surrounding a DSB independently of the Htp-C, suggesting that the phosphatase targets H2A.X phosphorylation after its displacement from DNA (Keogh et al., 2006). Moreover, the DNA checkpoint recovery defect imparted by the deletion of Pph3 results from the persistent phosphorylation of H2A.X (Keogh et al., 2006). Therefore, the dephosphorylation of H2A.X phosphorylation by the Htp-C may be necessary for efficient recovery from the DNA damage checkpoint.

### ***H3 serine 10 phosphorylation***

Core histone H3S10ph occurs during mitotic and meiotic chromatin condensation in Tetrahymena, yeast, worm and mammalian cells (Gurley et al., 1973; Paulson and Taylor, 1982; Wei et al., 1998; Cobb et al., 1999; Hsu et al., 2000). The link between H3 phosphorylation and chromosome condensation has



been supported by experiments that induce premature chromosome condensation (PCC). Drug-induced phosphorylation correlates with chromosome condensation, whereas, chromosome decondensation is observed when dephosphorylation is induced prematurely in mitotic cells (Ajiro et al., 1996). In addition, inhibition of the putative H3 kinase by staurosporin, a non-specific kinase inhibitor, resulted in chromosome decondensation as well as elimination of phosphorylated H3 (Th'ng et al., 1994). Furthermore, the development of an antibody against histone H3S10ph has allowed *in vivo* studies of this event (Hendzel et al., 1997), and further supports the strong correlation between S10ph and chromosome condensation during mitosis and meiosis (Hendzel et al., 1997; Van Hooser et al., 1998; Hsu et al., 2000).

Consistent with a role for H3S10ph in chromosome function, a *Tetrahymena* mutant strain in which S10 of histone H3 is replaced by an alanine residue (H3 S10A) exhibits altered chromosome condensation (Wei et al., 1999). In addition, abnormal chromosome segregation was observed in this strain, which the authors hypothesize is associated with the perturbation of chromosome condensation (Wei et al., 1999). However, similar mutational analysis in yeast showed that the H3S10 to alanine (H3 S10A) mutant does not have altered generation time or cell cycle progression defects as compared to the wild-type (WT) strain (Hsu et al., 2000). In addition, *in vitro* chromatin condensation assays using *Xenopus* extracts indicated that neither H3S10ph nor the H3 N-terminal tail are required for mitotic chromatin condensation (de la Barre et al., 2001). Therefore, although H3S10ph may function in chromosome condensation or segregation in *Tetrahymena*, the requirement for the modification in these processes does not appear to be conserved in yeast and *Xenopus*.

### ***H3 serine 10 kinase - Aurora B***

The kinase responsible for the mitotic and meiotic H3S10ph in eukaryotes is the Ipl1/aurora B kinase family (Hsu et al., 2000; Zeitlin et al., 2001). The phenotype of the H3 S10A mutant in *Tetrahymena* resembles that of the yeast mutant lacking the only yeast aurora kinase, Ipl1 (Chan and Botstein, 1993; Wei et al., 1999). The recombinant Ipl1 can phosphorylate H3S10 *in vitro* and the temperature sensitive yeast mutant strain *Ipl1-2* shows a dramatic reduction of mitotic and meiotic H3S10ph *in vivo*. In *S. pombe*, Ark1, the aurora kinase, is associated with H3S10ph in mitosis (Petersen et al., 2001). Furthermore, H3S10ph in worms and mammalian cells require aurora B kinase (Hsu et al., 2000; Giet and Glover, 2001; Hauf et al., 2003). In agreement with these results, RNAi reduction of aurora B kinase in these organisms associates with a decrease in H3S10ph (Hsu et al., 2000; Giet and Glover, 2001; Hauf et al., 2003).

### ***H3 serine 28 phosphorylation***

H3S28 phosphorylation (H3S28ph) is increased during mitosis in mammalian cells (Goto et al., 1999). Although found in the same consensus sequence –ARKS– as S10 (see “Histone modification cassette” and the yellow box in Figure 5), H3S28ph displays a pattern different from that of H3S10ph. H3S28ph initiates in condensing chromosomes at prophase (Goto et al., 1999), but H3S10ph initiates in heterochromatin at late G2 (Hendzel et al., 1997). In contrast to H3S10ph, H3S28ph has never been observed in interphase. Instead it seems to be a mitotic event strictly related to mitotic chromosome condensation (Goto et al., 1999).

As is the case for H3S10ph, H3S28ph may be stimulus-inducible. The stimulation of the MAPK pathway by phorbol esters leads to an increase in both

S10ph and S28ph in ras-transformed fibroblast (Dunn and Davie, 2005), suggesting that these two modifications might work together. However, acid urea gel (AU) analysis determined that a significant portion of phosphorylated S28 and S10 exist on an H3 that has not been otherwise acetylated or phosphorylated (the mono-modified form), suggesting that the two modifications do not function in a cooperative manner (Dunn and Davie, 2005). Furthermore, this mono-modified form was present at the same time when the H3 phosphorylation is at a maximum (Dunn and Davie, 2005). Thus, H3S28ph is not dependent upon the phosphorylation of S10 or vice versa.

Despite these differences, H3S28ph and S10ph share a common kinase. Aurora B was shown to be responsible for the mitosis-specific phosphorylation of S28 (Goto et al., 2002). Similar to H3S10ph, H3S28ph is sensitive to treatment with PP1 (protein phosphatase) (Goto et al., 2002). PP1 is a phosphatase that counteracts aurora B (Murnion et al., 2001).

### ***Dephosphorylation of H3 serine 10 and serine 28***

The phosphorylation of S10 and S28 are reversible processes and both are likely mediated by PP1. In yeast, Glc7, also known as PP1 is shown to be the phosphatase that counteracts Ipl1 kinase (Francisco et al., 1994) and catalyzes dephosphorylation of S10 on H3 (Hsu et al., 2000). In *C. elegans*, H3S10 is also dephosphorylated *in vivo* by a type 1 phosphatase, namely Glc7 (Hsu et al., 2000). Moreover, as discussed earlier, the level of H3S28ph is diminished to undetectable levels by PP1 phosphatase (Goto et al., 2002). Therefore, PP1 is suspected of being responsible for the dephosphorylation of S28 in mammalian cells as well.

Although the casual relationship of H3 phosphorylation and chromosome condensation has not been firmly established in yeast and nematode, much evidence suggests that PP1 is important for mitotic chromosome transmission. For example, specific alleles of *glc7* in yeast are defective for kinetochore function (Bloecher and Tatchell, 1999; Sassoon et al., 1999). Defects in chromosome segregation and condensation have also been noted for PP1 mutants in *S. pombe* (Ohkura et al., 1989) and in *A. nidulans* (Doonan and Morris, 1989). Moreover, mutation of the *Drosophila* protein phosphatase gene, *Pp1-87B*, or inhibition of protein phosphatase activity in mammalian cells can cause severe mitotic defects and over-condensed chromosomes (Axton et al., 1990; Guo et al., 1998). Therefore, these studies suggest that histone H3 is one of the physiologically relevant substrates for PP1 in variety of organisms including yeast and nematode, and a possible link between H3 dephosphorylation and mitosis.

### ***H3 threonine phosphorylation***

Although H3T3 phosphorylation (H3T3ph) has been identified as mitosis-specific phosphorylation (Preuss et al., 2003; Polioudaki et al., 2004), it has a different kinetic and localization pattern from H3S10ph. For example, H3T3ph is absent in anaphase and telophase, while the signal for H3S10ph was clearly detectable in these stages of mitosis (Polioudake et al., 2004). In addition, the H3T3ph signal was concentrated in the central region of the metaphase plate and extending to the chromosome arms, while H3S10ph signal was more dominant in the periphery of the metaphase plate (Polioudake et al., 2004). Recently,

Haspin/Gsg2 (haploid germ cell-specific nuclear protein kinase/germ cell-specific gene-2) was identified as a responsible kinase for H3T3 (Dai et al., 2005).

H3T11 phosphorylation (H3T11ph) occurs from prophase to anaphase and appears to be particularly enriched at mammalian centromeres (Preuss et al., 2003). Dlk kinase (Death-associated kinase) is a nuclear serine/threonine kinase that can phosphorylate H3 and H4 *in vitro* (Preuss et al., 2003). It also co-localizes to the centromeres with H3T11 phosphorylation (H3T11ph; Preuss et al., 2003), suggesting Dlk as a possible T3 kinase. Recently, H3T11ph was identified in plant cells during mitosis and meiosis (Houben et al., 2005). Interestingly, treatment of cells with the phosphatase inhibitor cantharidin revealed a high level of T11ph in interphase cells (Houben et al., 2005). Taken together, these results demonstrate the role of H3T11ph in mediating the progression through mitosis.

### ***H2A serine1 phosphorylation***

Phosphorylation on S1 of H2A (H2AS1ph) is found to be involved in transcription regulation and cell cycle. Recently, it was shown that Msk1, which is a kinase for active transcription-related H3S10ph (Sassone-Corsi et al., 1999; Thomson et al., 1999), catalyzes the H2AS1ph, and inhibits transcription *in vitro* (Zhang et al., 2004). Therefore, Msk1 seems to regulate transcriptional activation and repression depending on the histone substrate. It has been postulated that the acetylated histones suppress a transcriptional repression-related phosphorylation by Msk1 to induce transcription. Indeed, acetylated H3 inhibits the phosphorylation of H2A by Msk1 (Zhang et al., 2004). During mitosis, the phosphorylation at both H2AS1 and H4S1 have similar timing and localization as

H3 phosphorylation, and closely correlates with the mitotic chromatin condensation (Barber et al., 2004; see below). These results suggest that phosphorylation of H2A may have dual purpose in mitotic chromatin condensation and transcriptional regulation.

#### ***H4 serine 1 phosphorylation***

H4S1 phosphorylation (H4S1ph) was first reported to occur in the cytoplasm prior to being imported into the nucleus. This phosphorylation has been linked to “new” histone synthesis during S-phase and deposition of H4 onto newly replicated DNA (Ruiz-Carrillo et al., 1975). Consistent with this result, H4S1ph is localized in the nucleus of early S-phase cells when histones are synthesized and assembled into chromatin (Barber et al., 2004). H4S1ph also correlates with mitotic chromatin condensation and displays kinetics and localization patterns similar to H3S10ph (Barber et al., 2004). Therefore, H4S1ph may have a dual purpose in chromatin condensation during mitosis and histone deposition during S-phase.

H4S1ph has been also linked to DNA damage repair. Upon treatment within the DNA-damage agent MMS, which introduces single- and double-strand breaks in DNA, the casein kinase 2 (CK2) phosphorylates histone H4 at S1 in yeast (Cheung et al., 2005; Utley et al., 2005). CK2 is a DNA damage-regulated kinase, and null or temperature-sensitive CK2 yeast mutants are defective for induction of H4S1ph upon DNA damage *in vivo* (Cheung et al., 2005). CK2 mediated H4S1ph plays a role in non-homologous end joining repair, but yeast histone H4S1 mutants display no sensitivity to the DNA-damaging agents (Cheung et al., 2005; Utley et al., 2005), indicating that this modification itself is

not the DNA damage response. Recently, the increase in H4S1ph during DNA damage was accompanied with a drop in acetylation of histone H4 (Utley et al., 2005). In addition, phosphorylation of S1 has a negative effect on acetylation by NuA4, which is a HAT complex that is recruited to a DSB site, *in vitro* (Utley et al. 2005). These data suggest that this modification is a part of the DNA-repair histone code.

### ***H2B serine 14 phosphorylation***

H2BS14 phosphorylation (H2BS14ph) is induced during apoptosis in mammalian cells. (Ajiro et al., 2000; Cheung et al., 2003). The kinase Mst1 (Mammalian sterile twenty) was identified as the kinase responsible for S14 apoptotic phosphorylation (Cheung et al., 2003). The onset of DNA damage marker H2A.XS139ph precedes H2BS14ph, suggesting a link between DNA damage repair and apoptosis. Their link is further confirmed by the observation that showed the phosphorylation of S14 coinciding with the site of DSB induced by ionizing radiation or laser treatment (Fernandez-Capetillo et al., 2004a). Given that unrepaired or incorrectly repaired DNA damage triggers apoptosis to eliminate these deregulated cells (Sancar et al., 2004), H2BS14ph may be the mechanism to promote apoptosis in these cells. In other words, H2BS14ph serves as an apoptotic “histone code.”

Given that S14ph is uniquely associated with apoptotic chromatin, H2BS14ph may function to facilitate the formation of chromatin in species ranging from frogs to humans (Cheung et al., 2003). So far, the direct link between H2BS14ph and chromatin condensation has been lacking *in vivo*, although the influence of the H2B N-terminal tail on chromatin condensation

was observed *in vitro* (de la Barre et al., 2000). In Chapter 2, I have extended this finding to unicellular eukaryotes by identifying a novel histone H2B phosphorylation during yeast apoptosis. I have also provided the first *in vivo* demonstration that H2B phosphorylation directly mediates chromatin condensation.

### ***Histone modification “cross-talk”***

The nature of the histone code predicts that histone modifications impinge on each other by acting as molecular switches, enabling or blocking the setting of other covalent marks that may specify unique downstream functions (Jenuwein and Allis, 2001; Fischle et al., 2003a; Fischle et al., 2003b). Indeed, this type of “cross-talk” between different histone modifications has emerged as a paradigm of chromatin mediated functions/cell biology (Jordan et al., 2000; Pawson and Nash, 2000). The first level of the complexity of histone modification cross-talk originates from the modular organization of chromatin itself (Fischle et al., 2003a). Since each core histone can be post-translationally modified in a large number of ways, this generates a vast number of possible combinations of marks for any chromatin domain. The second level of complexity comes from the modifications on a single histone, which are dependent on each other and interconnected via various mechanisms (Fischle et al., 2003a). The final level of complexity is from the fact that cross-talk exists between modifications on different histones. These effects might be restricted to a single nucleosome or might affect larger nucleosomal arrays or domains (Fischle et al., 2003a). Thus, the complexity and diversity that are generated by the modifications add to the capacity of the genome to store, inherit and release information.



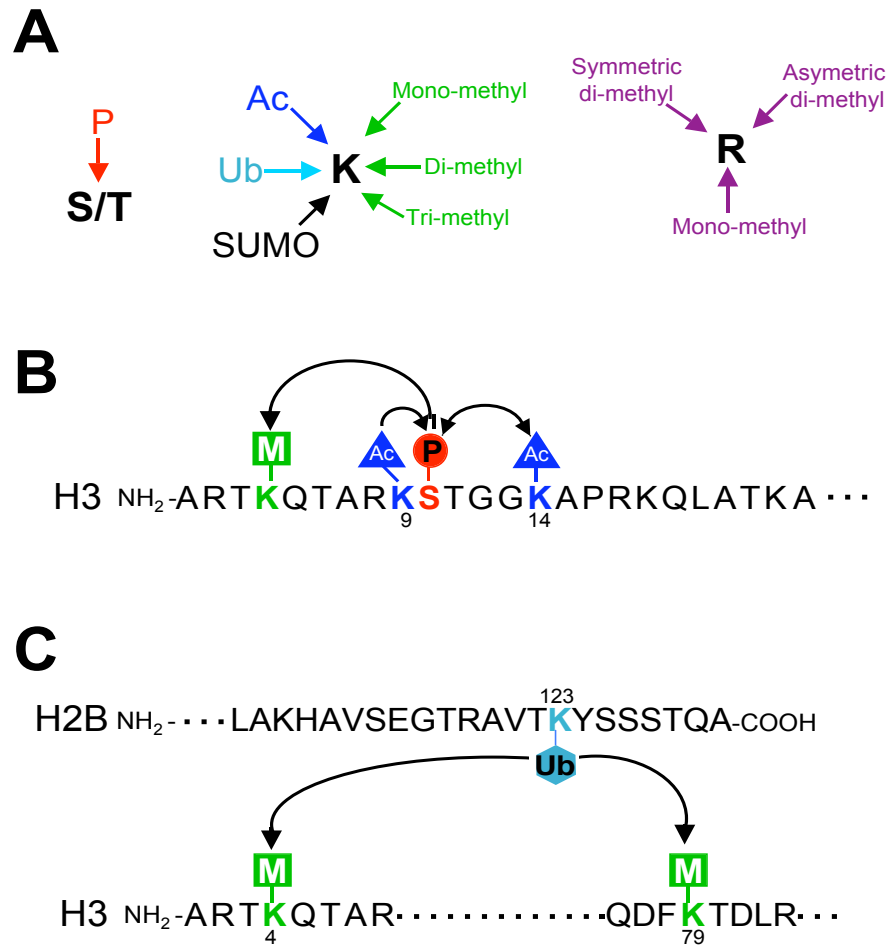


**Figure 4. "Cross-talk" between histone modifications**

(A) Potential "choices" of the modification status of different histone residues. Whereas serine (S) and threonine (T) residues are phospho-acceptor (P) sites, lysine (K) and arginine (R) residues have multiple choices of post-translational modification possibilities. Lysine residues can be acetylated (Ac), mono-ubiquitinated (Ub), sumoylated (Su), or (mono-, di-, tri-) methylated. Arginine might be mono- or di-methylated (symmetrical or asymmetrical). This figure was adapted from Fischle et al., 2003a.

(B) "Cross-talk" at the level of a single histone H3 amino-terminal tail. H3S10ph promotes acetylation on K14 following epidermal factor treatment. H3K9 and H3K14 acetylation stimulate H3S10ph during mitosis.

(C) "Cross-talk" between histone H2B and H3. In yeast, only H2B is known to be ubiquitinated (H2BK120 of the human sequence corresponds to H2BK123 in yeast). This modification is necessary for methylation of H3 on K4 and K79.

The histone modification choice of a single residue provides the first level of complexity of chromatin cross-talk (Fischle et al., 2003a). Particularly, lysine and arginine residues have multiple choices of post-translational modification possibilities. Lysine residues in histones can be acetylated, mono-ubiquitinated, or mono- or di-, and tri- methylated (Figure 4A). Similarly, arginine can be mono- or di-methylated symmetric or asymmetric (Zhang and Reinberg, 2001; Bannister et al., 2002). It is well documented that H3K9 and H3K14 can be either acetylated, or mono-, di-, and tri-methylated. Different modifications of a particular site can have different readouts with distinct biological functions. The H3K4me<sub>2</sub> occurs at both inactive and active euchromatic genes, whereas tri-methylation is present exclusively at active genes (Santos-Rosa et al., 2002). The acetylated state of H3K4, however, correlates with euchromatin, suggesting its involvement in active transcription (reviewed in Nowak and Corces, 2000). A similar paradigm also follows for H3K9. Pericentric heterochromatin is specifically enriched in H3K9me<sub>3</sub> leading to transcriptional repression, but the K9ac is found in euchromatin leading to transcriptional activation (reviewed in Lachner and Jenuwein, 2002; Kondo et al., 2003). Conversely, mono- and di-methylated H3K9 is found in silent domains within euchromatin (Rice et al., 2003), suggesting that K9me<sub>3</sub> is functionally distinct from the other H3K9-methyl modifications. Therefore, the cross-talk choices of single histone residues and the enzyme system that modifies them provide one level of complexity that impacts on genomic function and gene activity.

Histone modification cross-talk exists as a chronology in the establishment of a specific modification pattern. The methylation on H3K9, for example, appears to trigger sequential events leading ultimately to transcriptional

repression (Wang et al., 2001b). At least *in vitro*, this mark can inhibit acetylation of the H3 tail on K14, K18, and K23 by HAT (e.g. p300) (Wang et al., 2001b), and methylation on H3K4 by HMT (e.g. Set7) (Wang et al., 2001b). By contrast, H3K4me2 inhibits K9me2 by Su(var)3-9, but promotes acetylation of H3 by p300 (Wang et al., 2001b). The phosphorylation of histone H3S10 also facilitates acetylation of K14 and methylation of K4, and leads to gene activation (Lo et al., 2001; Milne et al., 2002; Cheung et al., 2000; Figure 4B). Thus, this is an example of a pre-existing modifications close to a site of methylation altering the recognition motif of protein methyltransferases to regulate gene activation.

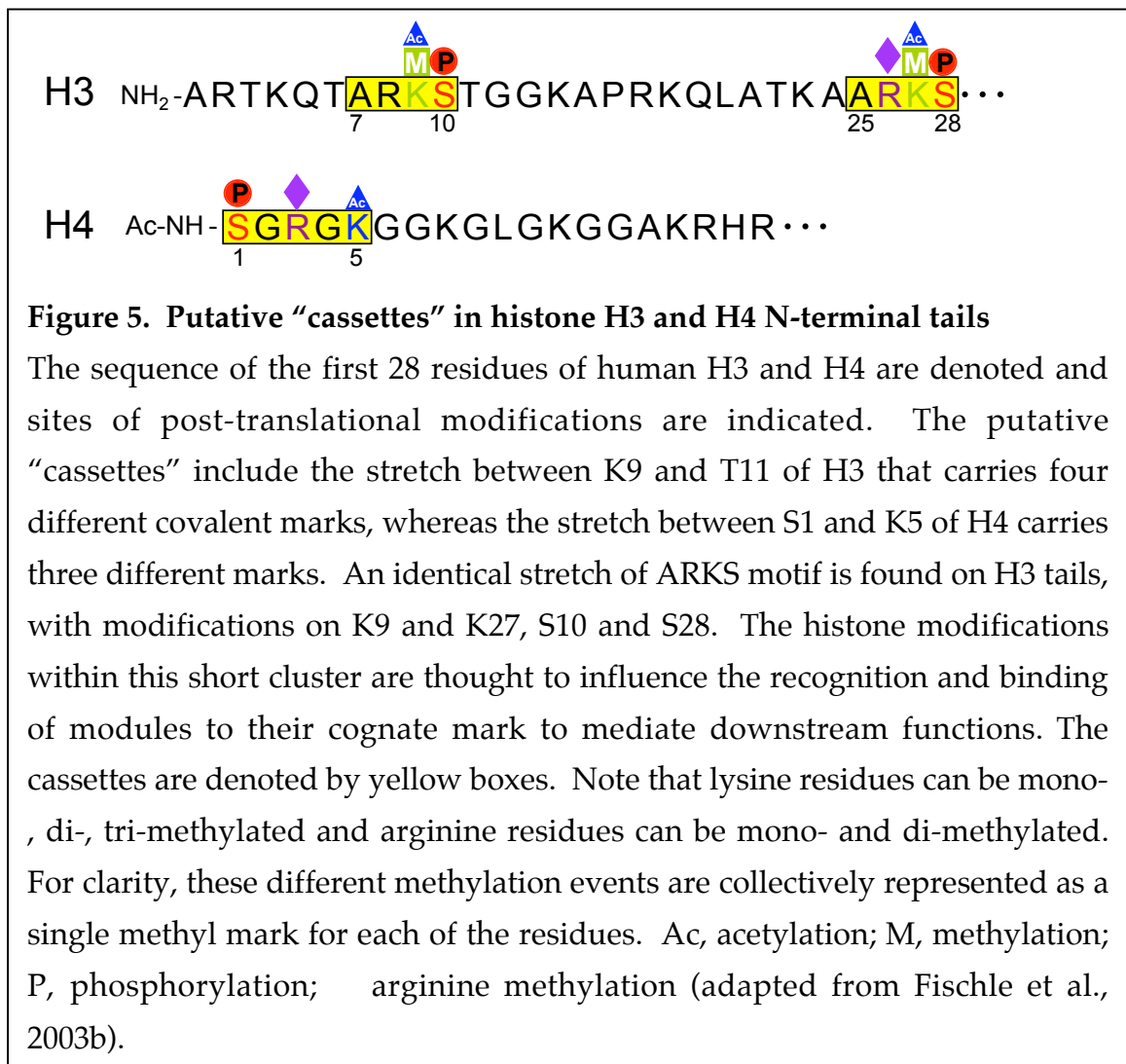
Finally, the histone modification cross-talk takes place even between marks on different histones. For example, ubiquitination of histone H2BK123 is required for methylation of H3K4 and H3K79, which are both involved in transcriptional activation (Sun and Allis, 2002; Briggs et al., 2002; Dover et al., 2002; Ng et al. 2002; Shahbazian et al., 2005; Dehe et al., 2005; Figure 4C).

The diversity of histone modification cross-talk establishes distinct biological functions. This can be achieved by a “code”, which is set up by singular as well as combinatorial histone modifications and read by cellular binding factors bringing about specific responses (e.g. chromodomain and bromodomain proteins; see “Trans mechanism”). Thus, in contrast to the straight flow of most signal transduction cascades, where the modification of one protein impacts directly on downstream effectors, signaling to and from chromatin appears to be far more complex. In my thesis, I have provided another example of histone modification cross-talk on the level of a single

histone, H2B, further supporting the complex nature of chromatin mediated function.

### *Histone modification “cassette”*

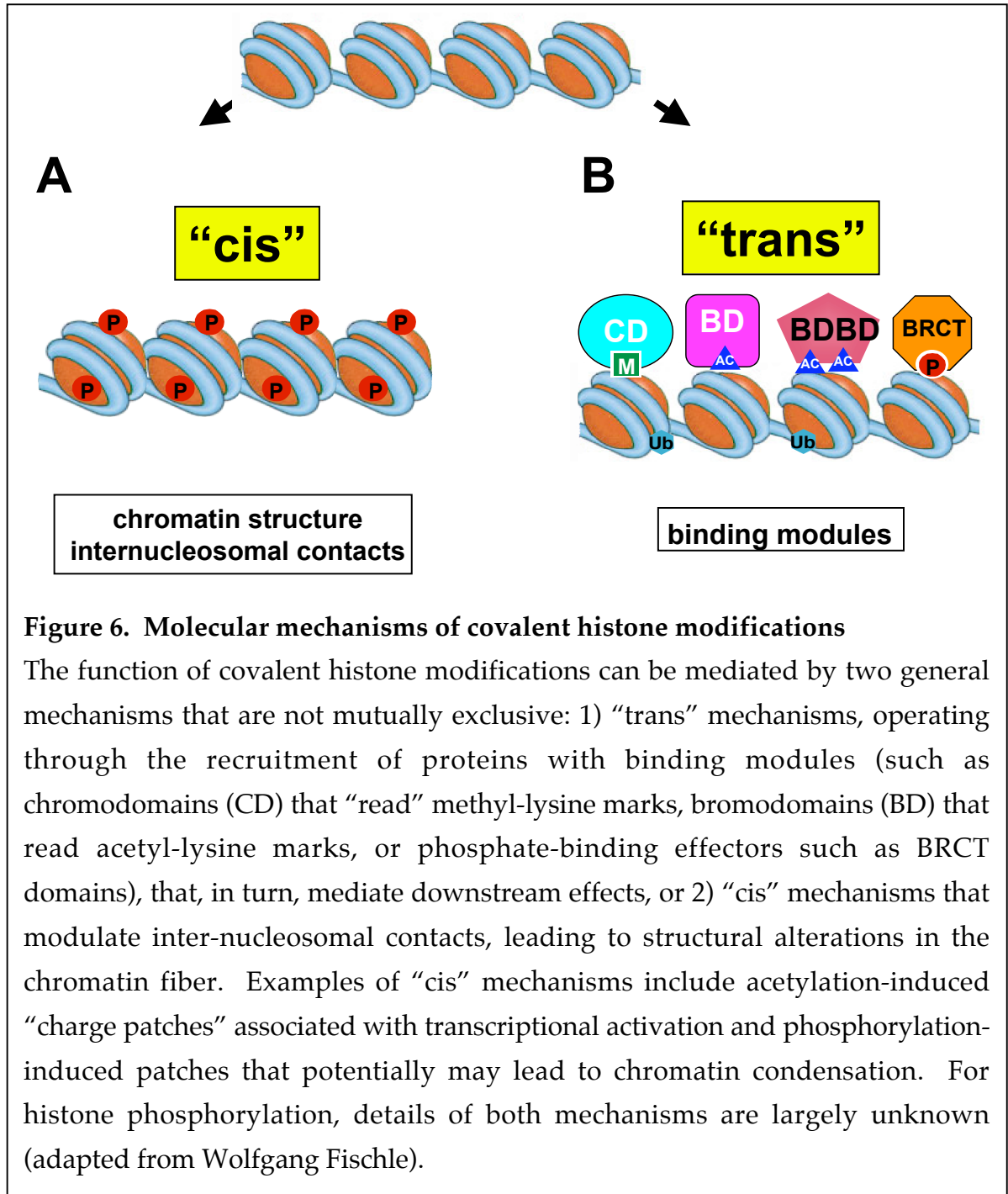
Another mechanism that might govern the biological readout of distinct modification patterns is the concept of “modification cassettes” (reviewed in Fischle et al., 2003b). In this hypothesis, the “cassette” refers to a short cluster of densely modifiable sites in histones with a distinct biological readout (Fischle et



al., 2003b). Rather than acting independently, this domain is situated at strategic locations in the histones and functions as a discrete information unit regulating and relaying different signals depending on its modification state (Fischle et al., 2003b). The best examples of short cassettes are readily spotted on the H3 and H4 N-terminal tail, where there are at least three out of five sites separated by no more than one residue that can be covalently modified; the stretch between K9 and T11 of H3 or S1 and K5 of H4 (see yellow box in Figure 5). The identical ARKS motifs are found in H3 tail with modifications on K9 and K27, S10 and S28 (yellow box in Figure 5). The histone modifications within this short cluster are thought to influence the recognition and binding of modules to their cognate mark to mediate downstream functions (see “trans mechanism”).

### **Functional mechanism of histone covalent modifications**

Different covalent modification patterns found in the highly basic core histone tail domains are essential determinants of chromatin fiber dynamics. Two general types of mechanisms have been proposed to explain the function of covalent histone modifications: 1) “cis” mechanisms that involve the covalent modifications inducing the structural alteration in the chromatin fiber by changing internucleosomal contacts (Figure 6A), 2) “trans” mechanisms that involve the binding of effectors to engage specific covalent modifications in a context-dependent fashion (Figure 6B).



### *Cis mechanism*

The “cis” mechanism postulates that covalent modifications directly affect the nucleosomal contacts and histone DNA interactions to alter the chromatin structure (Figure 6A). In this case, the N-terminal histone tails appear to mediate

chromatin condensation through multiple mechanisms, only one of which involves simple DNA charge neutralization. Most of the information available comes from studies involving “tail-less” nucleosome arrays that have the major portions of the core histone tails removed by selective proteolysis with trypsin. Trypsinized arrays are unable to fold into the most compact conformation or to oligomerize (Fletcher and Hansen, 1995; Garcia-Ramirez et al., 1992; Schwarz et al., 1996; Tse and Hansen, 1997). In addition, studies of “hybrid” trypsinized arrays lacking either their H2A/H2B or H3/H4 N-termini demonstrate that the core histone tail domain, and in particular the H3/H4 tetramer tails, mediate the solution-state conformational dynamics of the chromatin fiber (Krajewski and Ausio, 1996; Moore and Ausio, 1997; Tse and Hansen, 1997). Moreover, Richmond and colleagues have shown that the chromatin fibers lacking one of these histone tails with the exception of the H4 N-terminus lead to cation-dependent compaction (Dorigo et al., 2003). The detailed experiments revealed that the basic patch (amino acid residues 14-19) may be integral to the formation of nucleosome-nucleosome interactions in chromatin higher-order structure (Dorigo et al., 2003). The electrostatic interactions between the basic residues of the H4 N-terminal tail and the acidic patch of the H2A/H2B dimer from an adjacent nucleosome are thought to lead to a chromatin fiber compaction (Davey et al., 2002; Luger et al., 1997). Apart from the electrostatic component, protein-protein interactions, for example internucleosomal tail-tail interactions and/or binding of the tails to exposed protein domains on the surface of other nearby nucleosomes may also play a role (Hansen, 2002; Luger and Richmond, 1998). Furthermore, because of the extensive involvement of the tails in chromatin fiber

folding, it seems likely that at least some core histone tail post-translational modifications will have significant effects on chromatin fiber dynamics.

Currently, it is widely assumed that particular histone acetylation patterns lead to altered folding of the nucleosomal fiber that renders chromosomal domains more accessible. In this case, the reduction of the positive charge due to the acetylation of lysine and/or arginine residues in this region may contribute to a less stable, open structure (reviewed in Hansen, 2002). In support, the acetylated histones disrupted formation of the folded state *in vitro* (Garcia-Ramirez et al., 1995). Likewise, the acetylated histones also correlate with euchromatin *in vivo* (Vavra et al., 1982; Clarke et al., 1993; Bone et al., 1994; Hebbes et al., 1992; Hebbes et al., 1994). Recently, the acetylation of H4K16 was found to directly contribute to the decondensed chromatin *in vitro* (Shogren-Knaak et al., 2006). Given that H4K16ac has a role in transcriptional activation and the maintenance of euchromatin *in vivo* (Hilfiker et al., 1997; Suka et al., 2002) further reinforces that the functional status of the core histone tail domains can regulate the higher-order chromatin structure.

To date, the potential cis effects on chromatin structure, produced by adding or subtracting charge altering phosphates, remains poorly understood. In Chapter 4, I have provided evidence supporting the phosphorylation-induced patches leading to chromatin condensation via the cis mechanism.

### ***Trans mechanism***

According to the histone code hypothesis, the histone modification marks provide the binding sites for a series of effector proteins that would affect chromatin function (Jenuwein and Allis, 2001). Interestingly, the histone



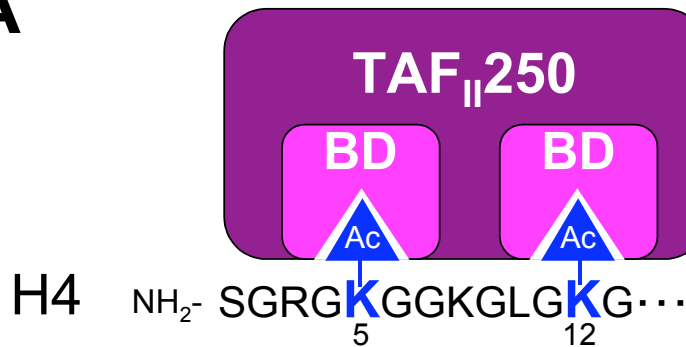
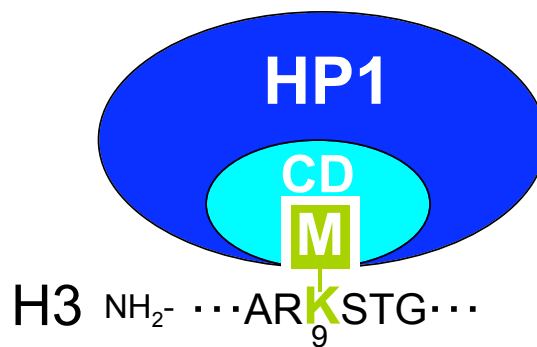
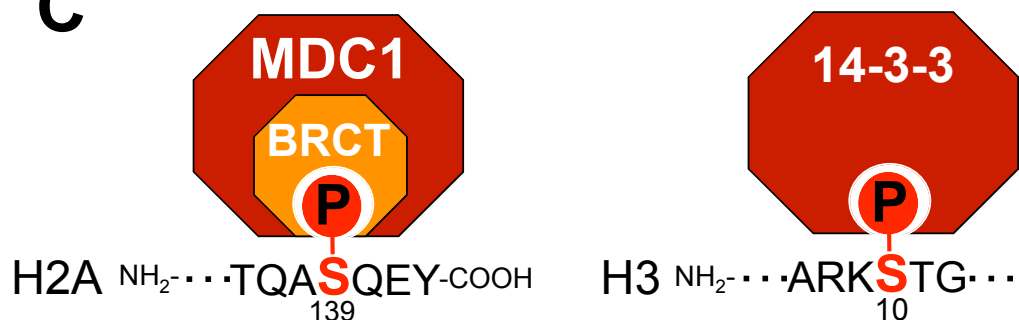
modifying enzymes are unable to access their substrates unless targeted there (Felsenfeld and Groudine, 2003; Johnson et al., 2005). In other words, the same enzyme will not modify all histones in all genes, at the same time; only that subset of genes that have recruited the modifying enzyme to the promoter will be regulated by it. This highlights the relevance of the targeting process, at the origin of the selectivity of the enzyme action, as an important feature of the regulation of histone modification. Within this context, it is clear that the protein domains able to interact with chromatin and/or its modified components (e.g. bromodomain, chromodomain, BRCT domains) can play a crucial role in the targeting process (reviewed in de la Cruz et al., 2005; Stucki et al., 2005), and therefore, induce and direct downstream biological functions, which is referred to as “trans” mechanism (Figure 6B). Some of the best known histone binding domains will be discussed below.

### ***Bromodomain***

Bromodomains (Brahma organization modifier) are small protein domains that are found in many chromatin-associated proteins and most HATs (reviewed in Horn and Peterson, 2001; Zeng and Zhou, 2002). Bromodomains function as acetylated lysine binding domains (Bottomley, 2004; Hudson et al., 2000; Owen et al., 2000; Jacobson et al., 2000). A direct interaction between bromodomains and acetylated lysines was initially suggested by NMR structural studies of PCAF's bromodomain and confirmed by *in vitro* peptide binding and mutagenesis experiments (Dhalluin et al., 1999). Indeed, the acetylation of tail lysines at the IFN- $\gamma$  promoter by GCN5/PCAF turns out to be highly specific both *in vivo* and *in vitro* and marks three residues: H4K8, and H3K9 and H3K14

(Agalioti et al., 2002). Using mutated and modified recombinant histones, these acetylations were found to provide distinct signals for the sequential recruitment of the bromodomain-containing proteins BRG1, a component of the SWI/SNF complex, and TAFII250, a component of TFIID (Agalioti et al., 2002; Figure 7A). Mutating H4K8 to alanine abolished the ability to recruit BRG1, whereas mutating H3K9 or K14 to alanine abolished the ability to recruit TAFII250 (Agalioti et al., 2002). These studies argue that these interactions are the result of unique protein-recognition surfaces created by the modifications and thus represent a histone acetylation code for the IFN- $\gamma$  promoter (Agalioti et al., 2002).

The crystallographic analyses of the double bromodomain of human TAFII250 showed that these modules have the capacity to bind histones that are multiply acetylated (Jacobson et al., 2000). Interestingly, the distance between the two binding pockets ideally suits the interaction with acetylated lysines that are seven amino acids apart, a configuration that is seen on H4 *in vivo* (K5, K8, K12, and K16 of the N-terminal tail are known to be acetylated (Thorne et al., 1990). Furthermore, *in vitro* peptide binding assays showed that multiply acetylated H4 peptides bind to the double bromodomain with much greater affinity than unacetylated peptides (Dey et al., 2003). Given that TAFII250 is a component of TFIID (Ruppert et al., 1993; Weinzierl et al., 1993), these findings immediately suggest a model whereby acetylation of histones, particularly at H4, may serve to recruit TFIID to relevant promoters and facilitate the assembly of preinitiation complexes. Taken together these studies demonstrate that sequential recruitment and anchoring of bromodomain-containing factors and complexes to the promoter region are indeed crucial for activation of some genes.

**A****B****C**

**Figure 7. Examples of “trans” mechanism for the effect of histone modifications**

(A) The pair of acetyl-groups (Ac flags) on H4 functions as an interaction module and binds to the double-bromodomains (BD) of TAFII250.

(B) By analogy, the methyl-group (M flags) on H3 functions as a unique epitope that specifically interacts with the chromodomain of HP1.

(C) The phospho-group on H2A.XS139 interacts with the BRCT domain of MDC1/NFBD1, whereas H3S10ph interacts with 14-3-3 protein.

### ***Chromodomain***

The chromodomain (chromatin organization modifier) was first identified as a common domain between two distinct regulators of chromatin structure in *Drosophila*: heterochromatin protein 1 (HP1) and Polycomb (Pc) (Paro and Hogness, 1991). Proteins containing chromodomains, have been shown to have affinity for methylated lysines (Jacobs and Khorasanizadeh, 2002; Fischle et al., 2003c). The structure of the HP1 chromodomain consists of three-stranded antiparallel  $\beta$ -sheet supported by an  $\alpha$ -helix that runs across the sheet. The binding pocket consists of three aromatic side chains that become ordered on binding the methylated histone H3 peptide (Nielsen et al., 2002; Jacobs and Khorasanizadeh, 2002; Fischle et al., 2003c; Bottomley, 2004). In fact, HP1 binds to methylated (mono-, di-, tri) H3-K9 (Figure 7B) and silencing protein Pc also binds tri-methylated H3K9 and all methylated state of H3K27 (Cao et al., 2002; Czermin et al., 2002; Kuzmichev et al., 2002; Fischle et al., 2003c), thus directing the binding of other proteins to mediate the formation of heterochromatin and gene silencing (Bannister et al., 2001; Lachner et al., 2001; Nakayama et al., 2001).

### ***BRCT domains***

BRCA1-C-terminal (BRCT) domain contains a pair of tandem repeats that are essential for the tumor suppressor function (reviewed in Glover et al., 2004). Similar repeat sequences have been identified in many proteins, such as Nbs1, the p53 binding protein 53BP1 and MDC1, that mediate cellular mechanisms for dealing with DNA damage (Celeste et al., 2002; Bassing et al., 2002). The BRCT domain was recently shown to constitute a module for recognizing phosphorylated peptides (Williams et al., 2004).

NBS1, the gene product defective in Nijmegen breakage syndrome (NBS) (Matsuura et al., 1998; Carney et al., 1998; Varon et al., 1998), physically interacts with histone, rather than damaged DNA, by direct binding to H2A.XS139ph (Kobayashi et al., 2002). The N-terminal region of Nbs1 contains both the fork-head associated (FHA) and the BRCT domain (Tauchi et al., 2001). Both FHA and BRCT domains of Nbs1 are essential for this physical interaction, since NBS1 lacking either domains failed to bind to H2A.XS139ph. In addition, recombinant FHA or BRCT domains alone can bind to phosphorylated H2A.X (Kobayashi et al., 2002). Thus, the phosphorylated H2A.XS139 and the FHA and BRCT domain of Nbs1 may define a signaling/recognition module pair for DNA damage.

Recently, the BRCT domain of mammalian MDC1/NFBD has also been shown to directly bind to H2A.XS139ph by specifically interacting with the phospho-epitope at the H2A.X carboxyl terminus following DNA damage (Stucki et al., 2005; Figure 7C). In addition, MDC1/NFBD1-H2A.X complex formation regulates H2A.X phosphorylation and is required for normal radioresistance and efficient accumulation of DNA-damage-response proteins on damaged chromatin (Stucki et al., 2005). Therefore, binding of MDC1/NFBD1 to phosphorylated H2A.X plays a central role in the mammalian response to DNA damage.

### ***14-3-3 domain***

The term "14-3-3" denotes a family of dimeric  $\alpha$ -helical proteins present in high abundance in all eukaryotic cells (Fu et al., 2000). 14-3-3 proteins were the first molecules to be recognized as distinct phosphorylated serine/threonine binding proteins, forming tight complexes with phosphorylated ligands (Yaffe et al.,

1997a; Rittinger et al., 1999). In fact, 14-3-3 binds to histone H3 tail in a strictly S10ph-dependent manner (Macdonald et al., 2005; Figure 7C). In addition, the acetylation of H3K9 and K14 does not impede 14-3-3 binding to H3S10ph (Macdonald et al., 2005). *In vivo*, 14-3-3 is inducibly recruited to *c-fos* and *c-jun* nucleosomes upon gene activation, concomitant with phosphorylation and acetylation of H3 (Macdonald et al., 2005). 14-3-3 isoforms thus represent a class of proteins that mediate the effect of histone phosphorylation at inducible genes.

## **Apoptosis**

Since my thesis deals with histone phosphorylation during cell death, in this section, I will discuss some of the critical pathways that affect apoptosis. As grim as this term sounds, cell death plays an essential part in development in adult life of multicellular organisms (Clarke and Clarke, 1996). In general there are two categories of cell death: passive and active cell death (reviewed in Jin and El-Deiry, 2005). For passive cell death, also known as necrosis, cells die with slow integration and without features of active cell death. Active cell death is known as apoptosis or programmed cell death (PCD), which refers to cells that are “programmed” to die during normal development.

The word apoptosis comes from the Greek word meaning “dropping or falling off of petals from a flower or leaves from a tree” and it plays a complementary but opposite role to mitosis in the regulation of animal cell populations (Kerr et al., 1972). Apoptosis is initially defined by its morphological and biochemical characteristics such as exposure of phosphatidylserine on the cell surface, cell shrinkage, membrane “blebbing,” production of reactive oxygen species (ROS), chromatin condensation and nuclear fragmentation (Kerr et al.,

1972; Figure 8). The nucleus condenses completely and is segregated into several fragments, although the other organelles are generally left intact (reviewed in Hacker, 2000). The entire condensed cell is reorganized into “apoptotic bodies” which are small membrane-bound vesicles varying in size and composition (Kerr et al., 1972). The “apoptotic bodies” can contain whole organelles, parts of condensed nuclei or cytosolic elements, which are phagocytosed by neighboring cells. Apoptosis is a silent type of cell death, since it does not induce a local inflammatory response, and has no effects to the surrounding cells (reviewed in Armstrong, 2006; Jin and El-Deiry, 2005). In this respect, it differs from the

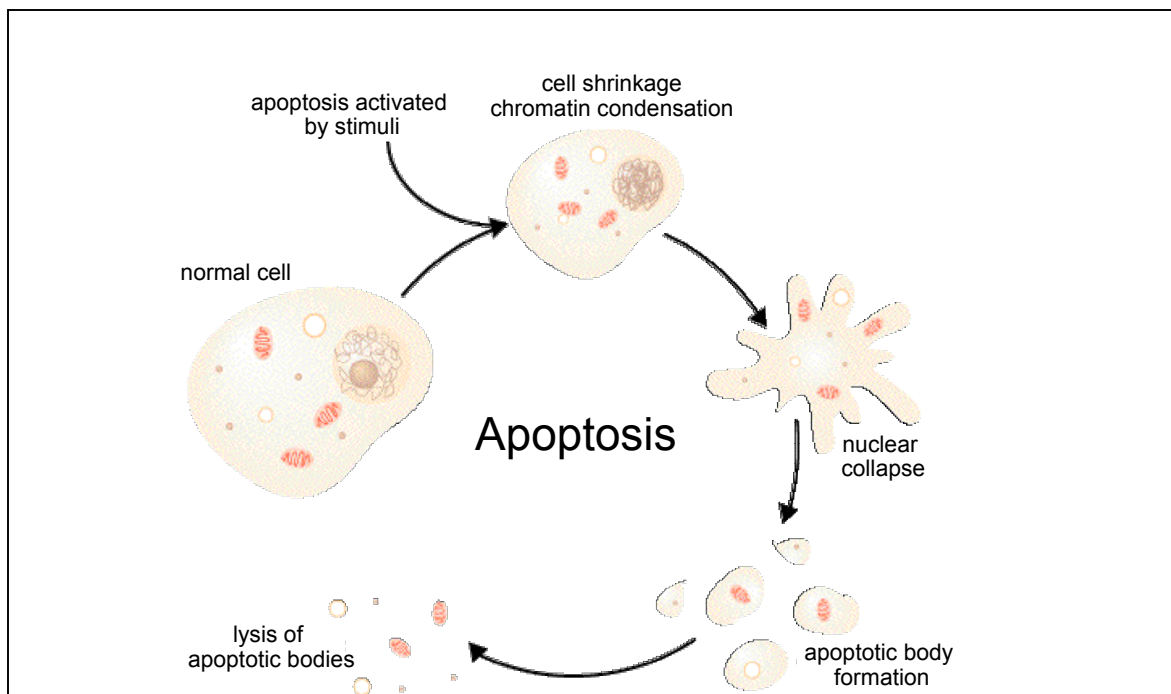


**Figure 8. Apoptosis - the programmed death of a cell**

Apoptosis is defined by its morphological and biochemical characteristics. During apoptosis, the genome of the cell fractures, followed by cell shrinkage and chromatin condensation. Part of the cell disintegrates into smaller apoptotic bodies which are phagocytosed by neighboring cells.

(adapted from <http://www.bioteach.ubc.ca/CellBiology/Apoptosis/>)

necrotic type of cell death, in which cells die through swelling, influx of calcium ions and water, followed by cell lysis (Armstrong, 2006; Jin and El-Deiry, 2005). This process is associated mostly with pathological death and it results in cell injury and an inflammatory reaction (Leist and Jaattela, 2001). The dying apoptotic cells simply disappear without leaving any traces (reviewed in Savill and Fadok, 2000).

Apoptosis is essential in normal development and homeostasis and acts as a defense mechanism in response to cellular abnormalities in multicellular organisms including human (reviewed in Fadeel and Orrenius, 2005). Apoptosis occurs during normal embryological development and during normal tissue turnover (Fadeel and Orrenius, 2005). Moreover, dysregulation of this cell death process has been postulated to play a role in the pathogenesis of a variety of human diseases (reviewed in Thompson, 1995; Osborne, 1996; Winoto, 1997). For example, a reduced propensity to die is thought to be important for both the development of tumors and the acquisition of resistance to chemotherapy (reviewed in Hanahan and Weinberg, 2000). Diminished apoptosis has been linked to autoimmune syndromes, whereas excessive apoptosis has been implicated in neurodegenerative diseases and in part of the tissue destruction that occurs after vascular occlusions in the brain and heart (reviewed in Fadeel and Orrenius, 2005). These facets have made apoptotic pathways the objective of intense interest and as result, enhanced our understanding of the complex networks of apoptotic signal transduction pathways. In this section, I will describe some of these pathways that can influence chromatin during apoptosis. Finally, I will describe an apoptotic mechanism in lower eukaryotes, particularly in budding yeast.



### *Apoptotic pathways*

In mammals, a wide array of external signals may trigger two major apoptotic pathways, namely the extrinsic pathway (death receptor pathway) or the intrinsic pathway (the mitochondrial pathway) within a cell (Savill and Fadok, 2000; Green and Kroemer, 2004). The extrinsic pathway is activated by apoptotic stimuli comprising extrinsic signals such as the binding of death inducing ligands to cell surface receptors (Jin and El-Deiry, 2005; Green and Kroemer, 2004; Figure 9). In other cases, apoptosis is initiated following intrinsic signals including DNA damage induced by irradiation or chemicals, growth factor deprivation or oxidative stress (Jin and El-Deiry, 2005; Green and Kroemer, 2004; Figure 9). In general intrinsic signals initiate apoptosis via the involvement of mitochondria (Green and Kroemer, 2004). The induction and execution of apoptosis require the cooperation of a series of molecules including signal molecules, receptors, enzymes and gene regulating proteins. Among them, the caspase-cascade signaling system, regulated by various molecules such as the inhibitor of apoptosis protein (IAP), Bcl-2 family proteins, and calpain, is vital in the process of apoptosis (Launay et al., 2005; Figure 9).

### *Caspases dependent apoptotic pathway*

Caspases, the interleukin-1 $\beta$ -converting enzyme family proteases, are highly homologous to *C. elegans* cell death gene CED-3 (Cerretti et al., 1992; Zimmermann et al., 2001; Yuan et al., 1993; Xue et al., 1996). Fourteen caspases have been identified so far, all of which share some common properties. They are all aspartate-specific cysteine proteases and contain three domains: N-terminal prodomain, large domain with the conservative pentapeptide active site

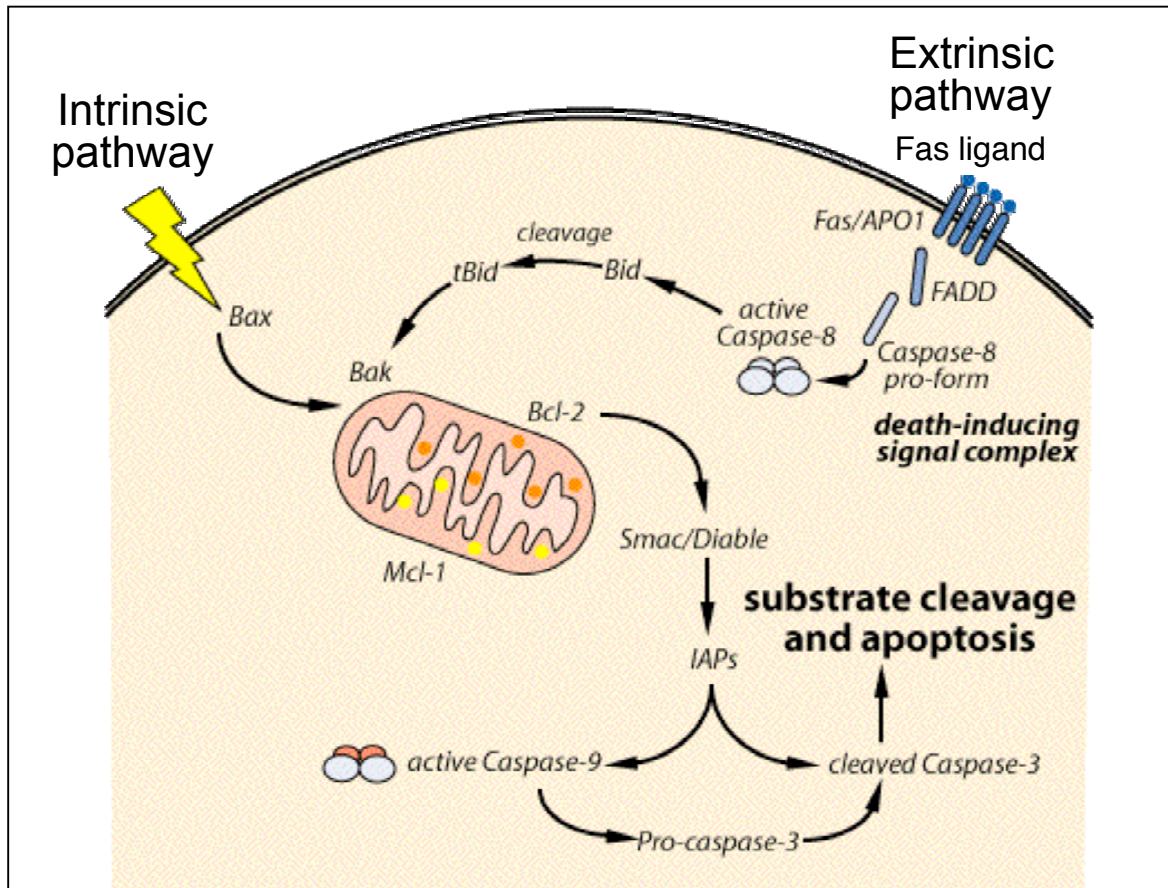


**Figure 9. The intrinsic and extrinsic pathways leading to mammalian apoptosis**

Apoptosis is triggered in a cell through either the intrinsic pathway or the extrinsic pathway. The intrinsic pathway is triggered by cellular stress, specifically mitochondrial stress caused by factors such as DNA damage and heat shock. In contrast, the extrinsic pathway is initiated through the stimulation of the transmembrane death receptors, such as the Fas receptors, located on the cell membrane.

(adapted from <http://www.bioteach.ubc.ca/CellBiology/Apoptosis/>)

“QACXG” (X can be R, Q or D), and C-terminal domain (reviewed in Ho and Hawkins, 2005; Boyce et al., 2004). In addition, their precursors are all zymogens known as procaspases (Ho and Hawkins, 2005). The activation of caspases involve cleavage of the C-terminal domain and the N-terminal prodomain

(Thornberry et al., 1997). The C-terminal domains bind to the large domain to form a dimer with the catalytically active site between them (Thornberry et al., 1997). The binding of two dimers then forms an active caspase (reviewed in Degterev et al., 2003; Ho and Hawkins, 2005). Even though the N-terminal prodomain is not a part of the active caspase, it contains critical signals such as caspase-recruitment domain (CARD) or death effector domain (DED) for interacting with activator molecules (Hofmann et al., 1997; Ashkenazi and Dixit, 1998). Initiator caspases (caspases-2, -8, -9, and -10) can cleave downstream effector caspases (caspase-3, -6, and -7) also known as “executioners” (Degterev et al., 2003).

Generally, there are two pathways through which the initiator caspase can be activated: one is the death signal-induced, death receptor-mediated pathway; the other is the stress-induced, mitochondria-mediated pathway (Jin and El-Deiry, 2005).

#### *Death receptor-mediated initiator caspase-activation pathway*

Cell death signals, such as Fas ligand (FasL) and tumor necrosis factor (TNF)-2, can be specifically recognized by their corresponding death receptors, such as Fas or TNF receptor (TNFR)-1, in the plasma membrane (reviewed in Schultz et al., 2003). Their binding will in turn activate the death receptors. Fas can bind to the Fas-associated death domain (FADD) or TNFR-associated death domains, TRADD, and causes FADD aggregation and the emergence of DEDs (Strasser et al., 2000; Hengartner, 2000; Ashkenazi and Dixit, 1998). These exposed DEDs interact with the DEDs in the prodomain of procaspase-8, which will induce the oligomerization of procaspase-8 localized on the cytosolic side of the plasma

membrane (Chinnaiyan et al., 1995; Schultz et al., 2003). Then a massive molecular complex known as the death-inducing signal complex (DISC) is formed (Kischkel et al., 1995; Peter et al., 1998). In DISC, two linear subunits of procaspase-8 compact to each other followed by procaspase-8 autoactivation to caspase-8 (reviewed in Walczak and Krammer, 2000). The activation of the downstream pathways of caspase-8 varies with different cell types. In some lymphoid cell lines, caspase-8 is vigorously activated and can directly activate the downstream effector caspases such as caspase-3 (Degterev et al., 2003). In most cells, caspase-8 activates the mitochondrion-mediated pathway by truncating Bid (a pro-apoptotic Bcl-2-family member), a kind of proapoptotic protein in the cytosol, into its active form, tBid (Budihardjo et al., 1999; Ho and Hawkins, 2005). tBid will trigger the activation of the mitochondria pathway: cytochrome c, apoptosis-inducing factor (AIF) and other molecules are released from mitochondria, and apoptosis will be induced (Wang et al., 2005; Arnoult et al., 2003;).

#### *Mitochondria-mediated initiator caspase-activation pathway*

Anti-apoptotic Bcl-2 (B-cell lymphoma) homology domain (BH)-containing proteins such as Bcl-2 and Bcl-XL reside on the mitochondrial outer membrane while pro-apoptotic Bcl-2 family member, Bax, Bid, and Bad are in the cytosol (reviewed in Green and Kroemer, 2004). When cellular stresses such as DNA damage occurs, Bax, Bid, and Bad are translocated to the mitochondria, and subsequently these proapoptotic proteins will be activated (reviewed in Zimmermann et al., 2001). Their activation will in turn induce the opening of mitochondria permeability transition pores (MPTPs) and as a result, cytochrome

c localized in mitochondria will be released to the cytosol (Newmeyer et al., 2003; Green and Kroemer, 2004). With the presence of cytosolic dATP or ATP, apoptotic protease activation factor-1 (Apaf-1) oligomerizes (Li et al., 1997). Together with cytosolic procaspase-9, dATP and cytochrome c, oligomerized Apaf-1 can result in the formation of a massive complex known as apoptosome (Zou et al., 1997; Zou et al., 1999). The N-terminus of Apaf-1 and the prodomain of procaspase-9 both have CARDs, with complementary shapes and opposite charges (Rodriguez and Lazebnik, 1999). They interact with each other by CARDs and form a complex in the proportion of 1:1 (Arnoult et al., 2003). Activated caspase-9 can in turn activate effector caspase-3 and caspase-7 (Ho and Hawkins, 2005).

Once activated, apoptosis effector caspases such as caspase-3, -6, and -7, then cleave many substrates, such as structural components of the cytoskeleton and nucleus and signaling molecules, to promote apoptotic features. Membrane blebbing is most likely mediated through caspase cleavage of the cytoplasmic structural proteins gelsolin (Kothakota et al., 1997), actin (Mashima et al., 1995; Kayalar et al., 1996), and spectrin  $\alpha$ -fodrin (Cryns et al., 1996; Martin et al., 1995). Effector caspases also might enhance nuclear condensation through cleaving nuclear structural proteins lamin A (Lazebnik et al., 1994), lamin B (Kaufmann, 1989), and nuclear mitotic apparatus proteins (NuMA) (Hirata et al., 1998). DNase responsible for DNA fragmentation during apoptosis are also activated by caspase-mediated cleavage (Liu et al., 1997; Enari et al., 1998). Finally, many members of the signaling pathways are substrates of caspases, and they are believed to be activated or inhibited for the proper progression of apoptosis. For example, protein kinase c (PKC), p21-activated kinases (PAK2), mammalian

sterile twenty-like kinase (Mst1), focal adhesion kinase (FAK), NF-KB (nuclear factor KB), and others are all cleaved by caspases and some of these truncations have documented roles in apoptosis (Jin and El-Deiry, 2005). For instance, PAK2 is activated by caspase-mediated cleavage, then participates in remodeling the actin-cytoskeleton for apoptotic cell morphology (Rudel and Bokoch, 1997; Lee et al., 1997). Cleaving FAK will inactivate it and results in loss of organization of focal adhesions and hence early detachment of cells from the extracellular matrix (Wen et al., 1997; Levkau et al., 1998; Bannerman et al., 1998). In addition, the activation of Mst1 upon cleavage by caspase-3 will in turn phosphorylate histone H2B at S14 and mediates mammalian apoptotic features including chromatin condensation (Cheung et al., 2003).

#### *Caspase-independent apoptotic pathway*

Apoptosis can be mediated by a caspase-independent mechanism (reviewed in Kroemer and Martin, 2005). Early cell-death studies in *C. elegans* hinted that PCD could occur in the absence of caspases. Characterization of *C. elegans ced-3* mutants using light microscopy revealed that the migratory leader cell of the male gonad, the linker cell, underwent PCD even in the absence of *ced-3* (Ellis and Horvitz, 1986). Subsequent findings are consistent with the existence of *ced-3*-independent PCD; these include reports that, in the anterior pharynx, some cells die even in animals harboring a deletion of the entire protease-encoding domain of *ced-3* (Shaham et al., 1999). One hint to how a *ced-3*-independent pathway might promote PCD came from genetic studies. In a *ced-4* loss-of-function mutant of *C. elegans*, PCD is blocked, suggesting that CED-4, a caspase activator, is required for PCD (Ellis and Horvitz, 1986). Epistasis experiments

placed *ced-4* activity upstream of *ced-3* (Shaham and H.R. Horvitz, 1996). When CED-4 is overexpressed in the ALM neurons of *C. elegans*, it is able to kill these cells (Shaham and H.R. Horvitz, 1996). Surprisingly, killing is reduced but not completely blocked in a *ced-3* mutant background (Shaham and H.R. Horvitz, 1996). This result suggests that *ced-4* can kill cells independently of *ced-3*.

In mammals, there is also evidence for caspase-independent PCD (reviewed in Kroemer and Martin, 2005). Genetic studies on PCD induced by 3-domain-only proteins, such as tBID, BIM and BAD, showed that these proteins, which have been shown to promote caspase activation and apoptosis, can also kill cells independently of *Apaf-1* and downstream caspases (Mills et al., 2006; Villunger et al., 2004; Cheng et al., 2001). Specifically, *Apaf-1*<sup>-/-</sup> mouse embryonic fibroblasts (MEFs) could still die in response to the overexpression of BH3-domain-only proteins (Cheng *et al.*, 2001). The cell death was reported as apoptotic, because dying cells displayed apoptotic features including DNA fragmentation, chromatin condensation, and externalization of phosphatidylserine (Cheng *et al.*, 2001). However, caspase activation was not detected in the dying cells when assayed with fluorogenic substrates for caspase-2, -3, -6 or -7, nor could cell death be blocked by the pan-caspase inhibitor zVAD.fmk (Cheng *et al.*, 2001), suggesting a caspase-independent cell death.

### ***Apoptotic chromatin condensation***

Internucleosomal chromatin fragmentation is a biochemical hallmark of apoptosis (Jin and El-Deiry, 2005). Apoptotic chromatin condensation has been attributed to caspase-6 mediated cleavage of nuclear structural proteins such as A- and B-type lamins (Rao et al., 1996; Neamati et al., 1995; Orth et al., 1996;

Lazebnik et al., 1995). Lamins are the most abundant peripheral proteins of the nuclear envelope and are attached to the inner nuclear membranes (reviewed in Buendia et al., 2001). During apoptosis, lamins are cleaved at the conserved aspartic residue in a hinge region and this cleavage generates a carboxy-terminal proteolytic fragment of 46 kDa, disrupting the interior structure of the nucleus (Takahashi et al., 1996; Orth et al., 1996).

Besides lamin, Acinus was identified as a nuclear factor that induces apoptotic chromatin condensation after cleavage by caspases (Sahara *et al*, 1999). Acinus is predominantly located in the nucleus and expressed in three different isoforms, termed Acinus-L, Acinus-S and Acinus-S'. They contain 1341, 583 and 568 amino-acid residues, respectively, with apparent molecular weights at 220, 98 and 94 kDa. Acinus is cleaved by caspases on both its N- and C-termini, producing a p17 active form (amino acid residues 987–1093), which triggers chromatin condensation in the absence of caspase-3. Full-length acinus-S is unable to condense chromatin, suggesting that caspase-mediated cleavage is necessary for this activity. Acinus undergoes several proteolytic cleavages during apoptosis, and p17 is one of the active forms to induce chromatin condensation. Although its function is still unclear, Acinus is a direct target of Akt, a serine/threonine kinase which promotes cell survival by phosphorylation and inhibiting components of the intrinsic cell death machinery. The phosphorylation of Acinus by Akt prevents its proteolytic cleavage mediated by caspase-3 and inhibits apoptotic chromatin condensation and apoptosis (Hu et al., 2005). Therefore, these results suggest that the regulation of apoptotic chromatin condensation is crucial for apoptosis.



### *Yeast apoptosis*

Often regarded as a phenomenon confined to multicellular organisms, an apoptotic-like phenotype, characterized by DNA fragmentation and modest chromatin changes, has been demonstrated in *S. cerevisiae* (Ludovico et al., 2001; Madeo et al., 1999; Severin and Hyman, 2002). When the complete genome sequence of yeast became available in 1997, no relative of the most central players in apoptosis (e.g. the caspases, members of the Bcl-2/Bax family or Apaf-1) were found, supporting the idea of a purely metazoan apoptosis (reviewed in Madeo et al., 2002a). However, several early studies determined that expression of pro-apoptotic proteins in yeast can cause cell death. These included human Bax and Bak and the related *C. elegans* protein, Ced4/Apaf-1 (Greenhalf et al., 1996; Ligr et al., 1998; James et al., 1997). In addition to these proteins, expression of both mammalian caspases-1 and -3 in fission yeast also can lead to cell death (Kang et al., 1999; Ryser et al., 1999). Both caspases are processed normally, are fully active when expressed in fission yeast, and are capable of cleaving co-expressed anti-apoptotic Bcl-2 at predicted sites for caspase cleavage (Kang et al., 1999; Ryser et al., 1999). Therefore, these results suggest that despite the failure to detect apoptotic components, a single-celled organism such as yeast might contain an endogenous cell death program that is in part homologous to the metazoan apoptotic machinery.

Now, it is clear that budding yeast can undergo apoptosis independently of the expression of mammalian pro-apoptotic proteins (reviewed in Frohlich and Madeo, 2000). The first clear evidence was obtained in studies of a yeast strain harboring a point mutation in the *CDC48* gene, *cdc48*<sup>S565G</sup> (Madeo et al., 1997), which encodes a protein required for vesicle trafficking (Latterich et al.,

1995). This mutant displayed a rapid loss in cell viability following a shift to the restrictive temperature, which was accompanied by the appearance of many of the same apoptotic markers found in mammalian cells (Madeo et al., 1997). Granot and colleagues showed that Bax-triggered apoptosis in yeast could be blocked by enhancing vesicle trafficking (Levine et al., 2001). Moreover, a downregulation of vesicular transport enhances the susceptibility of yeast cells to apoptosis (Madeo et al., 1997), providing an explanation for the *cdc48*<sup>S565G</sup>-mediated apoptosis. Interestingly, the human CDC48 orthologue VCP/p97 plays a role in mammalian apoptosis. Indeed, a mutated form of VCP, in a manner similar to the *cdc48*<sup>S565G</sup> mutation in yeast, dominantly induce apoptosis in B-cells (Shirogane et al., 1999; Wu et al., 1999). Cdc48/VCP was also shown to act as a cell-death effector molecule in the brain, suggesting that its concentration is critical for neurodegeneration (Higashiyama et al., 2002).

Cell death with apoptosis-like features has also been reported in yeast after treatment with acetic acid, UV-irradiation, and mating pheromone (Ludovico et al., 2001; Del Carratore et al., 2002; Severin and Hyman, 2002). Apoptosis was also observed in yeast exposed to low doses of H<sub>2</sub>O<sub>2</sub>, or accumulation of ROS by depletion of glutathione in wild-type yeast cells, indicating that as in metazoans, ROS are key regulators of yeast apoptosis (Madeo et al., 1999). Furthermore, addition of free radical scavengers to yeast cultures prior to inducing apoptosis led to a significant reduction in lethality, as did incubation in an anaerobic environment (Madeo et al., 1999), suggesting that ROS contribute to signaling in pathways leading to PCD. As discussed earlier, the production and accumulation of ROS are formed as a by-product of mitochondrial activity during mammalian apoptosis (Fleury et al., 2002) and

induces cytochrome c release and apoptosis (Shimizu et al., 2001). Since cytochrome c release occurs during yeast apoptosis induced by Bax, acetic acid, mating pheromone and  $H_2O_2$ , the accumulation of ROS in yeast may play a similar role as in mammals.

The conservation of yeast and mammalian apoptosis was further confirmed with the recent discovery of a caspase-related protease, Yca1, and its role in yeast apoptosis (Madeo et al., 2002b). Yca1 is processed in a caspase-typical manner and has proteolytic activity for caspase substrates (Madeo et al., 2002b). Overexpression of Yca1 in synergy with oxidative stress efficiently triggers yeast cell death, accompanied by markers of apoptosis (Madeo et al., 2002b). Conversely, Yca1 disruption increases tolerance against  $H_2O_2$ . Yca1 belongs to the family of metacaspases, which encompass members in fungi, plants and protists (Uren et al., 2000). Currently, the yeast metacaspase substrates are unknown. Recently, an AIF orthologue, Aif1, was identified in yeast (Wissing et al., 2004). Similar to mammalian AIF, yeast Aif1 is located in mitochondria and translocates to the nucleus of yeast cells in response to apoptotic stimuli such as  $H_2O_2$  (Wissing et al., 2004). While overexpression of Aif1 strongly stimulates apoptotic cell death induced by  $H_2O_2$ , this effect is attenuated by disruption of Aif1 along with the yeast caspase Yca1, suggesting that Aif1 is a caspase dependent cell death effector (Wissing et al., 2004). Together, these results suggest the common evolutionary origin of yeast and mammalian apoptosis.

Yeast can also stimulate apoptosis in a caspase-independent mechanism (Severin and Hyman et al., 2002). It was shown that treatment with pheromone at high concentrations is toxic to yeast cells and these dying cells displayed

apoptotic phenotypes including accumulation of ROS (Severin and Hyman et al., 2002). Interestingly, deletion of Ste20 kinase, the key component of the MAP kinase pathway, prevents pheromone-induced cell death and concomitantly prevents the formation of ROS. Given that Ste20 kinase is the homologue of Mst1 kinase that plays a role in mammalian apoptosis (Cheung et al., 2003), this study further reinforces the concept of a conservation of apoptotic machinery between yeast and mammalian cells.

Why would a single cell organism undergo programmed cell death? One reason for a unicellular organism to commit altruistic suicide may be to benefit the cell community (Severin and Hyman, 2002). Such a mechanism would improve the genetic fund of the community by eliminating the weak individuals. Yeast shows these aspects of communal behavior when they are damaged or infected with virus, or during mating. Damaged cells can compromise the viability of other members of the community by, for example, consuming scarce nutrients or spreading an infection. Moreover, yeast cells that were unable to mate after prolonged exposure to the opposite mating type might also be a detriment to the yeast community (Severin and Hyman, 2002). Therefore, a cellular suicide program that eliminates these cells would help to ensure the viability and reproductive success of healthier members of the community.

### *Histone modification in apoptosis*

Given the intimate connection between histones and DNA, the changes in DNA during apoptosis may be mediated by histone modifications. For example, the ubiquitination of H2A, which is associated with transcription, is decreased during apoptosis and this can be due to a decrease in transcription (Marushige

and Marushige, 1995; Mimnaugh et al., 1997; Mimnaugh et al., 2001; Jason et al., 2001; Jason et al., 2002). In addition, phosphorylation of a minor histone variant H2A.X at Ser139 has been shown to increase during DNA double-stranded breaks and DNA fragmentation in apoptosis (Rogakou et al., 1998; Rogaukou et al., 2000). However, H2A.X phosphorylation correlates with all double-stranded DNA breaks rather than with apoptotic chromatin condensation and apoptotic-specific oligonucleosomal DNA fragmentation (Cheung et al., 2003), suggesting it as a DNA damage marker rather than apoptotic marker. In mammalian cells, the only core histone modification that has been uniquely associated with apoptosis is histone H2B phosphorylation in the N-terminal tail as shown by *in vivo* labeling of apoptotic cells (Ajiro, 2000). In addition, a cell-free *Xenopus* chromatin condensation system shows that the H2B N-terminus, but not other histone tails, is essential for chromatin condensation (de la Barre et al., 2001). In 2003, Dr. Wang L. Cheung, a former graduate student, identified that H2B S14 phosphorylation closely associates with apoptosis in multicellular eukaryotes (Cheung et al., 2003). The onset of this phosphorylation event is mediated and dependent upon the cleavage of Mst1 by caspase-3 (Cheung et al., 2003). Although H2BS14ph has been correlated with apoptotic chromatin condensation, it is still unclear whether phosphorylation of H2B at S14 is required for apoptosis due to the lack of histone genetics in mammalian cells. Yeast, on the other hand, is one of the few organisms that provide a powerful combination of genetics and molecular tools to study biology. Because yeast can undergo mammalian-like apoptosis, yeast has been emerging as a model system to study the complex

nature of apoptosis. Therefore, I started my thesis by identifying and characterizing a histone modification mark that regulates chromatin condensation and/or alter chromatin structure during yeast apoptosis (Chapter 2).

## CHAPTER 2

# STERILE 20 KINASE PHOSPHORYLATES HISTONE H2B AT SERINE 10 DURING HYDROGEN PEROXIDE-INDUCED YEAST APOPTOSIS

### Introduction

Apoptosis is the most common form of cell death and plays a central role in development and cellular homeostasis in higher eukaryotes. In vertebrates, apoptosis has evolved as a mechanism to remove injured, infected or superfluous cells via a non-inflammatory pathway. As discussed in Chapter 1, apoptotic cell death is characterized by distinctive morphological and biochemical changes that include DNA laddering and chromatin condensation, typically late-stage events in the apoptotic pathway (reviewed in Kerr et al., 1978; Figure 8). Despite significant progress in identifying networks of upstream apoptotic regulators and effectors (reviewed in Kaufmann and Hengartner, 2001), the molecular details of downstream events, such as large-scale changes in chromatin structure, are largely unknown.

Often regarded as a phenomenon confined to multicellular organisms, mounting evidence suggests that some features of apoptosis may extend to unicellular organisms such as *Saccharomyces cerevisiae*. An apoptotic-like phenotype, characterized by DNA fragmentation and modest chromatin

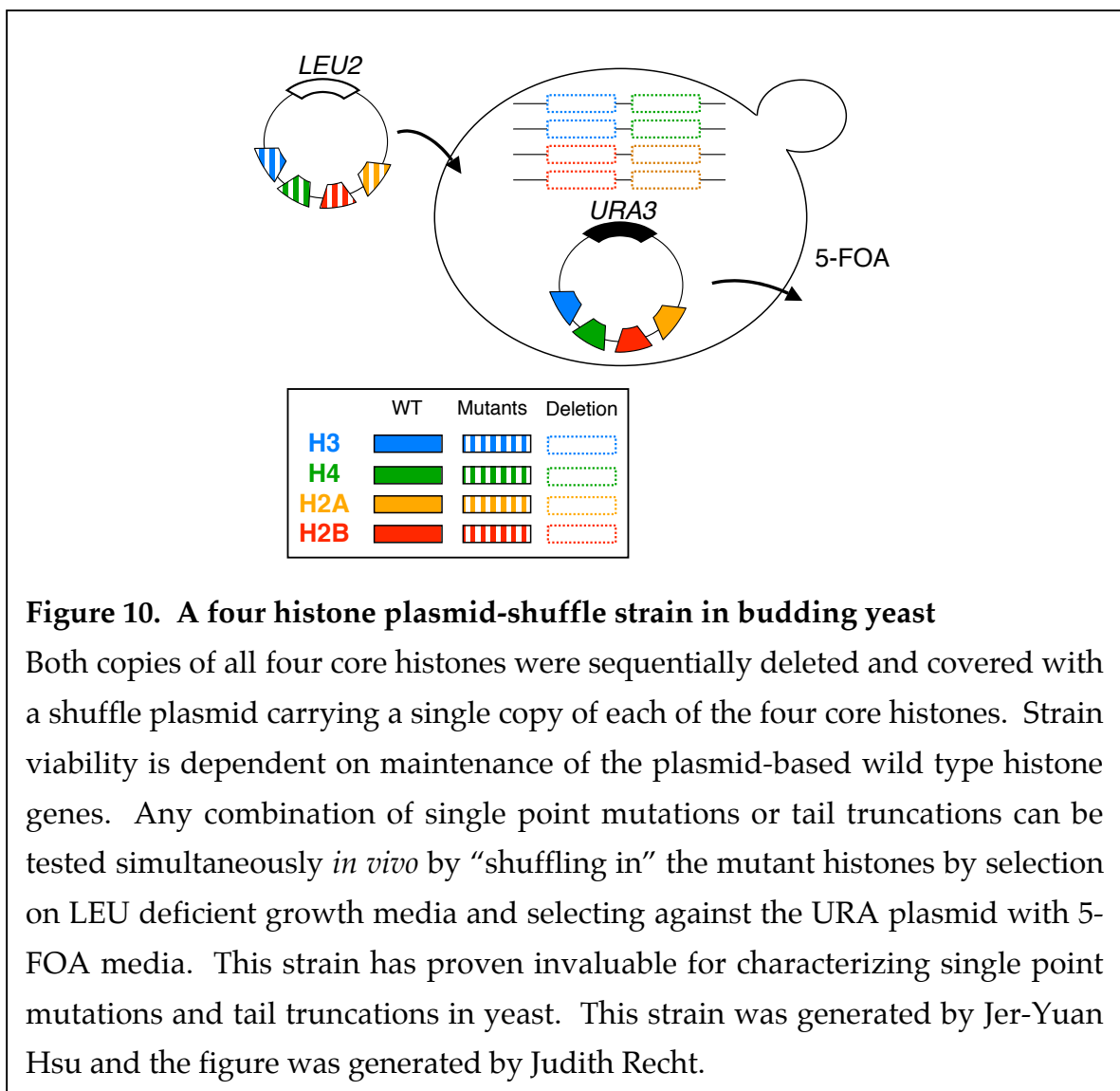
changes, has been demonstrated in *S. cerevisiae* when treated with various agents including acetic acid, osmotin, oxygen radical and pheromone (Ludovico et al., 2001; Madeo et al., 1999; Severin and Hyman, 2002). While not every identified mammalian gene involved in apoptosis has a clear counterpart in *S. cerevisiae*, a caspase-like protease of unknown function has been reported in *S. cerevisiae* (Madeo et al., 2002b).

In eukaryotic cells, DNA is organized into nucleosomes, the fundamental repeating unit of chromatin (Luger et al., 1997; Richmond and Davey, 2003). One well-studied mechanism for introducing variation into the chromatin polymer is the addition of post-translational histone modifications (e.g. acetylation, phosphorylation, methylation, etc.) whose importance in a wide range of DNA-templated processes is becoming clear (reviewed in Jenuwein and Allis, 2001; Felsenfeld and Groudine, 2003). To date, relatively few histone modifications have been firmly linked to apoptosis-induced chromatin changes. Phosphorylation of the histone variant H2A.X at S139 acts as a “DNA damage sensor” during the formation of DNA double-strand breaks (DSBs) induced by unnatural and natural means, including apoptosis (Rogakou et al., 2000). In *Xenopus*, chicken, and human cells, phosphorylation of H2B at S14 (H2BS14ph) by Mst1 kinase, the mammalian Sterile20-like kinase, is closely associated with apoptosis (Cheung et al., 2003) and radiation- induced damage foci (Fernandez-Capetillo et al., 2004a). However, the existence of this phosphorylation mark in invertebrates and unicellular eukaryotes has remained unclear, in part due to a lack of strict sequence conservation in H2B amino-terminal (N-terminal) tails. Thus, as is the case with mitotic (H3S10/H3S28) phosphorylation (Hsu et al.,



2000), no clear phenotypes, apoptotic or otherwise, have been linked to mutation of H2B (tail deletion or point mutation) or any other histone protein.

I initiated my thesis studies by surveying yeast cells (four histone plasmid-shuffle background; Figure 10) lacking specific histone N-terminal tails for loss of cell death upon H<sub>2</sub>O<sub>2</sub> treatment. In keeping with the H2B N-terminal tail's role in mammalian apoptosis, I found that a cell death property exists uniquely in the N-terminus of yeast H2B. Using both genetic and immunological



approaches, I have identified yeast H2B Serine 10 (H2BS10) as a yeast cell death phosphorylation mark. H2BS10A mutants are resistant to cell death elicited by H<sub>2</sub>O<sub>2</sub> while H2B S10E phospho-site mimics promote cell death and induce the “constitutive” formation of condensed chromatin. Finally, I identified Sterile 20 kinase (Ste20) as a bona fide yeast apoptotic H2BS10 kinase. Upon H<sub>2</sub>O<sub>2</sub> treatment, Ste20 kinase, a yeast homolog of mammalian Mst1 kinase, translocates into the nucleus in a caspase-independent fashion and directly phosphorylates H2B at S10.

## Results

### *Loss of the N-terminus of H2B, but no other histone N-terminal tails, abrogates hydrogen peroxide-induced cell death*

H2B phosphorylation and the H2B, but not other histones, N-terminal tails is essential for chromatin condensation in *Xenopus* cell-free systems (de la Barre et al., 2001). In addition, *in vivo* labeling studies showed that H2B phosphorylation occurs specially at the N-terminal tail during mammalian apoptosis (Aijiro et al., 2000). Because budding yeast may undergo apoptotic-like cell death (Madeo et al., 1999; Ludovico et al., 2001; Severin and Hyman, 2002), I sought to address whether the H2B N-terminus was involved. To this end, hydrogen peroxide (1 mM  $\text{H}_2\text{O}_2$ ) was added to wild-type (WT) yeast cells in a four histone plasmid-shuffle background that was generated by Dr. Jer-Yuan Hsu. In this strain, both copies of all four core histones were sequentially deleted and covered with a shuffle-plasmid carrying a single copy of each of the four core histones. By using a conventional plasmid-shuffle strategy, any combination of histone mutations can be tested *in vivo* (Figure 10). After a 200 minute incubation of  $\text{H}_2\text{O}_2$ , cell survival was assayed by plating assay (Madeo et al., 2002) and cell death was assayed by phloxin B (PB) staining which selectively stains only dead or dying yeast cells (Severin and Hyman, 2002). Consistent with previous findings (Madeo et al., 1999), a cell death phenotype was observed in WT cells after  $\text{H}_2\text{O}_2$  treatment. WT cells displayed 25-30% cell viability and 70-75% PB stained cells (Figure 11). These findings were not a result of cell necrosis, since protoplasts from cultures treated with  $\text{H}_2\text{O}_2$  maintained intact plasma membranes as illustrated by low yield of propidium iodide staining cells

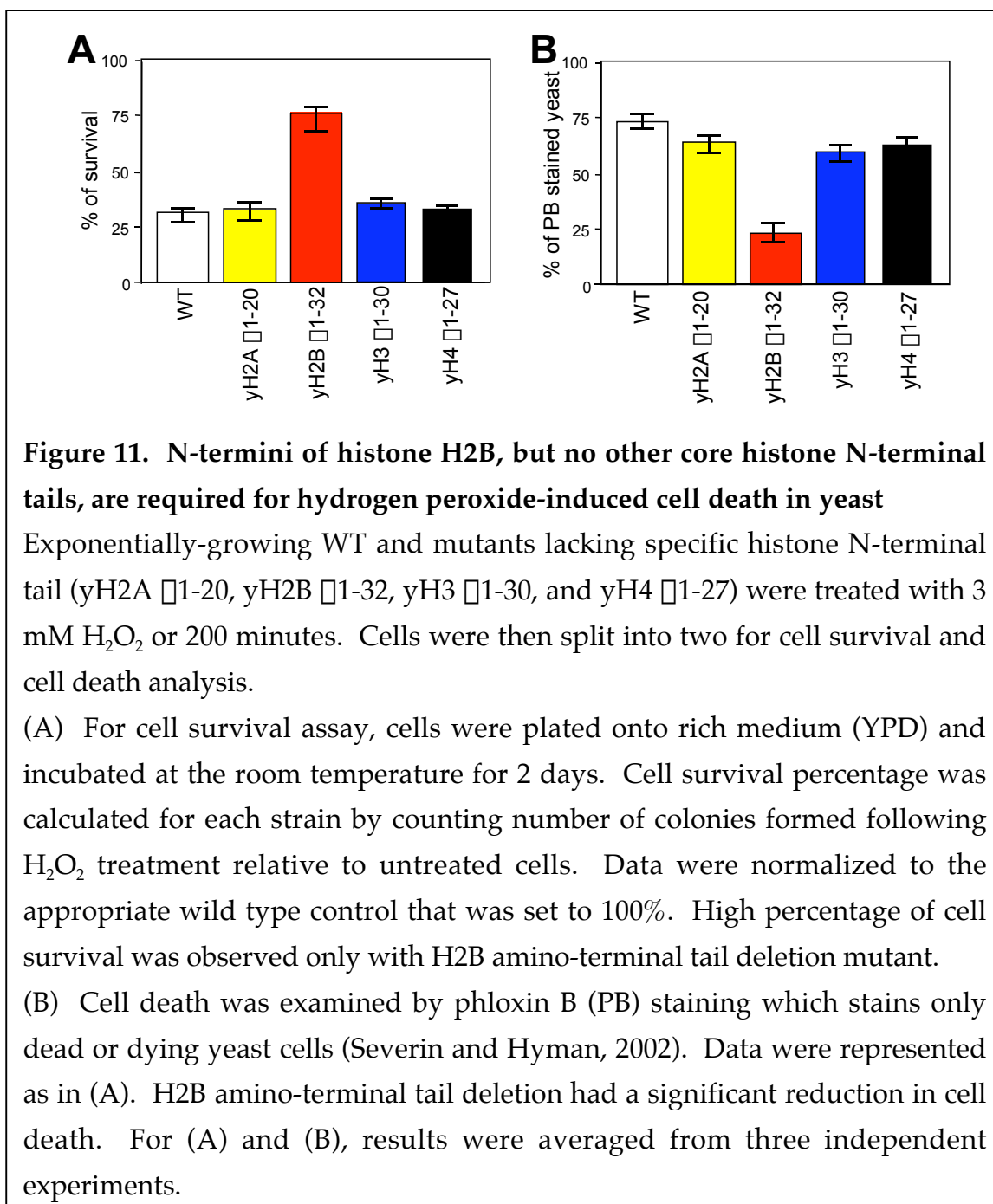
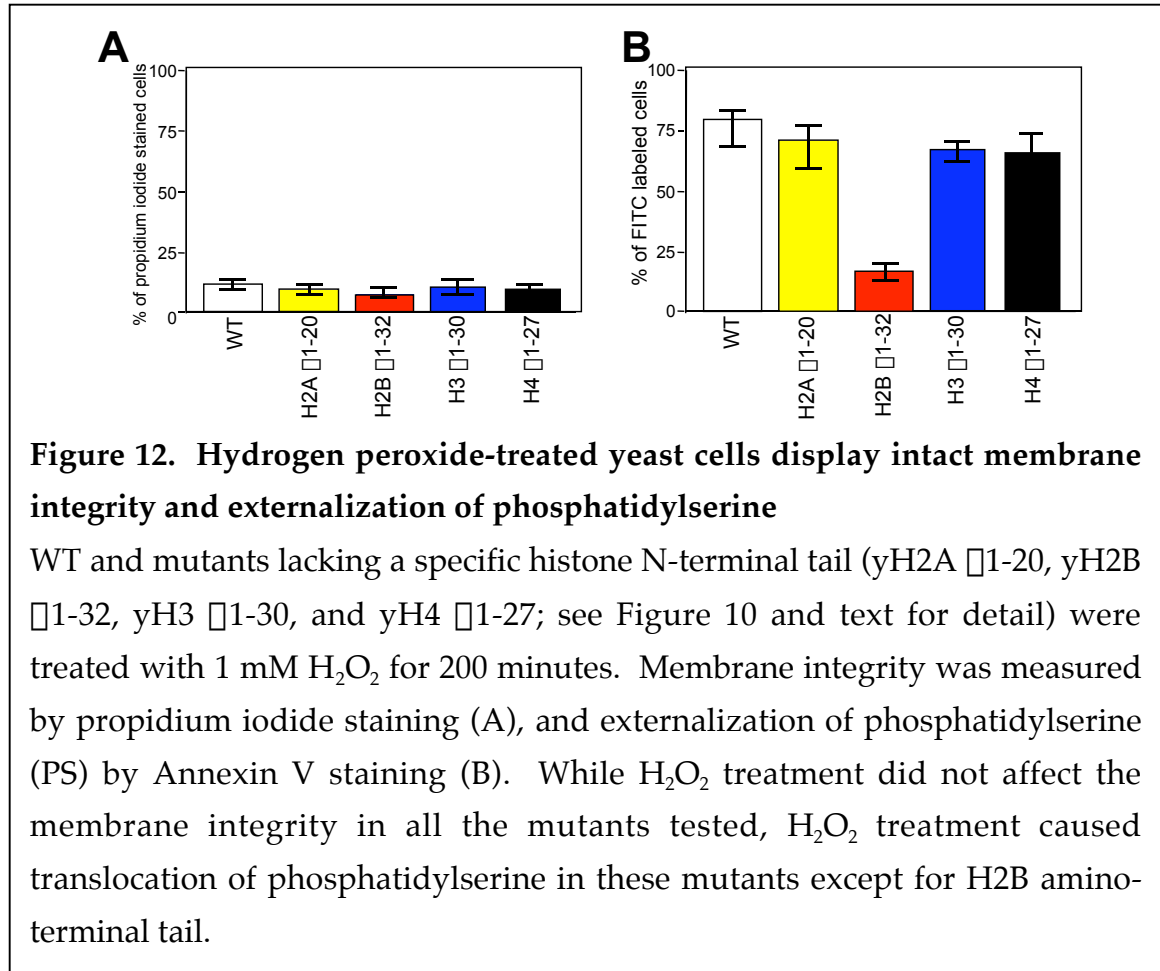


(Figure 12A). Furthermore, WT cells were stained with Annexin V, which detects the translocation of phosphatidylserine (PS) from the inner to the outer leaflet of membrane, an early event of apoptosis. About 80% of cells stained with Annexin V (Figure 12B), confirming that H<sub>2</sub>O<sub>2</sub> induces an apoptotic phenotype in yeast.

Competent with WT result,  $H_2O_2$  was added to isogenic yeast cells expressing separate N-terminal truncations of each of the four core histones, which include yH2A  $\Delta$ 1-20, yH2B  $\Delta$ 1-32, yH3  $\Delta$ 1-30, and yH4  $\Delta$ 1-27, all in identical histone-shuffle backgrounds that were generated by Dr. Jer-Yuan Hsu.

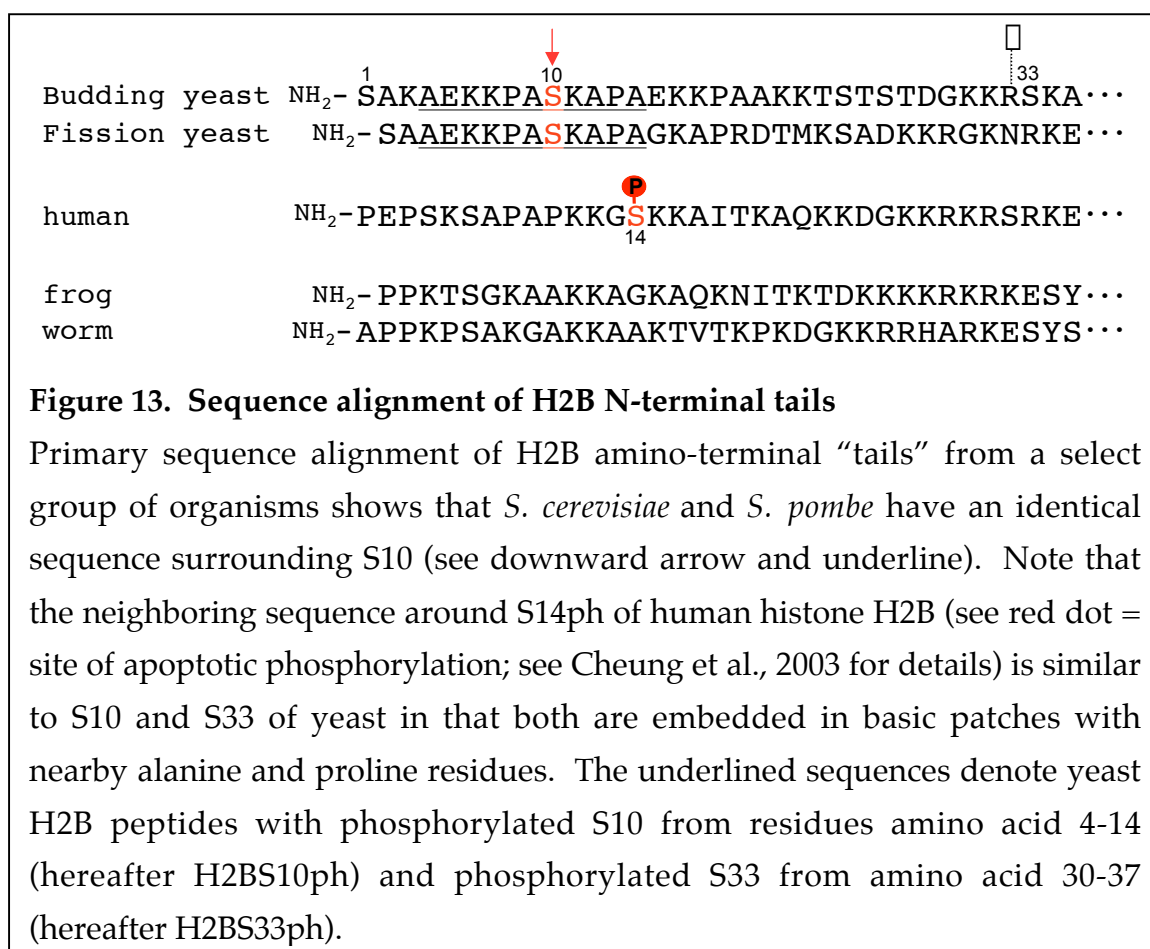


Interestingly, deletion of the N-terminus of H2B (yH2B  $\Delta$ 1-32) resulted in a reproducible resistance to  $H_2O_2$  (80-85% cell viability; 15-20% phloxin B stained cells; Figure 11A and 11B) with intact membrane integrity (Figure 12A). In addition, Annexin V staining was prevented to a larger extent in the H2B tail corresponding to the abrogation of cell death (Figure 12B). In contrast, levels of cell death similar to that of WT cells were observed with all other histone tail truncation mutants (yH2A  $\Delta$ 1-20, yH3  $\Delta$ 1-30, and yH4  $\Delta$ 1-27) (Figure 11 and 12).

These data suggested that a cell death property may exist uniquely in the N-terminus of yeast H2B. Given the similarities between this pathway and apoptosis, I will refer to the cell death as apoptosis.

### ***H2B S10A mutant abrogates hydrogen peroxide-induced yeast apoptosis***

Histone H2B is specifically phosphorylated at S14 in vertebrates undergoing programmed cell death (PCD; Cheung et al., 2003). Although H2B S14 and surrounding sequences are well conserved among vertebrates, they are not



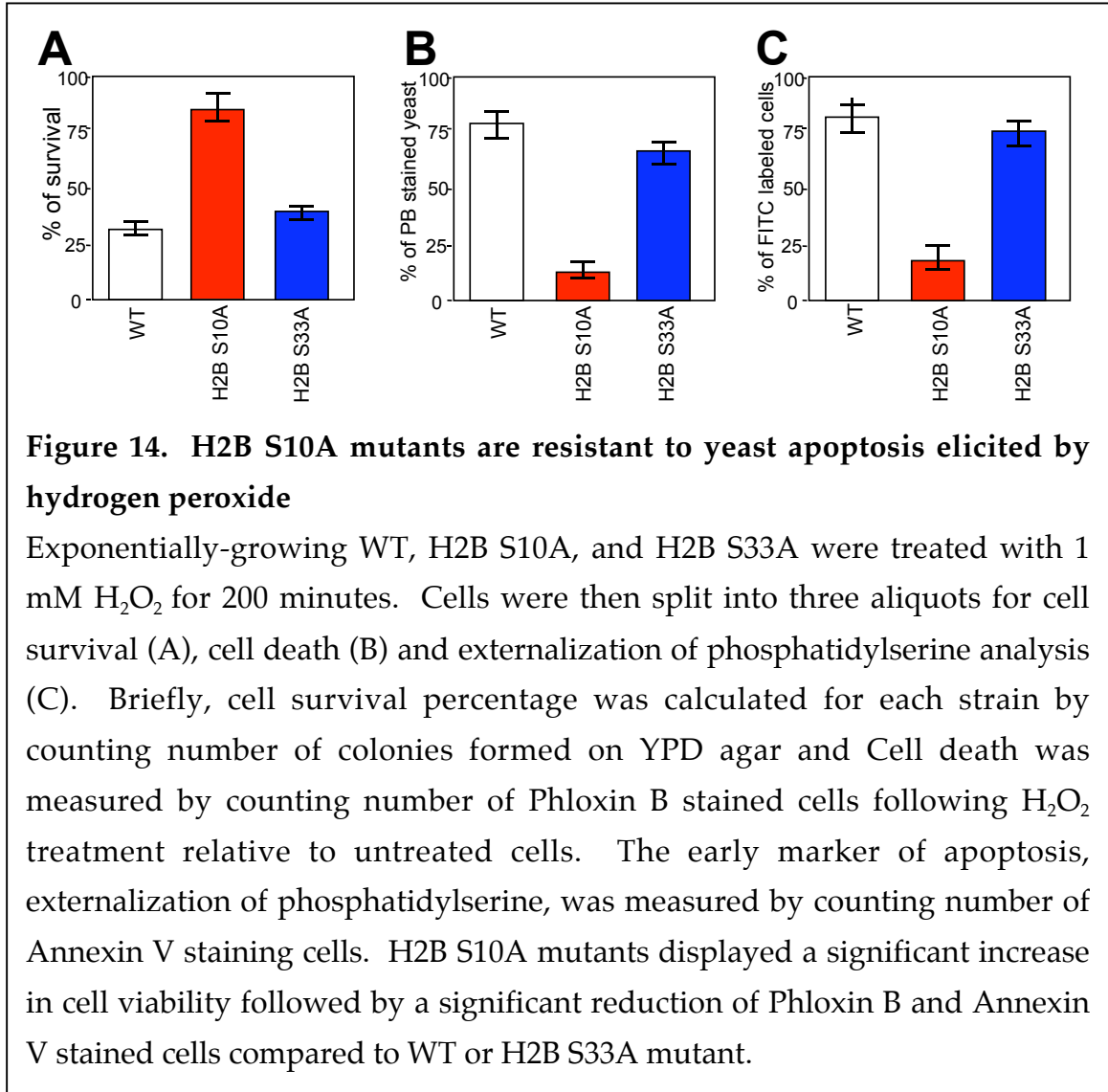
readily apparent in H2B tails of invertebrates and unicellular eukaryotes such as yeast (see red dot in Figure 13). Thus, it remained unclear whether any of the serine and/or threonine residues in the yeast H2B N-terminal tail could be

phosphorylated in an apoptosis-specific manner. As shown in Figure 13, numerous serine and threonine residues exist in the N-terminal tail of yeast histone H2B that could potentially serve as phosphate acceptor sites. Although serine 33 (S33) was embedded in a highly basic motif, similar to that of S14 in vertebrate H2B, S10 was surrounded in a basic motif that more closely resembled S14 in vertebrate H2B. This sequence, punctuated by conserved proline and alanine residues, was identical in *S. pombe* (see underline in Figure 13) suggestive of a conserved, but unknown, function for S10.

To analyze if S10 or S33 in yeast H2B serves a functional role in dying yeast, cells were generated expressing H2B in which S10, and S33 were separately mutated to alanine (S10A and S33A, respectively) into the four-histone plasmid-shuffle strain. While S33A H2B mutants were as sensitive to H<sub>2</sub>O<sub>2</sub>-treatment as WT cells, S10A H2B mutants were de-sensitized to H<sub>2</sub>O<sub>2</sub> treatment in much the same way as H2B tail truncation mutants (Figure 14). For example, H2B S10A mutants displayed high cell viability followed by low cell death judged by PB stained cells and low phosphatidylserine translocation by Annexin V (Figure 14). On the other hand, H2B S33A mutants conferred typical apoptotic phenotypes after treatment with H<sub>2</sub>O<sub>2</sub> (Figure 14). These results suggested the intriguing possibility that S10 in yeast H2B serves a comparable role to mammalian H2B at S14 by acting as a site of phosphorylation induced during H<sub>2</sub>O<sub>2</sub>-elicited apoptotic pathway.

### ***Histone H2B is specifically phosphorylated at serine 10 in dying yeast cells***

To directly test whether H2BS10 serves as a phosphorylation site during yeast apoptosis, a site-specific H2BS10 phospho-specific antibody (hereafter anti-



H2BS10ph) was generated. Peptides were synthesized at Baylor College of Medicine containing histone H2B residues 4-14 with unmodified or singly phosphorylated at S10 (hereafter H2BS10ph peptide; see underline in Figure 13 for the exact sequence). H2BS10ph peptide was then conjugated to carrier proteins and injected into rabbits by Covance (Denver, PA). Antisera from these rabbits were analyzed by enzyme-linked immunosorbent assay (ELISA) as described in Briggs et al., 2001. Anti- H2BS10ph immunoreacted strongly with the H2BS10ph peptide, but not the unmodified or H2BS33ph peptide (Figure 15).



While anti-H2BS10ph did not detect the H2B peptide that is singly acetylated at lysine 11 (H2BK11ac), but recognized peptide containing dual modifications of K11ac and S10ph of H2B, indicating that K11ac does not disrupt the epitope for anti-H2BS10ph (Figure 15). To further ensure that anti-H2BS10ph signal in the ELISA is specific, a competition was performed with unmodified and H2BS10ph peptide. As shown in Figure 15, only the H2BS10ph peptide was able to compete the anti-H2BS10ph signal away, suggesting that the antibody is specific to H2BS10ph peptide.

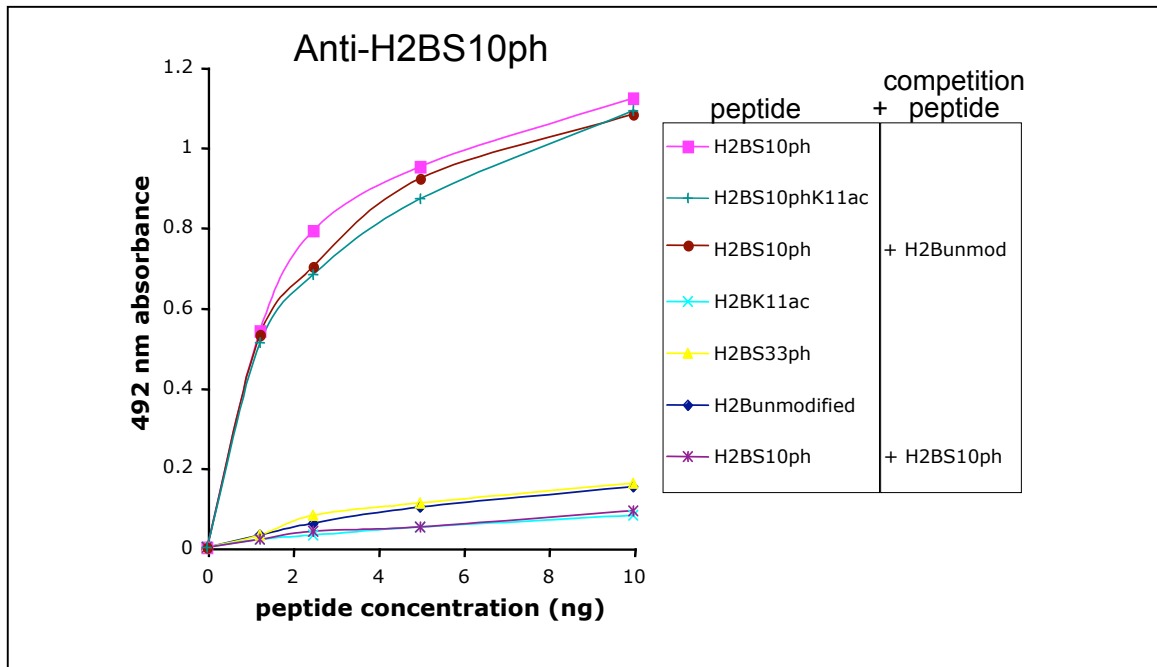


**Figure 15. ELISA of anti-H2BS10ph**

ELISA assay shows that this antiserum specifically recognizes the H2BS10ph peptide, but not H2BS33ph or H2BK11ac peptide. This antiserum also reacted with dually modified H2B peptide containing both S10ph and K11ac. Substrate specificity is supported by competition assays showing that only H2BS10ph peptide, and not the unmodified H2B peptide competes for binding of the antibody. Hereafter this antiserum will be referred to as anti-H2BS10ph.

With confidence in our new phospho-H2B antibody, I decided to test the hypothesis that yeast apoptotic H2B is phosphorylated at S10. Nuclei were prepared from logarithmically-growing cells treated with or without H<sub>2</sub>O<sub>2</sub> for 200 minutes and probed by immunoblotting using anti-H2BS10ph. As shown in Figure 16A, H2B from H<sub>2</sub>O<sub>2</sub>-treated WT cells reacted strongly with anti-H2BS10ph, suggesting that H2B is phosphorylated at S10 (H2BS10ph) upon H<sub>2</sub>O<sub>2</sub> treatment in yeast. As expected, anti-H2BS10ph antibody did not react with nuclei prepared from S10A mutant cells that were treated with H<sub>2</sub>O<sub>2</sub> (Figure 16A). To ensure equal loading, extracts were probed with H4 antibody generated against H4 residues from 1-20 amino acids (□-H4). In contrast, H2B from the S33A H2B mutant (H<sub>2</sub>O<sub>2</sub>-treated) displayed S10ph pattern similarly to WT (Figure 16A). To further confirm that anti-H2BS10ph is specific to histone H2B only, core histones were isolated by acid extraction followed by Western blotting analysis. H2BS10ph signal was detected from histone H2B isolated from H<sub>2</sub>O<sub>2</sub>-treated WT, and not H2B S10A mutants (Figure 16B). Ponceau staining ensured the equal loading of histone H2B, proving that lack of signal in H2B S10A mutant is not due to the absence of histone H2B. Reactivity with anti-H2BS10ph antibody was due to phosphorylation since treatment of the histone preparations with bacterial alkaline phosphatase (AP) resulted in a drastic loss of anti-H2BS10ph signal for both WT and S33A strains following H<sub>2</sub>O<sub>2</sub> treatment (Figure 16A). Thus, genetic and immunological approaches implicate phosphorylation of H2B at S10 in a cell death pathway brought about by H<sub>2</sub>O<sub>2</sub> treatment.

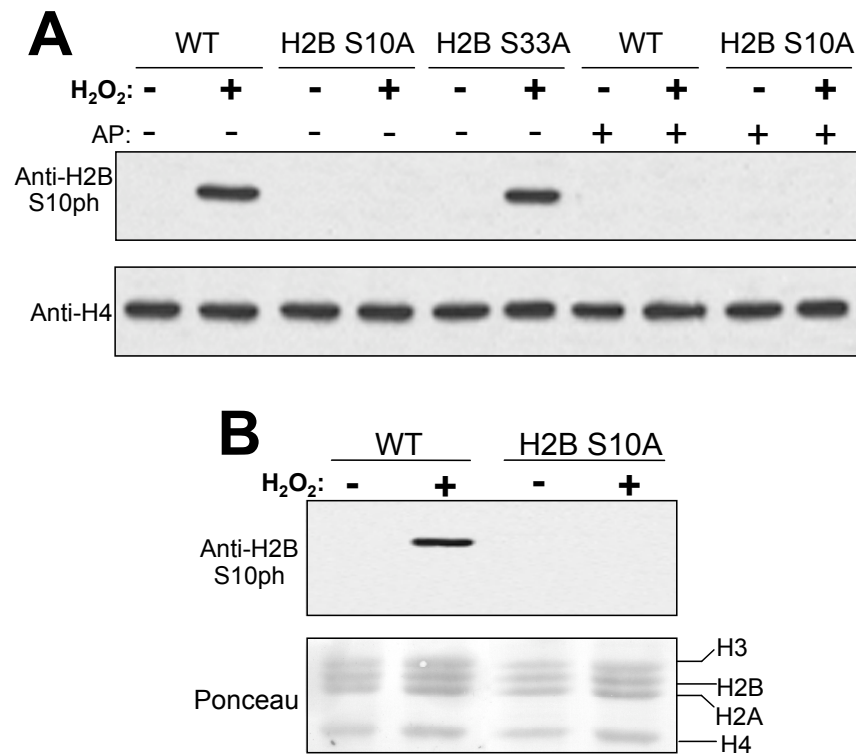


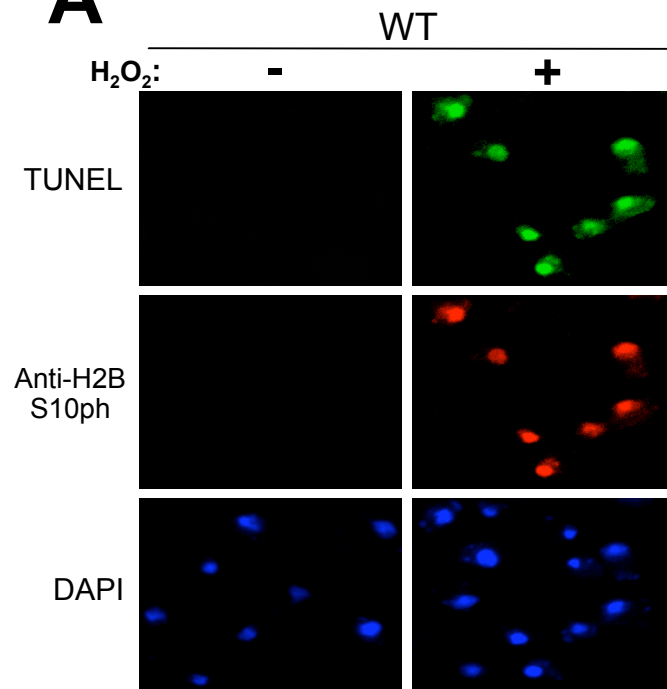
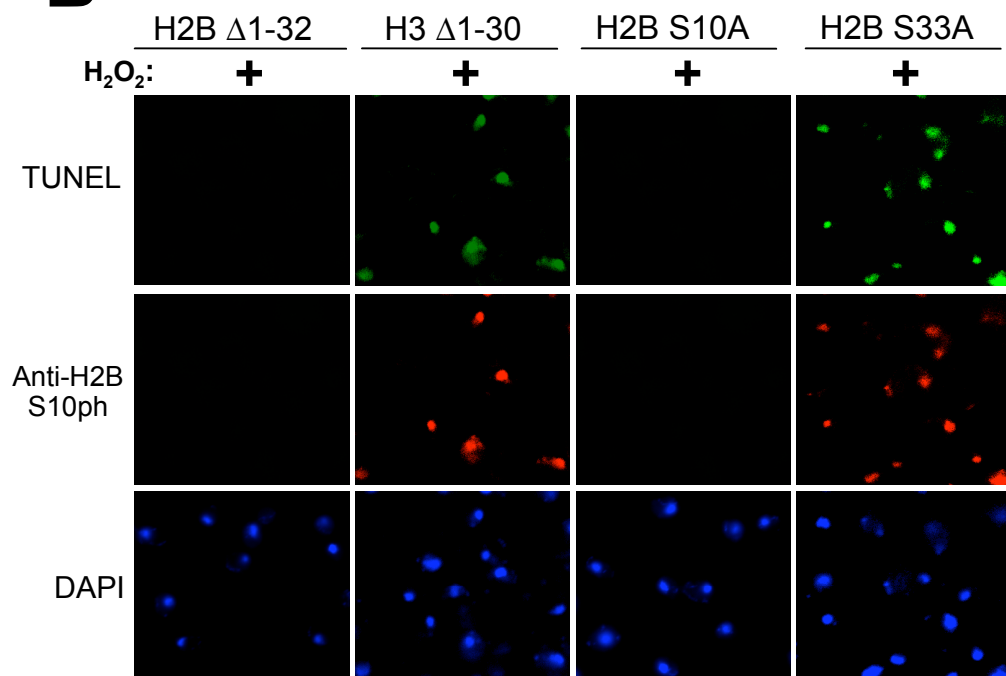
**Figure 16. Histone H2B is specifically phosphorylated at serine 10 in dying yeast cells**

(A) Total nuclear protein, isolated from cells treated with or without H<sub>2</sub>O<sub>2</sub>, was fractionated by SDS-PAGE before immunoblots were probed with anti-H2BS10ph antibody. Except for H2B, no other bands were detected with the anti-H2BS10ph from H<sub>2</sub>O<sub>2</sub>-treated WT or H2B S33A nuclear extracts. In contrast, anti-H2BS10ph antibody did not react with histones prepared from S10A mutant cells that were treated with H<sub>2</sub>O<sub>2</sub>. Where indicated, samples were treated with or without bacterial alkaline phosphatase (AP). Anti-H4 was used as a loading control.

(B) Histones were extracted from wild type and H2B S10A mutants treated with and without H<sub>2</sub>O<sub>2</sub> and analyzed by western blotting using anti-H2BS10ph and anti-H4. Equal loading was assessed by Ponceau staining. H2BS10ph signal was detected from histone H2B isolated from H<sub>2</sub>O<sub>2</sub> treated WT, and not H2B S10A mutants

**Figure 17. Antibodies to H2B serine 10 phosphorylation selectively stain TUNEL positive yeast apoptotic cells**

WT (A), or mutants lacking either H2B N-terminal tail (yH2B  $\Delta$ 1-32) and H3 N-terminal tail (yH3  $\Delta$ 1-30) (B), or H2B S10A, and S33A (B), treated with or without H<sub>2</sub>O<sub>2</sub>, were stained with TUNEL and anti-H2BS10ph. The same cells were counterstained with DAPI to detect nuclei. Note the excellent agreement of TUNEL and anti-H2BS10ph staining in all cells containing a H2B N-terminal tails or H2BS10.

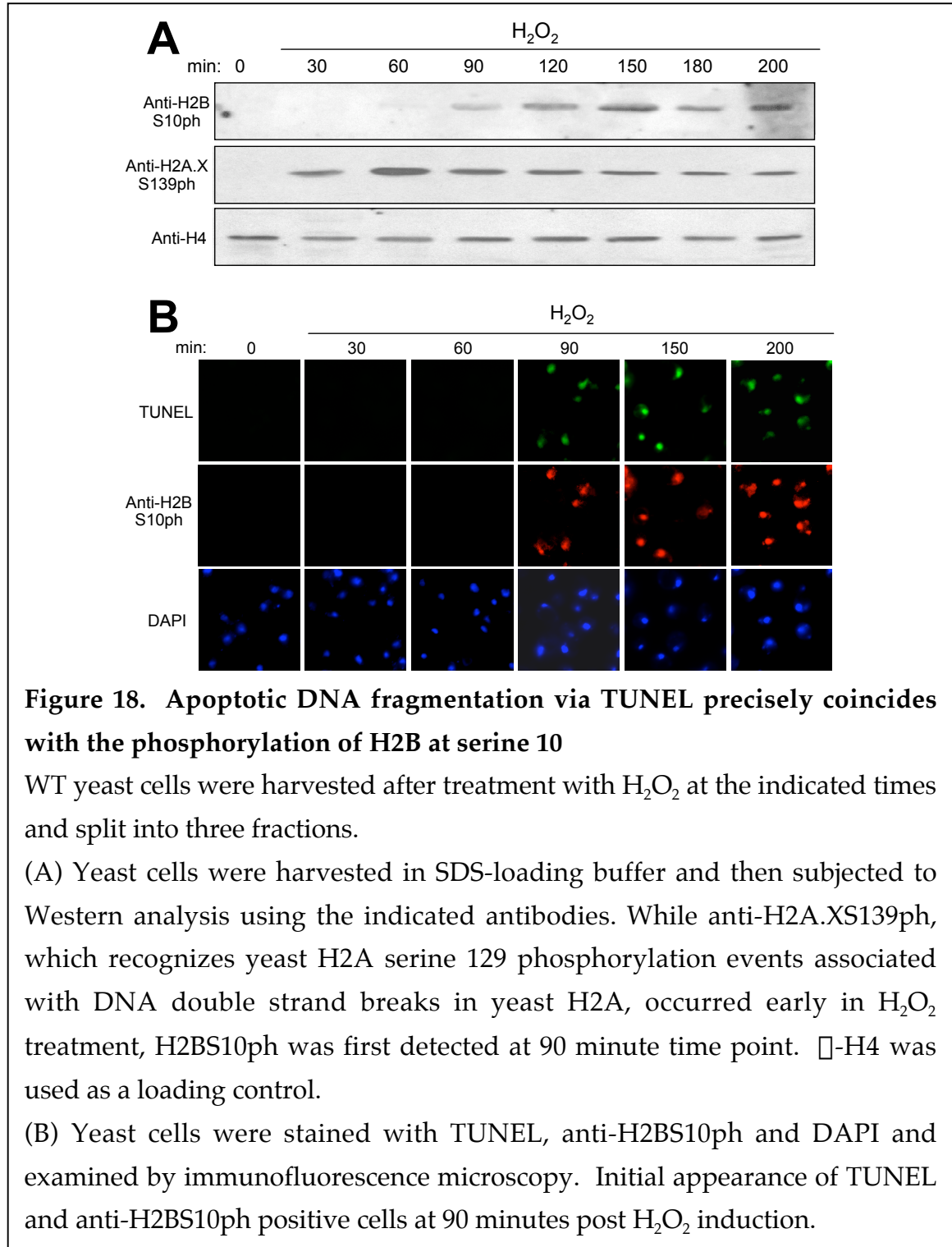
**A****B**

*Cells exhibiting phosphorylation of histone H2B at serine 10 display apoptotic DNA fragmentation*

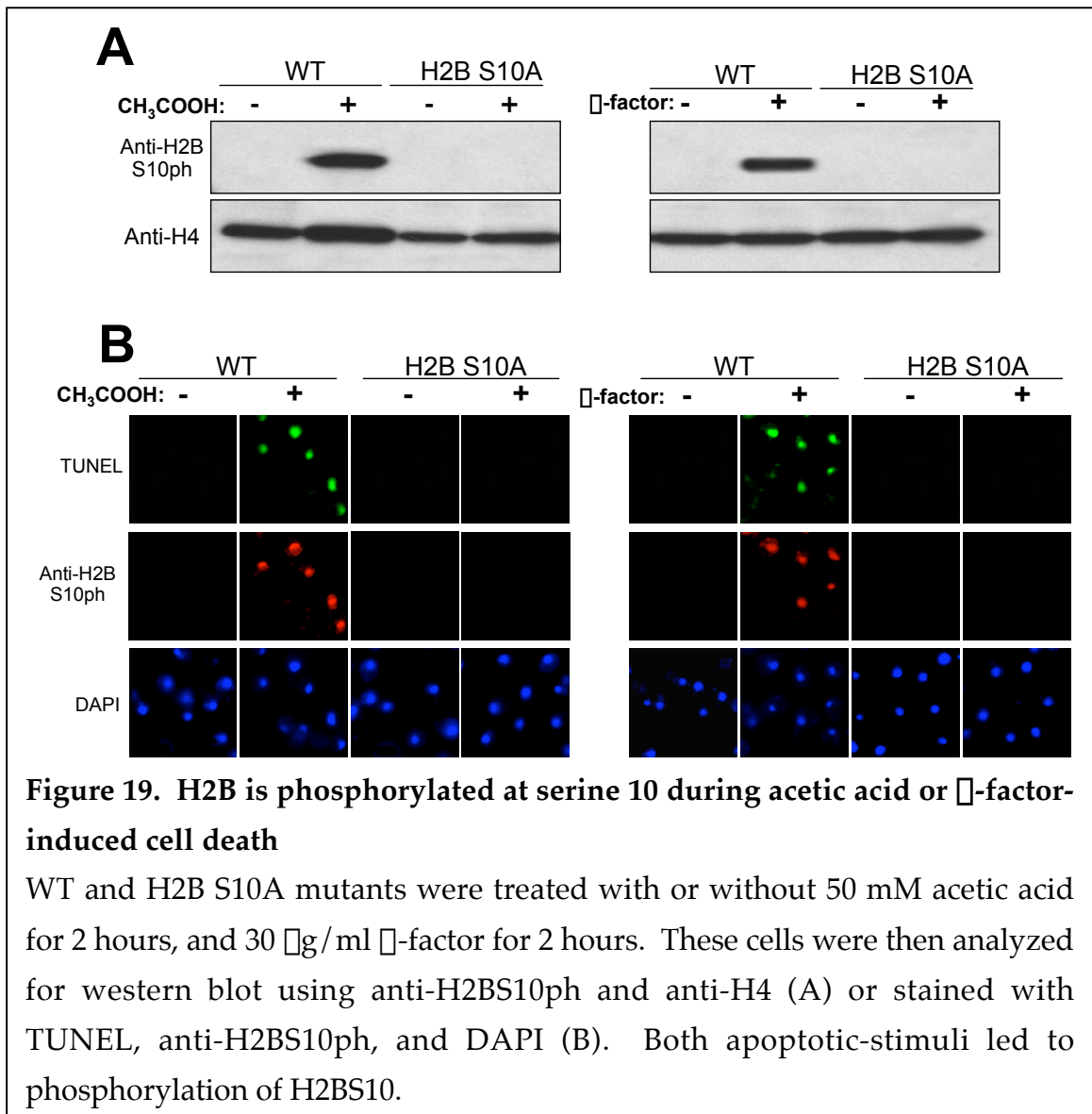
I wished to address whether phosphorylation of H2B at S10 has an analogous function to H2BS14ph during mammalian apoptosis. Yeast cells were double-stained with TUNEL and anti-H2BS10ph antibody and examined by immunofluorescence (IF) microscopy. In accordance with the loss of cell viability after treatment with H<sub>2</sub>O<sub>2</sub>, about 75-80% of WT cells showed TUNEL staining, a hallmark of apoptosis (Figure 17A). Strikingly, 100% of the TUNEL-positive cells were co-stained with the anti-H2BS10ph antibody demonstrating that apoptotic DNA fragmentation correlates precisely with H2B phosphorylation at S10 (Figure 17A). Similar positive staining patterns were observed with the S33A and the histone N-tail truncation mutants that included H3 (Figure 17B). However, in contrast, deletion of the N-terminus of H2B and the S10A mutants lacked these characteristic markers of apoptosis, even with H<sub>2</sub>O<sub>2</sub> treatment, further confirming that the H2B histone phosphorylation at S10 is required for apoptotic DNA fragmentation (Figure 17B).

The onset of mammalian H2BS14ph coincides with the appearance of apoptotic DNA fragmentation, suggesting that S14ph may play a role in establishing apoptotic DNA fragmentation (Cheung et al., 2003). Because of the similarities between yeast and mammalian apoptosis, I sought to determine the kinetics of apoptotic events and the onset of S10ph. For this purpose, WT cells induced to undergo apoptosis with H<sub>2</sub>O<sub>2</sub> were harvested at half-hour intervals for Western blot analyses using anti-H2BS10ph and anti-H2A.XS139ph, and IF. As discussed earlier, H2A.X phosphorylation at S139 has been correlated with DSBs (Rogakou et al., 1998; Rogakou et al., 2000) and occurs early in the

mammalian apoptosis after induction of etoposide such as VP16 (Cheung et al, 2003). Anti-H2A.XS139ph also recognizes serine 129 (S129) phosphorylation events associated with DSBs in yeast H2A (Figure 18A). Consistent with



mammalian H2BS14ph, yeast H2A phosphorylation preceded H2BS10ph, suggesting that DSBs occur early during the apoptotic pathway (Figure 18A). In addition, my time course analyses indicated that the onset of H2B phosphorylation coincides with the initial appearance of apoptotic DNA fragmentation evaluated by TUNEL staining (approximately 90 minutes post induction; Figure 18A and 18B). Taken together, these data suggest that H2B phosphorylation may play a role in establishing apoptotic DNA fragmentation and/or chromatin condensation, characteristic of late events in apoptosis.



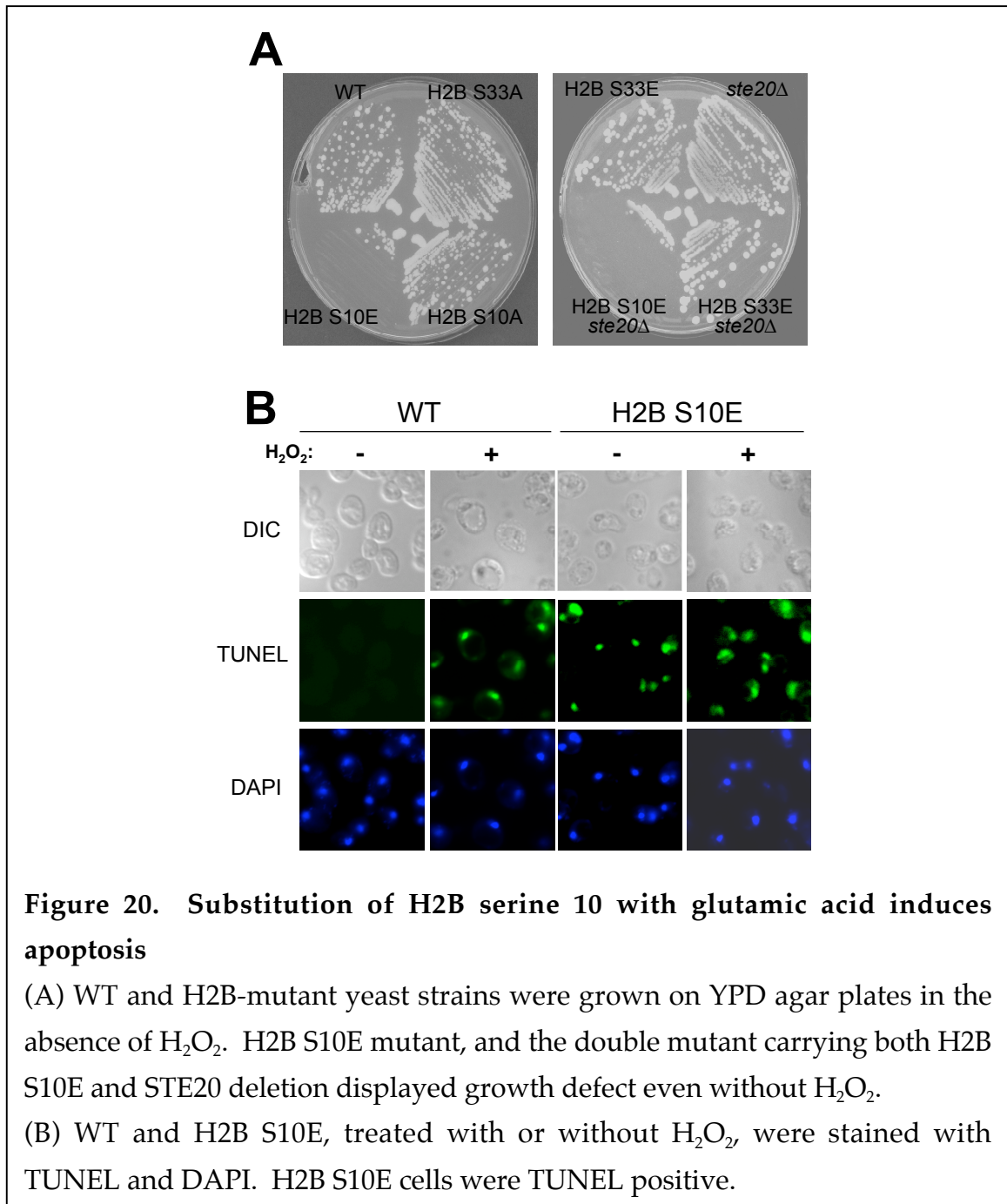


Next, I asked whether other yeast apoptotic stimuli could induce the enhancement of H2BS10ph. Nuclei were extracted from WT and H2B S10A that were treated with 50 mM acetic acid, or 30  $\mu$ g/ml  $\square$ -factor, chemicals reported by others to induce characteristics of cell death in mammalian cells (Ludovico et al., 2001; Severin and Hyman, 2002; Madeo et al., 1999). Similar to H<sub>2</sub>O<sub>2</sub> treatment, these apoptotic-stimuli led to H2BS10ph as demonstrated by immunoblotting analysis using anti-H2BS10ph . The phosphorylation band is H2BS10ph specific, since this band was absent in nuclear extracts from the H2B S10A mutant (Figure 19A). In addition, positive TUNEL staining was observed with WT cells treated with acetic acid or  $\square$ -factor, but not untreated cells or H2B S10A mutants (Figure 19B). This result demonstrates that this chromatin mark, H2BS10ph, is induced by a wide range of stimuli that bring about features of apoptotic cell death in yeast.

### *H2B S10E mutants induce apoptotic-like features including chromatin condensation*

To determine the role of H2BS10ph during H<sub>2</sub>O<sub>2</sub>-induced apoptosis, I separately mutated S10 and S33 to glutamic acid (S10E and S33E respectively) to mimic constitutive phosphorylation and to bypass the potential requirement for induced H2BS10 kinase activity. As shown in Figure 20A, the growth level of S10E mutations were drastically reduced on YPD agar plates, even in the absence of H<sub>2</sub>O<sub>2</sub>. Although few S10E H2B mutants grew under these conditions, surviving cells exhibited cell morphology similar to that of H<sub>2</sub>O<sub>2</sub>-treated WT cells (Figure 20B), indicating that the phosphorylation of this residue is important for

cell death. In addition, surviving S10E mutant cells were TUNEL-positive without  $H_2O_2$  treatment (Figure 20B). Upon the addition of  $H_2O_2$ , fewer S10E mutant colonies survived and these cells were also stained with TUNEL (Figure 20B). Together, these results suggest that S10E mutation induces apoptotic characteristics including DNA fragmentation.



Formation of condensed chromatin and fragmentation of DNA into oligonucleosomal lengths are hallmarks for apoptosis (Savill and Fadok, 2000). Thus, I asked whether H2BS10ph facilitates apoptotic chromatin condensation. With the help of Helen Shio from the Rockefeller University microscopy facility, the yeast nuclei of WT, H2B S10A and H2B S10E treated with or without H<sub>2</sub>O<sub>2</sub> were examined under electron microscopy. In agreement with published data (Madeo et al., 1999), WT cells incubated with H<sub>2</sub>O<sub>2</sub> revealed reproducible extensive chromatin condensation typical for apoptosis (Figure 21). No condensed chromatin was observed in S10A mutant with or without H<sub>2</sub>O<sub>2</sub>. In contrast, the S10E mutant displayed nuclei with striking patches of condensed chromatin (see arrows in Figure 21), even in the absence of H<sub>2</sub>O<sub>2</sub>. These data suggest that H2BS10ph and its phospho-mimic, S10E, correlate positively with “induced” and “constitutive” chromatin compaction *in vivo*. As far as I am aware, the H2B S10E point mutant is one of the more striking histone-tail mutations shown to promote large-scale chromatin compaction.

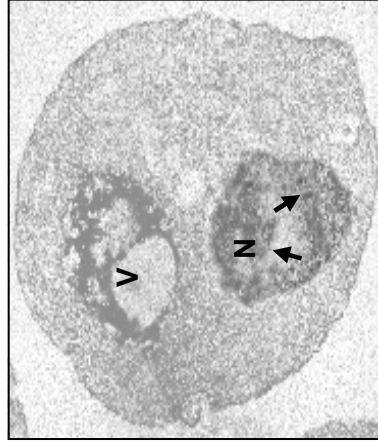
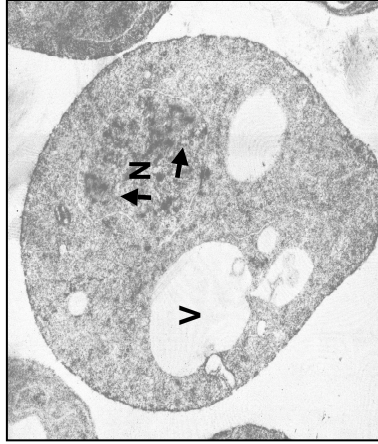
***Ste20 deletion mutants are resistant to hydrogen peroxide and abrogate H2B serine 10 phosphorylation***

During mammalian apoptosis, Mst1 kinase directly phosphorylates H2B at S14 both *in vivo* and *in vitro* (Cheung et al., 2003). Mst1 belongs to the PAK (p21-activated kinase) family, which also includes the yeast Ste20 kinase, and Mst1 and Ste20 kinase both share considerable sequence similarity throughout their catalytic domains (Creasy et al, 1996). Moreover, yeast containing a deletion of Ste20 kinase (*ste20 $\Delta$* ) was resistant to cell death elicited by pheromone treatment (Severin and Hyman, 2002). Thus, I sought to determine whether Ste20 kinase

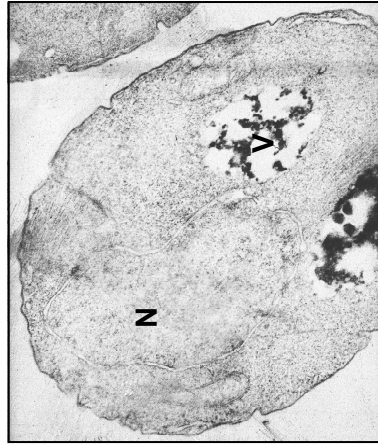
**Figure 21. H2B S10E mutant constitutively induces apoptotic chromatin condensation**

Exponentially grown WT, H2B S10A and H2B S10E that were untreated or treated with 1 mM H<sub>2</sub>O<sub>2</sub> were analyzed by electron microscopy. Arrows denote chromatin condensation. N denotes nucleus and V refers to the vacuole. Condensed chromatin was observed with H2B S10E. These images were taken by Helen Shio, from the microscopy facility at the Rockefeller University.

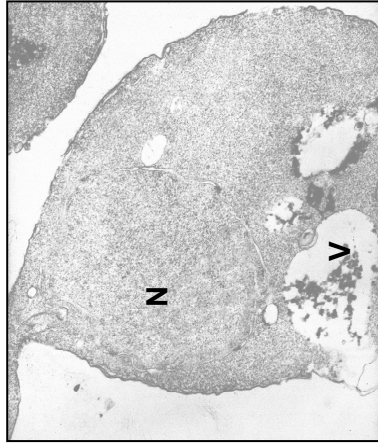
H2B S10E



H2B S10A



WT



$-H_2O_2$

$+H_2O_2$

function is necessary for yeast cell death *in vivo*. For this purpose, I generated a yeast strain containing a deletion mutation of Ste20 kinase in a four histone plasmid-shuffle strain background (*ste20*Δ) and tested for cell death upon H<sub>2</sub>O<sub>2</sub> induction. Similar to the survival pattern observed with the H2B S10A mutant cells, *ste20*Δ cells had a significant reduction of PB stained cells followed by a significant increase in cell viability as compared to its isogenic wild-type (Figure 22). In addition, *ste20*Δ cells lacked apoptotic DNA fragmentation evaluated by TUNEL staining (Figure 23A). Hence, these results demonstrate that Ste20 kinase is important for promoting cell death.

To determine whether the H<sub>2</sub>O<sub>2</sub>-induced cell death pathway includes both Ste20 kinase and H2BS10ph, I generated a double mutant carrying both H2B S10A and *STE20* deletion. After H<sub>2</sub>O<sub>2</sub> treatment, I observed no difference

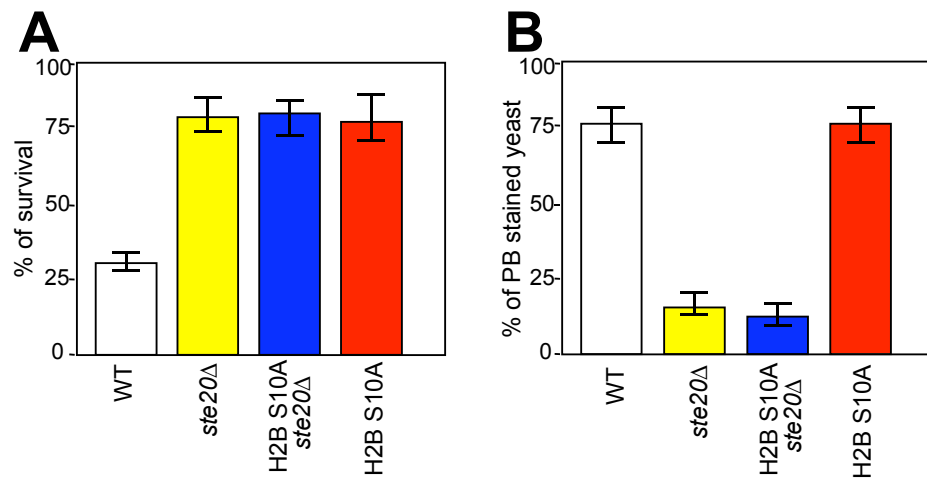


**Figure 22. Ste20 deletion mutants are resistant to hydrogen peroxide-induced yeast apoptosis**

H<sub>2</sub>O<sub>2</sub> was added to *ste20*Δ, H2B S10A and a double mutant carrying both H2B S10A and *ste20*Δ, and tested for cell survival (A), or cell death via Phloxin B staining (B) as described in Figure 11. Comparable cell survival pattern was observed with a single mutant or double mutant carrying *ste20*Δ and H2B S10A.

between a double mutant of H2B S10A and *ste20* $\Delta$ , as compared to each respective single mutant with regard to survival properties (Figure 22). All mutants conferred similar percentage of cell viability as well as cell death (Figure 22), suggesting that Ste20 kinase and H2BS10ph are in the same cell death pathway. Additionally, the double mutant carrying both S10E and *ste20* $\Delta$  conferred a growth level similar to S10E, whereas both single and double mutants carrying either S33E and/or *ste20* $\Delta$  survived as well as WT (Figure 20A). Taken together with the previous results reporting the importance of Ste20 during pheromone-elicited yeast death (Severin and Hyman, 2002), my *in vivo* results suggest that H<sub>2</sub>O<sub>2</sub> regulates a comparable cell death pathway to other yeast apoptotic stimuli via Ste20.

***Hydrogen peroxide-induced H2B serine 10 phosphorylation is mediated by Ste20 in vivo***

To investigate whether Ste20 could trigger the phosphorylation of H2B at S10 during conditions believed to induce yeast apoptosis, the level of H2BS10ph was assayed by immunoblotting. As shown in Figure 23B, no signal was detected by anti-H2BS10ph with H<sub>2</sub>O<sub>2</sub>-treated yeast lacking Ste20 (*ste20* $\Delta$ ) or double mutant carrying both H2B S10A and *ste20* $\Delta$ , suggesting that Ste20 may facilitate the phosphorylation of H2BS10. Ste20 has a specific kinase activity towards H2B at S10, since it does not phosphorylate H3 at S10 (Figure 23B). In addition, Ipl1, a kinase that phosphorylates both H2B and H3 *in vitro* (Hsu et al., 2000), fails to phosphorylate H2BS10 (Figure 23B).



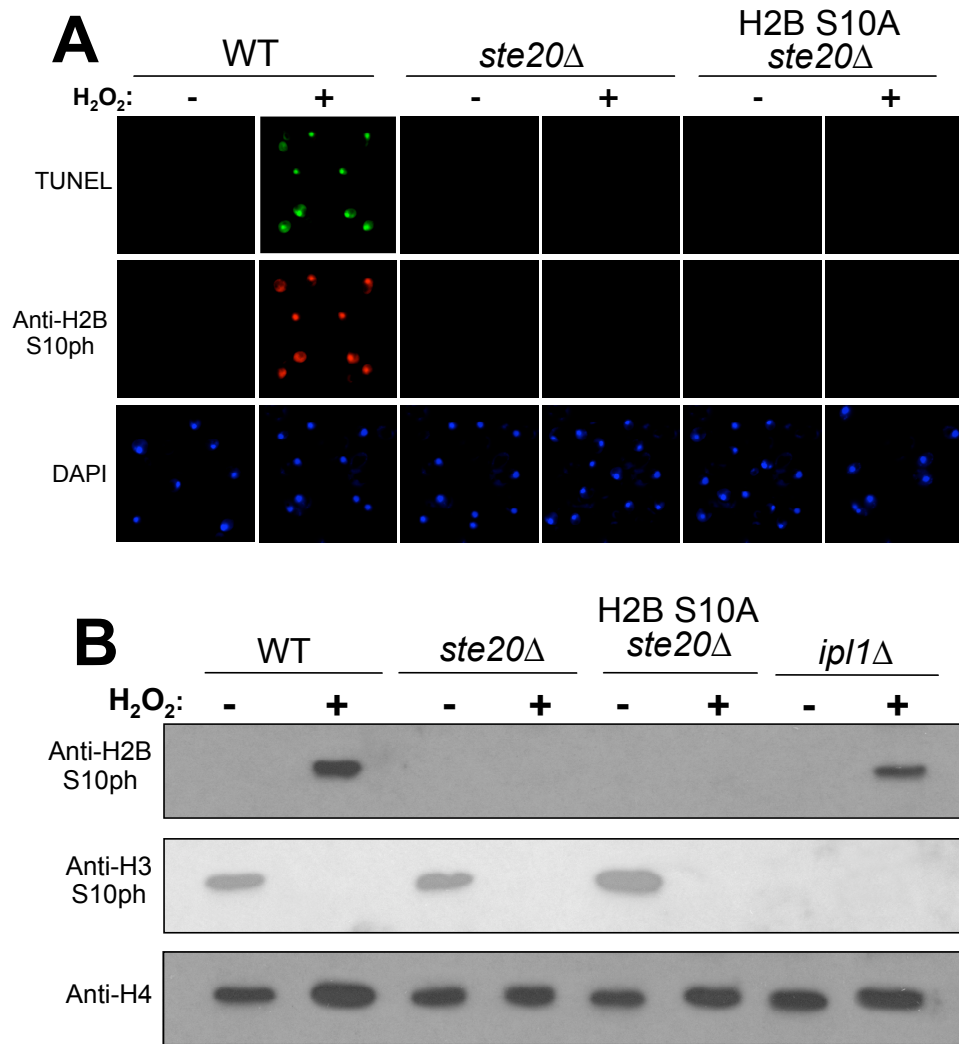


**Figure 23. Ste20 mediates hydrogen peroxide-induced H2B serine 10 phosphorylation *in vivo***

Log phased yeast cells from WT, *ste20Δ*, H2B S10A, and double mutant carrying both H2B S10A and *ste20Δ* were treated with 1 mM H<sub>2</sub>O<sub>2</sub> for 200 min.

(A) Half of the cells were stained with TUNEL, anti-H2BS10ph, and DAPI. No TUNEL or anti-H2BS10ph positive cells were observed with *ste20Δ* or H2B S10A or double mutants carrying both.

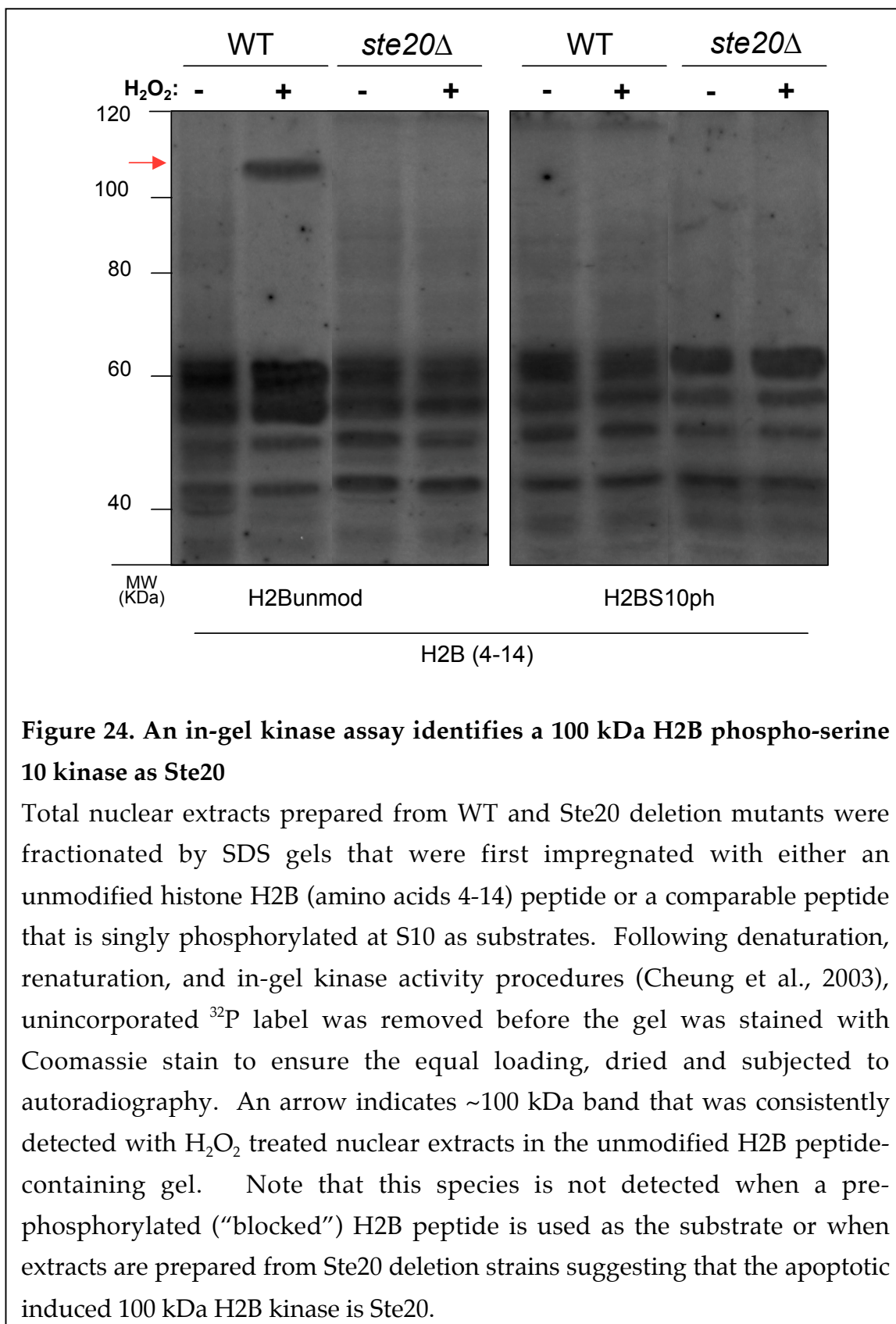
(B) The rest of the cells and H<sub>2</sub>O<sub>2</sub>-treated or untreated *ipl1Δ* were harvested and nuclear extracts were probed with anti-H2BS10ph and anti-H3S10ph for Western analysis. Anti-H4 was used as a loading control. Ste20 specifically phosphorylates H2BS10, whereas Ipl1 phosphorylates H3 at S10.



An in-gel kinase assay was employed to determine the molecular weight(s) of potential yeast apoptotic H2B kinases in total nuclear extracts. In this assay, nuclear extracts, prepared from H<sub>2</sub>O<sub>2</sub>-treated and untreated WT or *ste20* $\Delta$  cells, were separated by SDS-PAGE gels that were first impregnated with either unmodified (amino acids 4-14 of yeast H2B) or H2BS10ph peptides (Figure 24). Following renaturation and in-gel kinase assay, numerous bands were in common between these two peptide gels, likely due to autophosphorylation (Figure 24). However, a band with a molecular weight of approximately 100 kDa was consistently detected with H<sub>2</sub>O<sub>2</sub>-treated nuclear extracts in kinase activity gels containing the unmodified H2B peptide (see red arrow in Figure 24). This 100 kDa band was absent in identically treated in-gel kinase assays containing pre-H2BS10ph peptide or with yeast nuclear extracts prepared from *ste20* $\Delta$  cells (Figure 24). As 100 kDa is the predicted molecular mass of Ste20 protein, these data add further support that Ste20 kinase is an apoptosis-induced H2BS10 kinase.

#### ***Ste20 kinase phosphorylates histone H2B at serine 10 in vitro***

To further establish a direct role of Ste20 during H<sub>2</sub>O<sub>2</sub>-induced yeast cell death event, I developed a bacterial expression system which provided a source for recombinant full-length Ste20 (FL Ste20), and a kinase dead form of Ste20 (Ste20<sup>K649R</sup>; KD), containing an inactivating single point mutation changing lysine to arginine, that were N-terminally tagged with GST. Purified FL-Ste20 and KD were then incubated with yeast histone H2B peptides that contain residues 4-14 with unmodified or singly phosphorylated at S10 at 30 °C in the presence of



[ $^{32}$ P]ATP. After 1 hr incubation, the kinase activity was assayed by measuring incorporation of the [ $^{32}$ P] label into peptide substrates using a filter-binding assay. As shown in Figure 25A, FL Ste20 phosphorylated unmodified H2B peptide (amino acid residue 4-14), but not H2BS10ph peptide. As expected, no kinase activity was observed with KD as displayed by a drastic decrease of [ $^{32}$ P] incorporation into unmodified H2B peptide (Figure 25A), suggesting Ste20 as H2B kinase. Next, the specificity of Ste20 kinase was tested using any unmodified histone peptides that were available in our lab. Both FL Ste20 and KD were not able to phosphorylate unmodified peptides carrying H2B amino acids from 30-37, H2A from 1-9, H4 from 1-19 (Figure 25B), suggesting that Ste20 contains a strong histone kinase activity specific for H2B at S10. Interestingly, FL Ste20 phosphorylated an unmodified H2B peptide containing amino acids 6-16 from mammalian H2B (Figure 25B). In contrast, the phosphorylation level was significantly reduced with a similar peptide differing by a single phosphate at S14 (Figure 25B), demonstrating that yeast Ste20 can act similarly *in vitro* as mammalian Mst1, a H2BS14 kinase.

Ipl1, a H3S10 kinase, phosphorylates both H3 and H2B *in vitro* (Hsu et al., 2000) suggesting that H2B phosphorylation may be functionally redundant with H3 phosphorylation. Therefore, I sought to address whether Ste20 kinase can also phosphorylate H3 analyzed by *in vitro* kinase assay. Unlike Ipl1, FL Ste20 failed to phosphorylate H3 peptides that are either unmodified or singly phosphorylated at S10, disputing an existence of functional overlap between H2B and H3 phosphorylation by Ste20 (Figure 25A). As a positive control for unmodified H3 peptide, His10-Ipl1 was expressed in bacteria and purified for

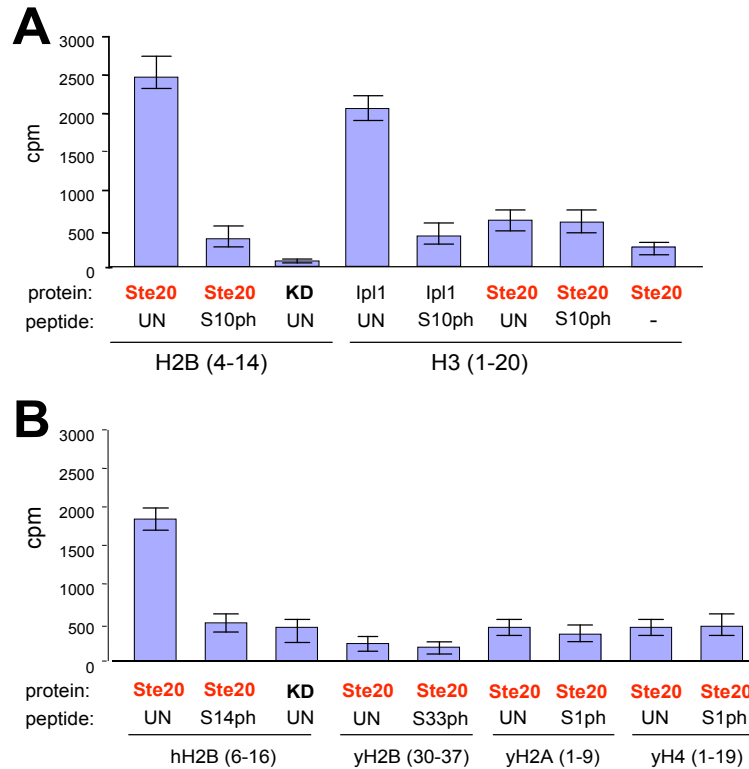


**Figure 25. Recombinant Ste20 kinase preferentially phosphorylates unmodified H2B peptide containing amino acid residue 4-14 *in vitro***

*In vitro* kinase assays were performed in the presence of GST-tagged full-length (FL Ste20), or kinase dead form of Ste20<sup>K649R</sup> (KD). Phosphorylation of indicated histone peptides was assessed by measuring incorporation of [<sup>32</sup>P]- $\gamma$ -ATP using a filter-binding. The indicated kinase activities were obtained from three independent experiments.

(A) H2B peptides from yeast (amino acids 4-14) or H3 peptides from yeast (amino acids 1-20) that were unmodified or singly phosphorylated at S10, were used as substrates for an *in vitro* kinase assay. FL Ste20, but not KD, only phosphorylates unmodified yeast H2B peptides. Ipl1 kinase was used as a positive control with H3 peptides (Hsu et al., 2000).

(B) As in (A), except that *in vitro* kinase assay was carried out with different histone peptide substrates including peptides from mammalian H2B (amino acids 6-16), yeast H2B (amino acids 30-37), yeast H2A (amino acids 1-9), and yeast H4 (amino acids 1-19). FL Ste20 phosphorylates mammalian H2B peptides that is unmodified but not singly phosphorylated at S14.

kinase assay. As expected, Ipl1 displayed a strong preference for unmodified H3 peptide, but not a comparable peptide that is singly phosphorylated at S10 of H3 (Figure 25A). No phosphorylation was observed with both H2B peptides (unmodified and S10ph containing amino acids 4-14), demonstrating that H2BS10 is not a suitable substrate for Ipl1.

Purified Ste20 was tested for its substrate preference using a collection of various composition and origin. They include recombinant histones, recombinant nucleosomes, and a mixture of core histones from yeast. The similar kinase reaction was carried out at 30 °C for 1 hr in the presence of [ $^{32}$ P]ATP. After stopping the reactions by SDS-loading buffer, proteins were separated on SDS-PAGE gel and analyzed by autoradiography. Incorporation of [ $^{32}$ P] label in H2B was detected in the reactions with FL Ste20, and not KD, when purified H2B, or a mixture of core histones was used as substrates (Figure 26A). Interestingly, FL Ste20 also phosphorylated nucleosomal H2B *in vitro* suggesting that Ste20 kinase has the potential to act on chromatin substrates *in vivo* (Figure 26A). Finally, parallel kinase reactions were performed with nonradioactive ATP and analyzed by western blotting. In agreement, only FL Ste20 phosphorylated H2B as detected by anti-H2BS10ph (Figure 26B). Taken together, these results demonstrate that Ste20 kinase can directly phosphorylate H2BS10 *in vitro* under these assay conditions. Thus, I suggest that Ste20, a bona fide cell death kinase in yeast, acts to bring about H2BS10ph through a direct enzyme-substrate interaction in a cascade triggered by H<sub>2</sub>O<sub>2</sub> treatment.

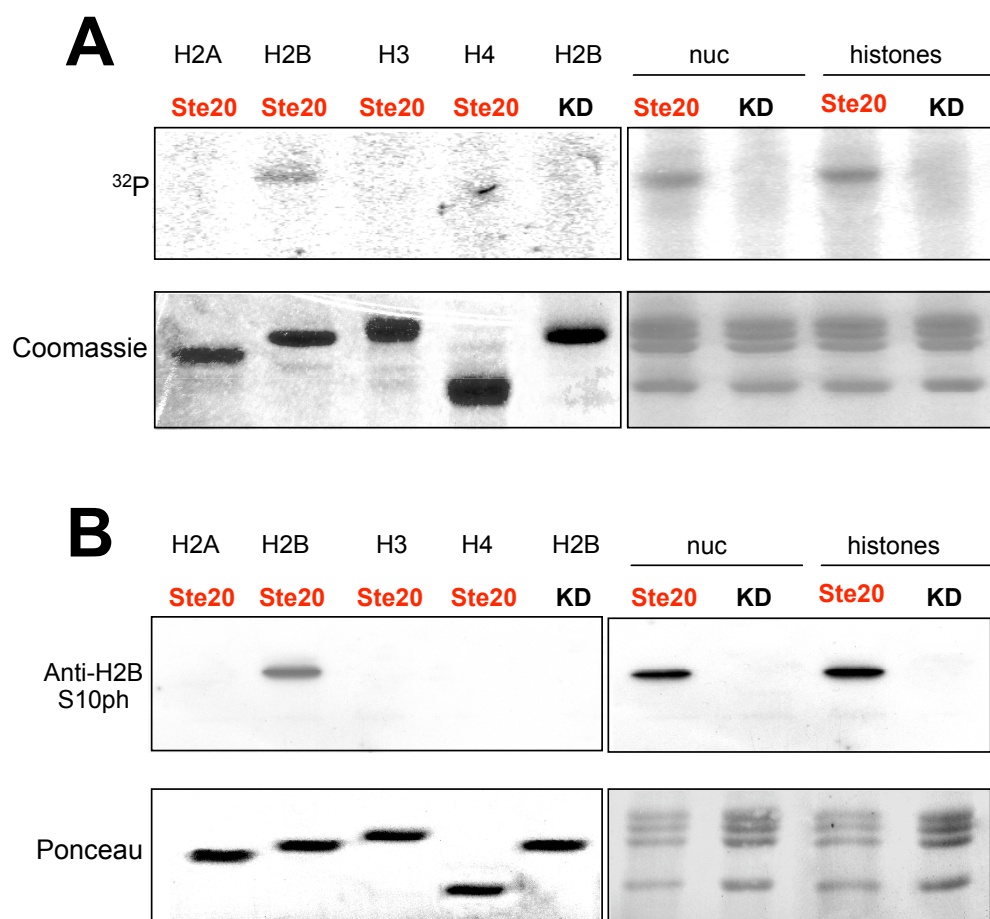


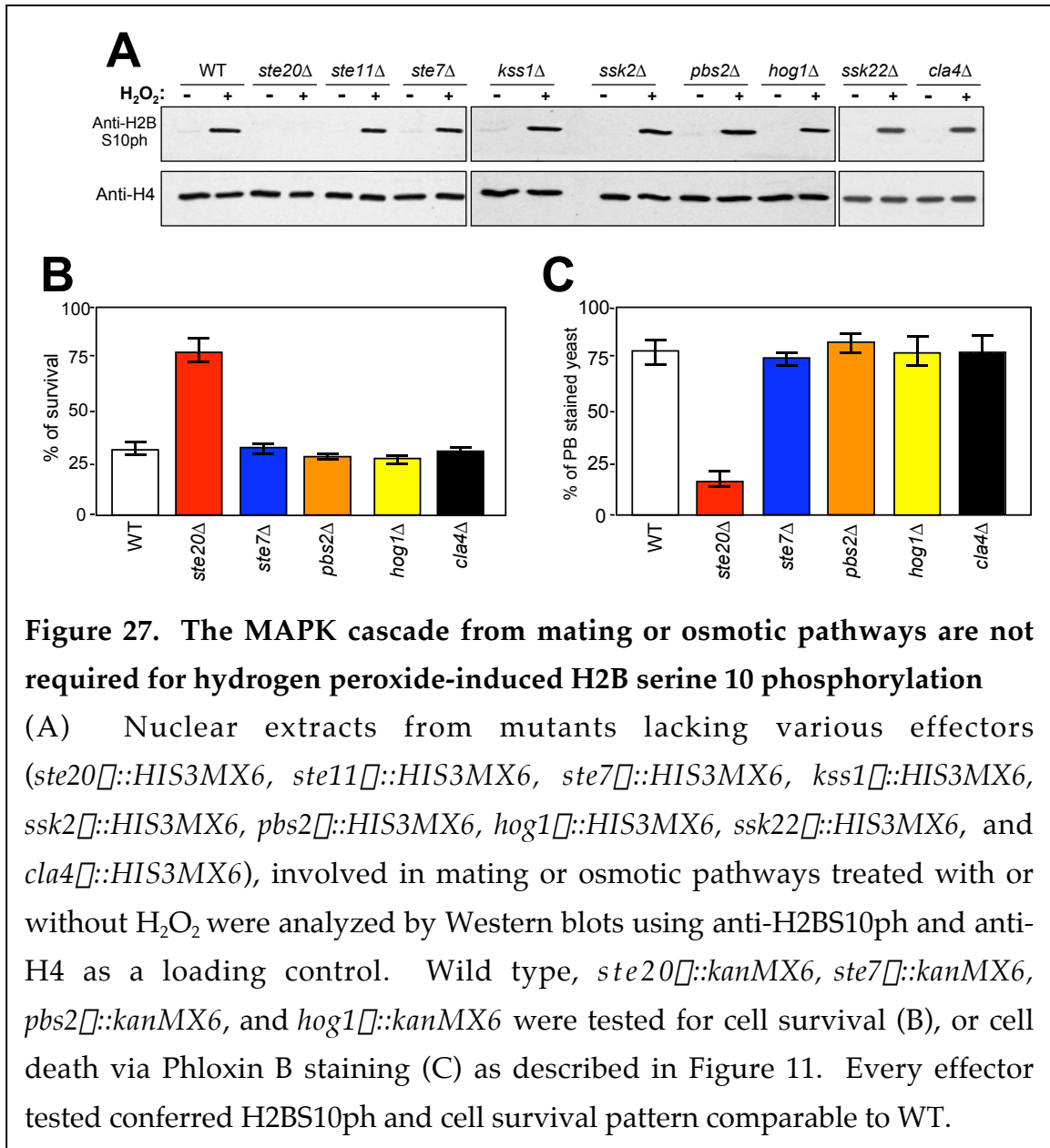
**Figure 26. Nucleosomal H2B is the substrate for Ste20 kinase *in vitro***

(A) Recombinant Ste20 (FL-Ste20) and the kinase dead form of Ste20<sup>K649R</sup> (KD) were incubated with various types of substrates, including recombinant H2B (H2B), recombinant nucleosomes (nuc), and a mixture core histones from yeast (histones). The kinase reactions were performed at 30 °C for 1hr in the presence of [<sup>32</sup>P]ATP. After stopping the reactions by SDS-loading buffer, proteins were separated on SDS-PAGE gel and visualized by Coomassie Blue staining (lower panel) to ensure the equal loading. Proteins radio-labeled with <sup>32</sup>P were detected by autoradiography (upper panel).

(B) As in (A), except that nonradioactive *in vitro* kinase assay was carried out without the [<sup>32</sup>P]ATP. Nonradioactive ATP was used as phosphate source. The phosphorylation of H2B was detected by Western analysis. FL Ste20 phosphorylated H2B as detected by anti-H2BS10ph.

**MAPK cascade signaling during mating or osmotic process and *Yca1* are not required for apoptotic H2B serine 10 phosphorylation**

The MEKK Ste20 kinase functions in three *Saccharomyces cerevisiae* MAPK cascades including the high osmolarity glycerol (HOG), pheromone response, and pseudohyphal/invasive growth pathways (Liu et al., 1993; Robers and Fink 1994; Davenport et al., 1995; Kamada et al., 1995; O'Rourke and Herskowitz,



1998). Therefore, I analyzed a series of strains defective in these pathways to determine whether they inhibit the enhancement of H2BS10ph. These include Ste11, Ste7, Kss1 from filamentous growth/pheromone response pathway, Ssk2, Pbs2, Hog1, Ssk22 from HOG pathway. In my hands, all the downstream effectors I tested displayed no changes in H2BS10ph (Figure 27A). Furthermore, yeast strains separately lacking these effectors had normal or increased amount of cell death as compared to WT (Figure 27B and 27C). Cla4 belong to Ste20 PAK kinase family and shares some essential function with Ste20 since double mutation of both kinases result in synthetic lethality (Cvrckova et al., 1995, Goehring et al., 2003). However, they do not share function in yeast apoptosis since Cla4 deletion mutant was sensitive to H<sub>2</sub>O<sub>2</sub>, accompanied by the appearance of apoptotic H2BS10ph (Figure 27). Thus, Ste20 kinase is so far the sole yeast apoptotic mediator that directly phosphorylates the histone H2BS10.

Caspases are integral components of many mammalian apoptotic pathways. The onset of apoptotic H2BS14ph is dependent upon cleaved of Mst1 by caspase-3 (Cheung et al., 2003) in vertebrates. Hence, I sought to determine whether H2BS10ph is controlled by Yca1, the only known yeast caspase. Yca1 gets cleaved in a caspase typical way and displays a caspase-like proteolytic activity which is activated during yeast apoptosis (Uren et al., 2000; Madeo et al., 2002b). As shown by Madeo et al. 2002, Ycal knockout in yeast decreased cell death induced by H<sub>2</sub>O<sub>2</sub> suggesting it as an apoptotic mediator (Figure 28A and 28B). However, the immunoblotting analysis showed that the level of H2BS10ph after H<sub>2</sub>O<sub>2</sub> treatment was normal in the Yca1 mutants (Figure 28C). Taken together, these results suggest that Yca1 and Ste20/H2BS10ph act in independent pathways modulating yeast cell death.



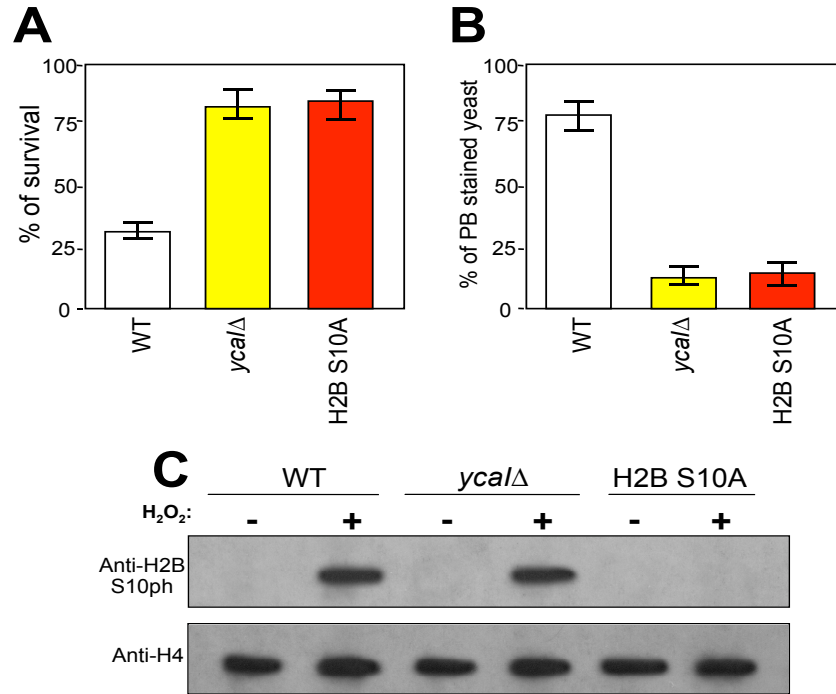


**Figure 28. Yca1 and H2B serine 10 phosphorylation act in independent pathways modulating yeast cell death.**

Log phased WT, *yca1*Δ and H2B S10A were treated with 1 mM H<sub>2</sub>O<sub>2</sub> for 200 minutes. Cells were then plated onto rich medium, YPD. After 2 days of growth, cells were counted to determine the cell viability (A), or cell death via Phloxin B staining (B) as described in Figure 11. As expected Yca1 plays a role in H<sub>2</sub>O<sub>2</sub>-induced cell death in yeast (Madeo et al., 2002b).

(C) Nuclear extracts of indicated yeast strains were separated on SDS-PAGE gel and immunoblots were probed with anti-H2BS10ph and anti-H4. Anti-H4 was used as a loading control. The H2BS10ph signal was detected in *yca1* deletion strain even after H<sub>2</sub>O<sub>2</sub> treatment.

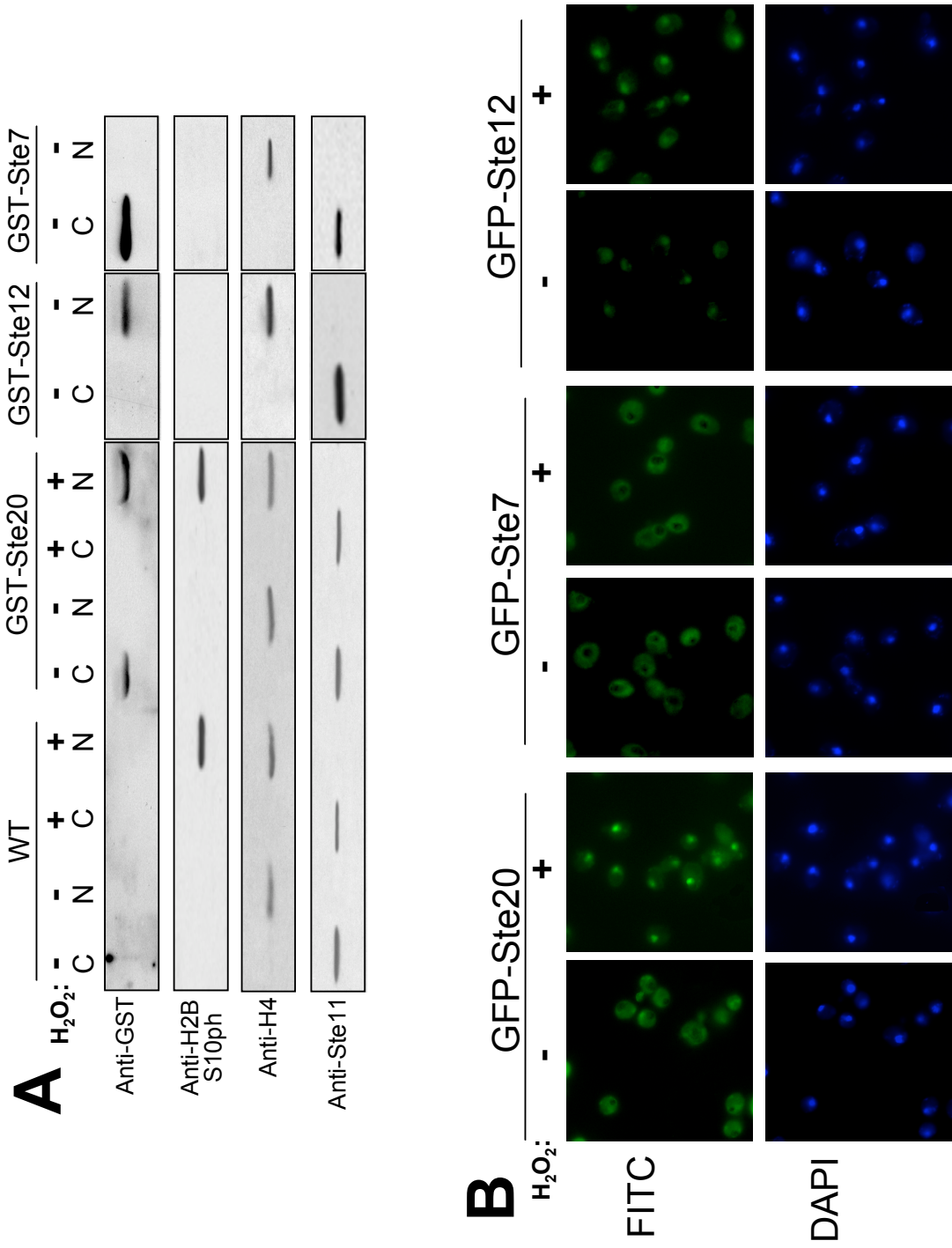
### *Hydrogen peroxide treatment stimulates translocation of Ste20 from cytoplasm into nucleus*

My results indicate that Ste20 directly acts to phosphorylate H2B *in vitro* and *in vivo*. I reasoned then that Ste20 kinase, which is normally present in the cytoplasm (Leberer et al., 1997), should be able to translocate from the cytoplasm

**Figure 29. Nuclear localization of GST-Ste20 upon hydrogen peroxide treatment**

(A) Cytoplasmic (C) and nuclear extracts (N) were obtained from GST-Ste20, GST-Ste12, and GST-Ste7 and analyzed by Western blotting using anti-GST following treatment with or without H<sub>2</sub>O<sub>2</sub>. Anti-H4 reacted with nuclear extracts while anti-Ste11 reacted with cytoplasmic extracts verifying the quality of the extracts. In addition, anti-GST reacted with nuclear extracts from GST-Ste12 and cytoplasmic extract from GST-Ste7. While GST-Ste20 was found in the cytoplasmic fraction from the mock-treated samples, 100 kDa full length Ste20 was found in the nuclear fraction from H<sub>2</sub>O<sub>2</sub>-treated samples.

(B) As in (A) except that Ste20, Ste7 and Ste12 was visually examined for the subcellular localization via the GFP tag with or without H<sub>2</sub>O<sub>2</sub> treatment. They were stained with DAPI for DNA. As expected, GFP-Ste7 localized in the cytoplasm and GFP-Ste12 localized in the nucleus. On the other hand, GFP-Ste20 and GFP-Ste20<sup>K649R</sup> translocated from cytoplasm into nucleus upon treatment with H<sub>2</sub>O<sub>2</sub>.



to the nucleus upon H<sub>2</sub>O<sub>2</sub> treatment, even though an obvious nuclear localization signal is not apparent in Ste20. To test this hypothesis, a yeast strain was generated in which the *STE20* gene was fused to GST at its N-terminus. This chimeric protein, under control of its endogenous *STE20* promoter, was fully functional as assessed by survival in H<sub>2</sub>O<sub>2</sub>, H2BS10ph, and ability to mate. Since Ste20 is localized in the growing bud tip and the plasma membrane during normal growth (Leberer et al., 1997), I predicted that GST-Ste20 would localize mostly in the cytoplasmic fraction without H<sub>2</sub>O<sub>2</sub> treatment. Hence, nuclei were extracted from H<sub>2</sub>O<sub>2</sub> treated or untreated GST-Ste20 cells and analyzed GST-Ste20's localization by Western blotting using anti-GST antibody. A high percentage of GST-Ste20 was found in the cytoplasmic fraction from the mock-treated samples (Figure 29A). Surprisingly, H<sub>2</sub>O<sub>2</sub> treatment facilitated the translocation of Ste20 into the nucleus as essentially all of GST-Ste20 was localized to the nuclear extracts following this treatment (Figure 29A).

Quality of the fractionation procedure was verified by determining the localization of known nuclear and cytoplasmic proteins. They include histone H4 and GST-Ste12 as nuclear proteins, and Ste11 and GST-Ste7 as cytoplasmic proteins. The localization of histone H4 and Ste11 was determined by immunoblotting analysis using anti-H4 and anti-Ste11 antibodies. As expected, all the nuclear extracts contained H4 signal whereas Ste11 was only present in cytoplasmic fractions (Figure 29A). GST-Ste12 and GST-Ste7 were generated as described for GST-Ste20, except that GST-Ste12 was under the control of *STE12* promoter and GST-Ste7 was under the control of *STE7* promoter. As shown in Figure 29A, GST-Ste12 was found in the nuclear fraction and GST-Ste7 was in cytoplasmic fractions in both H<sub>2</sub>O<sub>2</sub> untreated and treated conditions. Hence,

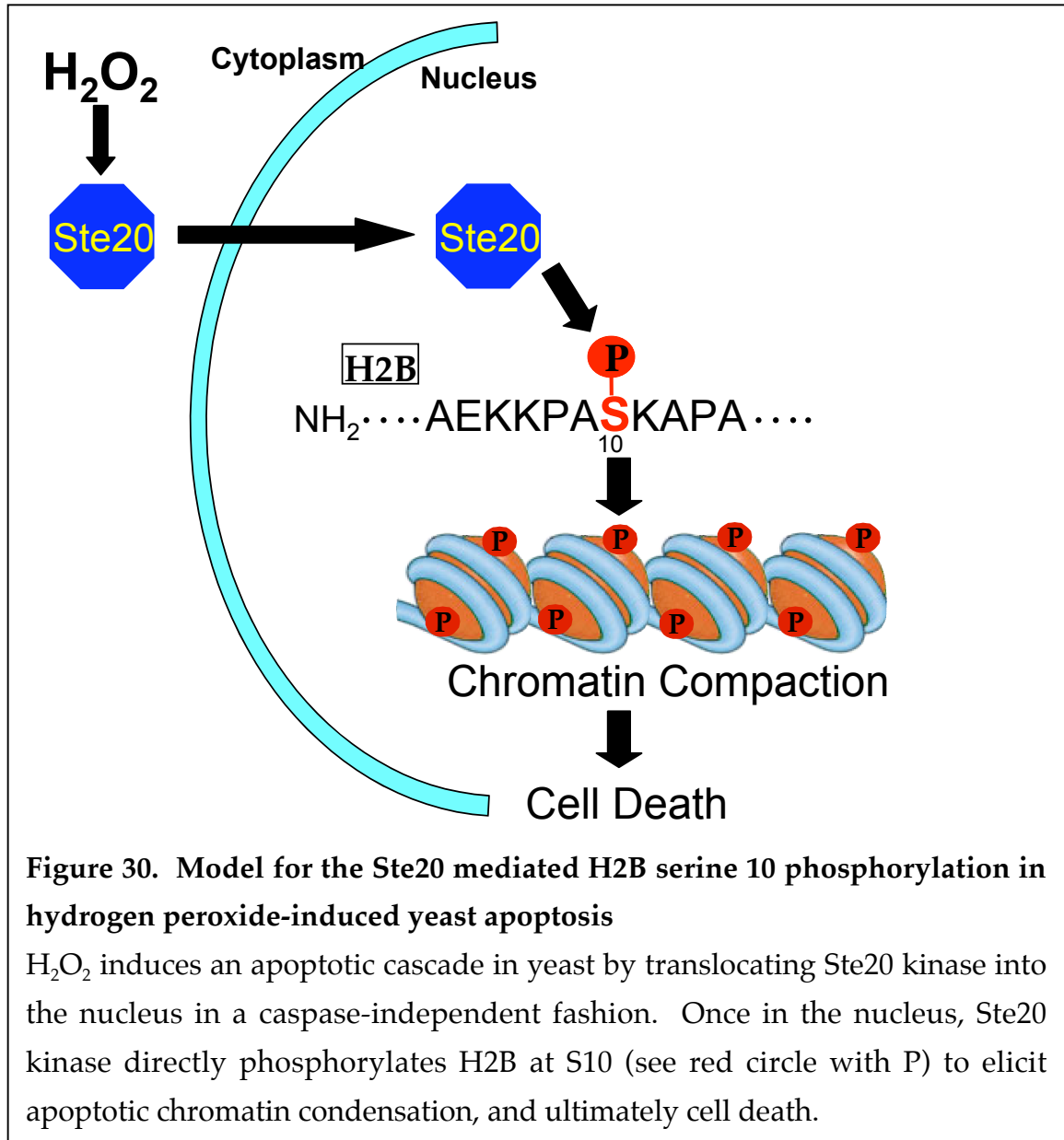
Ste20 translocated from the cytoplasm into the nucleus during H<sub>2</sub>O<sub>2</sub> -induced yeast apoptosis. Furthermore, an approximate 130 kDa band was consistently detected in H<sub>2</sub>O<sub>2</sub>-treated nuclear extracts, corroborating that full-length Ste20, and not a cleaved form of Ste20, is translocated into the nucleus (Figure 29A). These results are consistent with Yca1 operating in a separate pathway from Ste20-mediated H2BS10ph (Figure 28). Thus, my data underscore a difference between yeast and mammalian cells in that Ste20 does not appear to be a caspase-dependent apoptotic kinase in yeast.

Next, the sequence encoding green fluorescent protein (GFP (S65T)) was fused to the N-terminal sequence of *STE20* *in vivo* to examine the subcellular localization of Ste20 in response to H<sub>2</sub>O<sub>2</sub>. This chimeric protein displayed H<sub>2</sub>O<sub>2</sub> sensitivity, H2B phosphorylation and mating ability similar to that of WT cells. As shown in Figure 30B, in the absence of H<sub>2</sub>O<sub>2</sub> treatment, GFP-Ste20 was either concentrated at the site of bud emergence or appeared as a diffuse signal in normal growing cells, again correlating with previously documented results (Wu et al., 1995). However, upon treatment with H<sub>2</sub>O<sub>2</sub>, much of the fluorescent signal concentrated within nuclei, precisely coinciding with DAPI-stained nuclei. Ste20 kinase activity is not required for its nuclear translocation, since GFP-Ste20<sup>K649R</sup>, a catalytically-inactive form of Ste20, conferred a localization pattern similar to GFP-Ste20 (Figure 29B). These results are consistent with nuclear localization being an upstream event of histone H2B phosphorylation. As control, GFP was tagged N-terminal of Ste12 and Ste7 promoter to generate GFP-Ste7 and GFP-Ste12, respectively and their functionality was verified as both displayed H<sub>2</sub>O<sub>2</sub> sensitivity comparable to WT. GFP-Ste7 was concentrated in the cytoplasm, while GFP-Ste12 was in the nucleus (Figure 29B). Together, these results suggest

that  $\text{H}_2\text{O}_2$  induces a cell death cascade in yeast by translocating Ste20 into the nucleus in a caspase-independent fashion. I favor the view that Ste20, upon nuclear uptake, phosphorylates H2B at S10 directly to elicit chromatin compaction and re-organization that resembles to some extent what typically occurs during mammalian apoptosis (Figure 30).

## Discussion

Chromatin alterations, induced in part via covalent histone modifications, are proving to play ever-important roles in a wide range of DNA-templated processes. Here, I uncover a unique and previously unrecognized “death” function of the H2B N-terminal tails in *S. cerevisiae*. This function is unique to the H2B N-tail, and is not carried by the N-tails of H2A, H3 or H4. In keeping with results obtained in mammalian cells (Cheung et al., 2003), phosphorylation of S10 in yeast H2B serves a comparable role to phosphorylation of mammalian H2B at S14 and is catalyzed by Ste20 kinase, a yeast homolog of mammalian Mst1 kinase. I extended our mammalian studies by showing that phosphorylation of S10 in H2B in yeast is necessary to induce cell death *in vivo* and exhibit phenotypic hallmarks of apoptosis including DNA fragmentation and chromatin condensation. However, unlike H2BS14, I demonstrated that yeast cells containing a deletion mutation of Ste20 kinase (*ste20 $\Delta$* ), as well as mutants carrying H2B S10A, are resistant to cell death elicited by H<sub>2</sub>O<sub>2</sub>. Importantly, a phospho-mimic of S10, S10E, promotes the constitutive formation of highly compacted chromatin. Therefore, I favor the view that the Ste20 kinase, a yeast homolog of mammalian apoptotic Mst1 kinase, directly catalyzes phosphorylation of H2BS10 during H<sub>2</sub>O<sub>2</sub> induced yeast cell death upon its translocation into the nucleus in a caspase-independent manner (Figure 30). Together, these studies begin to define a phosphorylation-based H2B “death code” and elucidate a mechanism by which H2B phosphorylation regulates apoptosis, a pathway that appears conserved in significant detail from yeast to humans.



### *Yeast H2B serine 10 phosphorylation versus mammalian H2B serine 14 phosphorylation*

Previously, H2BS14 has been shown to serve as a site of phosphorylation induced during mammalian apoptosis (Cheung et al., 2003). The studies reported here suggest that H2BS10 functions as the counterpart of this event in yeast. In support, my proposed  $H_2O_2$ -induced yeast cell death signaling model is



similar to the previously described mammalian apoptotic cascade in which phosphorylation of vertebrate H2B at S14 is mediated by Mst1, a mammalian homolog of Ste20 (Cheung et al., 2003). My data are consistent with yeast H2BS10ph serving a role in mediating DNA fragmentation and chromatin condensation since H2B S10A mutants exhibit a loss of DNA fragmentation and chromatin condensation (Figures 18 and 20). Therefore, this phosphorylation event could serve as a mechanism mediating chromatin condensation during apoptosis *in vivo* (Cheung et al., 2003).

Interestingly, the Ste20-catalyzed cascade in yeast is distinct from mammalian Mst1 elicited pathway in that it does not require a proteolytic processing event. Instead, my data show that the full-length Ste20, and not the caspase-cleaved form, translocates into the nucleus upon H<sub>2</sub>O<sub>2</sub> treatment (Figure 29). Furthermore, Yca1, the only identified yeast caspase, is not required for H2BS10ph (Figure 28C), even though it serves as an apoptotic mediator during H<sub>2</sub>O<sub>2</sub>-induced cell death (Madeo et al., 2002b). Therefore, my results suggest that there may be two independent yeast cell death processes; one which is mediated by the caspase such as Yca1, and the other mediated by a caspase-independent mechanism involving H2BS10ph. Precedent for a non-caspase-mediated apoptosis has been observed in various human tumor cells after treatment with specific drugs (Wang et al., 2003). While no link to H2B phosphorylation has been made in this pathway, I cannot exclude the possibility that similar downstream effectors from yeast, may be regulating the caspase-independent apoptosis in vertebrates.

### *Ste20 kinase functions in a pathway distinct from known MAP kinase signaling cascade*

Although Ste20 is well known as an activator of MAP kinase pathway (Liu, 1993; Roberts and Fink, 1994; O'Rourke and Herskowitz, 1998), this role is not required for H2B phosphorylation induced by H<sub>2</sub>O<sub>2</sub> treatment. Instead, my data support a view wherein Ste20 facilitates phosphorylation of H2BS10 through a direct enzyme-substrate interaction without activating the classical MAPK pathway (Figure 27). In support, I show that Ste20 can translocate into the nucleus in response to H<sub>2</sub>O<sub>2</sub>, even though it lacks an obvious nuclear localization signal (Figure 29). It remains unclear whether yet unidentified factors interact with Ste20 to facilitate the nuclear translocation, or whether additional factors are required for catalytic-activity of Ste20 or its regulation. Interestingly, PAKs, such as Ste20, are commonly activated by small GTPases of Cdc42/Rac family, and Ste20 binds to Cdc42, a guanine nucleotide exchange factor (Burbelo et al., 1995). However, the role of this interaction is controversial since Ste20 lacking its entire Cdc42-binding domain still retains kinase activity and mating function (Peter et al., 1996; Leberer, et al., 1997). Thus, it is not surprising that Cdc42 may not be involved in activating Ste20 during H<sub>2</sub>O<sub>2</sub>-induced apoptosis. Instead, an autophosphorylation event might represent a crucial step in the activation of Ste20 since Ste20 exhibits autophosphorylation activity (Wu et al., 1995). Furthermore, p65<sup>PAK</sup>, another mammalian homologue of Ste20, has been shown to be activated *in vitro* by an autophosphorylation mechanism (Martin et al., 1995), as has Mst1 (Glantschnig et al., 2002). Thus, it is conceivable that yet unknown upstream regulators or other kinases may activate Ste20 via phosphorylation.

### *Conserved features of “apoptotic” H2B phosphorylation*

The finding of a potential “death code” in organisms as diverse as yeast and humans, suggests that similar sequences may exist in H2B tails from other organisms. In *S. pombe*, for example, the budding yeast S10, as well as its neighboring sequences, is identically found in its H2B N-terminal tail, suggesting an intriguing possibility of phosphorylation of S10 participating in apoptotic function in fission yeast. Interestingly, Pca1, a Yca1 homolog in *S. pombe*, appears to play an essential role in *S. pombe* apoptosis when induced with fatty acid (lipoapoptosis; Zhang et al., 2003). However, at this time, it is unknown if this process may be mediated by a mechanism similar to the budding yeast apoptosis described here.

Although apoptosis has been extensively studied in *Drosophila melanogaster* and *Caenorhabditis elegans*, it remains unclear whether N-terminal tail of H2B, or its phosphorylation, plays a significant role during cell death in these models. As shown in Figure 13, their H2B N-terminal tails are divergent, but potential phosphorylation acceptor candidates may include serine 5 in *Drosophila* and serine 6 in *C. elegans* as these serines are embedded in basic motifs near alanine/proline residues similar to that of vertebrate S14 and yeast S10. Moreover, hippo (Hpo), a *Drosophila* homolog of mammalian Mst1 and yeast Ste20 serine/threonine kinase, has been shown to modulate apoptosis in *Drosophila* (Harvey et al., 2003; Wu et al., 2003) and may facilitate phosphorylation of H2B during apoptosis. A comparable scenario may exist in *C. elegans* as well, since cMst, a *C. elegans* homolog of mammalian Mst1 (Lee et al., 2001), has been identified, although its role in apoptosis remains to be explored.

Although many of the major upstream apoptotic regulators described for mammalian cells have no apparent homolog in *S. cerevisiae*, a growing list of properties, including H2B phosphorylation, appear shared between them. Whether a “true” mammalian-like programmed cell death occurs in yeast is not answered by my study. Also unclear is whether “surviving” cells carrying the H2B S10A mutation are “normal” relative to WT cells or are refractory to other stress-induced insults. What benefits a suicide pathway serves a unicellular organism are also a matter of debate. It has been suggested that this mechanism may limit replication of viruses, reduce competition for nutrients during periods of starvation, or eliminate cells with damaged or mutated DNA to better maintain genomic integrity of future generations (Severin and Hyman, 2002).

Interestingly, H2BS14ph has recently been correlated with DNA damaged foci that also stain positively with H2A.X phosphorylation in mammalian cells (Fernandez-Capetillo et al., 2004a). Together, these data hint at a conserved pathway wherein histone phosphorylation of core histones (major and variant) create a specialized compacted chromatin structure that facilitates repair of DSBs as well as participates in the formation of condensed chromatin characteristic of dying cells. The precise role of these phosphorylation marks, whether inducing structural effects on chromatin packaging (“cis” mechanism), or allowing the binding of “death effectors” that, in turn, bring about downstream effects (“trans” mechanism), remains an open area of considerable interest. (discussed in Chapters 4 and 5).

In summary, while important differences in mechanistic details appear to exist between yeast and mammalian cells, my studies pave the way for a better understanding of apoptosis by defining the novel role of Ste20 in governing the

novel H2BS10ph in the yeast. The conservation of the covalent modification, the choice of the particular core histone tail substrate, and the enzyme system responsible for bringing about this mark, points to an ancient mechanism of cell death process conserved from yeast to human. My findings suggest the intriguing possibility that yeast can be used as model to provide a better understanding of the complex network of fundamental mechanisms of apoptosis, as well as furthering our understanding of link between covalent histone modifications and cell death. This theme will be further developed in the next chapter of my thesis.

## Materials and Methods

### *Reagents and media*

Restriction enzymes, T4 DNA ligase (for general cloning) and Vent DNA polymerase were purchased from New England Biolabs (NEB). The Pfu Turbo DNA polymerase (for DNA mutagenesis) was purchased from Stratagene. Hygromycin, G418 and microcystin-LR were purchased from Calbiochem. Yeast lytic enzyme was purchased from MP Biomedicals.  $\lambda$ -factor was purchased from Zymo research. Yeast extract, peptone, Bacto-Agar, and yeast nitrogen base were from Fischer Scientific Co. Amino acid drop out mix and 5-FOA were purchased from Bio101 systems. Reagents and enzymes purchased from Sigma include common lab chemicals, anti-GST antibody, diamidino-phenylindole (DAPI), phloxin B, phenylmethanesulfonyl fluoride (PMSF), leupeptin, aprotinin, pepstatin and salmon sperm DNA.

The commonly used yeast and bacterial media were prepared as described previously (Sherman et al., 1979). Bacterial cells were grown in LB medium (1% tryptone, 0.5% yeast extract, and 1% NaCl) or YT medium (6.0% tryptone, 1.0% yeast extract, 0.5% NaCl, plus antibiotics. These antibiotics include 100  $\mu$ g/ml ampicillin, 25  $\mu$ g/ml chloramphenicol, and 50  $\mu$ g/ml kanamycin). For yeast, rich media YPD consists of 1% yeast extract, 2% peptone and 2% dextrose. The synthetic complete (SC) medium consists of 0.36% yeast nitrogen base without amino acids, 2% dextrose, 1% ammonium sulfate, and amino acid drop out mix.

### ***General DNA manipulation***

*Escheirchia coli* strain DH5 $\alpha$  [*supE44*  $\Delta$ *lacU169* ( $\Delta$ 80 *lacZ*  $\Delta$ M15) *hsdR17 recA1 endA1 gyrA96 thi-1 relA1*] was used for general cloning. Plasmid DNA were purified using the Qiagen Midi Prep kit (Qiagen). DNA digestions with restriction enzymes were carried out according to the manufacturer's instruction. DNA fragmentations were isolated using QIAquick Gel extraction kit (Qiagen). DNA ligation was performed using T4 DNA ligase (NEB) and the buffer provided by the manufacturer in a 30  $\mu$ l reaction at room temperature (RT) for 3 hr.

### ***Mutation of histone genes***

A procedure based on the 'QuickChange Site-Directed Mutagenesis' protocol by Stratagene was used for the introduction of point mutations in plasmid-born histone genes. Plasmid pQQ18 (CEN *LEU2*, CEN, *HTA1-HTB1-HHF2-HHT2*), which contain the genomic fragment of *HTA1-HTB1* and *HHF2-HHT2* in pRS315 (Sikorski and Hieter), was used as template. Two mutagenic primers with complementary sequences were designed for each mutation. The desired mutation was placed in the middle of the primer with 15 base correct sequences on both sides. PCR reactions were performed in 0.5 ml Eppendorf tubes in a total reaction volume of 50  $\mu$ l, containing 125 ng of the PAGE-purified oligonucleotide containing the desired base substitution, 1x pFU Turbo DNA polymerase buffer, 250  $\mu$ M dNTP, 20  $\mu$ M oligonucleotides and 1 unit pFU Turbo polymerase. The following PCR program was used on the PTC-200 thermocycler: 95°C 30 seconds  $\square$  16x (95°C 30 seconds, 55°C 1 min, 68°C 10 min)  $\square$  75°C 10 min  $\square$  4°C. After completion of the thermocycling, the products were

digested with 1  $\mu$ l of *Dpn* I restriction enzyme (NEB) at 37°C for 4 hr to digest the parental (i.e., the nonmutated) supercoiled dsDNA. After heat inactivation at 85°C for 15 min, the digestion products were used to transform *E. coli* DH5 $\alpha$  competent cells. Desired mutations were confirmed by DNA sequencing and the minimal DNA fragment containing the mutated region was sub-cloned to the original parental pQQ18 plasmid to avoid secondary mutations on the plasmid.

### ***Plasmids***

pSA17 (*HTB1-S10A*), pSA18 (*HTB1-S33A*), pSA65(*HTB1-S10E*), pSA67 (*HTB1-S33E*), were created by PCR and sub-cloned into pQQ18. pSA51 and pSA52 carrying the *STE20* promoter, were created by replacing *GAL1* promoter in pFA6a-His3MX6-pGAL1-GFP and pFA6a-His3MX6-pGAL1-GST (Longtine et al., 1998), respectively, with the *STE20* promoter amplified by PCR using yeast genomic DNA from wild type yeast cells as template.

### ***Yeast transformation***

Yeast transformations were performed by a lithium acetate procedure based on that of Gietz et al. 1992. Briefly, yeast cells were grown in YPD medium at 30° C shaker with 200 rpm. When these cells reached  $1 \times 10^7$  cells/ml, they were harvested by centrifugation at 3000 g for 5 min, washed cells in 5 ml of 1X TE/LioAc (made fresh from 10X TE pH 7.5 and 10X LioAc [1M LioAc pH 7.5, adjusted with diluted acetic acid]) and resuspend in 50  $\mu$ l of 1X LioAc. The yeast cell suspension was then mixed with 1  $\mu$ g transforming DNA, 50  $\mu$ g of single stranded salmon sperm carrier DNA that was previously boiled 5 min and



chilled in ice for 10 min, and 300  $\mu$ l of sterile 40% PEG 3500 solution (40% PEG 4000, 1X TE, and 1X LioAc made fresh from sterile 50% PEG stock, sterile 10X TE and 10X LioAc). The yeast cell suspension was incubated at 30° C with agitation for 30 min, heat shocked in a 42°C water bath for 15 min, then 10 ml YPD was added and incubated at 30°C with agitation for 1 hr. After centrifugation at 3000 g for 5 min, the supernatant was discarded and cells were resuspended with 300  $\mu$ l of water. These cells were then plated onto appropriate SC selection plates.

### ***Yeast Strains***

Yeast strains are listed in Table 1 and all strains are derived from either S288C (BY4741; Research Genetics) background. JHY205, the histone shuffle strain with pJH33 plasmid, was used to generate yeast cells carrying histone mutations. Briefly, plasmids with histone gene mutations were transformed into JHY311, grown on SC-LEU medium at 30 C, and then colonies were streaked on a 5-FOA plate to select for cells that have ‘looped out’ the pJH33 plasmid. Cells having retained histone mutations were screened by plasmid rescue followed by DNA sequencing. pSA17 or pSA18 was transformed into JHY205 to replace pJH33 and generated SAY2 (*htb1-S10A*) or SAY3 (*htb1-S33A*), respectively. PSA65 or pSA67 was transformed into JHY205 to replace pJH33 and generated SAY168 (*htb1-S10E*) or SAY170 (*htb1-S33E*), respectively.

Yeast strains carrying gene deletions (*STE20*, *STE12*, *STE7*, *KSS1*, *STE11*, *PBS2*, *SSK22*, *SSK2*, *CLA4*, *HOG1*, and *YCA1*) were constructed by PCR amplification of a  $P_{TEF}$  promoter-driven bacterial kanamycin-resistance gene as described by Longtine et al., 1998. PCR products were then transformed into

JHY311 to create strains that lacked the full ORF (ATG-Stop). Correct integration of the marker was confirmed by a series of PCR analysis. These strains include SAY152 (*yca1*Δ::*kanMX6*), SAY153 (*ste11*Δ::*kanMX6*), SAY154(*ste7*Δ::*kanMX6*), SAY155 (*kss1*Δ::*kanMX6*), SAY156(*ssk22*Δ::*kanMX6*), SAY157 (*cla4*Δ::*kanMX6*), SAY158 (*pbs2*Δ::*kanMX6*), SAY159 (*hog1*Δ::*kanMX6*), SAY160 (*ssk2*Δ::*kanMX6*), and SAY148 (*ste20*Δ::*kanMX6*). No morphologic or growth phenotype was apparent between SAY 148 or SAY111 (gift from S.J. Kron). SAY151, a double mutant carrying both H2B S10A and *ste20*Δ::*kanMX6*, was created by transforming SAY2 (*HTB1-S10A*) with PCR product as described (Longtine et al., 1998). The GFP-Ste20 fusion gene under the control of *STE20* promoter was generated by introducing a fragment amplified by PCR, using pSA51 as template, into JHY311 or BY4741 cells to create SAY144 and SAY145, respectively. SAY146 and SAY147 carrying the GST-Ste20 fusion gene under the control of *STE20* promoter (from -405 to -1, 5' to the *STE20* ORF) was generated by introducing a fragment amplified by PCR using pSA52 as template, into JHY311 or BY4741. The GFP-Ste12 (SAY 161) and GFP-Ste7 (SAY162) were generated as described for GFP-Ste20, except that GFP-Ste12 was under the control of *STE12* promoter and GFP-Ste7 was under the control of *STE7* promoter. The gene disruption and epitope tagging in each strain were confirmed by PCR. Ste20<sup>K649R</sup> (SAY150) was constructed using the marker-fusion PCR method as previously described (Kitazono et al., 2002). Genomic DNA from SAY149, in which His3MX6 cassette from pFA6a-His3MX6-P<sub>*STE20*</sub>-GFP (Longtine et al., 1998) was integrated into 100 bp downstream of the *STE20* stop codon (Kitazono et al., 2002), was used as template to generate Ste20<sup>K649R</sup>.

Table 1. Genotypes of yeast strains

| Strain | Genotype  | Source            |
|--------|---|-------------------|
| BY4741 | <i>MATa his3Δ1 leu2Δ0 met15Δ0 ura3Δ0</i>  | Research Genetics |
| JHY205 | <i>MATa his3Δ1 leu2Δ0 met15Δ0 ura3Δ0 hht1-hhf1::KAN hhf-2hht2::NAT hta1-htb1::HPH hta2-htb2::NAT pJH33[CEN URA3 HTA1-HTB1 HHT2-HHF2]</i>  | This study        |
| JHY293 | <i>MATa his3Δ1 leu2Δ0 met15Δ0 ura3Δ0 hht1-hhf1::KAN hhf-2hht2::NAT hta1-htb1::HPH hta2-htb2::NAT pJH53[CEN LEU2 hta1-Δ1-20-HTB1 HHT2-HHF2]</i>                                      | This study        |
| JHY297 | <i>MATa his3Δ1 leu2Δ0 met15Δ0 ura3Δ0 hht1-hhf1::KAN hhf-2hht2::NAT hta1-htb1::HPH hta2-htb2::NAT pJH49[CEN LEU2 HTA1-htb1Δ1-32 HHT2-HHF2]</i>                                       | This study        |
| JHY307 | <i>MATa his3Δ1 leu2Δ0 met15Δ0 ura3Δ0 hht1-hhf1::KAN hhf-2hht2::NAT hta1-htb1::HPH hta2-htb2::NAT pJH57[CEN LEU2 HTA1-HTB1 hht2Δ1-30-HHF2]</i>                                       | This study        |
| JHY311 | <i>MATa his3Δ1 leu2Δ0 met15Δ0 ura3Δ0 hht1-hhf1::KAN hhf-2hht2::NAT hta1-htb1::HPH hta2-htb2::NAT pQQ18[CEN LEU2 HTA1-HTB1 HHT2-HHF2]</i>  | This study        |
| JHY315 | <i>MATa his3Δ1 leu2Δ0 met15Δ0 ura3Δ0 hht1-hhf1::KAN hhf-2hht2::NAT hta1-htb1::HPH hta2-htb2::NAT pJH45[CEN LEU2 HTA1-HTB1 HHT2-hhf2Δ1-27]</i>                                       | This study        |
| SAY2   | <i>MATa his3Δ1 leu2Δ0 met15Δ0 ura3Δ0 hht1-hhf1::KAN hhf-2hht2::NAT hta1-htb1::HPH hta2-htb2::NAT pSA17[CEN LEU2 HTA1-htb1-S10A HHT2-HHF2]</i>                                       | This study        |
| SAY3   | <i>MATa his3Δ1 leu2Δ0 met15Δ0 ura3Δ0 hht1-hhf1::KAN hhf-2hht2::NAT hta1-htb1::HPH hta2-htb2::NAT pSA18[CEN LEU2 HTA1-htb1-S33A HHT2-HHF2]</i>                                       | This study        |
| SAY111 | <i>MATa ura3-52 leu2::hisG ste20Δ::kanMX6</i>   | S. J. Kron        |
| SAY144 | <i>MATa his3Δ1 leu2Δ0 met15Δ0 ura3Δ0 HIS3MX6::P<sub>STE20</sub>-GFP-STE20 hht1-hhf1::KAN hhf-2hht2::NAT hta1-htb1::HPH hta2-htb2::NAT pQQ18[CEN LEU2 HTA1-HTB1 HHT2-HHF2]</i>       | This study        |
| SAY145 | <i>MATa his3Δ1 leu2Δ0 met15Δ0 ura3Δ0 HIS3MX6::P<sub>STE20</sub>-GFP-STE20</i>   | This study        |
| SAY146 | <i>MATa his3Δ1 leu2Δ0 met15Δ0 ura3Δ0 HIS3MX6::P<sub>STE20</sub>-GST-STE20 hht1-hhf1::KAN hhf-2hht2::NAT hta1-htb1::HPH hta2-htb2::NAT pQQ18[CEN LEU2 HTA1-HTB1 HHT2-HHF2]</i>       | This study        |
| SAY147 | <i>MATa his3Δ1 leu2Δ0 met15Δ0 ura3Δ0 HIS3MX6::P<sub>STE20</sub>-GST-STE20</i>   | This study        |
| SAY148 | <i>MATa his3Δ1 leu2Δ0 met15Δ0 ura3Δ0 ste20Δ::HIS3MX6 hht1-hhf1::KAN hhf-2hht2::NAT hta1-htb1::HPH hta2-htb2::NAT pQQ18[CEN LEU2 HTA1-HTB1 HHT2-HHF2]</i>                            | This study        |
| SAY149 | <i>MATa his3Δ1 leu2Δ0 met15Δ0 ura3Δ0 STE20::HIS3MX6</i>   | This study        |
| SAY150 | <i>MATa his3Δ1 leu2Δ0 met15Δ0 ura3Δ0 HIS3MX6::P<sub>STE20</sub>-GFP-Ste20-K649R hht1-hhf1::KAN hhf-2hht2::NAT hta1-htb1::HPH hta2-htb2::NAT pQQ18[CEN LEU2 HTA1-HTB1 HHT2-HHF2]</i> | This study        |
| SAY151 | <i>MATa his3Δ1 leu2Δ0 met15Δ0 ura3Δ0 ste20Δ::HIS3MX6 hht1-hhf1::KAN hhf-2hht2::NAT hta1-htb1::HPH hta2-htb2::NAT pSA17[CEN LEU2 HTA1-htb1-S10A HHT2-HHF2]</i>                       | This study        |
| SAY152 | <i>MATa his3Δ1 leu2Δ0 met15Δ0 ura3Δ0 yca1Δ::HIS3MX6 hht1-hhf1::KAN hhf-2hht2::NAT hta1-htb1::HPH hta2-htb2::NAT pQQ18[CEN LEU2 HTA1-HTB1 HHT2-HHF2]</i>                             | This study        |

| Strain | Genotype  | Source     |
|--------|---|------------|
| SAY154 | MATa <i>his3Δ1 leu2Δ0 met15Δ0 ura3Δ0 ste7Δ::HIS3MX6 hht1-hhf1::KAN hhf-2hht2::NAT hta1-htb1::HPH hta2-htb2::NAT pQQ18[CEN LEU2 HTA1-HTB1 HHT2-HHF2]</i>                       | This study |
| SAY155 | MATa <i>his3Δ1 leu2Δ0 met15Δ0 ura3Δ0 kss1Δ::HIS3MX6 hht1-hhf1::KAN hhf-2hht2::NAT hta1-htb1::HPH hta2-htb2::NAT pQQ18[CEN LEU2 HTA1-HTB1 HHT2-HHF2]</i>                       | This study |
| SAY156 | MATa <i>his3Δ1 leu2Δ0 met15Δ0 ura3Δ0 ssk22Δ::HIS3MX6 hht1-hhf1::KAN hhf-2hht2::NAT hta1-htb1::HPH hta2-htb2::NAT pQQ18[CEN LEU2 HTA1-HTB1 HHT2-HHF2]</i>                      | This study |
| SAY157 | MATa <i>his3Δ1 leu2Δ0 met15Δ0 ura3Δ0 cla4Δ::HIS3MX6 hht1-hhf1::KAN hhf-2hht2::NAT hta1-htb1::HPH hta2-htb2::NAT pQQ18[CEN LEU2 HTA1-HTB1 HHT2-HHF2]</i>                       | This study |
| SAY158 | MATa <i>his3Δ1 leu2Δ0 met15Δ0 ura3Δ0 pbs2Δ::HIS3MX6 hht1-hhf1::KAN hhf-2hht2::NAT hta1-htb1::HPH hta2-htb2::NAT pQQ18[CEN LEU2 HTA1-HTB1 HHT2-HHF2]</i>                       | This study |
| SAY159 | MATa <i>his3Δ1 leu2Δ0 met15Δ0 ura3Δ0 hog1Δ::HIS3MX6 hht1-hhf1::KAN hhf-2hht2::NAT hta1-htb1::HPH hta2-htb2::NAT pQQ18[CEN LEU2 HTA1-HTB1 HHT2-HHF2]</i>                       | This study |
| SAY160 | MATa <i>his3Δ1 leu2Δ0 met15Δ0 ura3Δ0 ssk2Δ::HIS3MX6 hht1-hhf1::KAN hhf-2hht2::NAT hta1-htb1::HPH hta2-htb2::NAT pQQ18[CEN LEU2 HTA1-HTB1 HHT2-HHF2]</i>                       | This study |
| SAY161 | MATa <i>his3Δ1 leu2Δ0 met15Δ0 ura3Δ HIS3MX6::P<sub>STE12</sub>-GFP-STE12 hht1-hhf1::KAN hhf-2hht2::NAT hta1-htb1::HPH hta2-htb2::NAT pQQ18[CEN LEU2 HTA1-HTB1 HHT2-HHF2]</i>  | This study |
| SAY162 | MATa <i>his3Δ1 leu2Δ0 met15Δ0 ura3Δ0 HIS3MX6::P<sub>STE7</sub>-GFP-STE7 hht1-hhf1::KAN hhf-2hht2::NAT hta1-htb1::HPH hta2-htb2::NAT pQQ18[CEN LEU2 HTA1-HTB1 HHT2-HHF2]</i>   | This study |
| SAY163 | MATa <i>his3Δ1 leu2Δ0 met15Δ0 ura3Δ0 yca1Δ::HIS3MX6 hht1-hhf1::KAN hhf-2hht2::NAT hta1-htb1::HPH hta2-htb2::NAT pSA17[CEN LEU2 HTA1-htb1-S10A HHT2-HHF2]</i>                  | This study |
| SAY164 | MATa <i>his3Δ1 leu2Δ0 met15Δ0 ura3Δ0 HIS3MX6::P<sub>STE12</sub>-GST-STE12 hht1-hhf1::KAN hhf-2hht2::NAT hta1-htb1::HPH hta2-htb2::NAT pQQ18[CEN LEU2 HTA1-HTB1 HHT2-HHF2]</i> | This study |
| SAY165 | MATa <i>his3Δ1 leu2Δ0 met15Δ0 ura3Δ0 HIS3MX6::P<sub>STE7</sub>-GST-STE7 hht1-hhf1::KAN hhf-2hht2::NAT hta1-htb1::HPH hta2-htb2::NAT pQQ18[CEN LEU2 HTA1-HTB1 HHT2-HHF2]</i>   | This study |
| SAY168 | MATa <i>his3Δ1 leu2Δ0 met15Δ0 ura3Δ0 hht1-hhf1::KAN hhf-2hht2::NAT hta1-htb1::HPH hta2-htb2::NAT pSA65[CEN LEU2 HTA1-htb1-S10E HHT2-HHF2]</i>                                 | This study |
| SAY170 | MATa <i>his3Δ1 leu2Δ0 met15Δ0 ura3Δ0 hht1-hhf1::KAN hhf-2hht2::NAT hta1-htb1::HPH hta2-htb2::NAT pSA67[CEN LEU2 HTA1-htb1-S33E HHT2-HHF2]</i>                                 | This study |
| SAY172 | MATa <i>his3Δ1 leu2Δ0 met15Δ0 ura3Δ0 ste20Δ::HIS3MX6 hht1-hhf1::KAN hhf-2hht2::NAT hta1-htb1::HPH hta2-htb2::NAT pSA65[CEN LEU2 HTA1-htb1-S10E HHT2-HHF2]</i>                 | This study |
| SAY174 | MATa <i>his3Δ1 leu2Δ0 met15Δ0 ura3Δ0 ste20Δ::HIS3MX6 hht1-hhf1::KAN hhf-2hht2::NAT hta1-htb1::HPH hta2-htb2::NAT pSA67[CEN LEU2 HTA1-htb1-S33E HHT2-HHF2]</i>                 | This study |
| SAY180 | MATa <i>his3Δ1 leu2Δ0 met15Δ0 ura3Δ0 hht1-hhf1::KAN hhf-2hht2::NAT hta1-htb1::HPH hta2-htb2::NAT pSA17[CEN LEU2 HTA1-htb1-K11R HHT2-HHF2]</i>                                 | This study |

| Strain | Genotype  | Source            |
|--------|---|-------------------|
| SAY182 | <i>MATa his3Δ1 leu2Δ0 met15Δ0 ura3Δ0 hht1-hhf1::KAN hhf-2hht2::NAT hta1-htb1::HPH hta2-htb2::NAT pSA17[CEN LEU2 HTA1-htb1-S10A K11R HHT2-HHF2]</i>            | This study        |
| SAY183 | <i>MATa his3Δ1 leu2Δ0 met15Δ0 ura3Δ0 hht1-hhf1::KAN hhf-2hht2::NAT hta1-htb1::HPH hta2-htb2::NAT pSA18[CEN LEU2 HTA1-htb1-S10A K11Q HHT2-HHF2]</i>            | This study        |
| SAY184 | <i>MATa his3Δ1 leu2Δ0 met15Δ0 ura3Δ0 hht1-hhf1::KAN hhf-2hht2::NAT hta1-htb1::HPH hta2-htb2::NAT pSA17[CEN LEU2 HTA1-htb1-S10E K11R HHT2-HHF2]</i>            | This study        |
| SAY185 | <i>MATa his3Δ1 leu2Δ0 met15Δ0 ura3Δ0 hht1-hhf1::KAN hhf-2hht2::NAT hta1-htb1::HPH hta2-htb2::NAT pSA18[CEN LEU2 HTA1-htb1-S10E K11Q HHT2-HHF2]</i>            | This study        |
| SAY186 | <i>MATa his3Δ1 leu2Δ0 met15Δ0 ura3Δ0 hht1-hhf1::KAN hhf-2hht2::NAT hta1-htb1::HPH hta2-htb2::NAT pSA17[CEN LEU2 HTA1-htb1-K16R HHT2-HHF2]</i>                 | This study        |
| SAY187 | <i>MATa his3Δ1 leu2Δ0 met15Δ0 ura3Δ0 hht1-hhf1::KAN hhf-2hht2::NAT hta1-htb1::HPH hta2-htb2::NAT pSA18[CEN LEU2 HTA1-htb1-K16Q HHT2-HHF2]</i>                 | This study        |
| SAY188 | <i>MATa his3Δ1 leu2Δ0 met15Δ0 ura3Δ0 hht1-hhf1::KAN hhf-2hht2::NAT hta1-htb1::HPH hta2-htb2::NAT pSA17[CEN LEU2 HTA1-htb1-S10A K16R HHT2-HHF2]</i>            | This study        |
| SAY190 | <i>MATa ura3-52 leu2::hisG hos3Δ::kanMX6</i>  | Research Genetics |
| SAY191 | <i>MATa his3Δ1 leu2Δ0 met15Δ0 ura3Δ0 ste20Δ::HIS3MX6 hht1-hhf1::KAN hhf-2hht2::NAT hta1-htb1::HPH hta2-htb2::NAT pSA67[CEN LEU2 HTA1-htb1-K11R HHT2-HHF2]</i> | This study        |
| SAY192 | <i>MATa ura3-52 leu2::hisG rpd3Δ::kanMX6</i>  | Research Genetics |
| SAY193 | <i>MATa ura3-52 leu2::hisG hda1Δ::kanMX6</i>  | Research Genetics |
| SAY194 | <i>MATa ura3-52 leu2::hisG hos1Δ::kanMX6</i>  | Research Genetics |
| SAY195 | <i>MATa ura3-52 leu2::hisG hos2Δ::kanMX6</i>  | Research Genetics |
| SAY196 | <i>MATa ura3-52 leu2::hisG hda2Δ::kanMX6</i>  | Research Genetics |
| SAY197 | <i>MATa ura3-52 leu2::hisG hda3Δ::kanMX6</i>  | Research Genetics |
| SAY198 | <i>MATa ura3-52 leu2::hisG gcn5Δ::kanMX6</i>  | Research Genetics |
| SAY199 | <i>MATa ura3-52 leu2::hisG sas32Δ::kanMX6</i>   | Research Genetics |
| SAY200 | <i>MATa ura3-52 leu2::hisG hpa3Δ::kanMX6</i>  | Research Genetics |
| SAY201 | <i>MATa ura3-52 leu2::hisG spt10Δ::kanMX6</i>   | Research Genetics |
| SAY205 | <i>MATa his3Δ1 leu2Δ0 met15Δ0 ura3Δ0 hht1-hhf1::KAN hhf-2hht2::NAT hta1-htb1::HPH hta2-htb2::NAT pSA81[CEN LEU2 HTA1-htb1-P8A-P13A HHT2-HHF2]</i>             | This study        |
| SAY206 | <i>MATa his3Δ1 leu2Δ0 met15Δ0 ura3Δ0 hht1-hhf1::KAN hhf-2hht2::NAT hta1-htb1::HPH hta2-htb2::NAT pSA82[CEN LEU2 HTA1-HTB2-16-htb1Δ1-32 HHT2-HHF2]</i>         | This study        |

| Strain | Genotype  | Source            |
|--------|---|-------------------|
| SAY208 | <i>MATa his3Δ1 leu2Δ0 met15Δ0 ura3Δ0 hht1-hhf1::KAN hhf-2hht2::NAT hta1-htb1::HPH hta2-htb2::NAT pSA84[CEN LEU2 HTA+HTB2-16-S10E-htb1Δ1-32 HHT2-HHF2]</i> | This study        |
| SAY209 | <i>MATa ura3-52 leu2::hisG</i>  | S. Elledge        |
| SAY210 | <i>MATa ura3-52 leu2::hisG sml1Δ::URA3</i>  | S. Elledge        |
| SAY211 | <i>MATa ura3-52 leu2::hisG sml1Δ::URA3 rad53::HIS3</i>  | S. Elledge        |
| SAY212 | <i>MATa ura3-52 leu2::hisG RAD53::TAP::KanMX6</i>   | Research Genetics |
| SAY213 | <i>MATa ura3-52 leu2::hisG sml1Δ::URA3 rad53Δ6-66::HIS3</i>   | This study        |
| SKY10  | <i>MATa/MAT□ ho::LYS2/ho::LYS2 lys2/lys2 ura3/ura3 leu2::hisG/leu2::hisG spo11Δ::URA3/spo11Δ::URA3</i>  | S. Keeney         |
| SKY165 | <i>MATa/MAT□ ho::LYS2/ho::LYS2 lys2/lys2 ura3/ura3 leu2::hisG/leu2::hisG</i>  | S. Keeney         |
| SKY169 | <i>MATa/MAT□ ho::LYS2/ho::LYS2 lys2/lys2 ura3/ura3 leu2::hisG/leu2::hisG ndt80Δ::URA3/ndt80Δ::URA3</i>  | S. Keeney         |

### *Yeast culture conditions*

The induction of yeast apoptosis by hydrogen peroxide (H<sub>2</sub>O<sub>2</sub>) was carried out as previously described in Madeo et al., 1999. Briefly, 1 mM H<sub>2</sub>O<sub>2</sub> was added to yeast cells growing exponentially on YPD medium and after a 200-minute incubation at 30°C with agitation, cells were washed three times with sterilized distilled water. Yeast apoptosis was also induced by 50 mM acetic acid (Ludovico et al., 2001) and 100 µg/ml  $\alpha$ -factor (Severin and Hyman, 2002). Synthetic complete medium (SC) was used for maintaining plasmids and selecting gene replacements (Rose et al., 1990). G418 (Calbiochem) was added to YPD agar at 0.2 mg/mL. As for 5-FOA, 0.5 g of 5-FOA was added to 500 ml of SC medium with 15 g of Bacto-agar.

### *Test for Apoptosis and Immunofluorescence Staining*

The survival rate was carried out as previously described (Madeo et al., 2002). An aliquot of the cultures was counted, diluted in distilled water, and about 1000 cells were plated on YPD plates. After two days of growth at 28°C, colonies were counted.

The cell death analysis was carried out as previously described (Severin and Hyman, 2002). An aliquot of the cultures were incubated with 0.4 mg/ml phloxin B for 5 min, and visualized under 63x objective lens.

For TUNEL staining, yeast cells were fixed with 3.7% formaldehyde and prepared as described (Madeo et al., 1999), except that TUNEL staining kits were purchased from Promega and used as recommended by the manufacturer. For immunofluorescence, cells were fixed with 3.7% formaldehyde, digested with

yeast lytic enzyme and applied to a poly-lysine coated slide. After washing the slide three times with PBS, cells were blocked in 2% goat serum PBS (block) for 1 hour and then incubated with anti-H2BS10ph in block at 37°C. After more washes, cells were incubated for 1 hr in the goat anti-rabbit Cy3-conjugated secondary antibody (Jackson), washed three times, and mounted in Vectashield mounting media containing DAPI. For double staining with TUNEL and anti-H2BS10ph, cells were stained with TUNEL first and then with  $\alpha$ -H2BS10ph.

Annexin V staining assay to detect the exposed phosphatidylserine was carried out as previously described (Madeo et al., 1997).

#### ***Yeast Nuclei and Histone Extraction***

Half a liter of yeast cells were grown to log phase ( $<5 \times 10^7$  cells/ml) in YPD and collected by centrifugation with 3000 rpm at room temperature for 5 min. Cell pellets were washed with 100 ml of water then resuspended in 100 ml of SP (1.1 M sorbitol, 0.02 M PIPES, pH 6.3) plus 0.5 ml of  $\alpha$ -mercaptoethanol. Cells were subjected to spheroplasting by adding 2-4 mg of lytic enzyme (ICN) and incubated at 30°C with slow shaking ( $<120$  rpm). Efficiency of spheroplasting was monitored by percentage of decrease in OD<sub>600</sub> reading of minute amount of cells (10-20  $\mu$ l) suspended in 1 ml of 1% SDS. When 80-90% of the cells were spheroplasted (usually 30 min to 1 hr), the spheroplasts were spun down, washed with 10 ml SPI (SP plus inhibitors for protease and phosphatases including 1 mg/ml of aprotinin, leupeptin, and pepstatin A, 1 mM PMSF, 1  $\mu$ M microcystin-LR, and 0.2 mM p-chloromercuriphenylsulfonic acid). All the procedures hereafter were processed on ice or at 4° C unless noted otherwise.



The spheroplasts were collected by centrifugation and the pellets were resuspended in 20 ml of FPMI (18% Ficoll, 20 mM PIPES, 1 mM  $\text{MgCl}_2$ , pH 6.3 plus protease and phosphatase inhibitors) and transferred to a Dounce homogenizer. Spheroplasts were lysed by <200 strikes with B pestle and then transferred to a centrifuge tube and chilled on ice for 10 min. The released nuclei were separated from the debris and unbroken cells by centrifugation at 3000g for 10 min. The supernatants were carefully transferred to an ultracentrifuge tube (14 x 95 mm, Beckman) and then centrifuged at 50,000g for 30 min (SW-40 rotor, Beckman L7-65). The pellets containing nuclei were resuspended in 10 ml of NP (0.34 M sucrose, 20 mM Tris-HCl, 50 mM KCl, 5 mM  $\text{MgCl}_2$ , pH 7.4 plus protease and phosphatase inhibitors) and centrifuged through a 2 ml sucrose cushion buffer (1.7 M sucrose, 20 mM Tris-HCl, 50 mM KCl, and 5 mM  $\text{MgCl}_2$ , pH 7.4) at 30,000g for 30 min. The resulting nuclei pellets were resuspended in 1 ml of NP buffer and split to 1.5 ml centrifuge tubes before frozen at  $-80^\circ\text{C}$ .

To extract histones, nuclei in 1 ml of NP were washed with 1 ml of buffer A (10 mM Tris-HCl, 0.5% NP-40, 75 mM NaCl, pH 8.0 plus protease and phosphatase inhibitors) extensively by pipetting the pellets up and down. Each washing solution was discarded after 5 min spinning in a benchtop mini-centrifuge. After the final wash, pellets were resuspended in 500  $\mu\text{l}$  of buffer B (10 mM Tris-HCl, 0.4 M NaCl, pH 8.0) and then added gradually with 50  $\mu\text{l}$  of 4 N  $\text{H}_2\text{SO}_4$  and were gently agitated on a rotator for >30 min. The suspension was centrifuged and the histones in the solution were precipitated by adding TCA to 25% final concentration and incubated on ice for >1 hr. Precipitated histones were centrifuged and washed with acetone containing 0.1% HCl

followed by another wash with acetone. The protein pellets are dissolved in 200  $\mu$ l of water and the protein concentration was estimated by measuring OD<sub>218</sub> (0.15  $\mu$ g/ $\mu$ l/OD) or Coomassie Blue staining after SDS-PAGE.

### ***Peptide synthesis and ELISA assay***

Unmodified H2B peptide was synthesized corresponding to residues 4-14 of yeast histone H2B (AEKKPASKAPA). Phosphorylated yeast H2B peptide was synthesized with a single phosphorylated serine residue at position 10 (AEKKPAS[p]KAPA). [p] denotes phosphate. Both peptides contain an artificial cysteine residue at position 15 for coupling to Keyhole limpet hemocyanin for the antibody generation.

ELISA procedures were performed as described (Muller et al., 1987). All antisera were diluted 1:1000. For peptide competition experiments, 100  $\mu$ l of antiserum was incubated with 100 mg of peptide for 1 hr at room temperature prior to ELISA. The bound enzyme conjugate was quantified by turnover of p-nitrophenyl phosphate substrate (Sigma), as described by absorbance at 492 nm.

### ***Western Blot***

Approximately 1.5  $\mu$ g of yeast histone proteins were analyzed by SDS-PAGE on 8% or 15% gels and then transferred to a piece of PVDF membrane (Immobilon-P Millipore) with Towin buffer (192 mM glycine, 25 mM Tris-Cl, 0.1% SDS, and 20% methanol, pH 8.0) by a Semi-dry system (Hoefer). The proteins transferred were examined by Ponceau S staining (0.4% w/v Ponceau S in 2% acetic acid and 8% TCA). The membrane was blocked with 5% non-fat dry milk dissolved in

TBS (20 mM Tris-Cl, pH 7.6, and 137 mM NaCl) at 4°C for overnight or at room temperature for 1 hr. After blocking, the membrane was immersed in 5 % milk/TBS-T buffer (TBS plus 0.1% Tween-20) containing appropriate dilution of desired antibody in a heat-sealable plastic bag and incubated at room temperature for 2hr on a horizontal shaker. Antibodies were diluted as follows: anti-H2BS10ph: 1:5,000, anti-H4: 1:5,000, anti-GST: 1:10,000 (Sigma). Following the primary antibody incubation, the membrane was washed with TBS-T for 10 min three times. The membrane was then incubated with appropriate secondary antibody diluted in 5% milk/TBS-T and incubated for 2 hr at room temperature. A HRP-conjugated rabbit secondary antibody (Amersham Pharmacia) was used as the secondary antibody for the primary rabbit polyclonal antibodies. The membrane was finally washed three times with TBS-T for 10 min and then subjected to chemiluminescence detection by ECL plus kit (Amersham Pharmacia). For an alkaline phosphatase (AP) treatment, histones were incubated with 1  $\mu$ l of shrimp alkaline phosphatase (Promega) at 37°C for 2 hr, boosted with another 1  $\mu$ l of enzyme, and then the incubation continued for another 1-2 hr. Six times concentrated Laemmli sample buffer was added to stop the reaction.

### ***Protein Kinase***

GST-Ste20 and GST-Ste20<sup>K649R</sup> were constructed by PCR using yeast genomic DNA from wild type yeast cells and SAY149 (GST- Ste20<sup>K649R</sup>) and then ligating into pENTRY and then into pDEST15 (GST). The GST fusion proteins were expressed in *E. Coli* strain BL21-Codon Plus (DE3)-RIL(Stratagene) at 30°C for

2hr, bound to glutathione-Sepharose beads, and eluted with glutathione according to the manufacturer's instructions (Amersham).

Kinase assays were performed in 40  $\mu$ L of 20 mM Tris-HCl (pH 7.0), 5 mM MgCl<sub>2</sub>, 1 mM EGTA, 90  $\mu$ M ATP, 0.75  $\mu$ Ci of [<sup>32</sup>P]- $\gamma$ -ATP, and 1  $\mu$ g of recombinant Ste20 or Ste20<sup>K649R</sup>, in the presence of 5  $\mu$ g of the indicated H2B or H3 peptides. After 1 hr incubation at 30°C, 10  $\mu$ L of the reaction mixture was removed and spotted onto P81 filter paper. The filter paper was then washed, dried and subjected to scintillation counting. Alternatively, Ste20 or Ste20<sup>K649R</sup> was incubated as above with either recombinant yeast H2B (2  $\mu$ g), a mixture of acid-extracted yeast free histone (2.5  $\mu$ g) or yeast nucleosomes (0.5  $\mu$ g). Assay mixtures were resolved by SDS-PAGE (15% gels) and processed for autoradiography. For nonradioactive (cold) reactions, no [<sup>32</sup>P]- $\gamma$ -ATP was used and the reactions were run in an SDS-PAGE gel for Western blot analysis.

### *In-Gel Kinase Assay*

The in-gel kinase assay was done as described (Cheung et al., 2003), except that 5  $\mu$ g/ml unmodified (amino acids 4-14 of yeast H2B) or S10-phosphorylated H2B peptides were added to 10% SDS-PAGE gels. In-gel assays were performed as essentially described in Sassone-Corsi et al., 1999). Following electrophoresis, gels were washed in 30 mM Tris-HCl pH 7.4, 1 mM DTT, 0.1 mM EDTA, 20% (v/v) isopropanol for 20 min and this was repeated three times. Gels were then incubated in 8 M urea, 30 mM Tris-HCl pH 7.4, 1 mM DTT, 0.1 mM EDTA for 1 hr. The gel was then immersed in 30 mM Tris-HCl, pH 7.4, 5 mM MgCl<sub>2</sub>, 2 mM MnCl<sub>2</sub>, 1 mM DTT, 100 mM NaCl, 0.05% Tween 40 at 4°C overnight to renature

the proteins. After renaturation, the *in vitro* kinase reaction was performed using 50  $\mu$ Ci of  $\gamma$ -ATP in 30 mM Tris-HCl pH 7.4, 5 mM MgCl<sub>2</sub>, 2 mM MnCl<sub>2</sub>, 1 mM DTT at 30°C for 2 hr. Gels were then stained with Coomassie Blue, destained, and dried for autoradiography.

## CHAPTER 3

# HISTONE MODIFICATION “CROSS-TALK” BETWEEN YEAST H2B SERINE 10 PHOSPHORYLATION AND LYSINE 11 ACETYLATION

### Introduction

Histone proteins are well-known substrates for numerous covalent post-translational modifications. Combinations of post-translational marks on single histones, single nucleosomes and nucleosomal domains can be altered by multiple extracellular and intracellular stimuli, and they in turn convey information that regulates the dynamics of the genome over the lifespan of a cell/organism (Strahl and Allis, 2000; Turner, 2000; Fischle et al., 2003a). In contrast to the straightforward flow of most signal transduction cascades, where the modification of one protein impacts directly on downstream effectors, signaling to and from chromatin appears to be far more complex. Indeed, each core histone, notably H3 and H4, can be post-translationally modified in a remarkably large number of ways, thus generating the potential for histone modification “cross-talk”, defined as positive or negative “communication” between different covalent modifications on one or more histone tails.

As discussed in Chapter 1, the “cross-talk” between post-translationally modified histones occurs at the level of single histone tails (Figure 4).

Phosphorylation of histone H3 at serine 10 (H3S10ph) has been linked, for example, to the acetylation of lysine 14 (H3K14ac) resulting in an open chromatin conformation and gene activation (Cheung et al., 2000; Lo et al., 2001; Figure 4B). Indeed, Snf1 and Gcn5, the enzymes that phosphorylate H3S10 and acetylate H3K14, respectively, appear to work synergistically to mediate these events (Lo et al., 2001; Clements et al., 2003). Serving as an example of cross-talk at the level of the nucleosome, the ubiquitination of yeast H2B K123 by Rad6 has been shown to be a prerequisite for the methylation of H3 on K4 and K79 (Sun and Allis., 2002; Dover et al., 2002; Figure 4C). This specific “cross-talk” is unidirectional since abolishment of H3 K4 methylation has no effect on H2B ubiquitination (Sun and Allis, 2002). As shown in Figure 4A, individual residues such as lysine have many potential states of modification. It is well documented that H3 K9 can be either acetylated or (mono-, di-, tri-) methylated (Zhang and Reinberg, 2000; Bannister et al., 2002). Since different marks on the same site cannot co-exist, they therefore exclude each other and perhaps then influence subsequent modifications made on that histone tail and/or nucleosome.

Previous studies have documented that H2B lysine11 is acetylated (H2BK11ac) in logarithmically-growing yeast (Suka et al., 2001). Since K11 is located adjacent to S10 in H2B, a site that correlates with the yeast cell death, I sought to address whether a potential interplay exists between these two histone modifications in the yeast H2Btail. In this chapter, I show that acetylation of histone H2B at K11 inhibits the phosphorylation of an adjacent site S10, catalyzed by Ste20 kinase, pointing to a mutually exclusive existence of the K11ac and S10ph marks in the tail of H2B. In support, yeast undergoing apoptosis lacked K11 acetylation, but displayed high levels of Ste20-mediated H2BS10ph. In

addition, K11Q, an acetyl-mimic mutant in H2B, failed to activate the apoptotic pathway; in contrast, K11R, a mutant mimicking deacetylation, displayed apoptotic features including H2BS10ph upon induction of H<sub>2</sub>O<sub>2</sub>. Finally, I identified Hos3 as the HDAC responsible for removing the acetyl mark on K11. Together, these findings lend strong support to the general view that a regulatory network of phos/acetyl cross-talk serves to integrate input signals to the tail of yeast H2B controlling a switch from cell proliferation to cell death.



## Results

### *H2B K11R mutants are resistant to hydrogen peroxide-induced yeast apoptosis*

As discussed in Chapter 2, the histone H2B is specifically phosphorylated at S10 in a hydrogen peroxide ( $\text{H}_2\text{O}_2$ )-induced cell death pathway in *S. cerevisiae* (Ahn et al., 2005). As shown in Figure 31A, S10 is located adjacent to K11 in H2B, a site known to be acetylated in growing yeast (Suka et al., 2001). As phosphorylation of the adjacent S10 correlates precisely with the cell death, I sought to address whether a potential interplay (cross-talk) exists between these two histone modifications in the yeast H2B tail. To this end, yeast cells were generated expressing H2B in which K11 was mutated to either glutamine to mimic constitutive acetylation (K11Q), or arginine, to mimic constitutive deacetylation (K11R), in a four-histone plasmid shuffle strain. No growth difference was apparent between these H2BK11 point mutants compared to wild type (WT), as indicated by their growth rate, suggesting that other acetylation events may compensate for lack of H2BK11ac during cell growth.

Upon treatment with 1 mM  $\text{H}_2\text{O}_2$  for 200 minutes, no difference was observed between WT and the H2B K11R mutant with regard to survival properties (Figure 31B). Both strains displayed 20-30% cell viability measured by a plating assay (Figure 31B), followed by 70-80% cell death measured by phloxin B-stained cells (Figure 31C). Interestingly, however, K11Q resulted in a reproducible resistance to  $\text{H}_2\text{O}_2$  with 70-80% cell viability and 20-30% phloxin B-stained cells, comparable to the S10A mutant (Figure 31B and 31C; also see Figure 14). Furthermore, H2BK16, another known acetylation site in yeast H2B (Suka et al., 2001; see Figure 31A), displayed a phenotype similar to WT in both

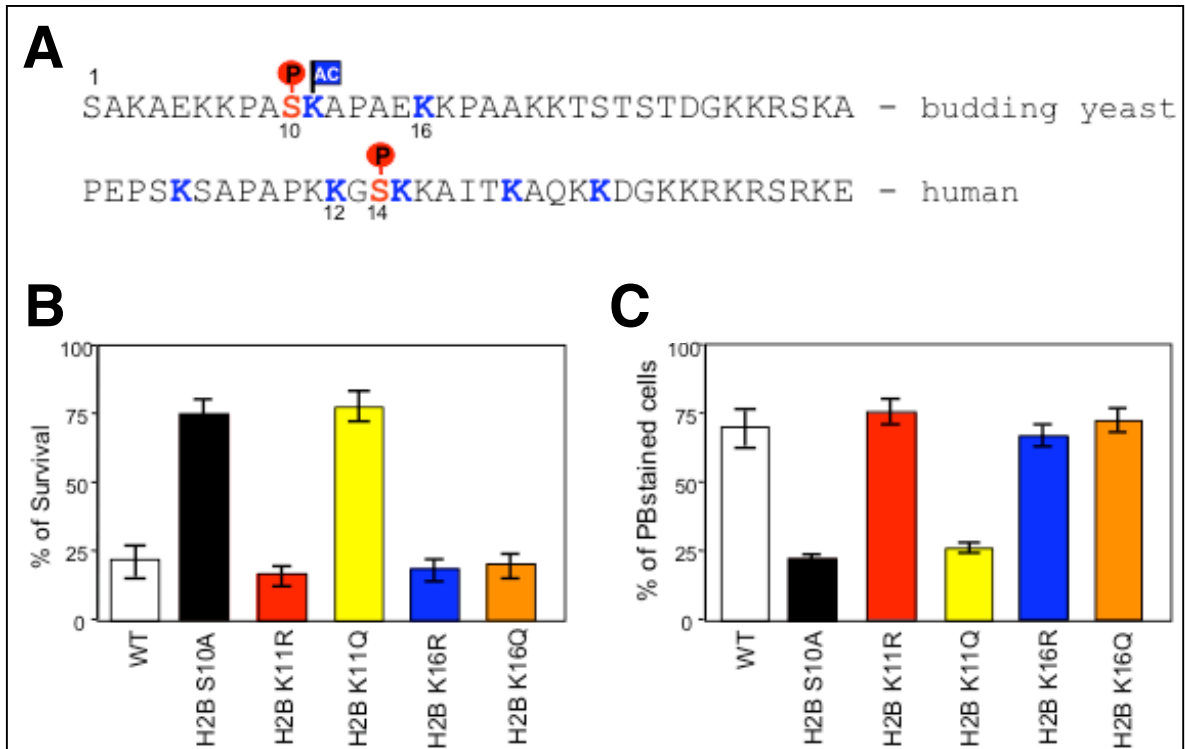


**Figure 31. Histone H2B is specifically deacetylated at lysine 11 in dying yeast cells**

(A) Primary sequence alignment of the amino-terminal tails of yeast and human H2B. In yeast, lysine 11 (K11) is located adjacent to serine 10 (S10), an apoptotic phosphorylation site (Chapter 2). Both K11 and K16 are acetylated in logarithmically-growing yeast (Suka et al., 2001). Note that K15, also known to be acetylated in mammalian cells (Thorne et al. 1990), is also adjacent to a mammalian apoptotic H2BS14ph site (Cheung et al., 2003). Other known acetylation marks are highlighted with blue “Ks”.

(B & C) Exponentially-growing WT, H2B S10A, H2B K11R, H2B K11Q, H2B K16R, and H2B K16Q strains were treated with 1 mM H<sub>2</sub>O<sub>2</sub> for 200 minutes. Cells were then split into two aliquots for cell survival (B), and cell death assays (C). Briefly, cell survival percentage was calculated for each strain by counting number of colonies formed on YPD agar; cell death was measured by counting the number of phloxin B stained cells following H<sub>2</sub>O<sub>2</sub> treatment relative to untreated cells, as described in Figure 11. Note that, while the H2B K11R mutant was as sensitive to H<sub>2</sub>O<sub>2</sub> as WT cells, the H2B K11Q mutant was resistant to H<sub>2</sub>O<sub>2</sub> treatment in either assay.

assays when K16 was mutated to R or Q. (Figure 31B and 31C). These data suggest that K11 in the yeast H2B tail, but not other H2B acetylation sites, needs to be deacetylated as part of a pathway leading to yeast cell death.

### *Characterization of anti-H2BK11ac antibody*

To directly test whether the deacetylation at H2B K11 correlates with cell death, a site-specific H2BK11 acetyl-specific antibody (hereafter anti-H2BK11ac) was used to evaluate the acetylation state of K11 during H<sub>2</sub>O<sub>2</sub>-induced yeast apoptosis. Anti-H2BK11ac antibody was a gift from Dr. Michael Grunstein (University of California; Los Angeles, CA). This antibody was generated against the peptide containing amino acids 8-17 with singly acetylated at K11 (hereafter H2BK11ac peptide; see Figure 31A for the sequence). The specificity of anti-H2BK11ac was analyzed by ELISA as described earlier for anti-H2BS10ph antiserum (see Figure 15 for anti-H2BS10ph). Anti-H2BK11ac reacted strongly with the H2BK11ac peptide, but not the unmodified counterpart (Figure 32A). This reaction was shown to be specific because only the H2BK11ac peptide and not the unmodified peptide competed this signal away (Figure 32A). Anti-H2BK11ac did not recognize the H2BS10ph peptide, but recognized peptide containing dual modification of both S10ph and K11ac (Figure 32A). Further, anti-H2BK11ac failed to react with the histone H2B peptide containing amino acids 12-21 with a single acetyl mark at K16 (H2BK16ac peptide) or a yeast H4 peptide (amino acids 1-22) with a single acetyl mark at K5 (H4K4ac peptide). These data suggest that anti-H2BK11ac specifically recognizes H2BK11ac and not just any acetyl-histone epitope.

Next, I decided to test the hypothesis that yeast H2B is deacetylated at K11 during yeast apoptosis. Nuclei were isolated from logarithmically-growing cells treated with or without H<sub>2</sub>O<sub>2</sub> before histones were extracted and probed by immunoblotting using anti-H2BS10ph and anti-H2BK11ac antibodies (Figure 32B). H2B from logarithmically-grown WT yeast nuclei was recognized by anti-H2BK11ac, but not by anti-H2BS10ph, demonstrating that H2BK11 acetylation is found in growing yeast cells, as expected (Suka et al., 2001). In contrast, H2B from H<sub>2</sub>O<sub>2</sub>-treated WT reacted strongly with anti-H2BS10ph, but not with anti-H2BK11ac (Figure 32B). S10ph was only detected in H<sub>2</sub>O<sub>2</sub>-treated K11R, but not in K11Q (Figure 32B), suggesting that H2BK11ac mark might interfere with the onset of S10ph. Anti-H2BK11ac did not recognize either the K11R or K11Q mutant (Figure 32B), likely due to the lost epitope. However, the H2B K16R mutant displayed H2BS10ph and K11ac behavior (reactivity to both antibodies) similar to WT cells (Figure 32B), suggesting that the induction of H2BS10ph is not affected by acetylation/deacetylation at other known H2Bac sites. In addition, the global acetylation pattern of H3 and H4 appeared to remain the same with or without H<sub>2</sub>O<sub>2</sub> treatment, as judged by anti-H4ac and anti-H3K14ac (Figure 32B), demonstrating that the H<sub>2</sub>O<sub>2</sub>-induced cell death may be specific for H2BK11. These results provided us with an early hint that the changes in yeast histone H2BK11ac and S10ph may be linked in a signaling pathway leading to chromatin compaction during yeast apoptosis.

**Figure 32. Characterization of anti-H2BK11ac antibody**

(A) ELISAs were performed using the H2BK11ac - specific antibody raised against H2BK11ac peptide residues 8-17 (see Figure 31 for the sequence; Suka et al., 2001). For indicated peptide competitions, antibody was incubated with 1 mg/ml competing peptide prior to dilution. Note that the anti-H2BK11ac immunoreacted strongly with the H2BK11ac peptide (amino acids 1-20) or a H2B peptide containing both S10ph and K11ac (amino acids 1-20). Substrate specificity is supported by competition assays showing that only H2BK11ac peptide, and not the unmodified H2B peptide, competes for binding of the antibody.

(B) Exponentially growing WT, H2B K11R, H2B K11Q and H2B K16R strains were treated with 1 mM H<sub>2</sub>O<sub>2</sub> for 200 min. Total nuclear protein was then prepared from these cells before being resolved on SDS-PAGE gel for Western analysis; blots were then probed with anti-H2BK11ac, anti-H2BS10ph, anti-H4ac, anti-H3K14ac, and anti-H3. As expected, anti-H2BS10ph reacted strongly with WT cells following oxidative stress. Note, in contrast, that anti-H2BK11ac only reacted with nuclear extracts from untreated cultures, but did not react with extracts from H<sub>2</sub>O<sub>2</sub>-treated cells. Characterization of this antibody suggests that this failure of antibody reactivity is not due to “epitope disruption” (see above). The level of anti-H4ac and anti-H3K14ac stayed constant in all the nuclear extracts tested. Anti-H3 was used as a loading control.

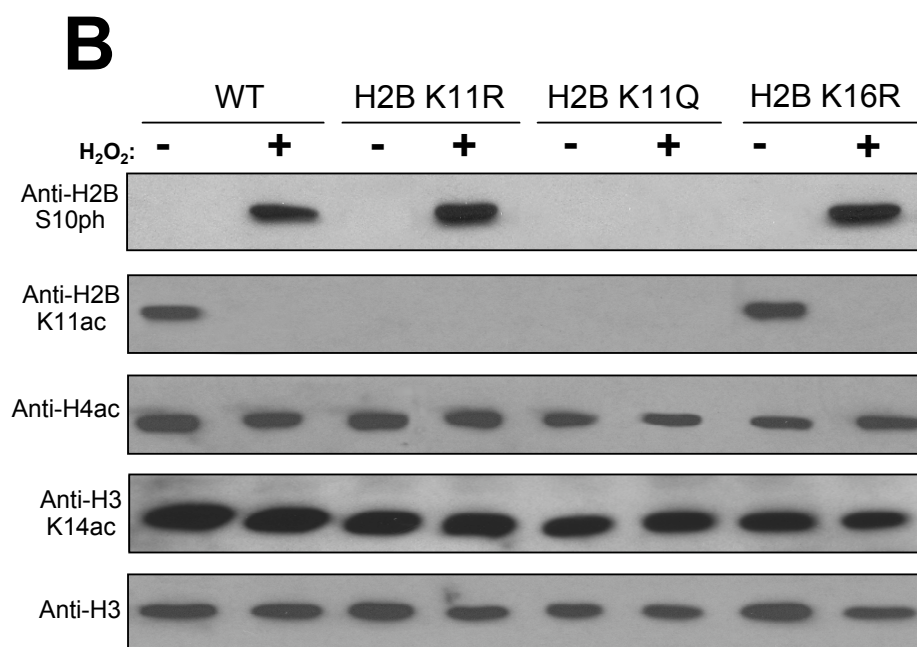
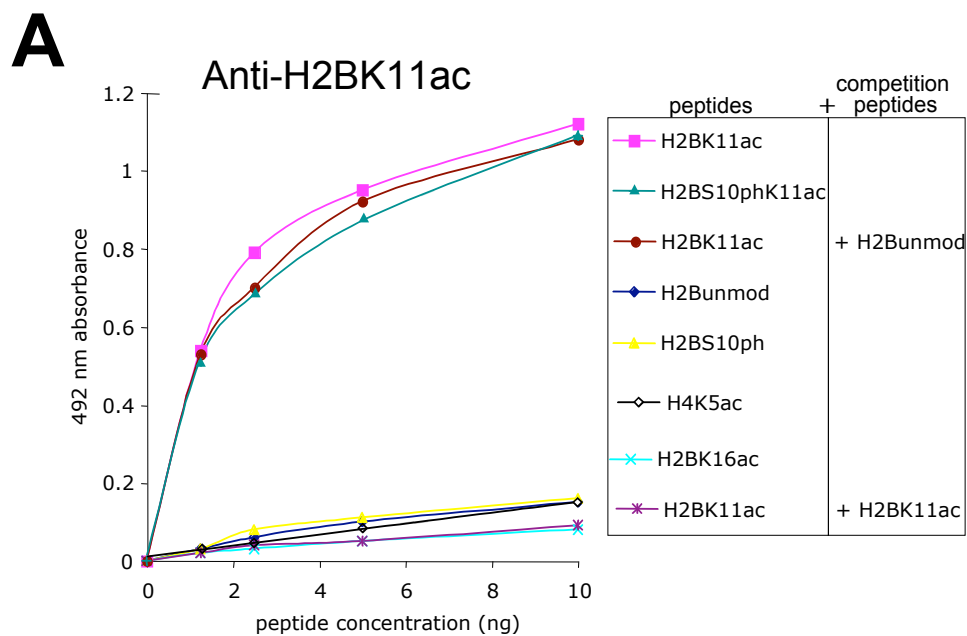
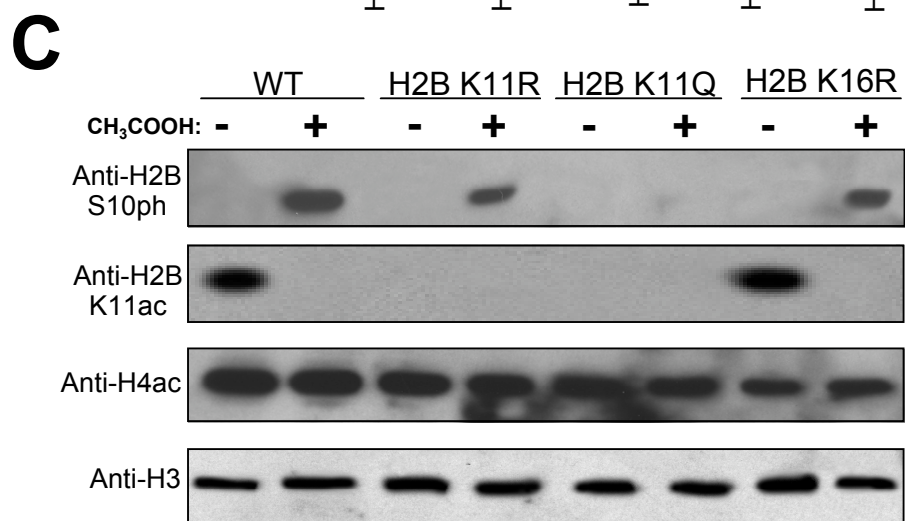
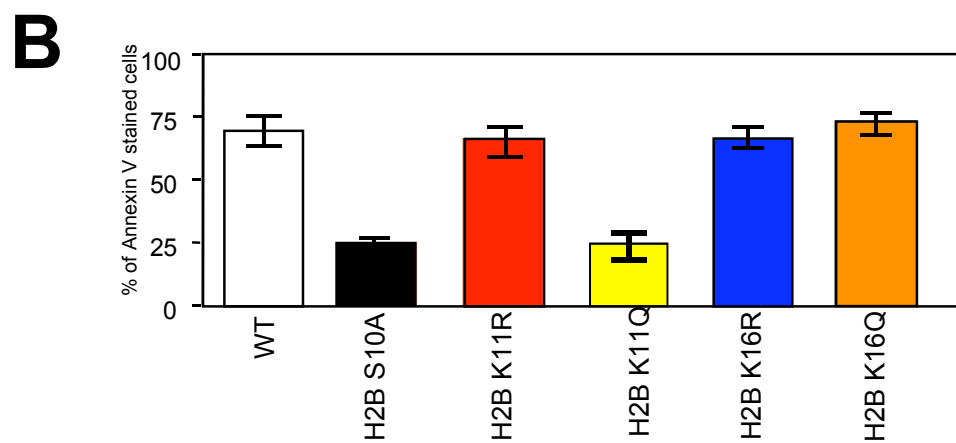
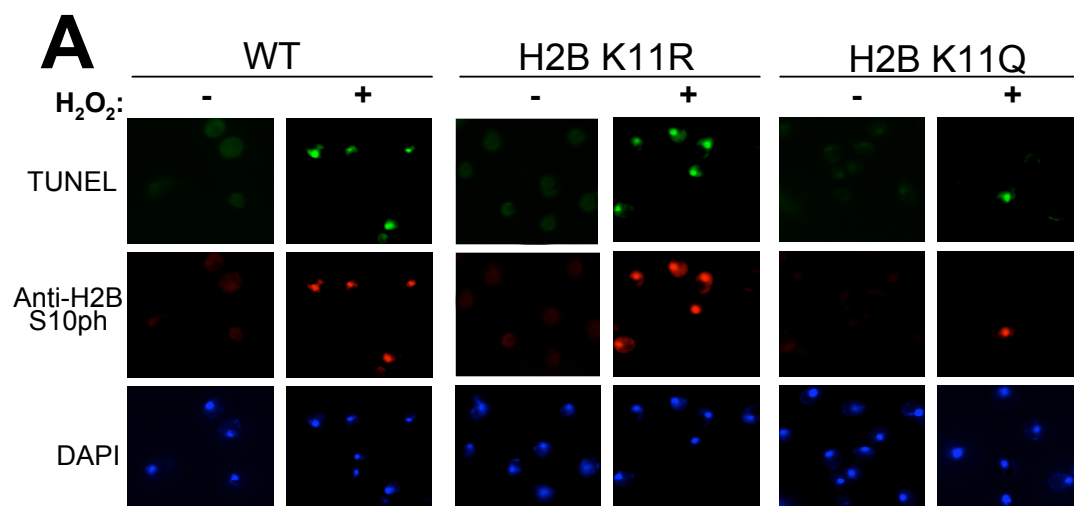


**Figure 33. Cells exhibiting “deacetylation” of histone H2B at K11 display TUNEL-positive DNA fragmentation**

(A) Exponentially-growing WT, H2B K11R, and H2B K11Q strains were treated with 1 mM H<sub>2</sub>O<sub>2</sub> for 200 minutes. Half of the cells were double-stained with TUNEL and anti-H2BS10ph after which cells were counterstained with DAPI for DNA. Cells carrying the H2B K11R mutant displayed immunostaining patterns similar to WT, while the K11Q mutant did not, suggesting that histone H2B K11 is deacetylated during H<sub>2</sub>O<sub>2</sub>-induced yeast apoptosis.

(B) Remaining cells from (A) were stained with Annexin V to measure the externalization of phosphatidylserine (PS), an early marker of yeast apoptosis (Koopman et al., 1994). 75% of WT cells and the K11R mutants displayed externalization of PS, further confirming deacetylation of H2BK11 is required for apoptosis.

(C) Nuclei were prepared from logarithmically-grown WT, H2B K11R, H2B K11Q, and H2B K16R strains that were treated with or without acetic acid, and resolved on SDS-PAGE for Western analysis using anti-H2BK11ac, anti-H2BS10ph, anti-H4ac, and anti-H3. Identical patterns of H2BS10ph and K11ac upon H<sub>2</sub>O<sub>2</sub> treatment (see Figure 32B) were observed with acetic acid. Anti-H3 was used as a loading control.





*Cells exhibiting deacetylation of histone H2B at lysine 11 display apoptotic phenotypes*

To confirm that deacetylation of H2B at K11 occurs specifically in apoptotic cells, H<sub>2</sub>O<sub>2</sub>-treated yeast cells were double-stained with TUNEL and anti-H2BS10ph antibody, and examined by immunofluorescence (IF). In accordance with the loss of cell viability after treatment with H<sub>2</sub>O<sub>2</sub>, about 75% of WT cells showed TUNEL staining, a hallmark of apoptosis (Figure 33A). Consistent with my previous findings in Chapter 2, 100% of the TUNEL-positive cells were co-stained with anti-H2BS10ph, indicating that apoptotic DNA fragmentation correlates precisely with H2B phosphorylation at S10 (Figure 33A). Similar positive staining patterns were observed with the K11R (70% TUNEL staining and anti-H2BS10ph staining; Figure 33A). However, K11Q mutants lacked both apoptotic DNA fragmentation and S10ph, even following H<sub>2</sub>O<sub>2</sub> treatment (20% TUNEL staining and anti-H2BS10ph staining; Figure 33A), suggesting that histone H2B must be deacetylated at K11 in a pathway linked to the formation of condensed apoptotic chromatin. Furthermore, translocation of phosphatidylserine (PS) from the inner to the outer leaflet of membrane, an early event of apoptosis detected by Annexin V staining (Koopman et al., 1994), was prevented in the H2B K11Q mutants (Figure 33B). In contrast, 80% of WT cells and the K11R mutants displayed externalization of PS. These results further confirm that deacetylation at H2BK11 is required for these apoptosis-like properties in yeast.

Because acetic acid can also induce yeast apoptosis (Ludovico et al., 2001; Madeo et al., 1999; Figure 19), I asked whether this apoptotic stimulus could induce the deacetylation of H2BK11. Exponentially-growing WT cells were

incubated with acetic acid, and nuclear extracts were prepared and subjected to SDS-PAGE for Western analysis. As shown in Figure 33C, acetic acid treatment lead to deacetylation at K11 and phosphorylation at S10, demonstrating that the “off/on” behavior of these chromatin marks is induced by a wide range of apoptotic stimuli.

***H2B lysine 11 deacetylation is upstream of serine 10 phosphorylation during yeast cell death***

To determine if an ordered hierarchy existed between H2BK11ac and S10ph, WT cells, induced to undergo apoptosis with H<sub>2</sub>O<sub>2</sub>, were harvested at various intervals for Western blot analysis. As shown in Figure 34, logarithmically growing yeast cells contained acetylated H2B at K11 and this mark was present through 60 minutes of H<sub>2</sub>O<sub>2</sub> treatment. However, after 90 minutes post H<sub>2</sub>O<sub>2</sub>

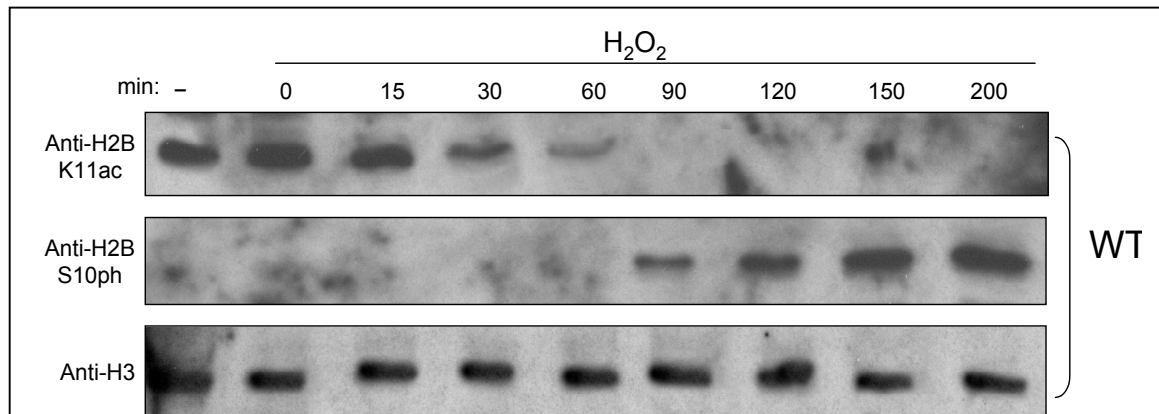


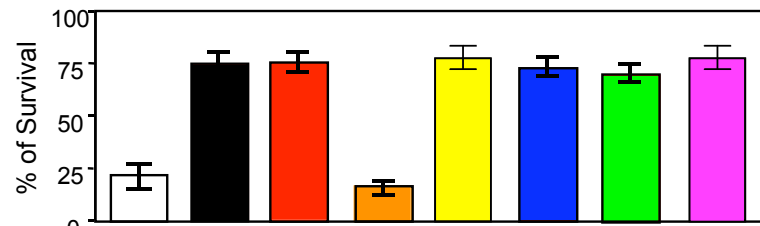
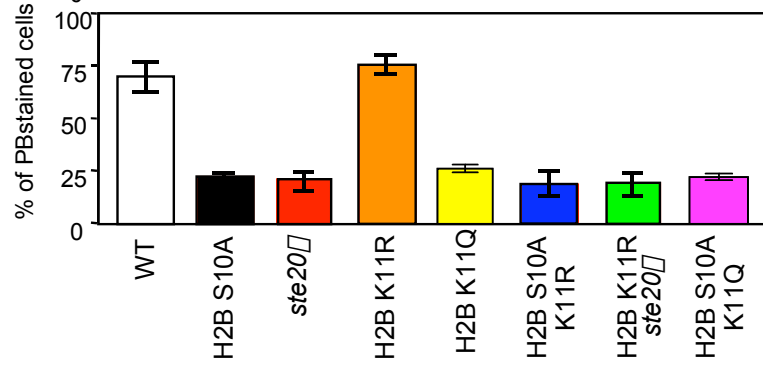
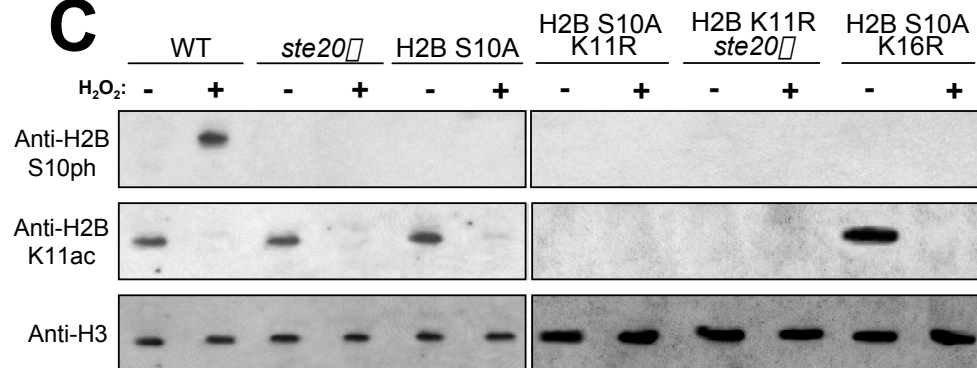
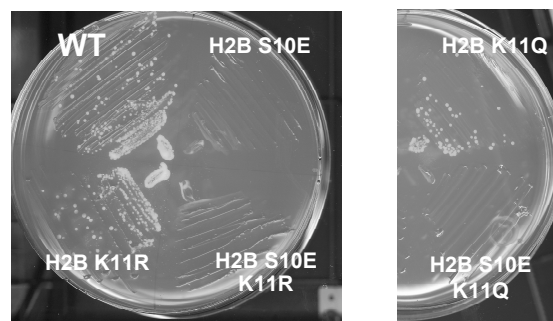
**Figure 34. Deacetylation of H2B lysine 11 precedes H2B serine 10 phosphorylation**

Logarithmically-growing WT cells were harvested after treatment with H<sub>2</sub>O<sub>2</sub> at the indicated times and their nuclear extracts were assayed by Western analysis using anti-H2BS10ph or anti-H2BK11ac. After H<sub>2</sub>O<sub>2</sub> treatment, progressive deacetylation of K11 coincides with the progressive increase in S10ph. Anti-H3 was used as a loading control.

**Figure 35. H2B lysine 11 deacetylation is upstream of H2B serine 10 phosphorylation during yeast apoptosis**

A, B, and C) Exponentially-growing yeast strains were treated with 1 mM H<sub>2</sub>O<sub>2</sub> for 200 minutes and tested for cell survival (A), cell death (B) and histone modifications as probed by modification-selective antibodies (C). Double mutants, carrying either H2B S10A or *ste20*Δ with K11R or K11Q, displayed comparable cell viability and cell death similar to single mutants containing H2B S10A or *ste20*Δ. Together, these results suggest that K11 deacetylation and S10ph act in the same pathway leading to cell death. (C) Immunoblots containing indicated nuclear extracts were probed with anti-H2BS10ph, anti-H2BK11ac, and anti-H3. H2BK11ac was present in logarithmically-growing cells, but not in H<sub>2</sub>O<sub>2</sub>-treated single mutants carrying H2B S10A or *ste20*Δ. None of the double mutants carrying either H2B S10A and K11R or K11R and *ste20*Δ, reacted with anti-H2BS10ph or anti-H2BK11ac.

(D) WT and H2B-mutant yeast strains were grown on YPD agar plates in the absence of H<sub>2</sub>O<sub>2</sub>. H2B S10E mutant, and the double mutant carrying both H2B S10E and K11R or K11Q displayed growth defects, even without H<sub>2</sub>O<sub>2</sub>.

**A****B****C****D**

induction, the disappearance of K11ac coincided with the onset of S10ph in H2B (Figure 34). Thus, it seems likely that H2B phosphorylation occurs after deacetylation of H2BK11 in yeast apoptotic pathway.

Yeast strains carrying mutations that either lack the S10ph site (S10A) or catalytic enzyme (*ste20Δ*) were combined with K11R or K11Q mutations to further assess the sequence of these covalent histone modifications during yeast apoptosis. Cells were treated with 1 mM H<sub>2</sub>O<sub>2</sub> for 200 minutes before cell survival was measured by a plating assay and cell death by phloxin B staining. Although low cell viability was observed with K11R, the double mutants carrying either S10A or *ste20Δ* in combination with K11R displayed similar resistance to H<sub>2</sub>O<sub>2</sub> as single mutants with S10A or *ste20Δ* (Figure 35A and 35B). Moreover, no difference was observed between double mutants carrying both K11Q and S10A or K11Q and *ste20Δ*, as compared to each respective single mutant with regard to survival properties (Figure 35A and 35B). Next, the level of H2B phosphorylation and acetylation were assayed by immunoblotting. As expected, no signal was detected by anti-H2BS10ph with H<sub>2</sub>O<sub>2</sub>-treated yeast double mutant carrying both H2B S10A or *ste20Δ* and each respective single mutant (Figure 35C). Consistent with the acetylation pattern of WT cells, untreated nuclear extracts of H2B S10A or *ste20Δ* or the double mutant carrying both mutations reacted strongly with anti-H2BK11ac (Figure 35C), suggesting that K11ac is not dependent on S10ph by Ste20. Upon H<sub>2</sub>O<sub>2</sub> treatment, only WT nuclear extracts displayed S10ph. K11ac was lost in all the mutants as well as WT (Figure 35C). This result further demonstrates that the inability to phosphorylate S10 does not interfere with the deacetylation of H2BK11, hence hinting that K11 deacetylation is upstream of S10ph during yeast apoptosis.

If the deacetylation of K11 is upstream of S10ph, one would expect that the slow growth of the phospho-mimic of H2BS10 (S10E), would be unaffected by a K11R mutation. As expected from cell viability assays and Western blots (Figure 35A and 35C), double mutants carrying either K11R or K11Q combined with S10E grew poorly on YPD agar plates even without H<sub>2</sub>O<sub>2</sub> treatment, and displayed growth levels similar to a S10E mutant (Figure 35D). Thus, these data indicate that deacetylation of K11 is upstream of S10ph.

### ***Hos3 is the HDAC for acetylated histone H2B lysine 11 during yeast apoptosis***

To identify the HDAC responsible for deacetylation of H2BK11 during yeast cell death, I surveyed HDAC knockout yeast strains and measured their cell viability after H<sub>2</sub>O<sub>2</sub> treatment. Yeast strains lacking Rpd3 (*rpd3Δ*), Hda1 (*hda1Δ*), or Hos3 (*hos3Δ*) were resistant to H<sub>2</sub>O<sub>2</sub> (Figure 36A and 36B), implicating them as possible H2BK11 HDAC candidates. For further analysis, nuclear extracts were prepared from *rpd3Δ*, *hda1Δ*, or *hos3Δ* and tested by immunoblotting with anti-H2BK11ac and anti-H2BS10ph. As shown in Figure 36C, Hos3 was identified as the HDAC for K11, since only the *HOS3* deletion strain failed to remove the K11ac mark after H<sub>2</sub>O<sub>2</sub> treatment. Moreover, the death-related H2BS10ph signal was lost in *hos3Δ*, further supporting that the deacetylation of K11 by Hos3 is upstream of S10ph during yeast apoptosis.

### ***Hos3 deacetylates H2B lysine 11 in vitro***

To further establish a direct role for Hos3 during H<sub>2</sub>O<sub>2</sub>-induced yeast cell death, full-length Hos3 (Hos3), full-length Ste20 (Ste20) and a kinase-dead form of Ste20 (KD; catalytically inactive point mutation K646R), were expressed in bacteria as

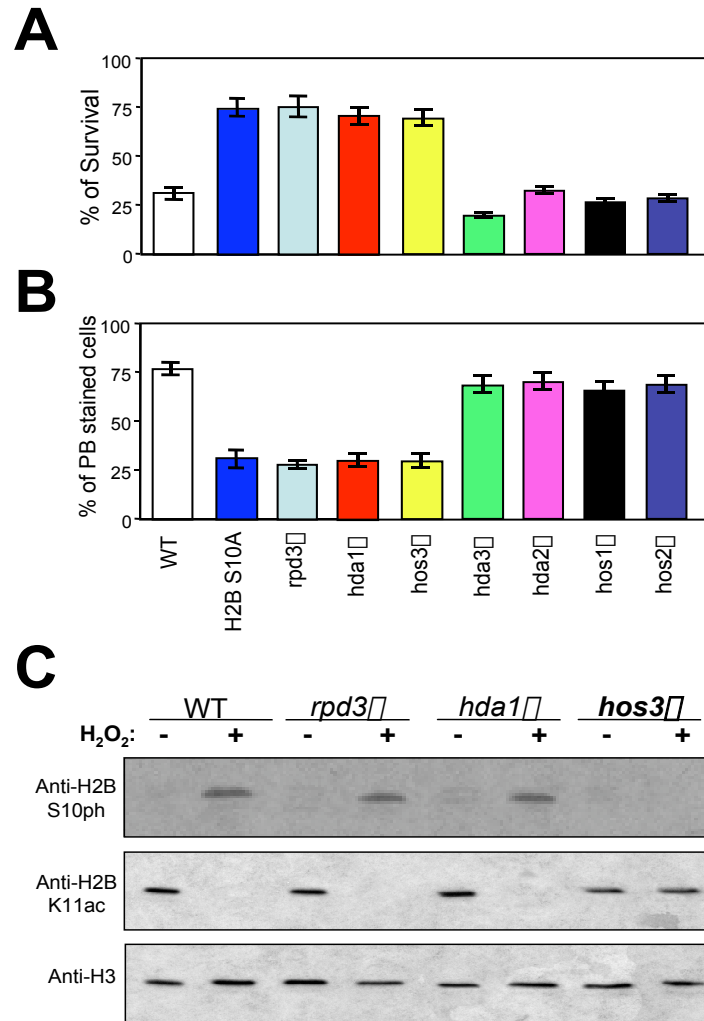


**Figure 36. Hos3 deacetylates H2B lysine 11 during hydrogen peroxide-induced yeast apoptosis**

Yeast HDAC knockout strains were treated with H<sub>2</sub>O<sub>2</sub> and tested for cell survival (A) and cell death (B). Possible HDAC candidates included: Rpd3, Hda1, and Hos3 since their knockout mutants displayed cell viability similar to H2B S10A.

(C) Yeast nuclear extracts from H<sub>2</sub>O<sub>2</sub>-treated or untreated WT, *rpd3*Δ, *hda1*Δ, and *hos3*Δ were probed with anti-H2BS10ph and anti-H2BK11ac. Only the *HOS3* deletion strain fails to remove the acetyl mark on K11 upon H<sub>2</sub>O<sub>2</sub> treatment. Moreover, the death-related H2BS10ph signal was not detected, suggesting that deacetylation of K11 is upstream of S10ph during H<sub>2</sub>O<sub>2</sub>-induced yeast apoptosis.

GST-fusions and purified for both HDAC and kinase assays. The HDAC assay was carried out with recombinant Hos3 and various combinations of H2B peptides at 37°C for 1 hour (Figure 37A). An ordered series of H2B peptide (amino acids 1-20) substrates for these reactions included: unmodified, S10ph, K11ac, or dual-modified at S10ph and K11ac. After quenching the reaction, the peptide substrate was extracted and the recombinant Ste20 was added for the kinase reaction. An identical *in vitro* kinase reaction was performed as described in Chapter 2. The kinase activity was assayed by measuring the incorporation of the [ $^{32}\text{P}$ ] label into peptide substrates (Figure 37A). In the absence of Hos3, Ste20 alone phosphorylated unmodified H2B peptide, but not H2B peptides containing either S10ph, K11ac or both modifications (Figure 37B). In contrast, [ $^{32}\text{P}$ ] incorporation with the K11ac peptide was significantly increased after the addition of both Hos3 and Ste20, supporting the idea that deacetylation of K11 by Hos3 is necessary for Ste20 mediated S10ph. (Figure 37B). Ste20 was not able to phosphorylate S10 in the K11ac peptide when inactive Hos3 was used in the HDAC reaction (Figure 37B). Therefore, these data support that Hos3 is an HDAC responsible for the dephosphorylation of H2B at K11.

The status of deacetylation and the phosphorylation on H2B peptides after the HDAC and kinase reaction were further verified by MALDI-TOF mass spectrometry with the help of Robert Diaz (Figure 37A). Initially, each H2B peptide tested displayed a sharp peak at the position corresponding to their expected molecular mass. For example, unmodified H2B peptide displayed a mass peak at 2721 Da (H2BS10K11 in Figure 37C), H2BS10ph peptide at 2801 Da (H2BS10ph in Figure 37C), H2BK11qc peptide at 2762 Da (H2BK11ac in Figure

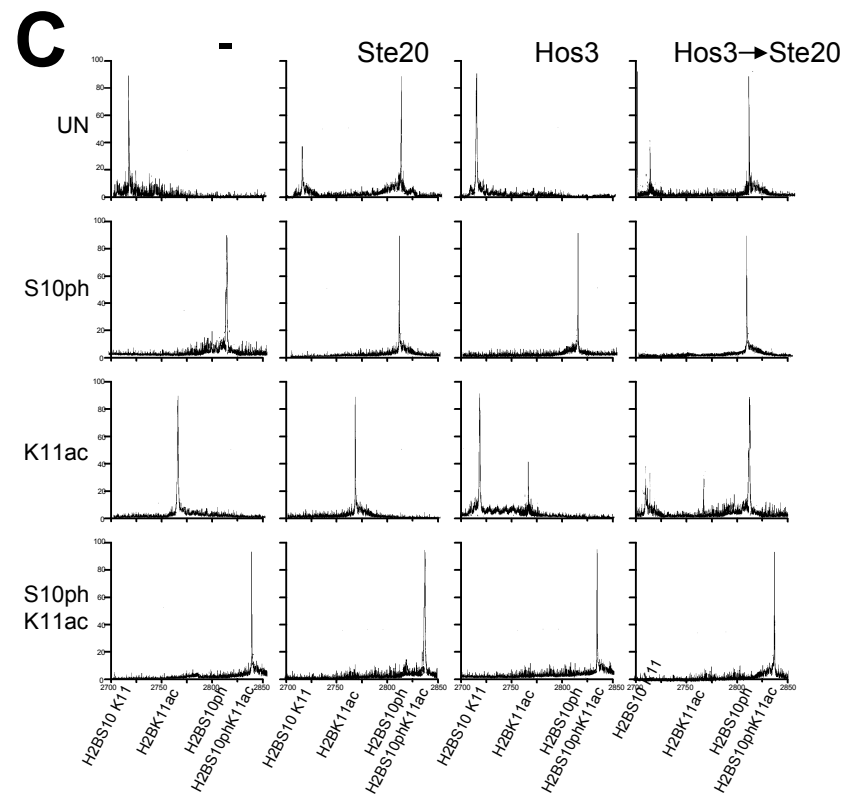
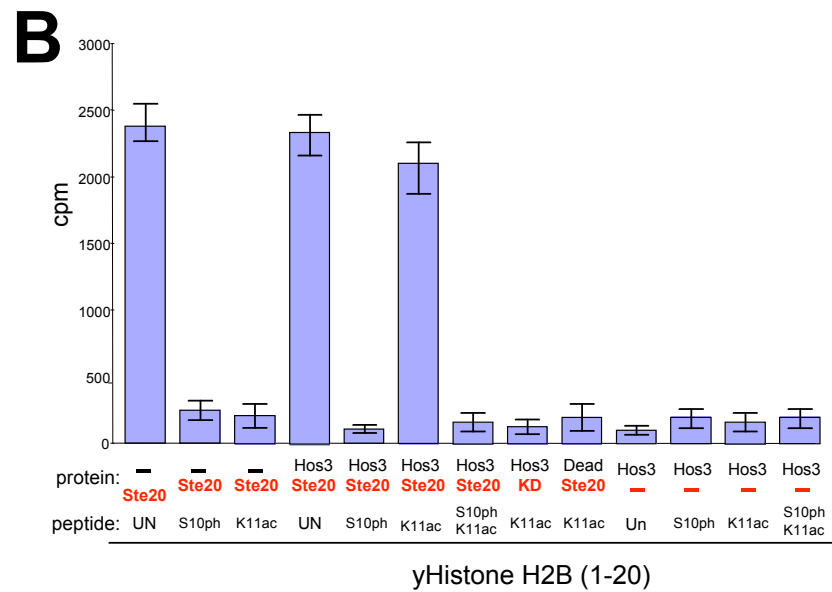
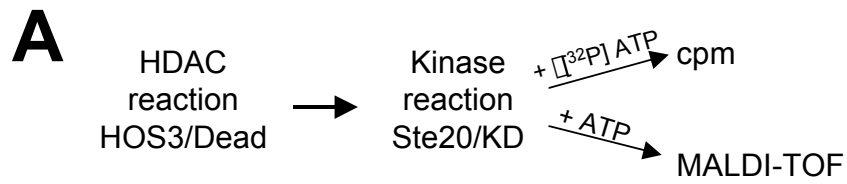


**Figure 37. Hos3 deacetylates H2B lysine 11 and promotes H2B serine 10 phosphorylation by Ste20 *in vitro***

(A) Schematic delineation of an *in vitro* HDAC and Kinase reactions. First, a HDAC reaction was carried out by incubating recombinant active (Hos3) or inactive Hos3 (Dead) with indicated H2B peptides as substrates. The peptides were then extracted and incubated with the recombinant active (Ste20) or inactive Ste20 (KD; Ste20<sup>K646R</sup>) for a kinase reaction. When [<sup>32</sup>P]ATP was used as phosphate source, the kinase activity was assayed by measuring incorporation of the [<sup>32</sup>P]ATP label into peptide substrates by scintillation counting (cpm). For non-radioactive reactions, unlabeled ATP was used instead, and the status of peptide was verified by MALDI-TOF mass spectrometry. As controls, the HDAC and kinase reactions were performed with Hos3 or Ste20 enzyme alone.

(B) *In vitro* HDAC reactions were followed by kinase reactions and carried out using indicated H2B peptides as substrates. For the HDAC reaction, peptides were incubated with recombinant Hos3, or Hos3 inactivated by boiling. After quenching the HDAC reaction, a kinase reaction was performed with recombinant Ste20 at 30 °C for 1 hour in the presence of [<sup>32</sup>P]ATP. The kinase reaction was stopped with the addition of phosphoric acid and spotted onto the filter paper; incorporation of [<sup>32</sup>P] on the substrate peptide was measured by scintillation counting. When H2BK11ac peptide was used as the substrate, incubation with both Hos3 and Ste20 yielded a significant increase in [<sup>32</sup>P] count compared to its incubation with Ste20 alone.

(C) Assays were performed as in (B), except that the *in vitro* kinase assay was carried out using a non-radioactive ATP as phosphate source. After HDAC and kinase reactions, the substrate peptides were analyzed by MALDI-TOF mass spectrometry. The appearance of a peak at 2721 Da corresponds to unmodified H2B peptide (H2BS10K11), at 2762 Da corresponds to acetylated K11 (H2BK11ac), at 2801 Da corresponds to phosphorylated S10 (H2BS10ph), and at 2843 Da corresponds H2B peptide containing dual modification of S10ph and K11ac (H2BS10phK11ac). All peptides tested contain amino acids 1-20 from yeast H2B. The addition of both Hos3 and Ste20 caused loss of peaks corresponding to unmodified and K11ac, but an increase of S10ph when H2BK11ac was used as a peptide substrate.



37C) and H2B peptide containing dual modification of S10ph and K11ac at 2843 Da (H2BS10phK11ac in Figure 37C). While Ste20 kinase was able to phosphorylate S10 in the unmodified peptide, it was unable to phosphorylate the same peptide acetylated at K11 (Figure 37C), further confirming that the acetyl mark on K11 inhibits H2BS10ph. As expected from my *in vivo* experiments (Figure 36C), Hos3 can deacetylate K11ac peptide, but not the unmodified or S10ph peptides (Figure 37C). In addition, I observed a loss of peaks corresponding to the unmodified and K11ac, and the emergence of a new peak at the expected mass for the H2BS10ph after sequential addition of Hos3 and Ste20 to the K11ac peptide (Figure 37C). Interestingly, with the H2B peptide containing both modifications of S10ph and K11ac, its mass profile remained the same even after incubation with Hos3, Ste20, or both enzymes (Figure 37C). These results are consistent with the notion that that K11ac and S10ph do not co-exist on the same H2B as part of signaling pathway leading to chromatin compaction during yeast apoptosis. Instead, my *in vivo* and *in vitro* data are most consistent with the idea that H2BK11ac mark is removed by Hos3 and effectively creates a substrate for Ste20 kinase to mediate H2BS10ph during yeast apoptosis (see Discussion and Figure 38).

## Discussion

“Cross-talk” between histone modifications postulates that covalent modifications can “communicate” between each other to specify unique downstream functions (Fischle et al., 2003a). Indeed, emerging evidence documents that histone modifications, often adjacent or nearby one another within a single histone tail, serve to regulate important signaling events that ultimately govern downstream chromatin and chromosome function (Fischle et al., 2003a). Perhaps the best documented cross-talk events are those that occur on a short stretch of the histone H3 tail, including various combinations of acetylation, methylation and phosphorylation marks on residues K9, S10 and K14 (Barratt et al., 1994; Cheung et al., 2000; Fischle et al., 2005).

Here, I extend this phenomenon by uncovering a cross-talk relationship between two neighboring residues within H2B that play an essential role in regulating yeast apoptosis, K11ac and S10ph. In keeping with earlier findings (Suka et al., 2001), H2BK11ac is found in asynchronously-growing yeast cells. However, I demonstrate that this mark blocks Ste20’s ability to phosphorylate its adjacent site, S10 (Figures 35 and 37). I further demonstrate that deacetylation of K11 occurs upon oxidative stress ( $H_2O_2$ ), mediated by the HDAC Hos3, an event upstream of H2BS10ph in yeast’s apoptotic cascade (Figure 36). In addition, K11Q, an acetyl-site mimic mutant, failed to activate the apoptotic pathway even in the addition of  $H_2O_2$ , whereas K11R, a mutant that can not be acetylated, displayed pronounced apoptotic features and induced H2BS10ph upon  $H_2O_2$  treatment (Figures 31 and 33). Based upon these findings, I propose a model for regulated cross-talk in H2B wherein Hos3 directly catalyzes the deacetylation of

H2BK11 that, in turn, mediates H2BS10ph by Ste20 kinase during H<sub>2</sub>O<sub>2</sub>-induced yeast cell death (see Figure 38).

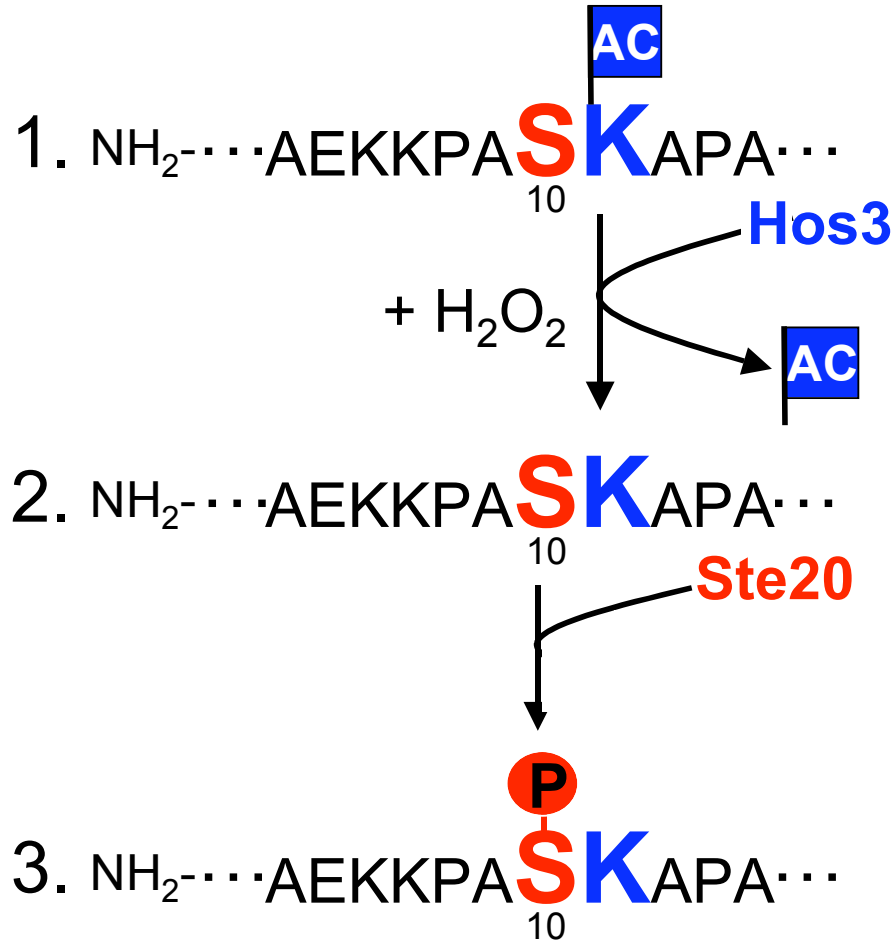


**Figure 38. Model for histone H2B “phos/acetyl cross-talk” (S10/K11) during hydrogen peroxide-induced yeast apoptosis**

K11 in H2B is acetylated in exponentially-growing yeast cells. Upon H<sub>2</sub>O<sub>2</sub> treatment, Hos3 HDAC directly catalyzes the deacetylation of H2BK11. This in turn, mediates H2BS10 phosphorylation by Ste20 kinase, which then leads to the activation of the yeast apoptotic cascade. We envision that deacetylation of K11 is required for H2BS10 phosphorylation (see text and discussion for details).

### ***Hos3 is the HDAC for lysine 11 during H<sub>2</sub>O<sub>2</sub>-induced yeast apoptosis***

HDACs, such as Rpd3, Hda1 and Hos3, are members of large, multi-protein complexes, which require specialized subunits within each complex for activity of the catalytic subunit (Rundlett et al., 1996; Kasten et al., 1997; Suka et al., 1998). Unlike Rpd3 and Hda1, Hos3 has intrinsic catalytic activity as a homodimer when expressed in *Escherichia coli* in the absence of other deacetylase complex components (Carmen et al., 1999). Early *in vitro* studies have suggested that Hos3 has specificity for various sites in each of the core histones, including H2B site at K11. Here, I demonstrate that Hos3 has histone deacetylase activity specifically on H2BK11 during H<sub>2</sub>O<sub>2</sub>-induced yeast apoptosis *in vivo* (Figures 36 and 37).

Interestingly, Rpd3 and Hda1 are also involved in H<sub>2</sub>O<sub>2</sub>-induced yeast apoptosis according to the cell survival assay (Figure 36). Although these HDACs have been shown to deacetylate H2BK11, as well as other acetylation sites in H3 and H4, during transcriptional repression (Suka et al., 2001; Wu et al., 2001), they do not seem to exhibit HDAC activity towards histone H2BK11 during yeast apoptosis. Rpd3 and Hda1 may deacetylate other histone or non-histone substrates that play an indirect role in yeast apoptosis. Since both Rpd3 and Hda1 regulate transcriptional silencing (Rundlett et al., 1996; Rundlett et al., 1998; Wu et al., 2001), they may, for example, repress transcription of an apoptotic regulator(s) that, in turn, acts in the apoptotic pathway.

### ***The existence of “cross-talk” between H2B serine 10 and lysine 11***

In this chapter, I provide *in vivo* and *in vitro* evidence for cross-talk between two histone neighboring residues (S10 and K11 of H2B) acting in a poorly

appreciated pathway leading to chromatin condensation in dying yeast cells as result of oxidative stress stimuli. My combined kinetic, biochemical and genetic experiments suggest that a pre-existing K11ac mark antagonizes Ste20-mediated phosphorylation at S10 in H2B. Moreover, I have identified Hos3 as a H2B K11 deacetylase that is induced upon oxidative stress and functions to remove this antagonistic acetyl mark from the H2B tail.

As shown in Figure 31A, numerous lysines are found around the mammalian H2BS14, a previously-characterized apoptotic phosphorylation site mediated by Mst1 kinase (Cheung et al., 2003) that in many ways acts similarly to S10 in yeast H2B. In particular, K15, located adjacent to S14, is acetylated in asynchronously-growing HeLa cells (Thorne et al., 1990) reminiscent of H2BK11ac in growing yeast (Suka et al., 2001). I suggest the intriguing possibility that phos/acetyl cross-talk also exists in mammalian cell H2B between S14 and K15.

### *Role of H2BK11 acetylation/deacetylation*

Previously, H2BK11 has been identified as one of the acetylation sites that correlate closely with euchromatin formation during transcriptional activation (Suka et al., 2001). Here, I have shown that deacetylation of H2BK11 correlates with the activation of the yeast apoptotic pathway including DNA fragmentation and chromatin compaction. Interestingly, H2B K11R, which is generally believed to mimic the deacetylated state of K11, did not display any growth defect (data not shown). One potential explanation for this observation is that other potentially-redundant acetylation sites may compensate for the loss of H2BK11ac. In growing yeast, at least six lysines is reported to be acetylated in

yeast core histones (Waterborg, 2000), and many of these sites of acetylation have been mapped using site-specific antibodies (Suka et al., 2001). Other studies have suggested that more flexible acetylation “charge patches” may govern chromatin function, which are not tied to specific residues (Dion et al., 2005; Ren and Gorovsky, 2001). My studies, however, provide a suggestion that H2BK11ac may serve a negative role governing H2BS10ph that is not provided by other acetylation sites such as H2BK16ac. The recent evidence of methyl/phos “switches” on H3K9me and H3S10ph (Fischle et al., 2005) lend support to the general concept that adjacent modification, or those that are extremely close within a short stretch, may be more attractive candidates for potential histone cross-talk regulation.

In summary, my studies provide *in vivo* evidence for histone modification cross-talk between H2BS10ph and K11ac. Not only do my results further elucidate the budding yeast apoptotic signaling mechanism by defining a novel role of Hos3 and deacetylation of H2BK11, but also underscore a critical interplay between different histone modifications on multiple structural and functional levels.



## Materials and Methods

### *Plasmids, Yeast strains and Culture Conditions*

Plasmid pQQ18 (CEN *LEU2*, CEN, *HTA1-HTB1-HHF2-HHT2*) was used to generate histone mutant plasmids; pSA70 (*htb1-K11R*), pSA71 (*htb1-K11Q*), pSA72 (*htb1-S10A K11R*), pSA73 (*htb1-S10A K11Q*), pSA74 (*htb1-S10E K11R*), pSA75 (*htb1-S10E K11Q*), pSA76 (*htb1-K16Q*), pSA77 (*htb1-K16R*), pSA78 (*htb1-S10A K16R*). These mutants were created by PCR and sub-cloned into pQQ18 as previously described in Mutations in histone genes (Chapter 2; Materials and Methods).

Yeast strains are listed in Table 1 and all strains are derived from S288C (BY4741; Research Genetics) background. Strain JHY205 was used to shuffle in plasmids containing histone H2B K11 or H2B K16 mutations (pSA60 through pSA68) using 5-FOA as a counterselecting agent for the URA3 plasmid. SAY191, a double mutant carrying both H2B K11R and *ste20 $\Delta$ ::kanMX6*, was created by transforming pSA60 plasmid into SAY148 (*ste20 $\Delta$ ::kanMX6*). Transformation of yeast cells was performed by the lithium acetate procedure, as described in Yeast transformation (Chapter 2; Materials and Methods).

### *Test for Apoptosis*

Yeast apoptotic induction by H<sub>2</sub>O<sub>2</sub> and acetic acids were carried out as described in Yeast culture conditions (Chapter 2; Materials and Methods). The cell survival, cell death analysis, TUNEL staining and immunofluorescence were done as described (Chapter 2; Materials and Methods).

### ***Yeast Nuclei and Histone Extraction, and Western Blot***

Yeast nuclei were prepared before histones were extracted as described in Chapter 2. Approximately 1.5  $\mu$ g of yeast histone proteins were analyzed by SDS-PAGE on 8% or 15% gels followed by Western blot analysis. HRP-conjugated rabbit secondary antibody (Amersham Pharmacia) was used. For chemiluminescence, the ECL plus kit (Amersham Pharmacia) was used for detection. For alkaline phosphatase (AP) treatments, histones were incubated with 1  $\mu$ L of shrimp alkaline phosphatase (Promega) at 37°C for 2 hr, boosted with another 1  $\mu$ L of enzyme, and then the incubation continued for another 1-2 hr. Six times concentrated Laemmli sample buffer was added to stop the reaction.

### ***Peptides Synthesis***

H2B peptides (amino acids 1-20 from yeast; SAKAEKKPASKAPAEKKPAA) were synthesized at the Rockefeller University Proteomics Resource Center. These peptides include; unmodified, phosphorylated at S10, acetylated at K11, or dual-modified at S10ph and K11ac. These peptides contain an artificial biotinylated residues at position 21 for linking to streptavidin beads or fluorescent dye.

### ***HDAC and Kinase Assays and MALDI-TOF***

GST-Ste20 and GST-Ste20<sup>K649R</sup> were purified as previously described in Chapter 2. The full-length Hos3 gene was cloned as described in Carmen et al., 1999. First, Hos3 was amplified by PCR, using oligonucleotide primers that added Bam HI

and Sma I sites then cloned into the Stratagene *E. coli* expression vector pCALn. The resulting plasmid was transformed and expressed in the *E. coli* strain BL21(DE3)pLysS. Cells with the HOS3 enzyme or vector alone were grown at 37° C in 2 liters of LB liquid medium plus ampicillin to OD<sub>600</sub> 0.4 and then induced with 1 mM isopropyl  $\beta$ -D-thiogalactoside for 2 hr at 30° C. Cells were harvested and resuspended in lysis buffer (50 mM Tris-HCl, pH 8, 250 mM NaCl, 2.5 mM DTT, 1.0 mM magnesium acetate, 1.0 mM imidazole, 2.0 mM PMSF) at 4°C. Cells were lysed by sonication and then centrifuged in a Beckman 45Ti rotor at 40,000 rpm for 45 min. The fusion protein was affinity-purified on calmodulin affinity resin (Stratagene) according to the manufacturer's instructions except that the wash and elution buffers contained 400 mM NaCl. This material was concentrated in vacuum dialysis in buffer DBHS (50 mM Tris, pH 8.0, 500 mM NaCl, 10  $\mu$ M ZnCl<sub>2</sub>, 2.5 mM DTT). The concentrated enzyme was purified further on a Superdex-200 column in the DBHS buffer. Hos3 was boiled for 30 min to inactivate the enzyme.

HDAC reaction was carried out before the kinase reaction. HDAC assay was carried out as described in Carmen et al., 1999. 2  $\mu$ g of recombinant active or inactive HOS3 enzyme was incubated with various histone substrates (5  $\mu$ g) in a 40  $\mu$ l reaction containing: 75 mM Tris-HCl, pH 7.0, 275 mM NaCl, 2.0 mM 2-mercaptoethanol, and 0.1 mM EDTA. The reactions were incubated at 30°C for 2 hr before adding 1 M HCl and 0.16 M acetic acid (50  $\mu$ l). The peptide substrate was extracted and the recombinant Ste20, Ste20<sup>K649R</sup> (KD), or no enzyme was added for the kinase reaction as indicated. Kinase assays were performed as described in Chapter 2. The reaction mixture was removed and spotted onto P81

filter paper. The filter paper was then washed, dried and subjected to scintillation counting.

Analysis of histone peptides was performed after the HDAC and kinase reactions as described above, except this time, unlabeled ATP was used instead of [ $^{32}\text{P}$ ]-ATP for the kinase reaction. 0.5  $\mu\text{l}$  alpha cyano-4-hydroxycinnamic acid (HCCA) was spotted on a Maldi plate followed by 2  $\mu\text{l}$  of each reaction, and analyzed on a Voyager DE-STR (Applied Biosystem) on reflector mode.

## CHAPTER 4

# THE ROLE OF THE H2B SERINE 10 PHOSPHORYLATION IN CHROMATIN FIBER FOLDING

### Introduction

The chromatin fiber is a dynamic macromolecular entity that is intimately involved in nuclear functions. Chromatin fiber allows the compression of meters of DNA molecules into a few micrometers of a cell's nucleus. This is accomplished by the folding of nucleosomes in 10 nm "bead-on-a-string" conformation into the 30-nm or condensed chromatin fiber (Figure 1). Once thought of solely in terms of chromosomal DNA packaging in the nucleus, chromatin fiber condensation is now recognized as having widespread biological functions, such as DNA replication, mitosis, meiosis, DNA repair and apoptosis (Fletcher and Hansen, 1996; Annunziato and Hansen, 2000). For example, the conformational dynamics of the chromatin fiber yields heterochromatin and euchromatin, which serve as a platform for transcriptional repression and activation in dividing cells (Rusche et al., 2003; Alvarez et al., 2003). Unique chromatin changes reminiscent of chromatin fiber compaction are also observed during apoptosis (Chapter 2), but the molecular determinants and mechanisms responsible for chromatin fiber dynamics remain elusive.

In order to understand the mechanism of chromatin condensation, the *in vitro* self-assembly system for nucleosome array is commonly used; recombinant, histone proteins that lack post-translational modification are combined with DNA of defined-sequence and undergo a reversible cation-dependent compaction in response to change in solution conditions (Hansen et al., 1989; Garcia-Ramirez et al., 1992; Schwarz and Hansen, 1994). Since the degree of chromatin fiber compaction depends strongly on the valency (mono or divalent cations) and concentration of salt present in the buffer (Ris and Kubai, 1970), it may be measured by a sedimentation velocity experiment using analytical ultracentrifugation following changes in the sedimentation coefficient upon addition of salt (Hansen et al., 1989). For divalent cations, concentrations in the 1-2 mM range are sufficient to induce compaction equivalent to that of the compacted 30-nm chromatin fiber, whereas monovalent ions compact the chromatin fiber at a 100 mM concentration (Hansen et al., 1989; Garcia-Ramirez et al., 1992; Schwarz and Hansen, 1994). As removal of salt re-establishes a single 10-nm diameter decondensed chromatin fiber (Hansen, 2002), all the transitions in the folding and self-association pathway are apparently reversible. Thus, the mechanisms and determinants of chromatin fiber dynamics characterized in this *in vitro* system have some relevance to *in vivo* events.

The consequences of histone modification on chromatin fiber are likely to be of key importance in regulating the folding of chromatin. In the case of hyperacetylation, it has been suggested that charge neutralization in structurally important regions of the histone tail offers a direct link to euchromatin structure (Tse et al., 1998; “cis” mechanism; Figure 6A). Although, most other modifications still lack a complete mechanistic explanation, it is generally

assumed that they serve as recognition modules for chromatin modification factors such as remodeler complexes, heterochromatin propagating proteins or the transcription machinery (Fischle et al., 2003b; “trans” mechanism; Figure 6B). In support of the cis mechanism of histone tail function, Dr. Timothy Richmond’s group (ETH Zurich, Switzerland) has shown that a “basic patch” of the H4 tail (residues 14-19) is sufficient to induce condensed chromatin structures (Dorigo et al., 2003). This result suggests that histone tails can directly establish the internucleosomal contacts and histone/DNA interactions that mediate chromatin condensation. This study elegantly demonstrated for the first time that histone tails are critically required for full fiber folding using the *in vitro* nucleosome array system, however, the influence of covalent histone modification within this basic stretch was not addressed. Recently, the acetylation of H4K16 was found to directly contribute to the decondensed chromatin *in vitro* (Shogren-Knaak et al., 2006). Taken together, these results reinforce that the covalent modification status of the core histone tail domains can regulate the higher-order chromatin structure.

As discussed in Chapter 2, yeast cells carrying a phospho-mimic H2BS10 mutation (S10E), but not a non-phospho mimic H2B S10A mutation, induced “constitutive” formation of condensed chromatin, suggesting that H2BS10ph mediates the chromatin condensation, a hallmark of apoptosis. In this chapter, I sought to gain a mechanistic insight into chromatin compaction mediated by H2BS10ph. I have found that peptides corresponding to the phosphorylated form of yeast H2B and human H2B (phosphorylated at S10 and S14, respectively) have the intrinsic mobility retardation in SDS-PAGE gel in accordance with cis mechanism (Cheung et al., 2003; Figure 39). This peptide mobility retardation

and cell death/apoptotic chromatin condensation function of H2BS10ph is dependent on the close proximity of proline residues (P8 and P13 in yeast H2B). In addition, *in vitro* nucleosome arrays carrying yeast H2B S10E or human H2B S14E affect nucleosomes to form the compacted chromatin fiber, as measured by analytical ultracentrifugation. This compaction is not dependent on linker histone H1, which was previously shown to influence the formation of chromatin fiber. Interestingly, the H2B N-terminus (amino acids 2-16) appears to function as a modular signaling “cassette,” since S10A and S10E H2B point mutations function in the context of a new histone tail as well as they do in the natural H2B tail. Together, these results support the idea that H2BS10ph plays a role in mediating chromatin condensation.



## Results

### *H2BS10ph peptide displays an intrinsic “aggregation” property in vitro*

Mammalian H2BS14ph peptide has been reported to migrate slower than its unmodified counterpart on a standard SDS-PAGE gel (Cheung et al., 2003). Since both yeast and mammalian H2B phosphorylation (S10 and S14, respectively) correlate with apoptosis in each respective organism, I decided to test whether this unusual migration property in H2BS14ph peptide extends to yeast H2B peptide. To this end, the unmodified and the H2BS10ph (amino acids 4-14) peptides were resolved on a 12% SDS-PAGE gel followed by coomassie staining. Similar to H2BS14ph peptide, H2BS10ph peptide showed slower migration compared to its unmodified counterpart (Figure 39B). The unmodified peptide migrated to a band corresponding to the expected molecular weight of the peptide (Figure 39B). To determine whether the high mobility bands are strictly due to the phosphate group, I treated yeast H2BS10ph and mammalian H2BS14ph (amino acids 6-16) peptides with shrimp alkaline phosphatase (AP) for 3 hours at 37°C, and re-electrophoresed them on a SDS-PAGE gel. As shown in Figure 39B, all of the high mobility bands in S10ph and S14ph peptides collapsed back to the expected size of the peptide, suggesting that the phosphorylation of the target serine contributes to these shifts. However, this shift was not common in all phosphorylated histone peptides as demonstrated by the absence of higher mobility bands in H2BS32ph, H2BS33ph, or Htz1S132ph peptides (Figure 39A). Therefore, this unique migration property exists only in our “apoptotic” phospho-serine H2B peptides.

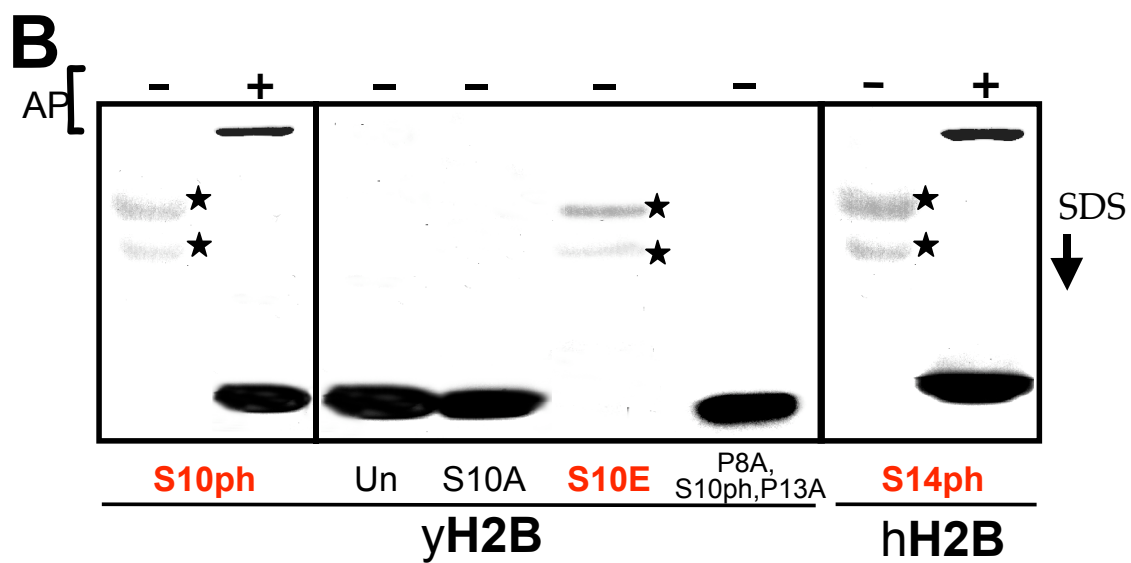
**Figure 39. “Death”-inducing phospho-peptides contain an intrinsic self-aggregation property *in vitro***

(A) List of peptide sequences and the status of their aggregation property. Apoptotic-inducing phospho-peptides, such as human H2BS14ph and yeast H2BS10ph, migrate anomalously in SDS-PAGE gels, a phenomenon we refer to as self-aggregation. This property is also observed with peptides containing glutamic acid in place of S10 (H2B S10E), or H3S28ph, a site followed by alanine and proline residues (labeled “YES” under “Aggregation.”) No other phospho histone peptide tested in this manner displayed this aggregation property, including a similar phospho-peptide from the C-tail of yeast Htz1 and the H3S10ph, which lacks an AP sequence (labeled “NO” under “Aggregation.”) When all prolines in the phospho-yeast H2B peptides were re-synthesized as alanine, aggregation is not observed. There, both phosphorylation and proximity to AP residues contribute to peptide aggregation. Note the strict correlation between peptide aggregation in this assay and *in vivo* chromatin condensation in yeast H2B S10A and S10E mutants.

(B) Various phosphorylated histone peptides listed above were incubated with 0.1 M DTT, then separated in standard SDS-PAGE gels following boiling in the sample buffer containing reducing agents. The aggregation effect, as indicated by higher molecular weight bands, (see red stars) is sensitive to alkaline phosphatase (AP) treatment.

**A**

| Peptide                  | Sequence                                     | Aggregation |
|--------------------------|--|-------------|
| 1. hH2BS14ph             | NH <sub>2</sub> -APAPKKGS <sup>14</sup> KK   | YES         |
| 2. yH2BS10ph             | NH <sub>2</sub> -AEKKPAS <sup>10</sup> SKAPA | YES         |
| yH2B S10E                | NH <sub>2</sub> -AEKKPAE <sup>10</sup> SKAPA | YES         |
| yH2B S10A                | NH <sub>2</sub> -AEKKPA <sup>10</sup> AKAPA  | NO          |
| yH2B P8A,<br>S10ph, P13A | NH <sub>2</sub> -AEKKA <sup>10</sup> SKAAA   | NO          |
| 3. yHtz1S132ph           | NH <sub>2</sub> -LKVEKKGS <sup>132</sup> KK  | NO          |
| 4. H3S10ph               | NH <sub>2</sub> -KQTARK <sup>10</sup> STGGKA | NO          |
| 5. H3S28ph               | NH <sub>2</sub> -AARKS <sup>28</sup> APATGGV | YES         |



Interestingly, yeast H3S28ph peptide displayed this unusual migration property, whereas it was absent in H3S10ph peptide in the same SDS-PAGE gel assay (Figure 39A). Although both H3 peptides contain identical –ARKS– motif, the serine phosphorylation site followed by alanine and proline residues (“AP” motif) are present in both H3S28ph and phospho-H2B peptides (see the yellow box in Figure 39A). Other phosphorylated peptides, which failed to yield high mobility bands, also lacked “AP” motif (H2BS32ph, H2BS33ph, or Htz1S132ph peptides; Figure 39A), suggest that prolines may be crucial in this *in vitro* peptide migration property. To test this hypothesis, a peptide with proline residues at 8<sup>th</sup> and 13<sup>th</sup> surrounding yeast H2BS10ph with replaced alanine (P8A, H2BS10ph, P13A H2B peptide) was subjected to same gel analysis. The unique migration property was not observed with this peptide even though a single phosphate was present at S10 (P8A, S10ph, P13A H2B peptide; Figure 39B). Therefore, the phosphorylation serine site and the proximity to AP sequence contribute to *in vitro* migration shift.

Next, I was curious whether the peptide containing glutamic acid in place of S10, S10E, would yield as dramatic a shift as H2BS10ph. As expected, the high mobility band was also observed with H2B S10E containing amino acids 4-14 of yeast histone H2B (Figure 39B). In contrast, the peptide containing the alanine in place of S10, S10A, displayed the band corresponding to the expected size of the peptide (Figure 39B). These *in vitro* result correlates well with my *in vivo* results (Figure 21). For example, H2B S10E displayed high mobility band *in vitro*, and condensed chromatin *in vivo*. In contrast, H2B S10A lacked this mobility shift in a peptide gel and conferred decondensed chromatin *in vivo*. Therefore, I hypothesize that the high mobility bands are “aggregation” of potential

secondary structure of H2BS10 or S14 that is dependent on the phosphate moiety and prolines. The proposed secondary structure could be a helix and the multimer of helices formed by self-interaction of H2B tails, which then yields the high mobility bands. In keeping with the cis mechanism, this direct interaction between phospho-H2B tails in the nucleosome may be the mechanism to form highly condensed chromatin as seen during apoptosis.

### ***H2B proline mutants are resistant to hydrogen peroxide treatment***

Phosphate-induced proline isomerization induces conformational changes in protein/peptide structure to mediate biological functions *in vivo* (Lim and Ping, 2005; Smet et al., 2004; Schutkowski et al., 1998; Yaffe et al., 1997b). Given that the occurrence of phospho-serine in conjunction with proline (H2BS14, H2BS10 and H3S28) can induce conformational changes in peptide structure (Figure 39), I hypothesized that the prolines may be important for altering chromatin structure as seen during apoptosis. For this purpose, two prolines, at amino acid position 8 and 13, surrounding yeast H2BS10 were separately mutated to alanine (H2B P8A P13A; Figure 40A) and tested for cell survival/death upon H<sub>2</sub>O<sub>2</sub> treatment as described in Chapter 2 (cell survival was tested by plating assay, cell death by phloxin B staining). This double mutant showed some resistance to H<sub>2</sub>O<sub>2</sub> compared to WT or H2B S10A mutants (Figure 40B and 40C). While WT and H2B S10A displayed 25% and 80% survival as judged by plating assays, respectively, the proline mutants showed 70% cell viability (Figure 40B). The proline mutants displayed 30% phloxin B stained cells compared with 70% for WT and 20% for H2B S10A mutants (Figure 40C). In accordance with the cell viability/death analysis, about 25-35% of H2B P8A P13A double mutants were

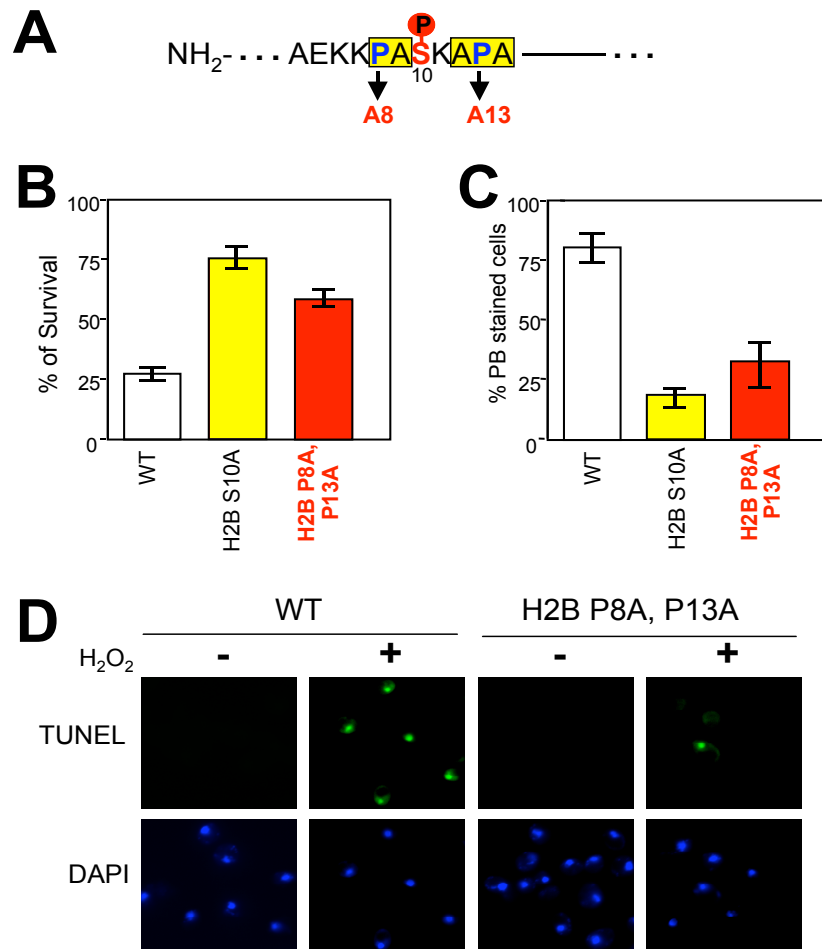


**Figure 40. Prolines in the yeast H2B “death motif”**

Prolines in close proximity to S10 in H2B have an aggregation property *in vitro* and a cell survival/ death function *in vivo*.

(A) Two prolines, at amino acid position 8 and 13, found in the yeast H2B “death motif” were separately mutated to alanine (H2B P8A P13A).

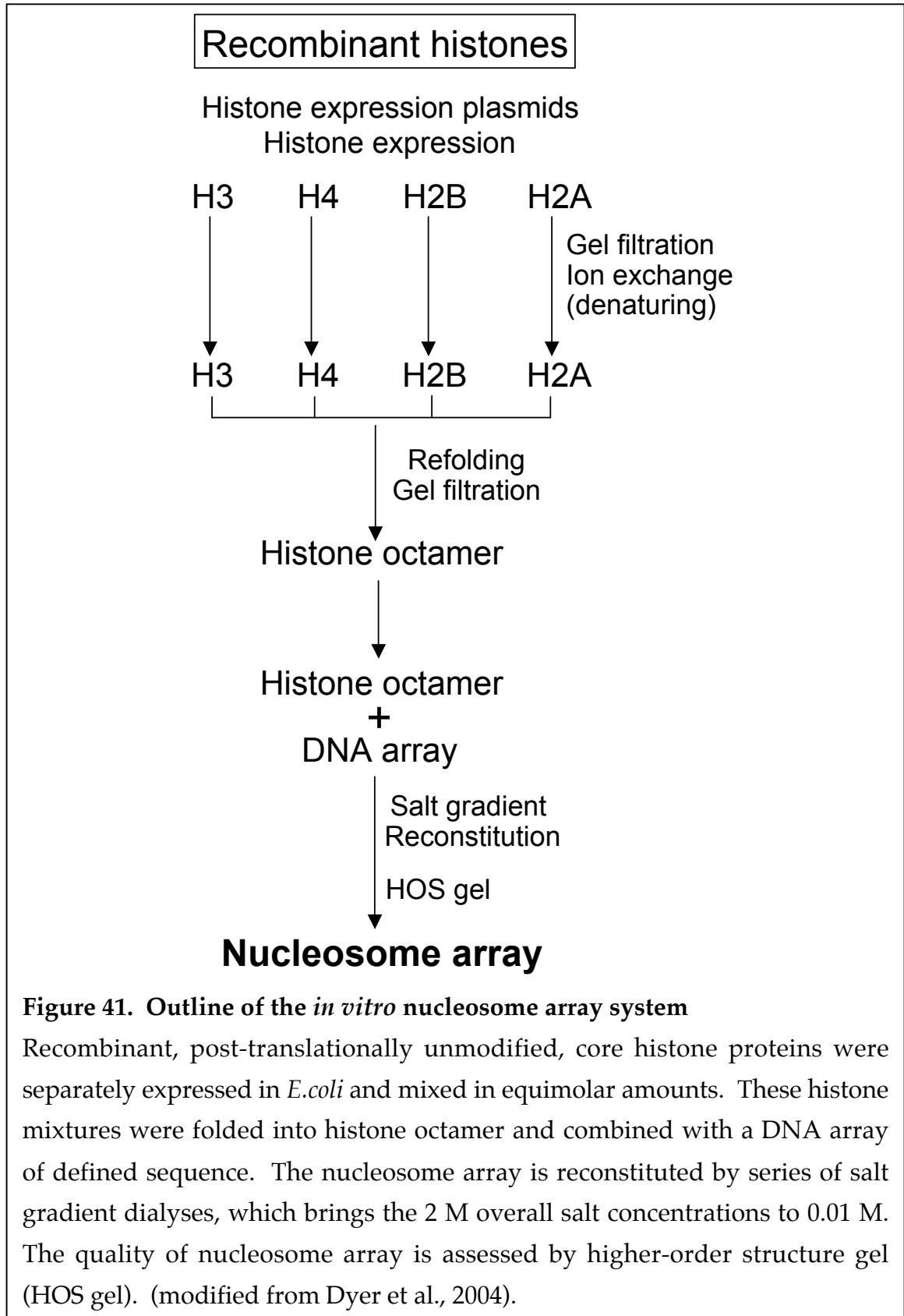
(B and C) H2B P8A P13A double mutants were tested for cell survival/ death upon H<sub>2</sub>O<sub>2</sub> treatment (cell survival was tested by a plating assay; cell death by phloxin B staining; See Figure 11 for detail). This double mutant shows some resistance to H<sub>2</sub>O<sub>2</sub> (60% survival, 30% death; see red arrows) compared to WT (25% survival, 75% death) or H2B S10A mutants (80% survival, 20% death).

(D) H<sub>2</sub>O<sub>2</sub> treated or untreated yeast cells were stained with TUNEL. In accordance with the cell viability/ death analysis, about 35% of H2B P8A P13A double mutants were stained with TUNEL (compare 80% TUNEL for WT; 15% for H2B S10A mutant). The same cells were counterstained with DAPI.

stained with TUNEL (compare 80% TUNEL for WT; 15% for H2B S10A mutant; Figure 40D). Taken together, these results underscore the importance of proline residues surrounding H2BS10ph during H<sub>2</sub>O<sub>2</sub>-induced yeast apoptosis. Since proline-mediated isomerization leads to the alteration of protein/peptide structure, prolines along with H2BS10ph may serve as a “facilitator” of chromatin condensation.

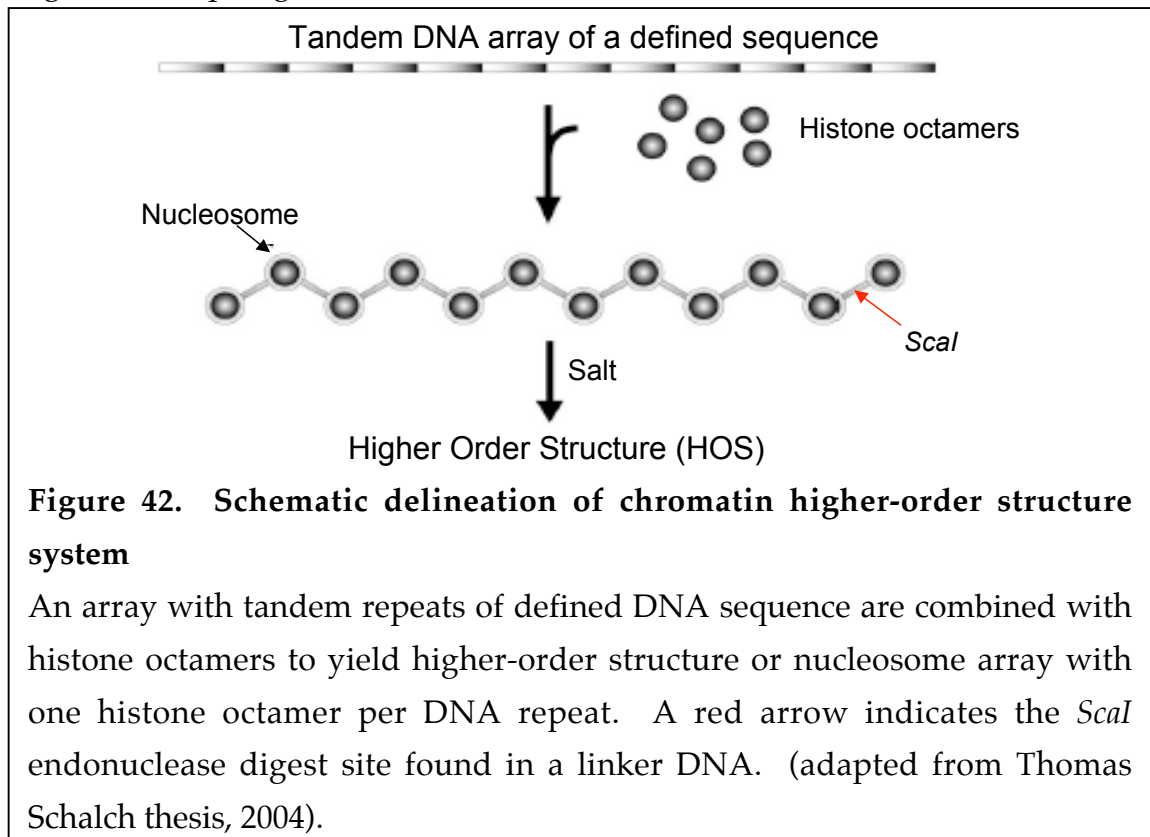
### *Nucleosome arrays of yeast H2B S10E*

To better understand the function(s) of histone H2B phosphorylation as it relates to apoptotic-chromosome compaction, I used the self-assembly system of the nucleosome array and *in vitro* chromatin-fiber folding assay. Dr. Timothy Richmond’s laboratory at ETH Zurich, Switzerland had previously identified that the basic path of H4 tails can induce condensed chromatin structures by using these *in vitro* assays (Dorigo et al., 2003). I spent two and half months at Dr. Richmond’s laboratory to learn these methods and to test whether yeast H2BS10ph directly effects chromatin compaction in collaboration with Dr. Richmond’s post-doc fellow, Dr. Thomas Schalch. Since the *in vitro* nucleosome array constitutes recombinant, post-translationally unmodified histone proteins, we decided to create nucleosome arrays containing yeast H2B S10E or H2B S10A. We expressed yeast histone H2B protein containing glutamic acid or alanine as the replacement of S10, and mixed them with the rest of yeast’s core histone proteins to form functionally refolded histone octamers (Figure 41). Nucleosome array reconstitution was achieved by mixing histone octamers containing different H2BS10 mutations with the DNA array in high-salt buffer (2M KCl) and slowly lowering the concentration of KCl to 10 mM by dialysis against

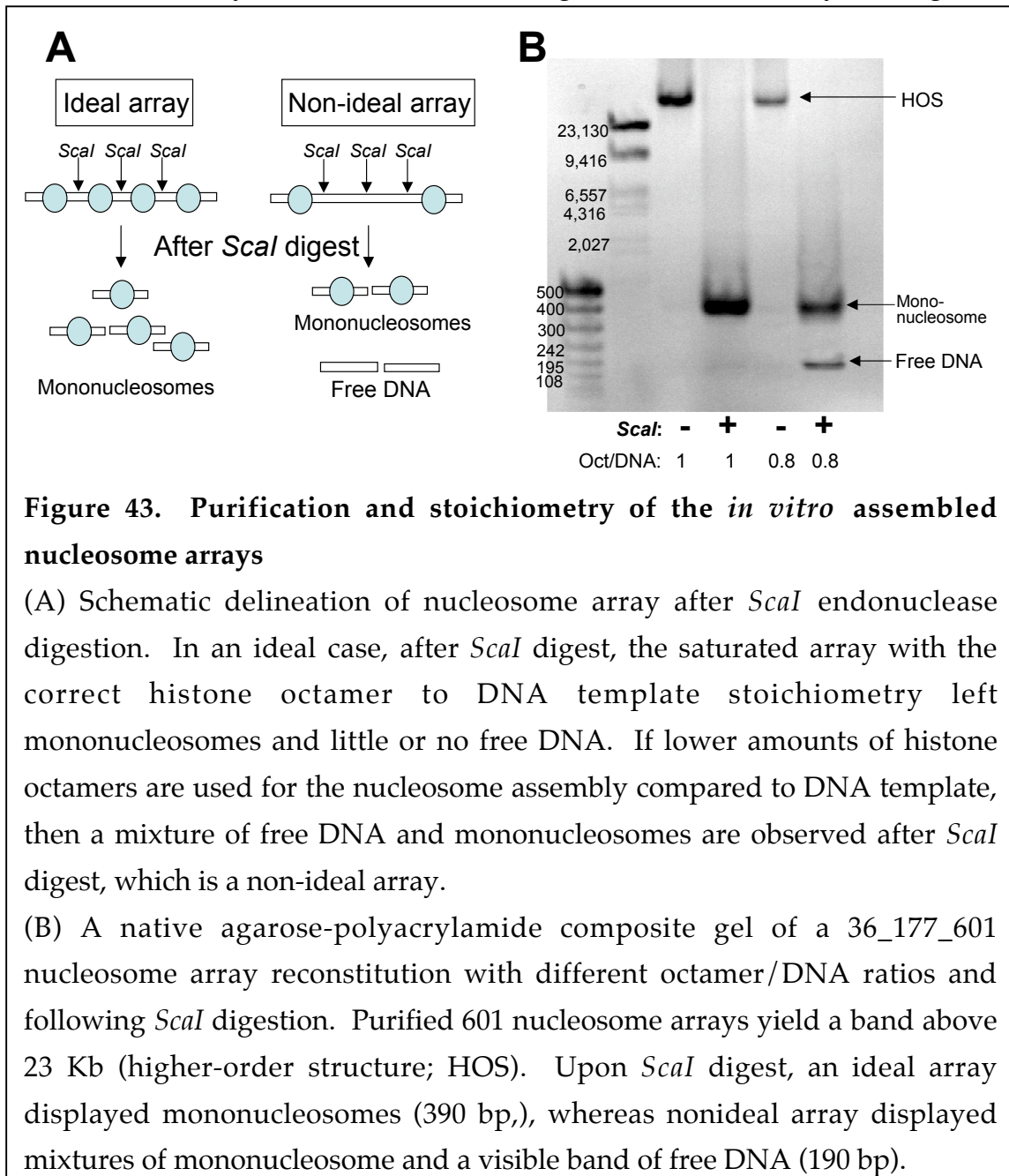




decreasing levels of salt (Figure 41). This step-wise salt dialysis allowed the deposition of one histone octamer per DNA repeat in an array by changing the ionic strength of the reconstitution reaction. For my studies, I used 36 tandem 177 bp repeats of the 601 DNA array (36\_177\_601 DNA array). The 601 DNA sequence which binds to histone octamers, contains repeats of alpha satellite sequence used for the nuclear core particle crystallization (Lowary and Widom, 1998). This DNA array was found to be the ideal choice for the chromatin fiber model because of its exceptional stability (Lowary and Widom, 1998). The repeat length of 177 bp was chosen from a list of preferentially quantized linker DNA lengths determined from a statistical analysis of nucleosome repeat lengths (Widom, 1992). Hence, the nucleosome array reconstituted with this particular DNA array yielded 36-nucleosome repeats of 601 DNA sequence with a repeat length of 177 bp (Figure 42).



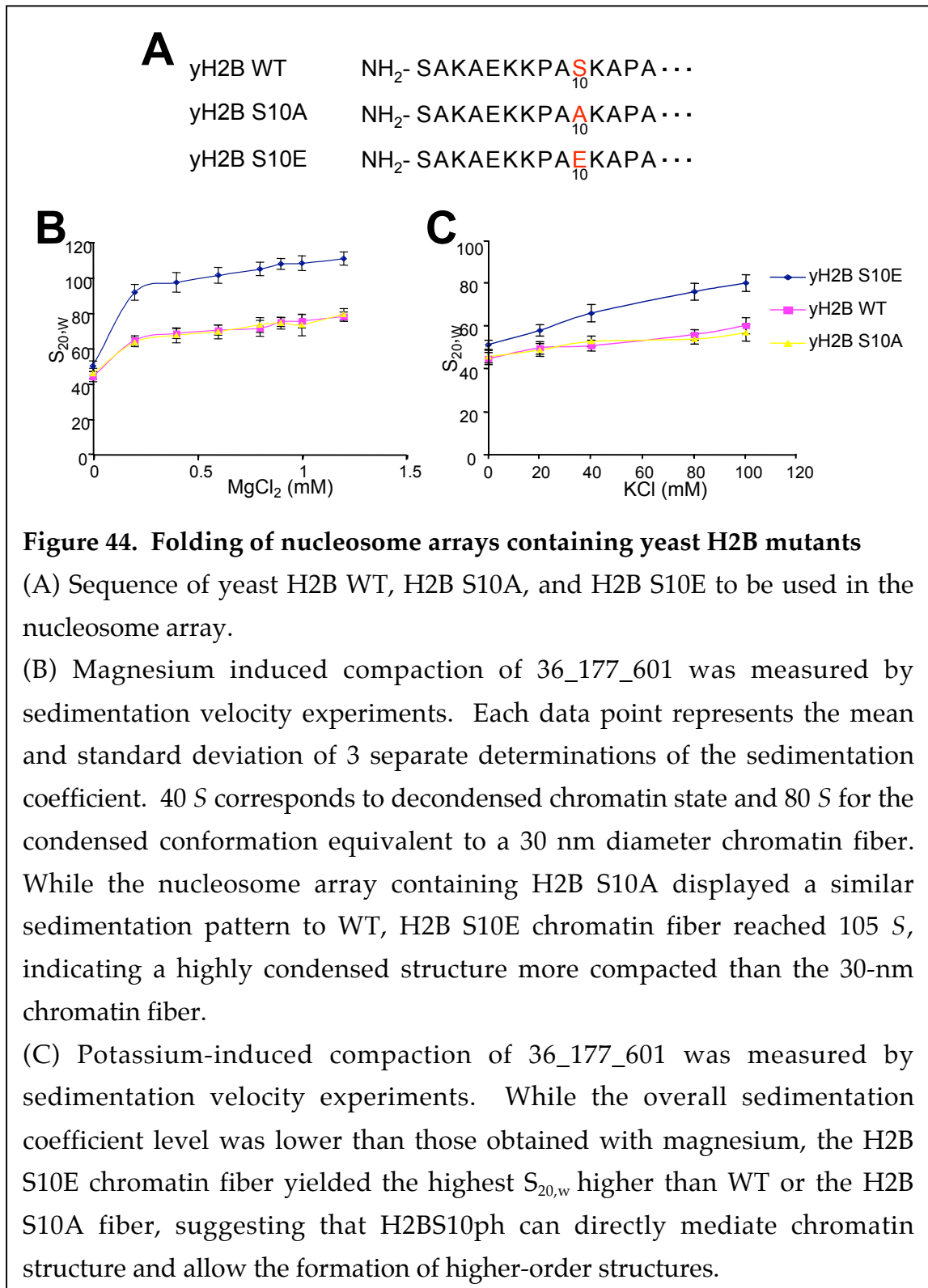
The biophysical properties of nucleosome array depend on the histone octamer to DNA stoichiometry (Dorigo et al., 2003). Therefore, it is crucial to find the ratio of histone octamers to DNA that would yield the homogeneous nucleosome array with one histone octamer occupying each DNA repeat (see “an ideal array” in Figure 43A). Histone octamer to DNA template stoichiometry was evaluated by *ScaI* endonuclease digestion followed by the agarose-



polyacrylamide gel electrophoresis (APAGE). The nucleosome arrays contain a *ScaI* restriction digest site in a linker DNA. After *ScaI* digest, the full-length arrays carrying one histone octamer per DNA repeat (occupied site) will be released as mononucleosomes and the arrays lacking histone octamers in the DNA repeat (unoccupied sites) as free DNA after *ScaI* digest (Figure 43A). The large full-length arrays as well as mononucleosome and single, free DNA repeats are visualized in APAGE. Run under denaturing conditions, the saturated array with the correct histone to DNA stoichiometry leaves mononucleosomes and no free DNA after *ScaI* digest (see left panel in Figure 43A). In contrast, free DNA is dominantly present in the nucleosome array with mis-positioned histone octamers after *ScaI* digest (see right panel in Figure 43A). Figure 43B shows the assembly products generated with increasing ratios of the WT histone octamer to DNA as well as corresponding *ScaI* digestion products. The undigested, large, full-length nucleosome array, also known as a higher-order structure (HOS), was displayed as a band above 23 Kb. Upon *ScaI* digest, I observed mixtures of bands corresponding to mononucleosomes (390 bp) and free DNA (190 bp) with the array prepared from a WT histone octamer to DNA repeat-stoichiometry of 0.8:1 (Figure 43B). On the other hand, the ratio of 1:1 yielded a single band representing mononucleosomes and left no free DNA (Figure 43B), indicative of the ideal array with a single, well-positioned octamer per DNA repeat. By using this analysis of *ScaI* digestion, the ratio of histone octamer to DNA was determined for each of the H2B nucleosome arrays.

The sedimentation velocity by analytical ultracentrifugation was used to measure the influence on chromatin compaction by H2BS10ph. The degree of chromatin compaction depends strongly on the valency and concentration of salt

in the buffer; concentrations in the 1-2 mM of  $\text{MgCl}_2$  divalent ion range are sufficient to induce compaction whereas monovalent ions (KCl) partially



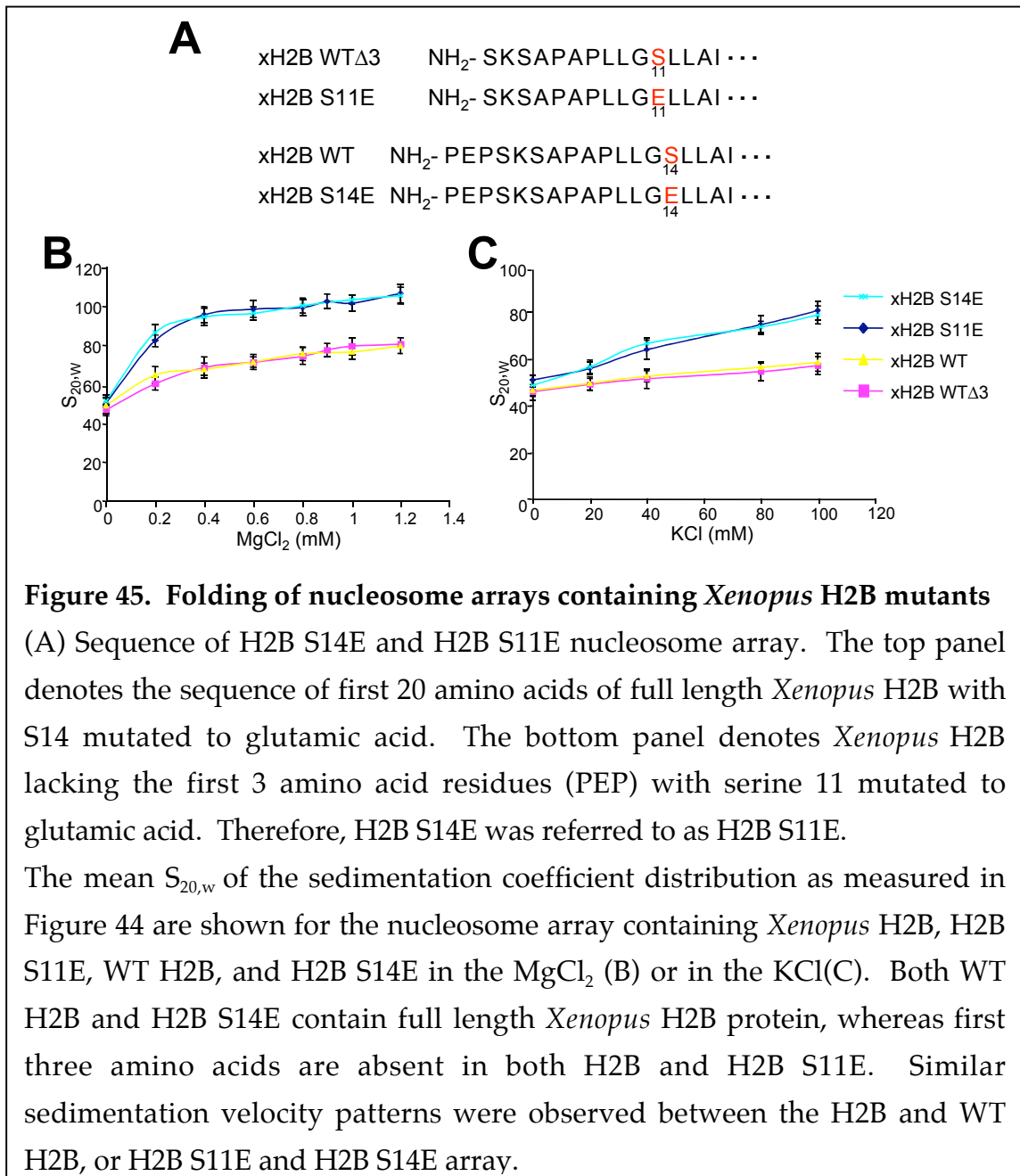
compact the chromatin fiber at 100 mM concentrations (Hansen, 2002). For the sedimentation velocity experiments, each of the nucleosome samples combined with varying concentration of salt were centrifuged at 12,000 rpm at 20°C collecting scans at 259 nm. We analyzed these data with the program, “Sedfit” (Schuk, 2000), and the sedimentation coefficient ( $S_{20,w}$  or  $S$ ) was determined. This coefficient reflects the status of the chromatin fiber; a low coefficient corresponds to the decondensed state of chromatin fiber, with a high sedimentation coefficient corresponds to the compacted state. The compact 30-nm chromatin fibers observed in mitosis were correlated with a 80  $S$  sedimentation coefficient. In WT array, such structure was only formed when  $MgCl_2$  concentration was raised to 1.2 mM (Figure 44A). Strikingly, H2B S10E mutant array formed a structure equivalent to 30-nm even at the lowest  $MgCl_2$  concentration (0.2 mM). When  $MgCl_2$  reached 1.2 mM, S10E array yielded a sedimentation coefficient above 100  $s$ , indicating a highly compacted structure (Figure 44A). In contrast, the H2B S10A nucleosome array, the nonphospho-mimic of yeast H2BS10, produced the same sedimentation coefficient as a WT nucleosome array (Figure 44A). Previously, aggregation of chromatin was observed when the concentration of salt is raised above the level required for compaction (Ris and Mirsky, 1949; Olins and Olins, 1972; Schwarz et al., 1996). We found that aggregation was consistently observed after 1.2 mM  $MgCl_2$  for all the arrays we tested, suggesting that 1.2 mM is the solubility boundary. These results indicate that the phospho-mimic S10E mutation causes a significant chromatin compaction *in vitro*. Since S10E  $S_{20,w}$  is much higher than WT, the H2B S10E nucleosome array could be more compacted than the 30-nm chromatin fiber seen during prophase of mitosis.

In our hands, the recombinant nucleosome arrays displayed compaction behavior without aggregation between 0 and 100 mM KCl, the monovalent cation salt (Figure 44B). The overall compaction levels achieved with KCl were 20 S lower than those obtained for the WT or H2B S10A array with  $\text{MgCl}_2$ . As shown in Figure 45B, the  $S_{20,w}$  for the WT and H2B S10A array was lower than 80, further supporting that arrays with KCl do not reach the fully compacted 30-nm chromatin fiber state. In contrast, H2B S10E array formed highly compacted chromatin fibers in the presence of monovalent cations, as demonstrated by 90 S, before reaching the solubility boundary at 100 mM KCl (Figure 44B). Taken together, these results further support that the nucleosome array containing H2BS10ph can directly mediate internucleosomal contact to form highly compacted chromatin *in vitro*.

#### ***Nucleosome array of *Xenopus* H2B S14E***

Since yeast H2BS10ph can directly mediate chromatin compaction *in vitro*, we decided to determine whether mammalian H2BS14ph would display similar level of chromatin compaction *in vitro*. With help from Dr. Thomas Schalch and Sywia Duda at Dr. Richmond's laboratory, we expressed all four *Xenopus* histone proteins along with the phospho-mimic H2B S14E. Then we combined these histone proteins with 36\_177\_601 DNA array to reconstitute the nucleosome array as described earlier. The first 3 amino acid residues (PEP) were missing from the *Xenopus* H2B construct, so H2B S14E was referred to as H2B S11E (Figure 45A). Both the WT and H2B S11E arrays reached the same extent of compaction as yeast WT and yeast H2B S10E, respectively (compare Figures 44 and 45). Similar to the yeast WT nucleosome, the *Xenopus* WT nucleosome array

reached a compacted state equivalent to 30-nm in 1.2 mM  $\text{MgCl}_2$ , and a partially compacted state in 100 mM KCl (Figure 45B and 45C). The S11E array reached a maximum of 105 S and 90 S before reaching the solubility boundary of  $\text{MgCl}_2$  and KCl (Figure 45B and 45C), respectively. Moreover, the addition of first 3 amino acids did not change the sedimentation coefficient; both full length WT H2B and H2B S14E arrays compacted in a similar level as WT and H2B S11E,



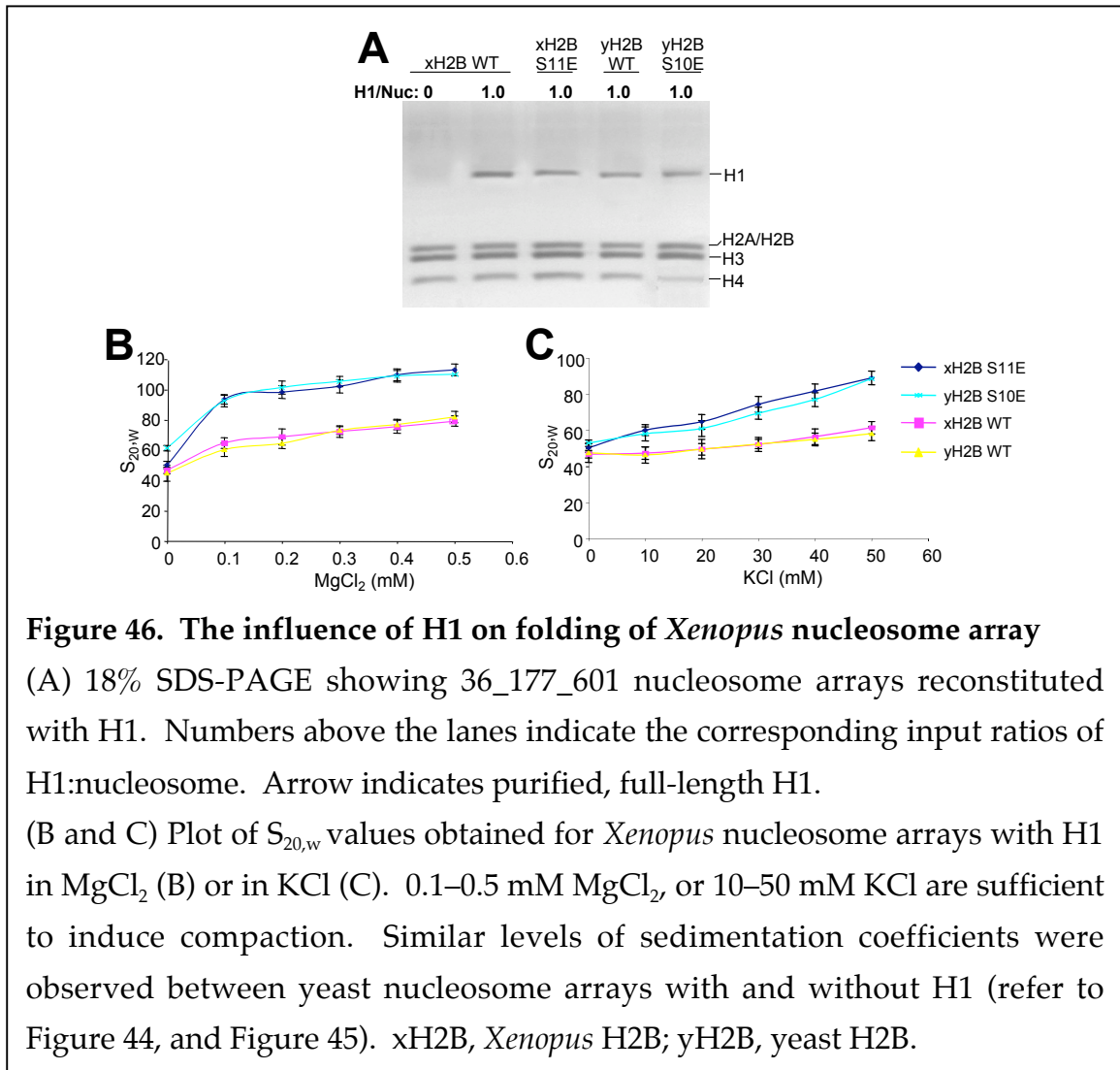
respectively (Figures 45C and 45C). These results further confirms that phosphorylation of H2B is critical for the chromatin condensation.

***Compaction of Xenopus H2B S11E and yeast H2B S10E are not dependent on linker histone H1***

Linker histones, such as H1, comprise a large family of chromatin associated proteins that bind to nucleosomes and influence chromatin fiber dynamics (Hansen, 2002). Because linker histones are considered to be necessary to induce folding of the chromatin fiber (Hansen, 2002), I investigated the influence of the H1 on compaction of the *Xenopus* H2B S11E chromatin fiber, which lacks the first 3 amino acids (PEP) of H2B. I reconstituted nucleosomes with full length H1 (gift of Dr. Chrysolula Leontinue at Dr. Richmond's laboratory) using input H1 to nucleosome ratio of 1:1 mimicking the *in vivo* nucleosome structure. The resulting nucleosome array contained 1 H1 per nucleosome and was verified by coomassie stained SDS gels. The quality of the nucleosome arrays was validated by observing histone octamers along with a 30 kDa band representing full length H1 (Figure 46A). The compaction was measured by analytical ultracentrifugation under several divalent or monovalent cation concentrations for each reconstitution. Compared arrays devoid of H1, arrays containing H1 compacted in less divalent or monovalent salt (Figure 46B and 46C). In the presence of divalent cation such as  $MgCl_2$ , concentrations in the range of 0.1-0.5 mM were sufficient to induce compaction whereas the monovalent ion, KCl, compacted the chromatin fiber at a 50 mM concentration and exceeding 0.5 mM  $MgCl_2$  or 50 mM KCl induces precipitation (Figure 46B and 46C). With an increasing  $MgCl_2$  concentration, we observed a comparable sedimentation



pattern for both arrays with or without H1;  $S_{20,w}$  value increased linearly and reached maximum of 80 S for array containing *Xenopus* WT with H1, or 110 S for *Xenopus* H2B S11E with H1 (Figure 46B). Similar to the compaction under a divalent cation, KCl also caused compaction between arrays with or without H1 (compare 60 S for *Xenopus* WT or 90 S for H2B S11E with or without H1; Figure 46C). Consistently, yeast nucleosome arrays of both WT and H2B S10E with H1 displayed comparable sedimentation coefficient as each respective H1-less nucleosome array. Together, these results suggest that *Xenopus* H2B S11E and yeast H2B S10E compaction are not enhanced by linker histone H1.



*Yeast H2B+H2A chimera mutants display hydrogen peroxide-induced yeast apoptosis*

Can the H2B “death function” be moved from the H2B tail to another core histone tail such as H2A, H3 or H4, where no H2BS10ph motif currently exists? Previously, domain-swap experiments have been executed between H3 and H4 N-terminal tail or H2A.Bbd domain and H2A C-terminal tail (Ling et al., 1996; Bao et al., 2004) to determine whether histones tail functions are limited to its native context. Having established that the C-terminal end of the H2B is not involved in yeast apoptosis, I next sought to address whether H2BS10ph motif serves as a modular histone modification “cassette.” In pilot experiments, I took a short stretch of the H2B N-terminal tail, corresponding to amino acids 2-16, and inserted it into the H2A N-terminal tail at amino acid position 2 in a plasmid shuffle strain lacking H2B N-terminal tail, yH2B  $\Delta$ 1-32 (Figure 47A). Hereafter, this chimera strain will be referred to as H2A+B. Given that H2B N-terminal tail is missing in the H2A+B chimera strain, the H2BS10ph motif was only present at H2A N-terminal tail (Figure 47A). The growth rate and the sensitivity to H<sub>2</sub>O<sub>2</sub> were comparable between the chimera strain and WT (Figure 47B and 47C, respectively). Unlike the H2B N-terminal tail deletion mutant, the H2A+B chimera was sensitive to H<sub>2</sub>O<sub>2</sub> treatment in a manner similar to WT; both displayed 30% cell viability and 70% cell death (Figure 47B and 47C). Next, H2BS10 was separately mutated to alanine or glutamic acid in H2A+B chimera mutant background and they were referred to as H2A+B S10A or H2A+B S10E, respectively. These chimera mutants displayed similar levels of cell viability and cell death as the H2BS10 mutants in their natural H2B N-terminus (Figure 47B and 47C); both S10A mutants in H2A+B or in native H2B N-terminus displayed

70% cell viability followed by 30% phloxin B staining, whereas S10E mutants in chimera or in native context conferred growth defect (Figure 47D). To determine whether H2A+B restores apoptotic phosphorylation in a H2B N-terminal tail deletion background, nuclear extracts purified from H<sub>2</sub>O<sub>2</sub>-treated or untreated chimera yeast cells were subjected to Western analysis. While H2B from H<sub>2</sub>O<sub>2</sub>-treated WT cells reacted strongly with anti-H2BS10ph antibody, the H2BS10ph signal was shifted to histone H2A in H<sub>2</sub>O<sub>2</sub>-treated chimera strains. In addition, the H2BS10ph signal was lost in H2A+B S10A mutant (Figure 47E). These results suggest that apoptotic H2BS10ph is re-established even in the absence of a wild-type copy of H2B N-terminal tail (Figure 47E). Given that H2A+B chimera mutants restore the cell death phenotype and apoptotic S10ph abolished by H2B N-terminal tail deletion, the H2B N-terminus (amino acids 2-16) appears to function as a modular signaling “cassette”, further supporting the existence of histone modification “cassettes” that are functionally modular.

#### *Chromatin compaction of yeast H2A+B chimera mutant*

Given that chromatin condensation correlates with yeast apoptosis, I sought to address whether phospho-H2B's role in chromatin compaction is still conserved in this H2A+B chimera mutant. The exact replica of the yeast H2A+B nucleosome was reconstituted *in vitro* using a 36\_177\_601 DNA array. In short, this nucleosome array contained a short stretch of the H2B N-terminal tail (amino acids 2-16) in the H2A at residue 2 and lacked the H2B N-terminus (H2A+B). I also generated identical nucleosome arrays that carry S10A or S10E H2B mutants (H2A+B S10A or H2A+B S10E, respectively; Figure 47). The degree of compaction was assessed by analytical ultracentrifugation in the presence of

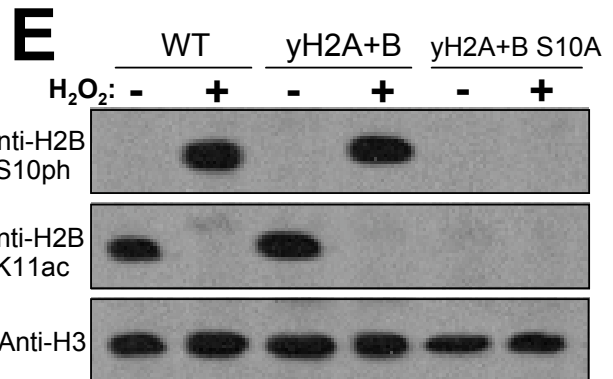
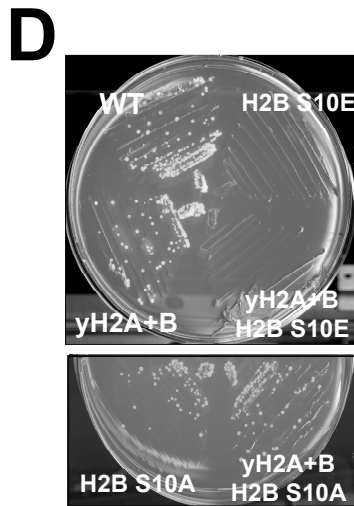
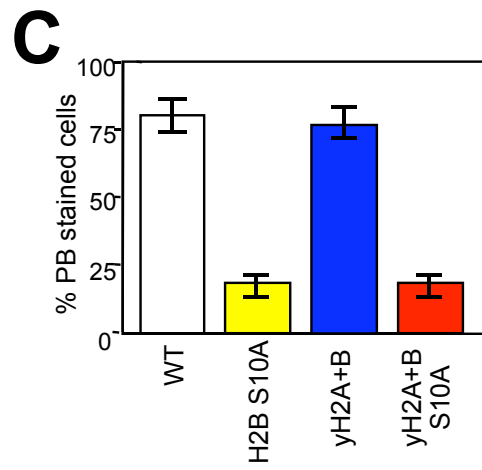
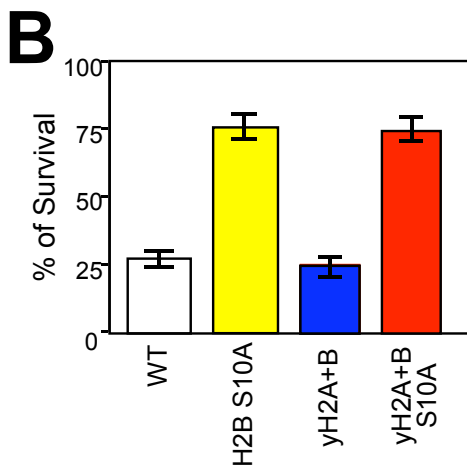
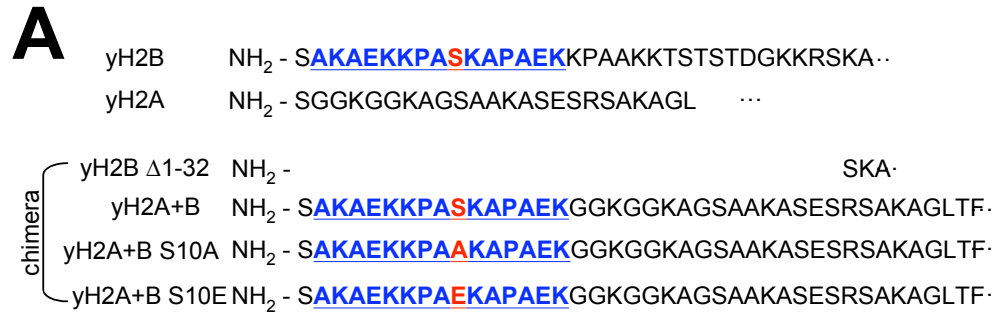
**Figure 47. Movable “death-cassette” in H2B**

(A) Sequence of yeast H2A+B chimera mutants. A short stretch of the yeast H2B N-terminal tail at amino acid position 2-16 (see blue underline) was inserted into the H2A N-terminal tail at amino acid position 2 in a plasmid shuffle strain lacking H2B N-terminal tail (yH2B  $\Delta$ 1-32). The H2BS10ph (denoted in red) was mutated to alanine or glutamic acid in the H2A+B chimera mutant background and hence forth referred to as H2A+B S10A or H2A+B S10E, respectively.

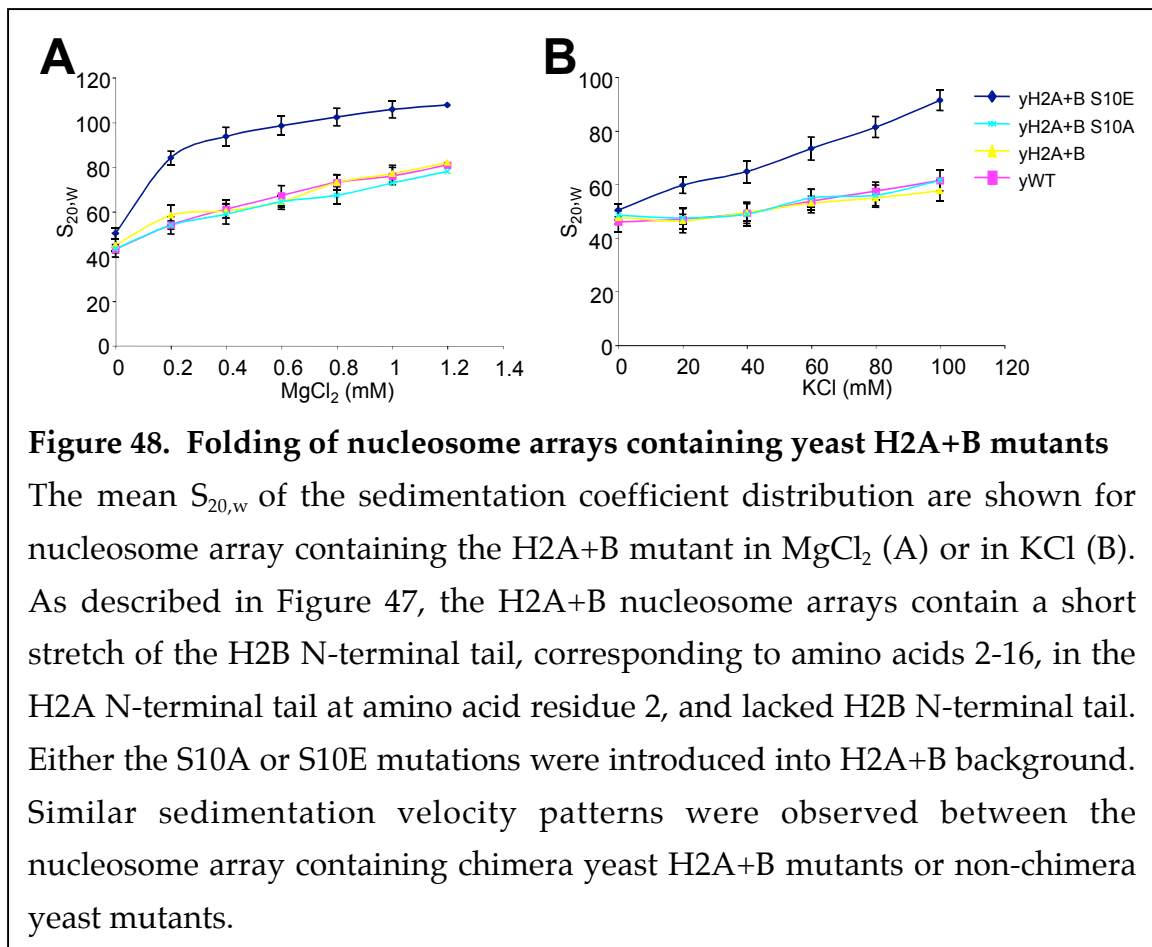
(B and C) yH2A+B chimera mutants were tested for cell survival/death upon H<sub>2</sub>O<sub>2</sub> treatment (cell survival was tested by plating assay; cell death by phloxin B staining; See Figure 11 for detail). Similar levels of sensitivity towards H<sub>2</sub>O<sub>2</sub> were observed between yH2A+B chimera (yH2A+B, yH2A+B S10A) and non-chimera mutants (WT, H2B S10A).

(D) WT, H2B S10E, yH2A+B, and yH2A+B S10E yeast strains were grown on YPD agar plates in the absence of H<sub>2</sub>O<sub>2</sub>. H2B S10E and yH2A+B S10E mutants displayed a growth defect even without H<sub>2</sub>O<sub>2</sub>.

(E) Nuclear extracts purified from H<sub>2</sub>O<sub>2</sub> treated or untreated WT, yH2A+B, and yH2A+B S10A were subjected to Western analysis using anti-H2BS10ph, anti-H2BK11ac and anti-H3 antibodies. Except for H2B, no other bands were detected with the anti-H2BS10ph or anti-H2BK11ac antibodies. Anti-H3 antibody was used as a loading control.



different divalent or monovalent cation concentrations. The overall sedimentation velocity pattern for nucleosome arrays with H2A+B chimera mutants was similar to yeast H2B mutant arrays (compare Figures 44 and 48). For example, the  $S_{20,w}$  value for the H2A+B chimera array starts at 40 S and reaches 80 S in 1.2 mM  $MgCl_2$ , or 70 S in 100 mM KCl, similar to the yeast WT nucleosome array (Figure 48A and 48B). S10A or S10E in H2A+B chimera also obtained the similar sedimentation coefficient values as arrays containing H2B S10A or S10E in a non-chimera background (Figure 48A and 48B). These results give credence to the idea that the H2B tail (amino acids 2-16) functions as a modular signaling platform to mediate yeast chromatin condensation further supporting the concept of a “death-cassette” in histone H2B.



## Discussion

Chromatin is a complex of DNA and proteins, primarily histones that organize the genetic material in the eukaryotic nucleus. The dynamics and structure of chromatin are directly involved in nuclear processes like apoptosis. In this chapter, I have described the role of H2BS10ph in mediating the dynamics of chromatin fiber folding. H2B peptides carrying S10ph or phospho-mimic of S10 (S10E) in the proper sequence context (i.e. close proximity to proline residues) induce an intrinsic aggregation property under reasonably harsh denaturing conditions (Figure 39). We observed that S10E mutants activate the yeast apoptotic pathway and chromatin condensation constitutively, whereas S10A mutants fail to activate it at all even upon cell-death stimuli (Chapter 2). Because this unusual *in vitro* property is mirrored by the *in vivo* phenotypes of the corresponding mutants, this property may be a mechanism for aggregating nucleosomes to form highly condensed apoptotic chromatin. To test this hypothesis, I have utilized *in vitro* homogeneous nucleosome array system and assessed the degree of compaction of chromatin fiber by analytical ultracentrifugation with help from Dr. Richmond's group. I determined that apoptotic markers in yeast and *Xenopus*, H2B S10E and H2B S14E respectively, are critical for condensation of chromatin fibers that are more compacted than the 30-nm chromatin fibers seen during mitosis (Figures 44 and 45). In addition, the H2BS10 motif serves as a modular signaling platform which functions in mediating yeast apoptotic chromatin condensation and apoptosis, which I refer to as "death-cassette". These results support that the yeast H2BS10ph can directly mediate the chromatin compaction (cis mechanism; see Figure 6).

### *In vitro* peptide aggregation and *in vivo* chromatin status

As shown in Figure 39, yeast H2BS10ph and mammalian H2BS14ph peptides migrated anomalously in the SDS-PAGE gel, however, most of the phospho-histone peptides migrated “normally” in this assay. I have found that two properties contribute to “aggregation” behavior in test peptides: 1) phosphorylation of the target serine residue and 2) the presence of nearby, often repeating, “AP” residues. In accordance with the above criteria, no aggregation was observed when the peptides were treated with alkaline phosphatase or when proline was replaced with alanine in the “aggregating” yeast H2BS10ph peptide (Figure 39B).

Without exception, phospho-peptides that displayed this unusual “aggregation” property, notably apoptotic phospho-peptides (yeast H2BS10ph and mammalian H2BS14ph), coincide precisely with condensed chromatin *in vivo* (Figures 39 and 21). These peptide data also correlate precisely with the *in vitro* chromatin compaction assay. Indeed, the H2B S10E phospho-mimic mutant displayed peptide “aggregation” in the simple gel assay (Figure 39), highly compacted chromatin fiber as measured by sedimentation velocity (Figure 44), and condensed chromatin *in vivo* (Figure 21). In contrast, the H2B S10A nonphospho-mimic mutant failed to aggregate in a peptide gel (Figure 39), and conferred decondensed chromatin fibers *in vitro* and *in vivo* (Figures 44 and 21). Thus, the peptide “aggregation assay” arises as one indicator for compacted chromatin fiber *in vitro* and *in vivo*.



### *The role of proline during yeast apoptosis*

Proline isomerization causes conformation changes in protein/peptide structure *in vivo* and controls important biological functions including apoptosis (Schutkowski et al., 1998; Lim and Ping 2004; Smet et al., 2004; Wulf et al., 2005; Berger et al., 2005). It was previously shown that the function of the tumor suppressor gene, p53, is regulated in its conformational changes by the proline isomerase, Pin1. For example, the mutation in the polyproline region (PPR) of p53 leads to the inhibition of Pin1-mediated conformational changes in p53, and in turn, impairs its apoptotic function (Berger, et al., 2005). A similar paradigm may be applied during yeast apoptosis. In this case, the proline residues found in histone H2B serves as a target for a proline isomerase, which induces conformational changes in H2B, and ultimately chromatin. In support, the importance of proline residues in yeast apoptosis was observed since the apoptotic phenotype is abrogated in the absence of prolines near the S10 phosphorylation site in H2B (Figure 40). It is implied that structural change in chromatin is dependent on both prolines and phosphorylated S10, but the proline isomerases that are responsible for facilitating these events are unclear at this time. Therefore, surveying the proyl-isomerase knockout yeast strains upon  $H_2O_2$  treatment should identify the responsible enzyme. Moreover, reconstituting the yeast nucleosome array containing proline mutants and measuring its sedimentation coefficient should determine whether S10 phosphate-induced proline isomerization plays a direct role in chromatin compaction (cis mechanism).

### *H2B “death-cassette”*

In this chapter, I have described the existence of a “cassette,” a short cluster of densely modifiable sites in histones with a distinct biological readout (Fischle et al., 2003b; see Figure 4). Rather than acting independently, this domain is situated at strategic locations in the histones and functions as a discrete information unit regulating and relaying different signals depending on its modification state (Fischle et al., 2003b). Already, several clusters of adjacent or closely-spaced modifiable residues are observed in all core histones and well studied hot spots of clustered marks punctuate the tails of H3 and H4 (Figure 5). Given that a cassette is a modular information domain, an intriguing possibility surfaces of a movable cassette in which its functions are not confined to its natural location. Although, this mobility has not been observed with cassettes from H3 or H4, I have found that the stretch consisting of yeast H2BS10ph does not need to be attached to its native H2B N-terminal tail (Figures 47 and 48). In support, it re-establishes both the cell-death phenotype upon in yeast H<sub>2</sub>O<sub>2</sub> treatment and the compaction of the nucleosome array when inserted into the H2A N-terminus (Figures 47 and 48). The post-translational modification patterns of H2BK11 and H2BS10 are also re-established on the H2A tail in H2A+B chimera strain (Figure 47), suggesting that this motif maintains its ability to serve as a target substrate of Ste20 kinase and Hos3 HDAC, even in the unnatural setting.

This “death-cassette” consists of 2 proline residues at the 8<sup>th</sup> and 13<sup>th</sup> residues as well as K11 and S10. Shortening the cassette may provide further insights into the influence of histone modifications facilitating yeast cell death. I hypothesize that the combination of K11 influencing S10ph and phosphate-

induced proline isomerization comprises the functional unit that relays an apoptotic signal. Since H2B and H2A form a dimer (Klug et al., 1980; Richmond et al., 1984), moving the H2B death-cassette into H2A might not alter the structure of nucleosome and disrupt its normal biological function. Therefore, moving this cassette to additional histone tails should determine how movable this histone modification cassette is. Nevertheless, my preliminary results identified a death-cassette in the histone H2B N-terminus that functions as a modular and movable histone covalent modification domain to recruit and facilitate yeast's apoptotic signaling cascade.

### *Influence of linker histone H1*

For many years it was thought that the formation of the 30-nm chromatin fibers depend on the presence of H1, but the sedimentation analysis of defined nucleosome arrays in  $\text{MgCl}_2$  has shown that compact fibers can form in the absence of linker histone H1 (Carruthers et al., 1998). I have observed that compaction of chromatin fibers in phospho-mimic H2B serine mutants are independent of H1 (Figure 46). In yeast, linker histones are nonessential (Ausio, 2000), further supporting that H1 does not mediate yeast chromatin condensation. H1 is essential in vertebrates (Georgel and Hansen, 2001), but the *in vitro* chromatin sedimentation analysis and the endogenous chromatin from *Xenopus* egg extracts suggest otherwise. In both cases, chromatin can fold into the highest levels of compaction similar to the metaphase chromosome even in the absence of H1 (Carruthers et al., 1998; Dasso et al., 1994; see Figure 46 for our *in vitro* chromatin sedimentation analysis). Therefore, we hypothesize that the

formation of higher-order chromatin structure is directed by core histones rather than H1.

In support of our hypothesis, studies of endogenous nucleosome arrays reassembled with linker histone indicate that the highly basic C-terminus of H1 is responsible for fiber stabilization, not condensation (Allan et al., 1986). *In vitro*, H1 has been shown to stabilize the folded and oligomeric states of chromatin fibers; less  $\text{MgCl}_2$  when compared to H1-less nucleosome arrays is required to induce folding (Carruthers et al., 1998). We have also observed that arrays containing H1 compact in less divalent salt compared to arrays devoid of H1 (Figure 46B). Taken together, our studies demonstrate that H2B phosphorylation can induce chromatin compaction directly without linker H1.

#### *In vitro nucleosome array and in vivo chromatin compaction status*

Perhaps the most obvious question when considering functional ramifications of chromatin fiber dynamics is whether the solution behavior of chromatin fibers *in vitro* is relevant *in vivo*. Short stretches of 10-nm and 30-nm chromatin fibers can exist in extensively coiled 100-200 nm diameter chromosomal domains without causing widespread chromosomal fiber decondensation (Belmont and Bruce, 1994). This suggests that local chromatin fiber dynamics and long-range chromosomal domain structures are uncoupled *in vivo*, a conclusion that also is consistent with the physical uncoupling of folding and oligomerization in nucleosomal arrays and chromatin fibers *in vitro* (Schwarz et al., 1996). Thus, the mechanisms and determinants of chromatin fiber dynamics characterized *in vitro* should have direct relevance to those regions of the genome that are assembled

into some type of stable, higher-order structure domains, such as those seen during apoptosis.

The yeast H2B S10E mutant, which mimics the phosphorylated state of S10, induces a highly-compacted chromatin state *in vivo* and *in vitro* in fibers that were previously uncondensed, suggesting that H2BS10ph regulates chromatin fiber condensation. Therefore, the compacted chromatin should be absent in a mutant lacking S10ph *in vitro* and *in vivo*. Indeed, both WT and H2B S10A nucleosome arrays, where S10ph was absent, displayed a sedimentation coefficient value much lower than that of the S10E array (Figure 44). These results not only validate the *in vitro* nucleosome array to the *in vivo* chromatin status, it also reinforces the idea that H2BS10ph are critical for condensation of chromatin fibers.

### ***“Cis” mechanism***

By using phospho-mimic mutants of yeast and *Xenopus* H2B, I have shown that H2B phosphorylation can directly cause internucleosomal contact and histone/DNA interaction in order to mediate chromatin condensation. It is remarkable that nucleosome arrays with one amino acid replacement, yeast H2B S10E or *Xenopus* H2B S14E, can cause a dramatic change in chromatin fiber folding (Figures 44 and 45). Yeast H2B motifs consisting of amino acid residues 2-16 appear to function as a modular signaling platform (Figures 47 and 48), so it can be argued that conformation change is solely dependent on the negative charge in the H2B motif and not necessarily on serine. In other words, chromatin fibers would form a compacted conformation as long as a negative charge is present within this motif. Dr. Grunstein’s group has shown that amino acid

residues 21-29 of the H4 N-tail is critical for the repression of silent mating loci and changing the charge of this motif by a single amino acid insertion or deletion are extremely detrimental (Johnson et al., 1992). This suggests that overall charge is crucial to the function of the H4 motif and a similar paradigm may exist in H2B as well. To test this hypothesis, replacing residues near phospho-targeted serine with glutamic acid *in vitro* (peptide or nucleosome array) or *in vivo* (yeast mutant) should elucidate the importance of the negative charge on serine or on any residues in the H2B histone tail for mediating chromatin compaction.

*In vitro* nucleosome array system allows one to examine the influence of histone in its proper and native context, although one shortcoming is that influence of covalent histone modifications cannot be addressed. Histone modifications play important roles in modulating nearly all DNA-associated processes. Therefore, it is essential to understand how post-translational modification of histones influence chromatin structure and the binding and function of chromatin-associated proteins. For this purpose, a native chemical-ligation strategy can be used to generate “designed” histones, which consist of covalently modified histone peptides linked to recombinant histone proteins (Shogren-Knaak et al., 2003; Blaschke et al., 2000). Unlike enzymatically-modified histones or those purified from cellular lysates, ligation provides homogeneously modified histones making it possible to study the effect of histone modification on chromatin structure and function where recognition or interaction between histone domains, octamer subunits, nucleosomes, or nucleosomal DNA is important. Yeast histone H2B could be “designed” by linking a peptide containing the N-terminus of H2B featuring single phosphate on S10 with recombinantly-expressed, C-terminal H2B protein. Then, this

“designed” H2B will be incorporated into histone octamers and reconstituted into nucleosome arrays to study the effects of H2BS10ph on chromatin structure.

In 1.2 mM  $\text{MgCl}_2$ , the sedimentation coefficient for yeast H2B S10E and *Xenopus* H2B S14E were higher than the WT nucleosome array that is equivalent to compacted 30-nm chromatin fiber (Figures 44 and 45). These results abet our finding that both phospho-mimic H2B mutants may display chromatin fibers that are more compacted than the 30-nm chromatin fiber. Elucidating the higher-order structure of compact nucleosome arrays should provide further insights into the role of H2B phosphorylation in apoptotic chromatin condensation. Recently, Dr. Richmond’s group had great success in visualizing chromatin fiber compaction by electron microscopy (Dorigo et al., 2004). Nucleosome arrays were stabilized by crosslinking with glutaraldehyde and were prepared under different salt conditions. At very low ionic strength, they observed the “bead-on-a-string” conformation (decondensed state) and in higher ionic strength, a round particle with a diameter 30-nm (condensed state). Employing a similar method of stabilization and visualization of the nucleosome array should determine the chromatin structure influenced by the phosphorylation of H2B.

In conclusion, I have illustrated the possible existence of cis mechanism as the function of H2BS10ph in mediating the yeast apoptotic cascade. The *in vitro* peptide and the nucleosome array containing phospho-mimic H2B S10E gives strength to the idea that H2BS10ph may serve as a “facilitator” during apoptotic chromatin condensation. It is still unclear whether this type of cis mechanism exists *in vivo*, but these results point to a potentially novel mode of histone phosphorylation directly affecting the chromatin structure.

## Materials and Methods

### *Histone Expression Plasmids*

The pET-3a plasmid containing the individual yeast or *Xenopus Laevis* histone were generated as previously described in Luger et al., 1997. For histone mutagenesis, a procedure based on the 'QuickChange Site-Directed Mutagenesis' protocol by Stratagene was used. For creating mutations in yeast histone H2B, pET-3a plasmid containing full-length yeast histone H2B gene was used as template. Two mutagenic primers with complementary sequences were designed for each mutation. The desired mutation was placed in the middle of the primer with 15 base correct sequences on both sides.

The pET-3a plasmid containing *Xenopus Laevis* histone H2B lacks sequences encoding first three amino acids (PEP). The expression plasmid with the full-length *Xenopus Laevis* histone H2B was generated by PCR. *Xenopus* H2B S14A or H2B S11A mutation was generated by PCR using pET-3a plasmid containing H2B gene with or without first 3 amino acids, respectively. Desired mutations were confirmed by DNA sequencing.

### *Histone Expression*

The pET-3a plasmid with histone genes was transformed into competent *E. coli* BL21 (DE3)pLysS cells as described in Bacterial transformation (Chapter 2; Materials and Methods) The cells were plated and incubated at 37°C for 10-18 hr on TYE plates (1.0% tryptone, 0.5% yeast extract, 0.8% NaCl, 1.5% agar, 100 µg/ml ampicillin and 25 µg/ml chloramphenicol) containing ampicillin and



chloramphenicol to select not only for the presence of the pET-3a plasmid, but also maintain the pLysS plasmid.

For the large scale expression, a 100 ml 2X TY (100 µg/ml ampicillin and 25 µg/ml chloramphenicol) starter culture was inoculated with six colonies from a transformation plate and grown at 37°C until the OD600 reached 0.4. Subsequently 12x 1 liter 2X TY with ampicillin and chloramphenicol was inoculated with 5 ml of the starter culture for 1 liter of medium and grown until the OD600 reached 0.6. Addition of 0.4 mM IPTG induced the expression of the lacUV5 dependent T7 RNA polymerase and therefore also the expression of the T7-promoter controlled histone gene. The cells were harvested after 2 hr by centrifugating at room temperature for 6 min at 6,000g in 500 ml containers. The pellet was resuspended in 200 ml wash buffer (50 mM Tris-HCl pH 7.5, 100 mM NaCl, 1 mM benzamidine, 1 mM  $\beta$ -mercaptoethanol), and frozen in liquid nitrogen.

### *Histone purification*

The purification protocol involves three steps: preparation of inclusion bodies, gel filtration under denaturing conditions, and HPLC-ion exchange chromatography under denaturing conditions.

### *Inclusion body preparation*

The frozen cells were lysed by thawing in a 37°C waterbath. The freeze-thawing disrupts the inner cell membrane and liberates T7 lysozyme, which can then digest the outer cell membrane. For homogenization, the viscous cell suspension

was mixed in the Ultra Turrax twice for 20 seconds. Inclusion bodies were collected by spinning at 4° C for 30 min at 17,000g. The pellet was resuspended in 50 ml 1% Triton X-100 in wash buffer and dounced, then spun at room temperature for 10 min at 17,000g. The washing of the pellet was repeated once with 1% Triton in wash buffer and twice with wash buffer only. The pellet was redissolved in 40 ml unfolding buffer and stirred at room temperature for 1 hr. The undissolved matter was spun down at room temperature for 60 min at 17,000g and the supernatant loaded onto the Sephacryl S-200 column.

#### *Gel filtration chromatography*

The Sephacryl S-200 column was equilibrated with 2 liters SAUDE 200 (7 M deionized urea, 20 mM NaAc pH 5.2, 200 mM NaCl, 1 mM  $\beta$ -mercaptoethanol, 1 mM EDTA). The fractions of the histone peak were run on a SDS-PAGE gel and the fractions containing the relatively pure histone were pooled, dialyzed in 6-8000 MWCO bags against 3 changes of 5 liters 5 mM  $\beta$ -mercaptoethanol, frozen in liquid nitrogen, lyophilized and stored at -20°C.

#### *Cation ion exchange chromatography*

The lyophilized S-200 histone was dissolved in SAUDE 200 and spun for 10 min at 20,000g. The 6 ml Resource S column was equilibrated with SAUDE 200 and a maximum of 50 mg per run was injected into the column. Using a flow rate of 2 ml/min, proteins were eluted with the following gradient with buffer A= SAUDE 200 and buffer B= SAUDE 600 (7 M deionized urea, 20 mM NaAc pH 5.2, 600 mM NaCl, 1 mM  $\beta$ -mercaptoethanol, 1 mM EDTA).

| Time (min) | B (%) |
|------------|-------|
| 0          | 0     |
| 6          | 0     |
| 7          | 10    |
| 20         | 60    |
| 21         | 100   |

### *Histone octamer refolding and purification*

Purified, lyophilized histone H2A, H2B, H3 and H4 were dissolved individually in unfolding buffer (7 M guanidine hydrochloride, 20 mM NaAc pH 5.2, 10 mM DTT) to a concentration of approximately 2 mg/ml. After at least 30 min at room temperature, the histone concentration was determined by measuring the OD<sub>276</sub> of the undiluted sample against unfolding buffer. The four histones were mixed in equimolar amounts and adjusted to a final protein concentration of 1 mg/ml with unfolding buffer and then dialyzed in 6-8000 MWCO dialysis bags against three changes of 2 liter refolding buffer at 4°C for at least 3 hr. The sample was spun for 20 min at 4,000g to remove the precipitate. The supernatant was concentrated in a Micropore Ultra 15 at 4°C to a final volume of 1-1.5 ml. The sample was spun twice at 4°C for 15 min at 20,000g and then loaded onto the Superose 6 column, which was pre-equilibrated with refolding buffer (2 M NaCl, 10 mM Tris-Cl pH 7.5, 1 mM EDTA, 5 mM  $\beta$ -mercaptoethanol, 1 mM EDTA) at 4°C. The first eluted peak contained aggregates, followed by a peak containing the octamer and finally a small peak of dimer. The fractions containing the

octamer were determined by SDS-PAGE, pooled and concentrated in a Micropore Ultrafree 4, then stored on ice.

The H2A/H2B dimer were reconstituted separately using the same protocol as used for the histone octamer.

### *Reconstitution of nucleosomes on 36-mer DNA fragment*

DNA, 5  $\mu$ M measured in nucleosome repeat, was mixed with 4 M KCl and water to yield a final concentration of 2 M KCl in a total volume of 100  $\mu$ l. The histone octamer was added such that the desired molar ratio of octamer/DNA was obtained (see Determination of octamer/DNA ratio). For reconstitutions with 601 based arrays 147 bp MMTV A DNA was added as a histone octamer buffer. The 100  $\mu$ l reconstitution reaction mixture was placed in a small dialysis bag (Spectra/Por 6-8000 MWCO membrane) and the dialysis protocol automatically executed overnight by a specially designed reconstitution apparatus. The reconstitution started in 200 ml of 1.4 mM KCl, 10 mM Tris pH 7.5, 0.1 mM EDTA. By stepwise dilution with End buffer (10 mM Tris pH 7.5, 10 mM KCl, 0.1 mM EDTA) the dialysis was brought to 0.6 M KCl. The step (in time and KCl concentration) were 70 min 1.4 M, 70 min 1.2 M, 420 min 1.0 M, 70 min 0.8 M, 70 min 0.6 M, following which the dialysis container was emptied and refilled with 200 ml of End buffer. After 180 min, the End buffer was exchanged again and the sample was dialyzed for another 180 min. The reconstituted arrays were recovered from the dialysis bag and centrifuged for 10 min with 20,000g at 4°C to remove precipitated material.

### *Determination of octamer/DNA ratio by ScaI digestion*

The stoichiometry of soluble material was assessed by digesting the assembled arrays with *ScaI* in 100 mM KCl, 10 mM Tris-Cl pH 7.5, 0.5 mM MgCl<sub>2</sub> for 4 hr at 22°C. Each repeat is separated by a *ScaI* restriction site. The ratio of free DNA to nucleosomal DNA was analyzed on an APAGE gel. A single well positioned octamer per DNA repeat yields a pattern showing no bands corresponding to free DNA and uncleaved DNA repeats.

### *Native agarose-polyacrylamid composite gels (APAGE)*

An aliquots of 60 ml MilliQ water containing 1% agarose was heated until the agarose was dissolved, following which 50x TAE was added to give 0.25x TAE. While the solution was still hot 2 ml acrylamide (40%, 20:1), 100  $\mu$ l of 25% AMPS and 30  $\mu$ l of TEMED were added. The solution was poured between assembled and preheated (60°C) glass plates (20 cm x 20 cm, 1.5 mm spacers, comb was inserted only few millimeters). The agarose was let harden for 20 min at room temperature, and the comb was removed very carefully and gel was mounted in the vertical gel box. The gel was prerun for 3 hr at 200 V in 0.25 x TAE with buffer recirculation. Approximately, 1-3 pmol of reconstituted material was loaded in native 5% sucrose and run under the same conditions for 3 hr. After electrophoresis, the gel was stained for 10 min in a 1  $\mu$ g/ml ethidium bromide solution and photographed on a MultiImage Light Cabinet.

### *Sedimentation velocity*

Sedimentation velocity experiments were performed using a Beckman XL-1 analytical ultracentrifuge and an AN-50 Ti rotor. The initial sample absorbance at 259 nm was between 0.6 and 0.8. Samples (350 to 400  $\mu$ l for sedimentation velocity) were equilibrated in their respective buffer solutions in the analytical ultracentrifuge chamber under vacuum for 30 min at 20°C prior to sedimentation at 12,000 rpm in 12 mm double sector cells and an 8 hole rotor. Scans were collected at 259 nm in continuous scan mode using 1 0.003 cm radial step size. Boundaries were analyzed by sedimentation boundary fitting using the *c(s)* distribution method provided by the program Sedfit (Schuck, 2000).

### *Plasmids, Yeast strains and Culture Conditions*

Plasmid pQQ18 (CEN *LEU2*, CEN, *HTA1-HTB1-HHF2-HHT2*) was used to generate histone mutant plasmids; pSA81 (*htb1-P8A P13A*) and pSA82. Plasmid pSA82 contains a short stretch of the H2B N-terminal tail, corresponding to amino acids 2-16, and inserted it into the H2A N-terminal tail at amino acid position 2 in a plasmid shuffle strain lacking H2B N-terminal tail, *htb1*  $\Delta$ 1-32. These mutants were created by PCR and sub-cloned into pQQ18 as previously described in Mutations in histone genes (Chapter 2; Materials and Methods).

Yeast strains are listed in Table 1 and all strains are derived from S288C (BY4741; Research Genetics) background. Strain JHY205 was used to shuffle in plasmids containing histone mutations using 5-FOA as a counterselecting agent for the URA3 plasmid. SAY206, a chimera mutant strain containing pSA82 is referred to as H2A+B. Transformation of yeast cells was performed by the

lithium acetate procedure, as described in Yeast transformation (Chapter 2; Materials and Methods).

#### *Test for Apoptosis and Western Blot*

Yeast apoptotic induction by H<sub>2</sub>O<sub>2</sub>, the cell survival, cell death analysis, TUNEL staining, immunofluorescence, yeast nuclei preparation and Western analysis were carried out as described in Chapter 2; Materials and Methods.

#### *In vitro peptide aggregation assay*

15 µg of peptides were mixed with 6X Lammeli buffer with 1 M DTT, boiled for 10 min and put in ice for 10 min. These peptides were run on 15% SDS-PAGE gel for 20 min at 220 V and stained with fresh filtered Coomassie for 1 hr. The gel was then destained for 10 min.

## CHAPTER 5

### **RAD53 ASSOCIATES WITH H2B SERINE10 PHOSPHORYLATION DURING YEAST APOPTOSIS**

#### **Introduction**

Understanding the biological roles of post-translational histone modifications requires understanding the mechanisms by which these marks are selectively recognized by protein modules (reviewed in Seet et al., 2006). One of the best illustrations of a histone modification in mediating protein-protein interactions is the recognition of methylated lysine residues by a structure known as the chromodomain (de la Cruz et al., 2005). The amino-terminal chromodomain found in heterochromatin protein 1 (HP1) has been shown to bind to the methylated H3K9, particularly in its di- and tri-methylated states (Bannister et al., 2001; Jacobs et al., 2001; Lachner et al., 2001; Figure 7B). It is thought that this interaction is crucial for establishing and maintaining regions of heterochromatin (Sims et al., 2003; Schotta et al., 2004). As for acetyl-lysines in histones, a motif known as the bromodomain, which is found in a number of nuclear histone acetyltransferases and transcription regulators, binds to acetylated histone H3 and H4 (Jeanmougin et al., 1997; Winston and Allis, 1999). The interaction between the double bromodomains of hTAF<sub>II</sub>250 and acetylated K5 and K8, or



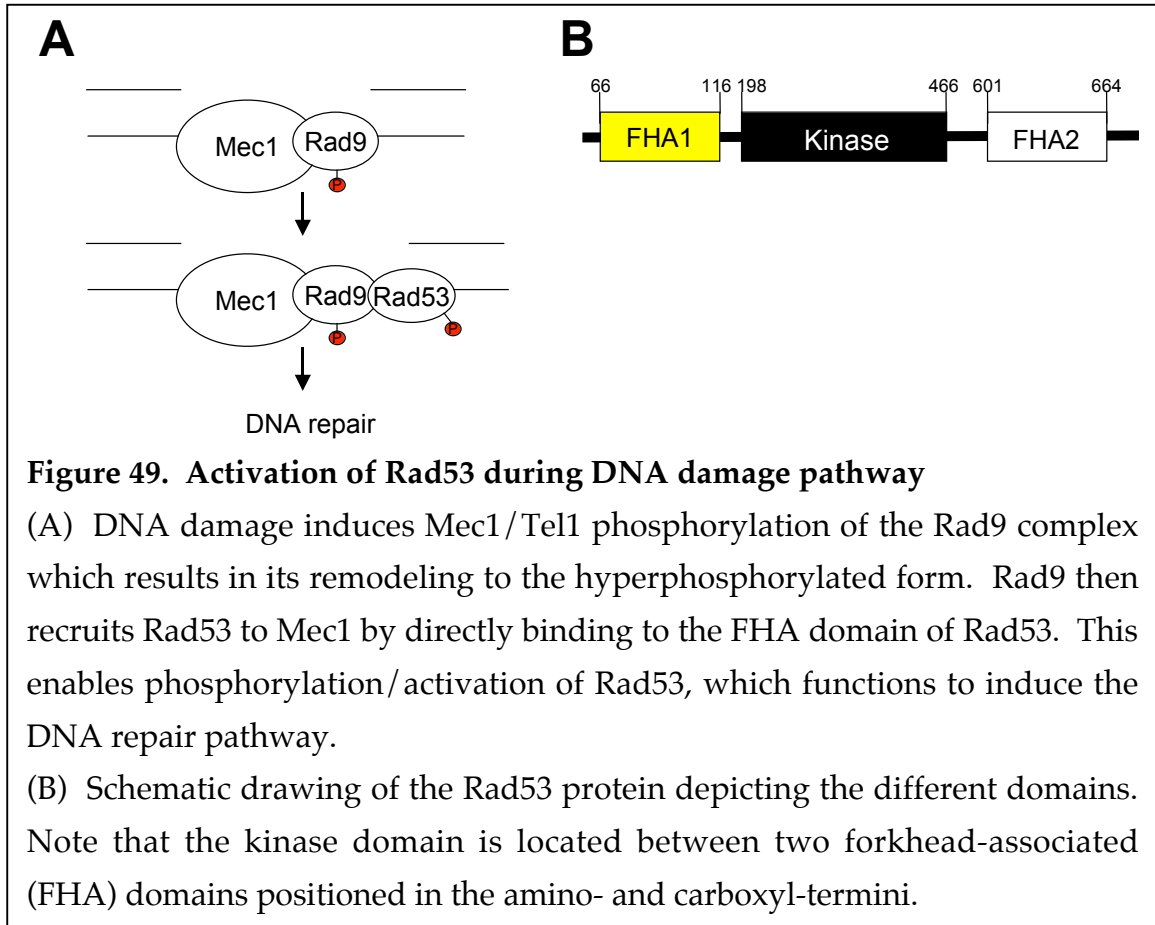
K12 and K16 of H4 leads to the assembly of preinitiation complexes for transcription activation (Mizzen et al., 1996; Rossignol et al., 1999; Figure 7B).

A docking module for a phosphorylated serine residue in the histone variant, H2A.X, has also been identified. The phosphorylation of this relatively minor histone variant, H2A.X S139 in mammalian cells and H2A S129 in yeast, correlates with double-stranded DNA breaks (DSB) induced by numerous stimuli, suggesting that this mark acts as a DNA-damage sensor (Rogakou et al., 1998, Rogakou et al., 2000). In mammalian cells, Mdc1/Nfbd1 directly interacts with H2A.XS139ph via its BRCT domain (Stucki et al., 2005). Their interaction then results in the recruitment of 53BP1, Nbs1 and phosphorylated ATM at sites of damaged chromatin, and is thought to mediate the DNA repair signaling cascade (Stucki et al., 2005; Figure 7C). The 14-3-3 protein has also been identified as a binding protein for H3S10ph (Macdonald et al., 2005; Figure 7C). Although H3 phosphorylation at S10 occurs during mitotic and meiotic chromatin condensation, a causal relationship between this phosphorylation event and chromosome dynamics has not yet been demonstrated; yeast mutants lacking S10 (H3 S10A) have generation times and cell cycle progression identical to those of the wild-type strain (Hsu et al., 2000). To date, the binding modules that “read” the covalent histone modifications associated with the chromatin compaction (e.g. H2BS14ph in mammalian cells and H2BS10ph in yeast) still remain elusive.

As discussed in Chapter 2, H2AS129ph occurs early and precedes apoptotic H2BS10ph in yeast (Figure 18); this suggests an intricate interplay between DNA damage/repair and apoptosis. If DSBs are unrepaired or repaired incorrectly, they can cause cell death (Sancar et al., 2004; Zhou and Elledge, 2000;

Modrich, 1997). Thus, cells react to DSBs by rapidly deploying a host of proteins to the damaged-chromatin regions. Some of these proteins engage in DNA repair, while others trigger a signaling pathway (DNA-damage checkpoint). In yeast, the central proteins involved in this DNA damage response are the checkpoint kinases Mec1, Rad53, Rad9, and Chk1. Mec1 and Rad53 are the central transducers of DNA damage response signals and they activate another kinase such as Dun1 to delay cell-cycle progression and coordinate repair processes (Zhou and Elledge, 2000; Paciotti et al., 2000; reviewed in Rouse and Jackson, 2002; Bashkirov et al., 2003; Figure 49A). The deletion of Rad53 disrupts the DNA repair pathway since *rad53Δ* is sensitive to DNA damage agents and leads to the loss of viability (Hammet et al., 2000; Pike et al., 2003). During DNA damage, the activation of Rad53 by phosphorylation requires the upstream kinase Mec1 and the mediator Rad9 (Sanchez et al., 1996; Sun et al., 1996). Multiple models for Rad53 activation have been proposed. In the first model, phosphorylated Rad9 may work as an adaptor to deliver Rad53 to Mec1 at sites of DNA damage (Sun et al., 1998; Schwartz et al., 2002). In another model, Rad53 is activated through intermolecular autophosphorylation after interaction with phosphorylated Rad9 (Gilbert et al., 2001; Schwartz et al., 2003). It is unclear whether the two mechanisms operate together to fully activate Rad53 and the DNA repair pathway *in vivo*. Nevertheless, the activation of the Rad53-dependent DNA repair pathway requires Rad53's interaction with phosphorylated Rad9 (Schwartz et al., 2003). Disruption of their association leads to the accumulation of DNA damage and failure to restore the continuity of the DNA duplex; the apoptotic signaling cascade is subsequently activated to

eliminate such heavily damaged or seriously deregulated cells (Sancar et al., 2004).



In keeping with the “trans” mechanism leading to chromatin compaction (Figure 6B), I sought to address the binding partner for H2BS10 phosphorylation during H<sub>2</sub>O<sub>2</sub>-induced yeast apoptosis. In collaboration with Dr. Sheng-Hong Chen at Ludwig Institute of Cancer, San Diego, CA, we found that Rad53 associates with the nucleosome carrying histone H2B phosphorylated at S10 upon H<sub>2</sub>O<sub>2</sub> insult. Rad53 contains two forkhead-associated homology domains (FHA1 and FHA2) that are hypothesized to be modular phospho-S/T binding domains (Hammet et al., 2000; Figure 49B). Using recombinantly-expressed individual Rad53 FHA domains, I demonstrated that the FHA1 domain of Rad53 binds to H2BS10ph peptide *in vitro*. Interestingly, during a H<sub>2</sub>O<sub>2</sub>-induced

apoptotic cascade, Rad53 is inactivated and it binds to H2BS10ph. Taken together, these results, while somewhat preliminary, provide support to the idea that inactivation of the DNA-damage checkpoint may promote the apoptotic cascade.

## Results

### *FHA1 of Rad53 specifically associates with phosphorylated serine 10 of H2B in vitro*

Previously, Dr. Sheng-Hong Chen at the Ludwig Institute of Cancer center (San Diego, CA), had identified that recombinant FHA1 from Rad53 interacts with histones upon H<sub>2</sub>O<sub>2</sub> treatment (Dr. Chen, personal communication). To this end, bacterially expressed recombinant GST-FHA1 or GST was immobilized on glutathione-sepharose beads and incubated with H<sub>2</sub>O<sub>2</sub>-treated or untreated WT yeast lysates. After the sepharose beads were pelleted by brief centrifugation, bound proteins were eluted and subjected for MS/MS analysis. Dr. Chen found that H2B binds specifically to GST-FHA1, but not GST alone (Dr. Chen, personal communication), suggesting that FHA1 from Rad53 is a possible binding protein domain for H2BS10ph during H<sub>2</sub>O<sub>2</sub>-induced yeast apoptosis. Therefore, I initiated a collaboration with Dr. Chen's group to further test this hypothesis.

To decipher whether FHA1 from Rad53 directly interacts with H2BS10ph, a peptide pull-down experiment was performed using either biotinylated histone H2B or H3 peptides each immobilized on avidin beads (Figure 50A). This method is commonly used in our laboratory and recently, Dr. Joanna Wysocka has successfully demonstrated the interaction between mammalian Wdr5 protein and H3K4me2 using this assay (Wysocka et al., 2005). Therefore, I adopted a similar system where the biotin moiety was attached at the N-terminus of synthetic peptides. Histone H2B peptides carried amino acids 1-20, with S10 either unmodified or singly phosphorylated; histone H3 peptides also carried amino acids 1-20 and included either unmodified or singly phosphorylated S10

(Figure 50B). These peptides were bound to streptavidin beads in a high salt buffer and then adjusted to a low salt buffer. To ensure specificity, excess BSA (20  $\mu$ g) was incubated with a 1:1 mixture of bacterially expressed recombinant GST-FHA1 and GST-FHA2 from Rad53 (each at 1  $\mu$ g). This mixture was used as input for the pull-down assay with the biotinylated histone peptides linked to streptavidin beads. The beads were washed extensively to remove the unbound proteins. As shown in Figure 50C, GST-FHA1, but not GST-FHA2, was enriched in the H2BS10ph peptide. In contrast, neither GST-FHA1 nor GST-FHA2 from Rad53 was enriched in the unmodified H2B or either of the H3 peptides. BSA failed to bind to any of these peptides (Figure 50C). Next, I tested binding ability of the recombinantly-purified FHA domain from Dun1 (GST-Dun1) to H2BS10ph peptide. Dun1 is a FHA domain kinase, which functions in the DNA damage and replication block (Zhou and Elledge, 1993; reviewed in Weinert, 1998; Zhou and Elledge, 2000). However, unlike Rad53, Dun1 contains only one FHA (Bashkirov et al., 2003). No interaction was observed between GST-Dun1 and H2BS10ph (Figure 50C). These results indicate that association between FHA1 of Rad53 and H2BS10ph is both direct and, within the context of the peptides and proteins used here, specific.

***In solution fluorescence polarization assay detects an interaction between FHA1 of Rad53 and H2BS10ph peptide***

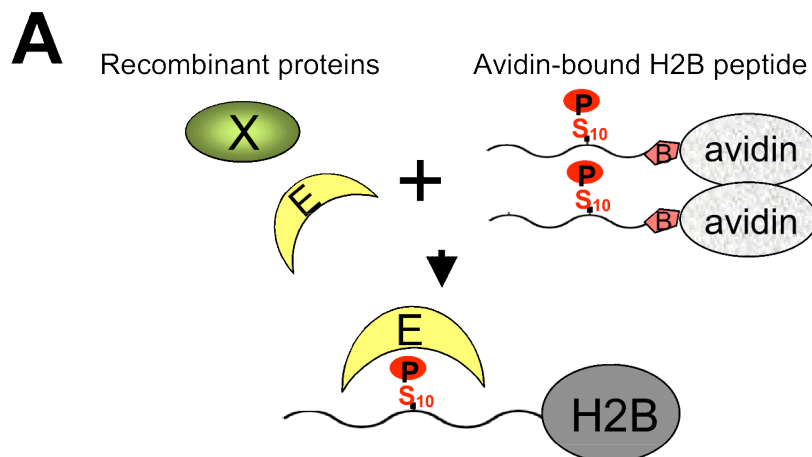
In order to further test an interaction between FHA1 of Rad53 and H2BS10ph, *in vitro* quantitative binding experiments were performed using fluorescently labeled H2B peptides and recombinant FHA1 or FHA2 of Rad53. As described

**Figure 50. FHA1 of Rad53 is a potential binding effector for H2B serine 10 phosphorylation *in vitro*.**

(A) Schematic drawing of histone peptide pull-down assays. Biotinylated histone peptides were linked to streptavidin beads and incubated with the recombinant proteins. After washing, bound proteins were eluted from the beads by glycine, and eluted fractions were separated on a SDS-PAGE gel.

(B) Amino acid sequence of histone peptides used for the peptide pull-down assays. Yeast H2B peptides contained amino acids 1-20 either unmodified (H2Bun) or singly phosphorylated at S10 (H2BS10ph). Yeast H3 peptides contained amino acids from 1-20 that were either unmodified (H3un), singly phosphorylated at T3 (H3T3ph) or at S10 (H3S10ph). [P] denotes phosphate.

(C) Excess BSA was incubated with equimolar amounts of purified recombinant GST-tagged FHA1 or FHA2 of Rad53, and GST-tagged FHA of Dun1. This mixture was used as input for the pull-down assay with indicated peptides. Bound proteins were analyzed by SDS-PAGE and silver staining. GST-tagged FHA1, but not FHA2, specifically binds to H2BS10ph biotinylated peptide (see red arrow). Note that FHA1 does not bind to other biotinylated peptides tested, including H3S10ph or H3T3ph peptide. No other band was detected in this gel assay. Pep, histone peptides.



**B**

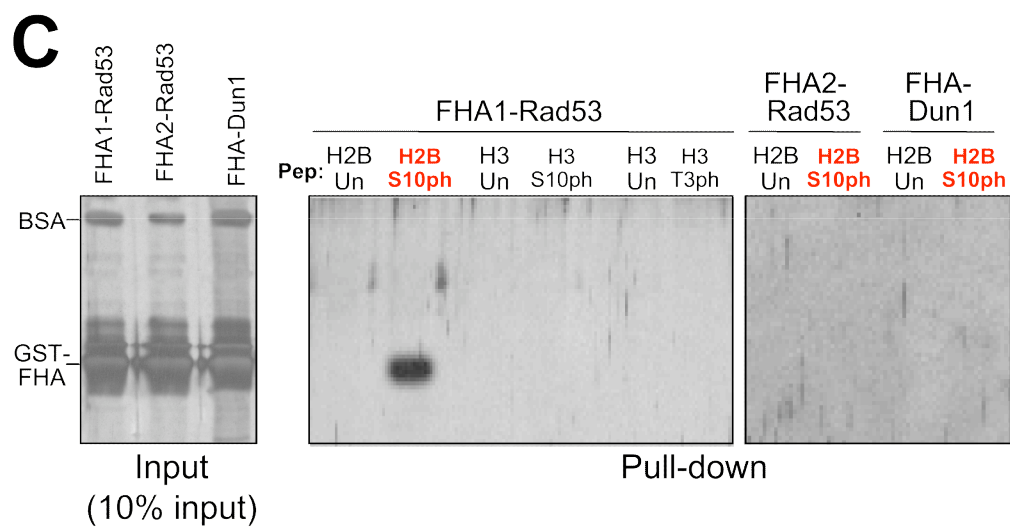
H2B<sub>un</sub>: S<sub>1</sub>AKAEKKPASKAPAEKKPAA<sub>20</sub>

H2BS10ph: S<sub>1</sub>AKAEKKPAS<sup>[P]</sup><sub>10</sub>KAPAEKKPAA<sub>20</sub>

H3<sub>un</sub>: A<sub>1</sub>RTKQTARKSTGGKAPRKQL<sub>20</sub>

H3T3ph: A<sub>1</sub>RT<sup>[P]</sup><sub>3</sub>KQTARKSTGGKAPRKQL<sub>20</sub>

H3S10ph: A<sub>1</sub>RTKQTARKS<sup>[P]</sup><sub>10</sub>TGGKAPRKQL<sub>20</sub>





in Figure 51A, upon excitation, the fluorescent peptides emit light that is polarized by a filter and the extent of depolarization of the emitted light (its anisotropy) depends on the mobility of the fluorescent molecule: the higher the rotational diffusion of a fluorescent molecule, the stronger the depolarization it causes. These differences in depolarization are exploited to measure the binding of a fluorophore-labeled peptide to a protein. If the peptide is bound to a protein, the rotational mobility of the peptide is drastically reduced compared to the free peptide. The emitted fluorescence is therefore polarized (Figure 51A). This method was previously used to measure the binding of chromodomain proteins such as HP1 and Polycomb (Pc) to H3K9me2 peptide (Jacobs et al., 2001; Fischle et al., 2003c; Fischle et al., 2005). I labeled various H2B (unmodified, H2BS10ph, H2BK11ac, or H2BS10phK11ac) and H3S10ph peptides by adding a FITC group to its N-terminus through NHS-mediated cross-linking. The quality of FITC labeling at the N-terminus of H2B peptides was verified by mass spectrometry analysis with help of Rob Diaz. The binding constants (dissociation constant,  $K_D$   $\mu$ M) were then determined by measuring the fluorescence anisotropy of the fluorophore-labeled peptides (100 nM) when different concentrations of recombinant FHA proteins were added. Consistent with the peptide pull-down experiment showing Rad53 FHA1 as the binding domain for H2BS10ph (Figure 50C), the fluorescence polarization measurements indicated a clear preference of the Rad53 FHA1 for the H2BS10ph, but not the unmodified H2BS10, or H3S10ph (Figure 51B). Specifically, the dissociation constant for the H2BS10ph peptide was 71  $\mu$ M, and that for the unmodified H2B peptide was 13,888  $\mu$ M (Figure 51B). Likewise, the binding constant for the

association between FHA1 and H2BK11ac peptide remained as high as the unmodified peptide. I also detected a significant loss in the affinity of Rad53 FHA1 for a dually modified H2BS10phK11ac peptide (Figure 51B), suggesting a putative function for the dual-mark combination of H2BS10phK11ac in the inhibition of Rad53 recruitment. Taken together, these results demonstrate that FHA1 domain of Rad53 specifically binds to H2BS10ph *in vitro*.

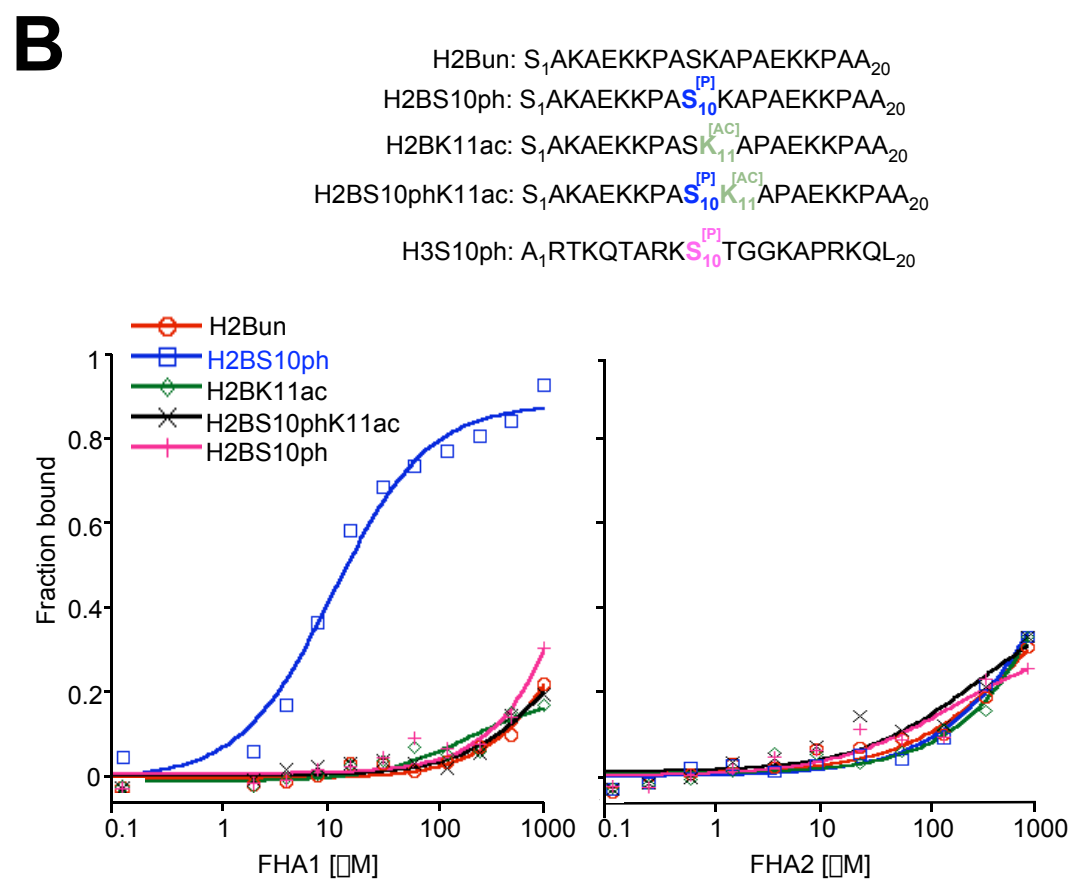
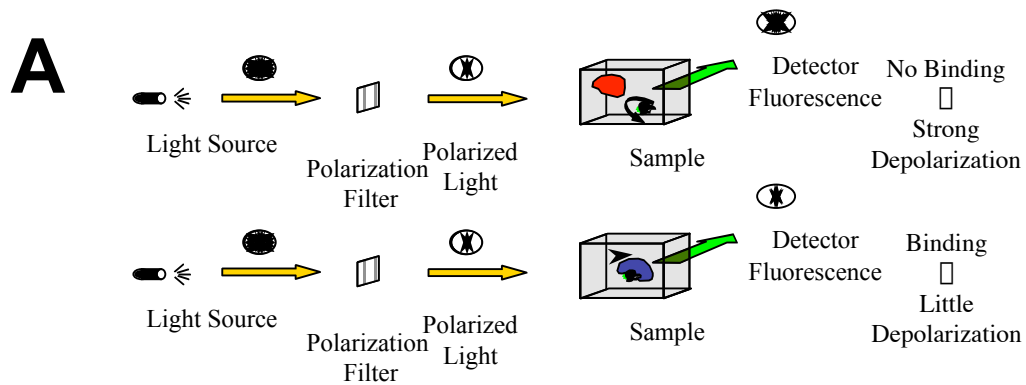
### ***Rad53 associates with phosphorylated serine 10 H2B***

To confirm the interaction between Rad53 and H2BS10ph *in vivo*, I turned to the peptide pull-down assay as described in Figure 50. This time, a series of biotinylated unmodified or appropriately modified H2B peptides (amino acids 1-20; see Figure 50B for the peptide sequence) immobilized on streptavidin beads were incubated with H<sub>2</sub>O<sub>2</sub>-treated or untreated WT nuclear extracts (Figure 52A). Bound polypeptides were then eluted from the resin, resolved by SDS-PAGE, and visualized by silver staining (Figure 52B). Although I observed numerous bands common between these pull-down eluted fractions, this analysis consistently revealed the presence of a 95 kDa band that was specifically enriched in the H2BS10ph peptide purification (See red arrow in Figure 52A). With the help of Dr. Alan Tackett from Dr. Brian Chait's laboratory at the Rockefeller University, we attempted to identify this polypeptide using mass spectrometry. Unfortunately, we were not able to identify it due to the insufficient amount of polypeptide extracted from this gel. However, 95 kDa is the predicted molecular mass of Rad53, so I tentatively predict that Rad53 associates with H2BS10ph.

**Figure 51. Binding studies of H2B tail peptides to FHA1 of Rad53**

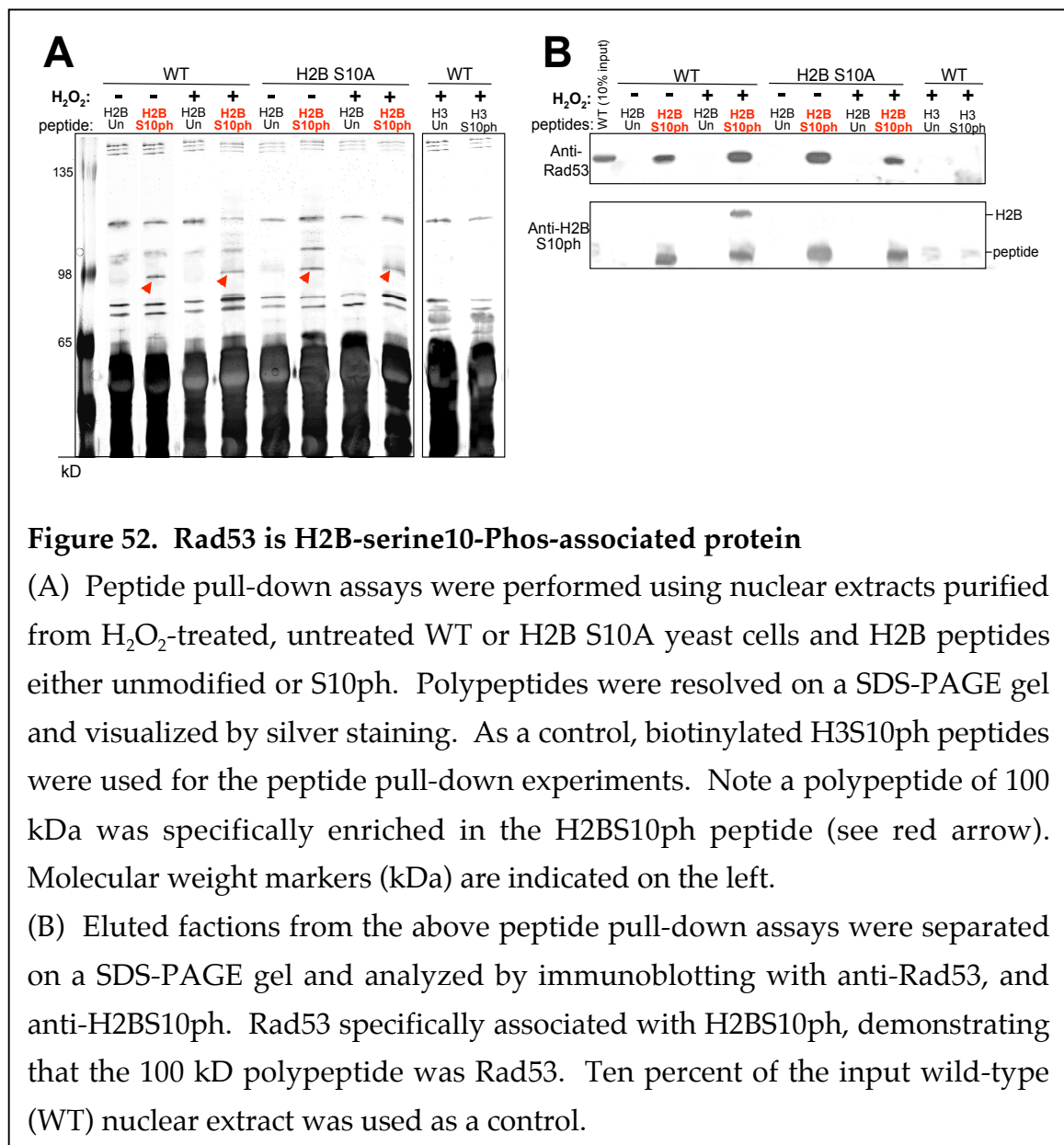
(A) Schematic delineation of fluorescence polarization measurement. When fluorophores are excited with polarized light, they emit polarized light and the extent of emission depends on the mobility, therefore on the size of the fluorescent molecule; the higher the rotational diffusion of a fluorescent molecule, the stronger is the depolarization it causes. These differences in the depolarization are exploited to measure the binding of a fluorophore-labeled peptide to a protein. If a fluorophore-labeled peptide does not bind to a protein, then the mobility of the fluorophore remains high, therefore, displays strong depolarization (Top panel). However, when there is an interaction between fluorophore-labeled peptide and a protein, then the rotational mobility of the peptide is drastically reduced compared to the free peptide, therefore results in little depolarization and change in its anisotropy (Bottom panel) (adapted from Holger Dorman).

(B) Binding of the FHA1 or FHA2 of Rad53 to H2B peptides containing residues from 1-20 with unmodified or S10ph, in a fluorescence polarization assay.  $K_D$  ( $\mu$ M) values are listed in the bottom. Note that FHA1 of Rad53 interacts with H2BS10ph peptide. Neither FHA domains interact with the unmodified H2B tail.



|      | H2B<br>unmod | H2B<br>S10ph | H2B<br>K11ac | H2B<br>S10phK11ac | H3<br>S10ph |
|------|--------------|--------------|--------------|-------------------|-------------|
| FHA1 | >1000        | 71 ± 9       | >1000        | >1000             | >1000       |
| FHA2 | >1000        | >1000        | >1000        | >1000             | >1000       |

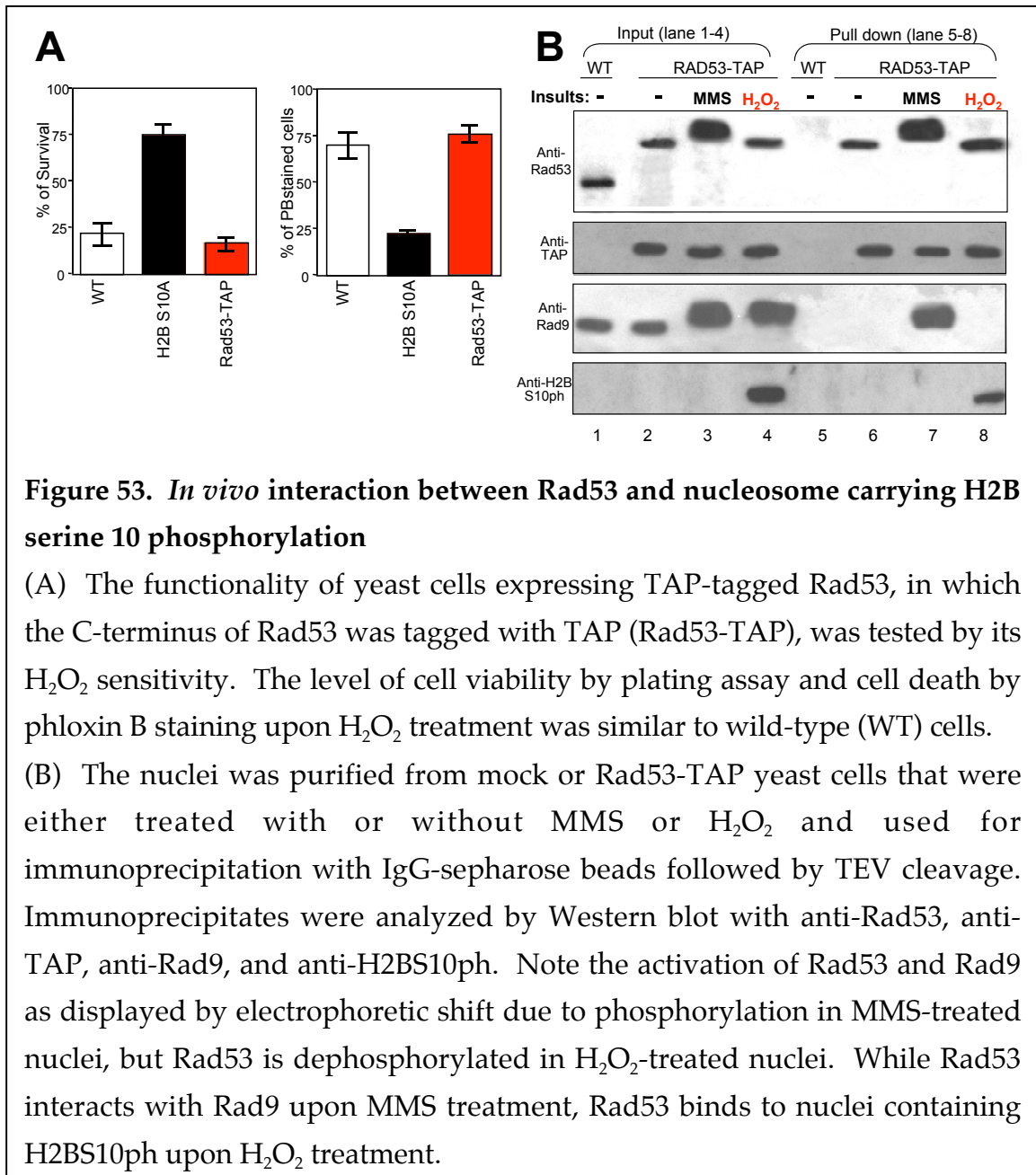
To confirm the specificity of the association between Rad53 and H2B tail phosphorylated at S10 during H<sub>2</sub>O<sub>2</sub>-induced yeast apoptosis, I performed a similar peptide pull-down assay with yeast extracts, but this time the eluted polypeptides were separated on SDS-PAGE gel and then subjected to immunoblotting to detect Rad53 (anti-Rad53 antibody). As expected, Rad53 associates specifically with the H2BS10ph, but not unmodified H2BS10 upon H<sub>2</sub>O<sub>2</sub> induction (Figure 52B). The interaction between Rad53 and H2BS10ph was



also consistently present in the absence of H<sub>2</sub>O<sub>2</sub> treatment or phosphorylation at S10 (H2B S10A) suggesting that synthetic H2BS10ph peptide can serve as a preferential binding substrate for Rad53 even in the absence of endogenous histone H2B with S10 phosphorylation. As a control, the same peptide pull-down experiments were performed with H3S10ph peptides. No interaction between Rad53 and H3S10ph were observed (Figure 52A and 52B), demonstrating that Rad53 is a major H2BS10ph associated protein.

To confirm the functional significance of Rad53 association with H2BS10ph, I sought to address whether an *in vivo* association of Rad53 with H2BS10 phosphorylated nucleosome exists. To this end, I employed a yeast strain expressing TAP -tagged full-length endogenous Rad53, in which the C-terminus of Rad53 was tagged with TAP. The functionality of this strain was tested by its growth rate and H<sub>2</sub>O<sub>2</sub> sensitivity. The level of cell viability and death was similar to WT (Figure 53A). Nuclei purified from H<sub>2</sub>O<sub>2</sub>-treated or untreated Rad53-TAP strains were used for immunoprecipitation experiments with glutathione-linked to sepharose beads, followed by glutathione elution. To monitor the specificity, nuclei from WT yeast cells untagged with Rad53 were used in parallel mock purifications. Immunoprecipitates were subsequently analyzed with antibodies against (1) Rad53 or (2) TAP to monitor immunoprecipitation efficiency; (3) Rad9, a known Rad53 associated protein, as a positive control; (4) H2BS10ph (Figure 53B). Consistent with published results of Rad53 activation upon DNA damage (Schwartz et al., 2003; 2002), I observed an electrophoretic mobility shift due to DNA-damage activated Rad53 phosphorylation upon treatment with a DNA damage agent, such as methyl methane sulfonate (MMS) (Figure 53B). In comparison, upon 1 mM H<sub>2</sub>O<sub>2</sub>

treatment for 200 minutes, phosphorylation of Rad53 was significantly reduced suggesting that H<sub>2</sub>O<sub>2</sub>-induced yeast apoptosis leads to inactivation of Rad53 (Figure 53B). On the other hand, the phosphorylation of Rad9 was present in both MMS and H<sub>2</sub>O<sub>2</sub> treatments, as indicated by the electrophoretic mobility shift (Figure 53B). H2BS10ph was observed with H<sub>2</sub>O<sub>2</sub>-treated, but not MMS-treated, yeast cells (Figure 53B).



Consistent with previous results showing the interaction between Rad53 and Rad9 (Sun et al., 19998; Schwartz et al., 2002), Rad53 coimmunoprecipitates with phosphorylated Rad9, but not with the phosphorylated H2B tail upon MMS treatment (Figure 53B). Interestingly, H<sub>2</sub>O<sub>2</sub>-treated Rad53-TAP specifically coimmunoprecipitated with the nuclei containing H2BS10ph, but it failed to interact with Rad9 (Figure 53B). These data illustrate that the nonphosphorylated form of Rad53 binds to H2B tail phosphorylated at S10 *in vivo* in the context of native nucleosomes during H<sub>2</sub>O<sub>2</sub>-induced yeast apoptosis.

***Rad53 is inactivated during hydrogen peroxide-induced yeast cell death pathway***

The H<sub>2</sub>O<sub>2</sub> treatment condition that resulted in dephosphorylated Rad53, as shown by electrophoretic mobility (Figure 53B), prompted me to determine the kinetics for Rad53 and Rad9. I harvested WT nuclei at different times post H<sub>2</sub>O<sub>2</sub> treatment and subjected them to Western analysis. The mobility shift characterizing Rad53 phosphorylation occurred early in H<sub>2</sub>O<sub>2</sub> treatments coinciding with the appearance of DSB, as indicated by the presence of anti-H2A.XS139 antibody (Figure 54A). Although the DSB signal remained constant throughout the H<sub>2</sub>O<sub>2</sub> treatment, the mobility shift due to phosphorylation of Rad53 was lost at the time point when the H2BS10ph signal first appeared (90 min post induction; Figure 54A). Rad9, on the other hand, remained phosphorylated throughout the H<sub>2</sub>O<sub>2</sub> treatment. These results suggest that Rad53 binds to phosphorylated Rad9 as an early consequence of the appearance of H<sub>2</sub>O<sub>2</sub>-induced DSBs. However, after 90 minutes of post induction,



dephosphorylated Rad53 interacts with H2BS10ph and subsequently inactivates the Rad53-dependent repair pathway and promotes apoptotic cascade.

To support this claim, immunoprecipitation analysis was carried out as described in Figure 53, but this time using nucleosomes purified from yeast

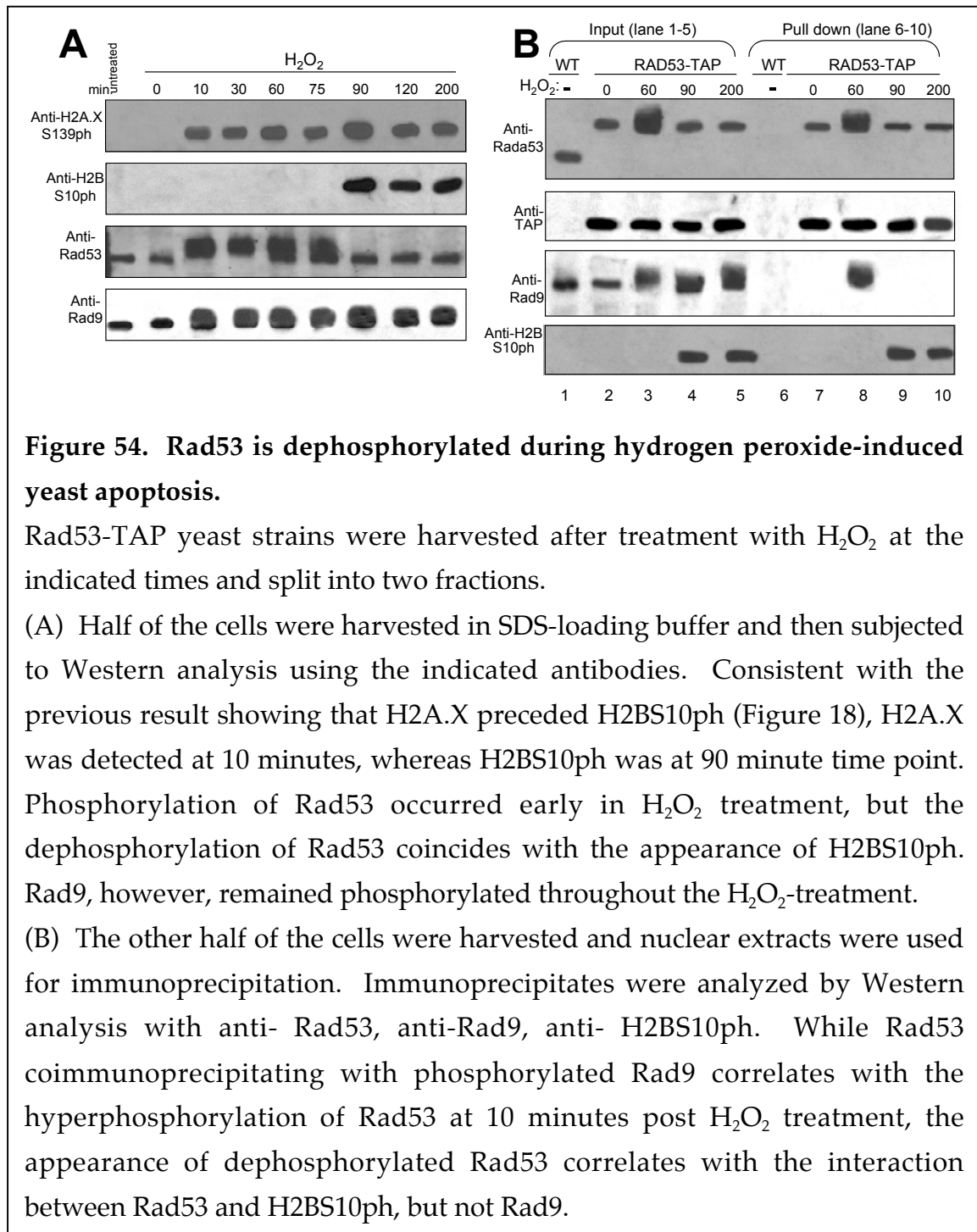


**Figure 54. Rad53 is dephosphorylated during hydrogen peroxide-induced yeast apoptosis.**

Rad53-TAP yeast strains were harvested after treatment with  $H_2O_2$  at the indicated times and split into two fractions.

(A) Half of the cells were harvested in SDS-loading buffer and then subjected to Western analysis using the indicated antibodies. Consistent with the previous result showing that H2A.X preceded H2BS10ph (Figure 18), H2A.X was detected at 10 minutes, whereas H2BS10ph was at 90 minute time point. Phosphorylation of Rad53 occurred early in  $H_2O_2$  treatment, but the dephosphorylation of Rad53 coincides with the appearance of H2BS10ph. Rad9, however, remained phosphorylated throughout the  $H_2O_2$ -treatment.

(B) The other half of the cells were harvested and nuclear extracts were used for immunoprecipitation. Immunoprecipitates were analyzed by Western analysis with anti- Rad53, anti-Rad9, anti- H2BS10ph. While Rad53 coimmunoprecipitating with phosphorylated Rad9 correlates with the hyperphosphorylation of Rad53 at 10 minutes post  $H_2O_2$  treatment, the appearance of dephosphorylated Rad53 correlates with the interaction between Rad53 and H2BS10ph, but not Rad9.

Rad53-TAP cells collected at different times post H<sub>2</sub>O<sub>2</sub> induction. A similar signaling pattern to that of WT was observed with Rad53-TAP in which the onset of H2BS10ph correlated with the disappearance of electrophoretic shift due to Rad53 phosphorylation (Figure 54B). As expected, Rad53 coimmunoprecipitates with nucleosomes containing phosphorylated Rad9 at early time points, suggesting that the DNA repair pathway is activated to remove DSBs (Figure 54B). In contrast, a direct interaction between Rad53 and the phosphorylated H2B tail, but not with phosphorylated Rad9, was observed at the 90 minutes time point (Figure 54B). Since the Rad53-Rad9 complex mediates the induction of the Rad53-dependent DNA repair pathway, these results support the idea that Rad53 binding to H2BS10ph, instead of Rad9, leads to the downregulation of DNA repair cascade, and activation of apoptosis.

#### ***Loss of FHA1 of Rad53 abrogates hydrogen peroxide-induced yeast apoptosis***

I wanted to address whether FHA1 of Rad53 is necessary for yeast cell death *in vivo*. A yeast strain lacking Rad53 (*rad53Δ*) is lethal, since the essential function of Rad53 is to promote deoxyribonucleotide triphosphate (dNTP) production during S phase to facilitate DNA replication (Zhao et al., 1998). This is achieved by phosphorylation and degradation of Sml1, a stoichiometric inhibitor of ribonucleotide reductase (Zhao et al., 1998). Therefore, the lethality of *rad53Δ* mutant is rescued by elevating dNTP levels through disruption of the *SML1* gene (Zhao et al., 2001). The yeast strain lacking Sml1 (*sml1Δ*) is in the four histone plasmid-shuffle strain background. As determined by cell viability and cell death as described in Figure 11, *sml1Δ* was as sensitive to H<sub>2</sub>O<sub>2</sub> treatment similar as WT (Figure 55). Next, I generated a yeast strain lacking either Rad53 FHA1

(amino acids 6-66; *FHA1* $\Delta$ ), Rad53 FHA2 (amino acids 601-664; *FHA2* $\Delta$ ) or full length Rad53 (*rad53* $\Delta$ ) in *sml1* $\Delta$  background and tested for cell viability upon H<sub>2</sub>O<sub>2</sub> induction. Similar to the survival pattern observed with the H2B S10A mutant cells, *FHA1* $\Delta$  and *rad53* $\Delta$ , but not *FHA2* $\Delta$ , cells had a significant reduction of phloxin B stained cells followed by a significant increase in cell viability as compared to its isogenic WT or *sml1* $\Delta$  (Figure 55). These results demonstrate that the FHA1 of Rad53 is important for promoting cell death.

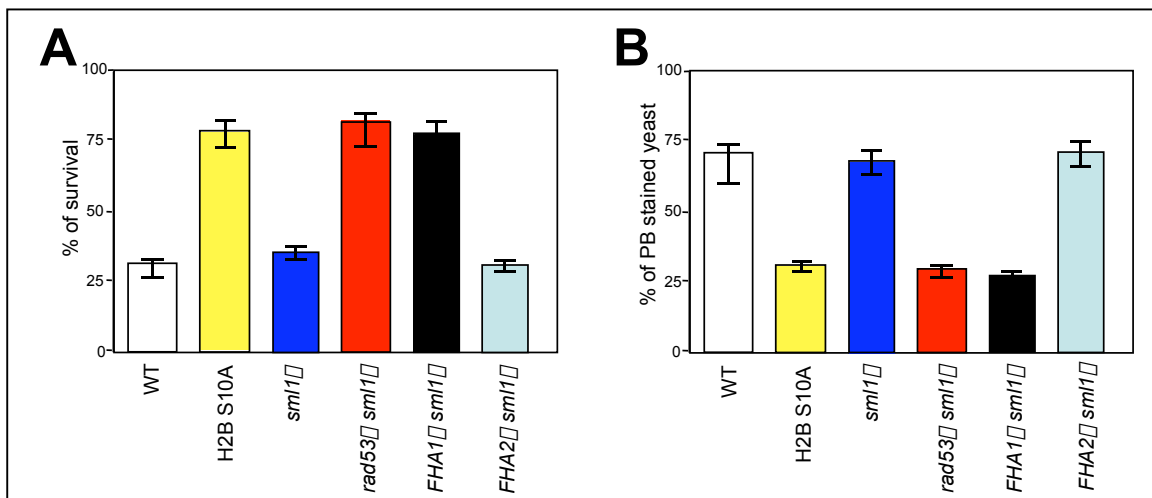


**Figure 55. FHA1 of Rad53 is required for hydrogen peroxide-induced yeast apoptosis.**

Log phase yeast wild-type (WT), cells lacking Rad53 FHA1 (residues 6-116; *FHA1* $\Delta$ ), cells lacking Rad53 FHA2 (residues 601-664; *FHA2* $\Delta$ ), or cells lacking full length Rad53 (*rad53* $\Delta$ ), were treated with 1 mM H<sub>2</sub>O<sub>2</sub> for 200 minutes, and measured the level of cell survival and cell death. Cell viability was judged by plating assay and cell death by phloxin B staining as described in Figure 11. The *FHA2* $\Delta$  mutants were sensitive, but *FHA1* $\Delta$  and *rad53* $\Delta$  were resistant to H<sub>2</sub>O<sub>2</sub> treatment.

## Discussion

The discovery of binding modules that “read” covalent marks on histones, a trans mechanism, has been crucial in our present understanding of gene regulation in the context of chromatin polymers (Seet et al., 2006). In this chapter, I have extended the understanding of this “trans-mechanism” by identifying Rad53 as a binding partner for yeast H2BS10ph during H<sub>2</sub>O<sub>2</sub>-induced yeast apoptosis. Although during the DNA damage pathway the interaction between Rad53 and Rad9 is important for the phosphorylation and subsequent activation of Rad53 (Sanchez et al., 1996; Sun et al., 1996), Rad53 becomes dephosphorylated during H<sub>2</sub>O<sub>2</sub>-induced yeast apoptosis (Figures 53 and 54). *In vivo*, this dephosphorylated form of Rad53 fails to interact with Rad9 (Figures 53 and 54). Instead, Rad53 coimmunoprecipitates with nucleosome carrying H<sub>2</sub>O<sub>2</sub>-induced H2BS10ph (Figures 53B and 54B). FHA1 of Rad53, but not FHA2, specifically associates with H2BS10ph peptide *in vitro* (Figures 50C and 51B). Moreover, H<sub>2</sub>O<sub>2</sub>-induced yeast apoptosis is abrogated in yeast cells lacking FHA1 (Figure 55). Taken together, these results allowed me to conclude that FHA1 of Rad53 is a binding domain for H2BS10ph *in vivo*. The consequence of this interaction may include the downregulation of DNA repair pathway and subsequently promotion of apoptotic cascade (Figure 56).

### *FHA1 of Rad53 as H2BS10ph binding effector protein*

Sequence-dependent phospho-serine/phospho-threonine specific binding domains include 14-3-3, BRCT, and FHA domains play essential roles in many cellular processes (reviewed in Yaffe and Elia, 2001). Recently, 14-3-3 has been

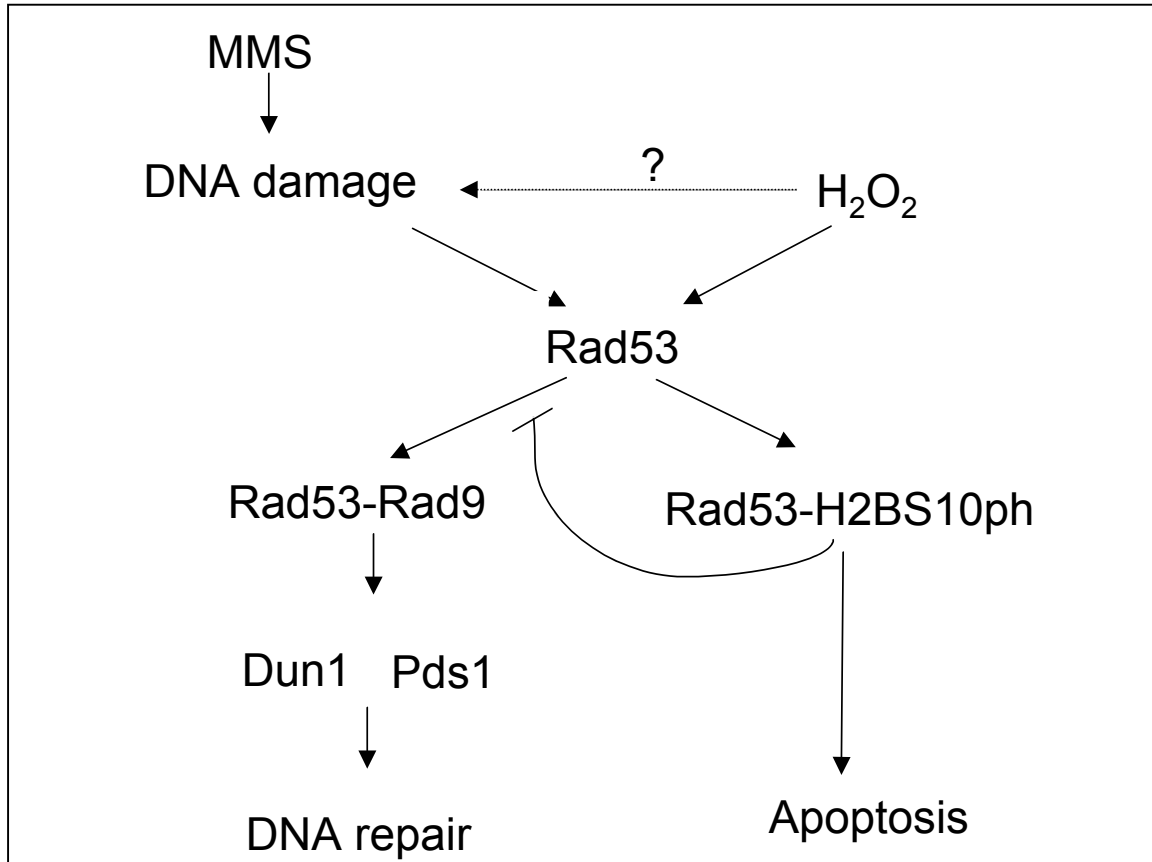


**Figure 56. Model for Rad53's role in yeast apoptosis**

During MMS-induced DNA damage, the direction association between phosphorylated Rad9 and Rad53 leads to the phosphorylation/activation of Rad53. Rad53 then activates downstream targets such as Dun1 or Pds1, and arrests the cell cycle and activates the DNA repair pathway. Upon H<sub>2</sub>O<sub>2</sub> treatment, Rad53 is initially activated and may promote DNA repair pathway similar to MMS induction. However, as DSB break accumulates, Rad53 dissociates from Rad9, and instead interacts with H2BS10ph via Rad53's FHA1 domain. Their interaction may inactivate DNA repair pathway and subsequently promote the apoptotic cascade.

identified as H3S10ph-specific binding protein and the BRCT domain from MDC1 as a binding protein for H2A.XS139ph (Macdonald et al., 2005; Stucki et al., 2005). I have now added FHA as a phospho-serine histone binding protein to this growing list of modular phosphate-binding domains. FHA domains contain

100–180 amino acid residues forming an 11-stranded  $\beta$ -sandwich (Durocher and Jackson, 2002). FHA domains are present in a large number of proteins in all phyla from bacteria to mammals and seem to be prevalent among proteins with cell cycle and DNA damage response functions. The FHA domain proteins include Nbs1 and Chk2, which are human DNA damage checkpoint proteins (Tauchi et al., 2001; Matsuoka et al., 1998). The yeast homolog of the Chk2 kinase, Rad53, is the only known protein to contain two FHA domains (Hammet et al., 2000). The Rad53 FHA1 domain is mapped to residues 14-164, which form 11  $\beta$  strands with 2 large twisted and anti-parallel  $\beta$ -sheets folding into a  $\beta$ -sandwich, a similar structure to that of FHA2 (Liao et al., 2000). However, several loops that link  $\beta$ -strands are significantly different between FHA1 and FHA2, and it has been proposed that this difference may contribute to the specificity of binding substrate (Byeon et al., 2001; Liao et al., 2000). In support, I have observed that only FHA1, but not FHA2, has binding affinity for the H2BS10ph peptide (Figures 50C and 51B). In addition, FHA of Dun1, which displays a different loop structure than the Rad53 FHA domains (Blanchard et al., 2001), did not interact with H2BS10ph peptide (Figures 50C and 51B), suggesting that structural difference in loops could be the key element in distinguishing the binding substrate.

Surface-plasmon resonance analysis has revealed that a pocket formed between residues (G69, R70, S85, N107, G133, G135) in this variable loop region and outside of the core FHA region is responsible for the interaction between FHA1 Rad53 and Rad9 (Liao et al., 2000; Yongkiettrakul et al., 2004). *In vitro*, a peptide containing a short stretch of Rad9 surrounding the threonine residue at

192 binds to FHA1 with a  $K_D$  value of 0.36  $\mu$ M (Liao et al., 2000). In this study, D at the +3 position and A at the +2 position to phospho-threonine, T(phos)XAD, is thought to be the absolute requirement for binding to the loop of Rad53 FHA1. In contrast, R70, S85 and N86, also located in the loop of FHA1, are thought to be responsible for binding to Rad9 peptide spanning amino acid residues from 188-200 that is singly phosphorylated at T192 *in vitro* (Liao et al., 2000). It remains to be established whether the FHA1 domain of Rad53 binds to a phospho-T192 of Rad9 *in vivo*. As for phospho-serine peptide, H2BS10ph peptide interacts with FHA1 *in vitro* as shown by the peptide pull down experiments and fluorescence anisotropy analysis (Figures 50C and Figure 51B). The latter measured the dissociation constant ( $K_D$ ) for their interaction to be 71  $\mu$ M (Figure 51B). The differences between  $K_D$  value for H2BS10ph peptide and phospho-T192 Rad9 peptide may reflect differences in detection sensitivity for binding analysis. Nevertheless, the  $K_D$  for binding of methylated H3 tail peptides to chromodomains of HP1 (Jacobs et al., 2001) and chromomethylase 3 (Lindroth et al., 2004) range from 10 to 100  $\mu$ M. In addition,  $K_D$  values for the association of multiple acetylated H4 tails and the hTAF<sub>II</sub>250 double bromodomains are between 1 and 50  $\mu$ M when measured by the fluorescent anisotropy (Jacobson et al., 2000). Moreover, the interaction between 14-3-3 and H3S10ph was determined to have  $K_D$  of 78  $\mu$ M (Macdonald et al., 2005). Thus, the strength of the FHA1/ H2BS10ph interaction is comparable to those of other chromatin binding modules to their respective histone modifications. Taken together, these results provide evidence that FHA1 of Rad53 is the binding effector of H2BS10ph *in vitro*.

Using yeast genetic approaches, I demonstrated that their interactions extends *in vivo* and correlate with H<sub>2</sub>O<sub>2</sub>-induced yeast apoptosis. Indeed, yeast cells lacking the FHA1 domain of Rad53 were resistant to H<sub>2</sub>O<sub>2</sub> treatment (Figure 55), demonstrating that the FHA1 domain plays a critical role during H<sub>2</sub>O<sub>2</sub>-induced yeast apoptosis. It is likely that the H2BS10ph may interact with the residues found in the loop of FHA1 and mediate yeast apoptosis. Detailed structural analysis using H2BS10ph peptide will provide better insights into understanding the structural basis of ligand specificity of FHA1 of Rad53.

#### ***Role of Rad53 and H2B serine 10 phosphorylation in yeast apoptosis***

What is the function of the association between Rad53 and H2BS10ph during yeast apoptosis? It is tempting to speculate that their interaction is important for disrupting DNA repair pathway and, as a result, mediate apoptosis and subsequently eliminate cells with damage beyond repair. Indeed, the activation of the Mec1- and Rad53-dependent DNA repair pathway has been correlated with the induction of apoptosis upon extensive MMS-induced DNA damage in both mammalian and yeast cells (Weinberger et al., 2005; Yoshida et al., 2002). As mentioned earlier, the activation of Rad53 in response to DSBs requires direct phosphorylation by Mec1, which is recruited by Rad9 upon Rad53-Rad9 interaction (Sun et al., 1998; Kondo et al., 2001; Schwartz et al., 2003; Lee et al., 2004). Accordingly, the direct interaction between phosphorylated Rad9 and Rad53 via its FHA domains is observed as DSBs are generated upon H<sub>2</sub>O<sub>2</sub> treatment (Figures 53B and 54). This may enable Rad53 phosphorylation/activation, and therefore, initiate the repairing of DSB. As H<sub>2</sub>O<sub>2</sub> treatment results in continuous DSBs, the H2BS10 is phosphorylated and



Rad53 is dephosphorylated (Figure 54), both of which are linked to the inactivation of DNA repair and cell death (Sancar et al., 2004). It is likely that heavily damaged cells exceeding the capacity for repair induce apoptosis by mediating the H2BS10ph and binding of Rad53. Whether their interaction directly affects the downstream targets of the DNA repair pathway or recruits apoptotic regulators or both is unknown at this time.

At this time, the mechanism behind the dephosphorylation of Rad53 is unknown. It could be mediated by a unknown phosphatase or simply a consequence of interaction with H2BS10ph. In the latter case, an interaction between Rad53 FHA1 and H2BS10ph may cause dissociation from Rad9. As a consequence, Rad53 would be no longer phosphorylated by Mec1 kinase. If this is the case, then H2BS10ph should have a binding affinity for both the phosphorylated and dephosphorylated form of Rad53. Since only dephosphorylated Rad53 interacts with the H2BS10ph (Figures 50, 53 and 54), in my hands, I favor the view that Rad53 is dephosphorylated by a phosphatase before binding to H2BS10ph. Detailed time course studies should determine the sequence of these events.

Both FHA1 and FHA2 of Rad53 interact with phosphorylated Rad9 and their interaction mediates the DNA repair pathway by phosphorylation and activation of Rad53 (Durocher et al., 1999). For example, mutations of both Rad53 FHA domains result in a strong reduction of the interaction of Rad53 with phosphorylated Rad9, and subsequently affect Rad9-dependent phosphorylation of Rad53. Thus, both Rad53 FHA domains are required for the robust interaction with Rad9 *in vivo* (Schwartz et al., 2003; Pike et al., 2003). Then what happens during yeast apoptosis? Since the initial reaction to H<sub>2</sub>O<sub>2</sub> induces DSBs, which

are similar to DSBs found during DNA damage/repair pathway, both FHA domains of Rad53 may be responsible for facilitating Rad53's interaction with Rad9. Therefore, I envision that FHA1 binding to H2BS10ph is antagonistic to the association between FHA2 and Rad9. As DSB break accumulates, FHA1, but not FHA2, of Rad53 is sufficient to downregulate Rad53-dependent DNA repair pathway and promote apoptotic cascade by docking at the phosphorylated H2B tail. Whether the FHA1-H2B tail complex causes conformation change on FHA2 of Rad53 or Rad9 leading to their dissociation remains to be seen.

A Rad53 homolog, Chk2, exists in mammalian cells and functions downstream of ATM (ataxia telangiectasia mutated) and ATR (ATM related) proteins during the DNA damage response pathway (reviewed in Rouse and Jackson, 2002; Rhind and Russell, 2000). Chk2 also participates in apoptosis via phosphorylation of the pro-apoptotic protein PML (Yang et al., 2002), E2F1 (Stevens et al., 2003), and the tumor suppressor protein p53 (Hirao et al., 2002). Unlike Rad53, Chk2 has one FHA domain and it is similar to FHA1 of Rad53 (Hofmann et al., 1995). Taken together, these relationships indicate an apoptotic mechanism with Chk2 as a binding protein for mammalian H2BS14ph. Employing similar peptide pull-down and immunoprecipitation experiments should determine their interaction.

In summary, I have provided necessary evidence supporting the assertion that Rad53 is the binding partner of H2BS10ph during H<sub>2</sub>O<sub>2</sub>-induced yeast apoptosis. Identifying the phospho-binding effector further strengthens the existence of a trans mechanism in mediating the role of H2BS10ph, and illustrates an intricate relationship between the DNA repair pathway and the apoptotic cascade. Whether the docking of Rad53 onto H2BS10ph directly

terminates the activation of DNA repair pathway is still debatable, but my results pave the way for a better understanding of apoptosis by defining a novel role of FHA1 of Rad53 and H2BS10ph.

## Materials and Methods

### *Recombinant FHA domain proteins*

Rad53 FHA1 (residues 2-279), Rad53 FHA2 (residues 543-801), Dun1 FHA (residues 2-264) cloned into pGEX4T1 were gifts from Dr. Sheng Hong Chen at the Ludwig Instituted, CA. These glutathione S-transferase (GST) fusion proteins were produced in *E. coli* BL21. Bacterial lysates were purified over glutathione Sepharose 4B (Amersham) as recommended by the manufacturer.

### *Plasmids and Yeast strains*

Yeast strains are listed in Table 1 and all strains are derived from W303C (BY4741; Research Genetics) background. Yeast strains carrying FHA1 deletion (residues 6-66; SAY 213), FHA2 deletion (residues 601-664; SAY 214) were constructed by PCR amplication of a  $P_{TEF}$  promoter-driven bacterial kanamycin-resistance gene as described by Longtine et al., 1998. PCR products were then transformed into SAY210 (*MATa ura3-52 leu2::hisG sml1Δ::URA3*) to create strains that lacked the full ORF (ATG-Stop).

### *Peptide-pull down*

Peptide pull-down assays were performed as described previously (Wysocka et al., 2005). About 1  $\mu$ g of peptide that were prebound to avidin beads for 3 hr at 4°C, was incubated with 1  $\mu$ g of recombinant protein plus 20-fold excess of bovine serum albumin (internal control) in assay buffer (100 mM KCl, 20 mM HEPES, and 0.2% Triton X-100), and beads were washed six times in assay buffer. Bound proteins were eluted from the resin two times with 100 mM

glycine (pH 2.8). Elutes were combined, neutralized using 1/10 volume of 1 M Tris (pH 8), and analyzed by SDS PAGE.

Yeast nuclear extracts were prepared as described in Yeast nuclei extraction (Chapter 2; Material and Methods) and the peptide pull-down assay was performed as described previously (Wysocka et al., 2005). These nuclear extracts were then incubated with 150 mM NaCl, 0.2% Triton X-100 with 25  $\mu$ l of avidin beads for 1 hr at room temperature. Meanwhile, 25  $\mu$ g biotinylated peptides were pre-bound to 100  $\mu$ l of avidin beads with 200  $\mu$ l 1X PBS for 3 hr at the room temperature. The bound peptides were separated from unbound peptides by washing 3 times in 1X PBS and resuspended in 100  $\mu$ l 1X PBS. The nuclear extracts were then spun and the supernatant was incubated with 20  $\mu$ l of bound biotinylated peptides (5  $\mu$ g of peptide per  $10^8$  cells were used per pull-down) for 5 hr at 4°C. Beads were then washed eight times by incubating beads with buffer containing 20 mM HEPES (pH 7.9), 150 mM KCl, 0.2% Triton X-100, 1 mM PMSF, and protease inhibitor cocktail (Roche) for 5 min at 4°C with gentle rotation and then pelleting the beads. A final wash was performed with buffer containing 4 mM HEPES (pH 7.9), 10 mM NaCl, 1 mM PMSF, and protease inhibitor cocktail (Roche). Bound proteins were eluted from the resin two times with 100 mM glycine (pH 2.8). Elutes were combined, neutralized using 1/10 volume of 1 M Tris-HCl pH 8.0, and analyzed by SDS PAGE.

### ***TAP-immunoprecipitation***

Nuclear extracts were prepared as described in Chapter 2 (Methods and Materials) from yeast cells stably expressing Rad53TAP and as a control from

yeast cells lacking ectopic Rad53. The TAP fusion proteins were precipitated by incubating nuclear extracts with IgG Sepharose 4 Fast Flow (Amersham Biosciences) with IP buffer (20 mM Hepes, pH 7.4, 5% glycerol, 5 mM MgCl<sub>2</sub>, 0.1 M KCl, 1 mM EDTA, 0.1% NP-40, protease inhibitor cocktail (Roche), and phosphatase inhibitor cocktail (Roche)) and incubated for 2 hr at 4°C with gentle rotation. Beads were collected by spinning at 1000 rpm and washed beads with IP buffer, each time incubating it for 5 min at 4°C with gentle rotation and then pelleting beads by centrifugation. For TEV protease cleavage, beads were washed with TEV cleavage buffer (10 mM Tris-HCl, pH 8.0, 150 mM NaCl, 0.1% NP50, 0.5 mM EDTA, 1 mM DTT), each time incubating it for 5 min at 4°C with gentle rotation and then pelleting beads by centrifugation, for three times. The TEV protease (Sigma) were added to the beads, rotated it for 2 hr at 4°C and then collected the supernatant by the centrifugation.

#### *Test for Apoptosis and Western Blot*

Yeast apoptotic induction by H<sub>2</sub>O<sub>2</sub>, the cell survival, cell death analysis, TUNEL staining, immunofluorescence, yeast nuclei preparation and Western analysis were carried out as described in Chapter 2; Materials and Methods.

#### *Fluorescence polarization assay*

Protein concentrations were determined by absorbance spectroscopy using predicted extinction coefficients (for FHA1 of Rad53  $\epsilon_{280} = 16980 \text{ cm}^{-1} \text{ M}^{-1}$ ; for FHA2 of Rad53  $\epsilon_{280} = 15700 \text{ cm}^{-1} \text{ M}^{-1}$ ). Peptide concentrations were estimated from the mass.

Fluorescence anisotropy binding assays were performed essentially as described previously (Fischle et al., 2003 *Genes and Dev*). Peptides were N-terminally labeled with fluorescein-5-EX succinimidyl ester (Molecular Probes) as recommended by the manufacturer. Fluorescinated peptides were then passed over a 0.5 ml G10 Sephadex (Pharmacia) column that has been pre-equilibrated with 100 mM KPO<sub>4</sub> pH 7.5 to remove free fluorescein and hydroxyl succinamide. Fractions containing the peptide were purified further by reversed phase chromatography. Binding assays were performed in 100. Fluorescence polarization binding measurements were performed under conditions of 20 mM imidazole (pH 8.0), 25 mM NaCl, 2 mM DTT, and 100 nM fluorescein-labeled peptide. For competition experiments, the competing peptide was unlabeled and added in excess to the final concentration of 200 nM. Fluorescence polarization (P) values were converted to anisotropy (A) values by the equation:  $A=2P/(3-P)$ . Binding curves were analyzed by non-linear least-squares fitting of the data using KaleidaGraph (Synergy Software). Data were fitted using the equation  $A=[A_f(A_b-A_f)][\text{protein}]/KD + [\text{protein}]$ , where  $A_f$  and  $A_b$  represent the anisotropy of the free and bound peptides, respectively.

## CHAPTER 6

# H2B SERINE 10 PHOSPHORYLATION IS INDUCED DURING MEIOSIS

### Introduction

To date, histone H2B phosphorylation has been best characterized during apoptosis. Chromatin condensation and DNA fragmentation, hallmark features of apoptosis, have been firmly linked to mammalian H2BS14ph catalyzed by Mst1 (Cheung et al., 2003). In the previous chapter, I uncovered an analogous serine (yeast H2BS10) catalyzed by Ste20 kinase that has a “death” function, which provides evidence for a chromatin-mediated apoptotic pathway that is remarkably well conserved between yeast and humans. The Nussenzweig group has previously shown that the phosphorylation of mammalian H2BS14 co-localizes with H2A.XS139ph in DNA-damage foci induced by  $\gamma$ -irradiation (Fernandez-Capetillo et al., 2004a). These results suggest that H2B phosphorylation in both mammalian (S14) and yeast (S10) may serve as markers for DNA double stranded breaks (DSBs), along with H2A.XS139ph. Besides ionizing radiation, DSBs can arise by the programmed action of endonucleases during meiosis (Haber, 2000). In particular, meiotic DSBs are generated by an evolutionarily conserved, meiosis-specific endonuclease, Spo11, which cuts the



DNA through a topoisomerase-like mechanism during meiotic prophase when chromatin is mostly condensed (Keeney, 2001). Since H2A.XS139ph correlates with DSBs during meiotic prophase (Mahadevaiah et al., 2001; Baarends et al., 2003), this suggests a link between DSBs and chromatin condensation arising from meiosis and DNA damage. From the following data, I propose that yeast H2BS10ph could play a role in mediating DSBs and chromatin condensation during meiosis.

In this chapter, I will characterize H2BS10ph during meiosis. In collaboration with Kiersten Henderson in Dr. Scott Keeny's laboratory at Cornell Medical Center, NY, we found that H2BS10ph is enriched during pachytene stage of meiotic prophase where chromosomes are condensed. In addition, deletion of Spo11 did not affect the H2BS10ph pattern, indicating that the H2BS10ph was not induced in response to the formation of the DSBs that initiate meiotic recombination. Taken together these results support that H2BS10ph correlates with meiotic chromosome condensation.

## Results

### *Histone H2B is specifically phosphorylated at serine 10 during yeast meiosis*

In mammalian cells, H2BS14ph co-localized with H2A.XS139ph in DNA-damage foci induced by  $\gamma$ -irradiation (IR; Fernandez-Capetillo et al., 2004a). Thus, we were interested in the possibility that the role of yeast H2BS10ph may extend to meiosis, and in particular, to the stage of meiotic prophase when DSBs are known to occur (Mahadevaiah et al., 2001).

To test this hypothesis, nuclear extracts were prepared from diploid yeast cells derived from rapidly-sporulating SK1 strains that were induced for synchronous sporulation (Bishop, 1994). Extracts from different meiotic stages were then resolved on an SDS-PAGE gel and examined by Western blotting using mitotic H3S10ph-specific (anti-H3S10ph) as well as apoptotic H2BS10ph-specific antibodies (anti-H2BS10ph). Interestingly, both H2BS10 and H3S10 phosphorylation events were enhanced at 2 hour and declined after 7 hour following induction into meiosis (Figure 57A), suggesting that similar to H3S10ph (Hsu et al., 2000), H2BS10ph occurs during meiotic prophase. Not all phosphorylation marks on core histones follow the above pattern suggesting some specificity. For example, S1 phosphorylation of histone H4 (H4S1ph), a mark known to correlate with mitosis (Barber et al., 2004) and damaged DNA (MMS-induced; Cheung et al., 2005), is induced at much later stages (9-11 hr) of meiosis (Figure 57A).

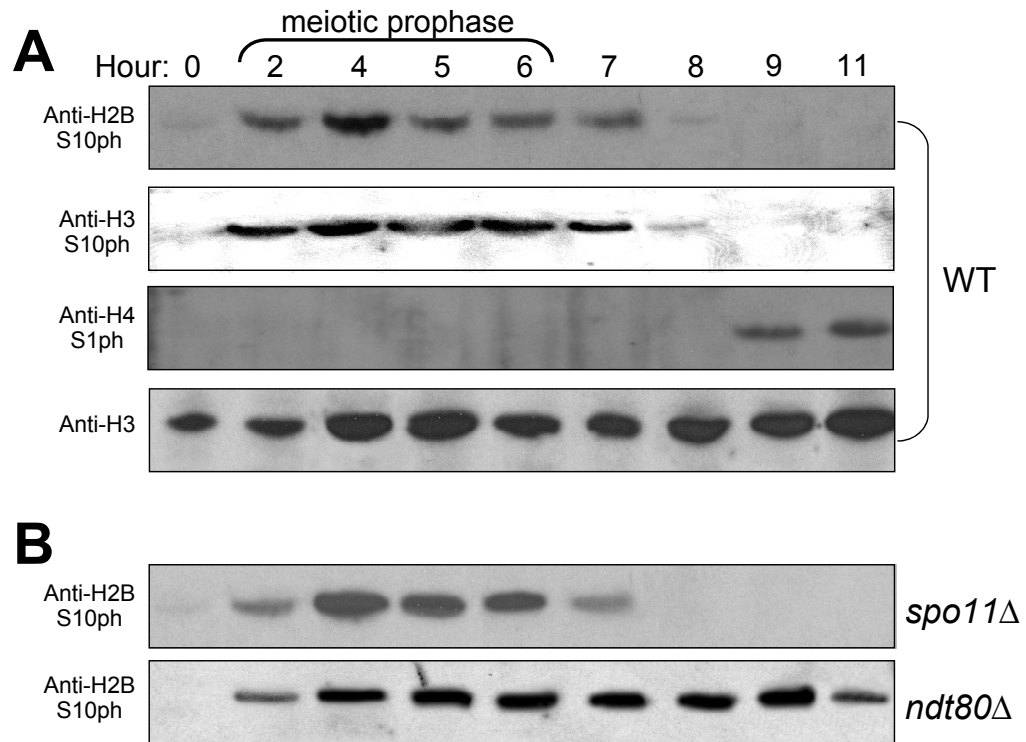


**Figure 57. H2B serine 10 phosphorylation is induced during meiotic prophase**  
 Synchronous meiotic yeast culture (diploid SK1 strains) were harvested at the indicated times and subjected for Western analysis using indicated antibodies (A) H2BS10ph is strongly induced during meiotic prophase. Antibodies to H3S10ph and H4S1ph demonstrate the unique timing and robustness of the signal obtained from anti-H2BS10ph. A general H3 antibody is used as a loading control.  
 (B) The wild-type-like H2BS10ph pattern is observed in *spo11* deletion mutants, whereas this phosphorylation level is maintained in *ndt80* deletion mutants.

### *H2B serine 10 phosphorylation is enriched in condensed meiotic chromosomes*

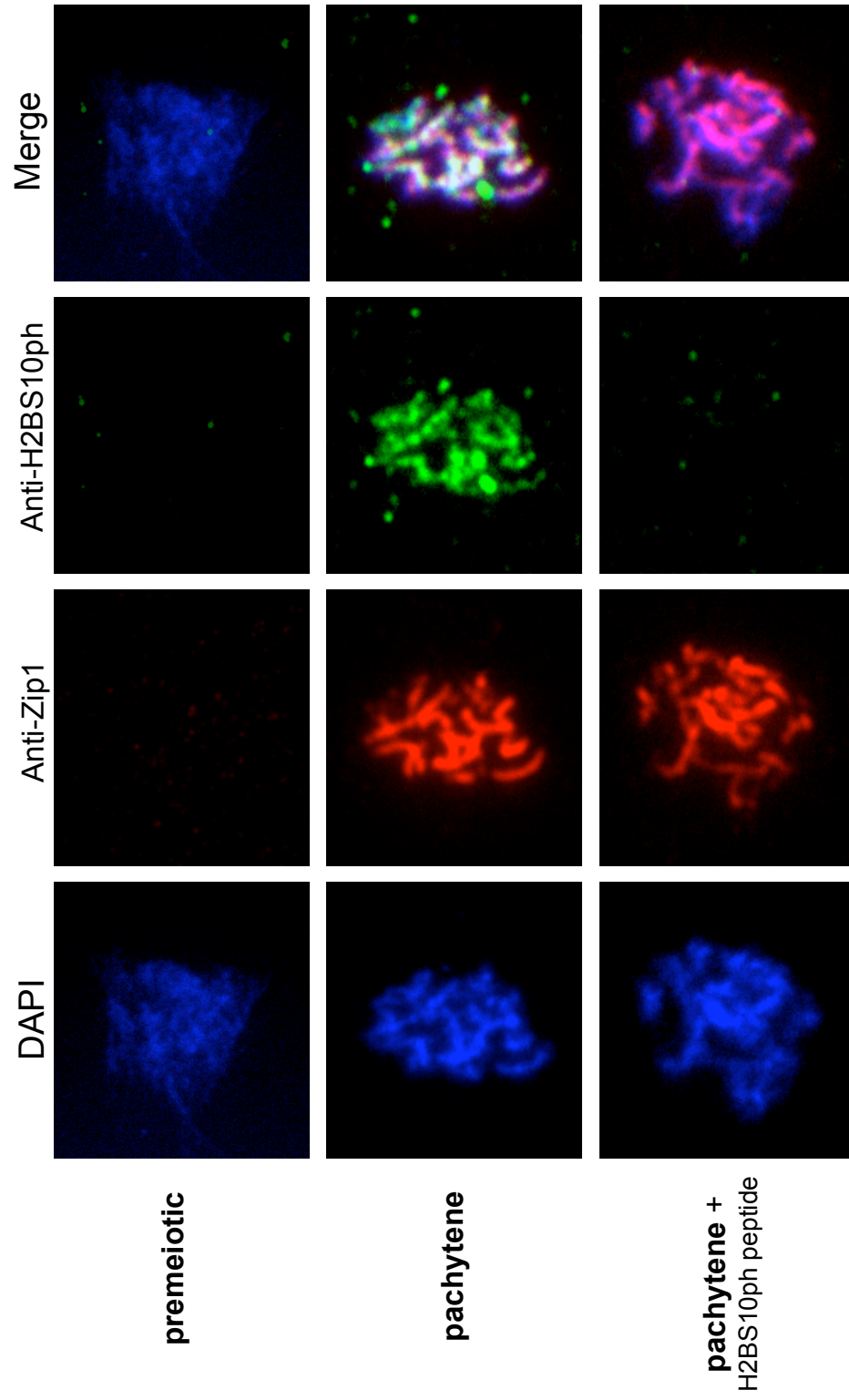
To better define the precise stage(s) of meiotic prophase when H2BS10ph is maximal, we performed double immunostaining of surface spread meiotic nuclei for H2BS10ph and Zip1, a component of the synaptonemal complex. The pattern of Zip1 localization indicates the stage in meiotic prophase, with extensive linear Zip1 staining denoting fully synapsed chromosomes (Sym et al., 1993), the

hallmark of the pachytene stage of prophase where chromosomes are condensed (Dresser and Giroux, 1988). As shown in Figure 58, prior to entry into meiosis (premeiotic), when Zip1 was absent, H2BS10ph was largely absent (93%; 63/70 nuclei). Consistent with the kinetics of H3S10ph (Hsu et al., 2000), H2BS10ph gradually increased as cells progressed through prophase and by pachytene the vast majority of nuclei (98%; 52/53) stained brightly with H2BS10ph-specific antibody. The H2BS10ph signal was specific as it was eliminated from pachytene nuclei upon competition with H2BS10ph (amino acids 4-14) peptide (Figure 58); this staining is not diminished when unmodified (control) H2B peptides were used in parallel competition experiments. Also consistent with the kinetics of H3S10ph, H2BS10ph, as detected by Western blot (Figure 57A), declined rapidly around the first meiotic division, which occurred at 8 hour in this culture. We further tested the correlation between high levels of H2BS10ph and the pachytene stage of meiosis by examining H2B phosphorylation in a *ndt80* mutant, which arrests at pachytene with condensed chromosomes (Chu and Herskowitz, 1998). The *ndt80* mutant failed to undergo meiotic divisions and maintained phosphorylated H2B at high levels (Figure 57B), suggesting that, like H3S10ph, maximal H2BS10ph occurs at the pachytene stage of meiotic prophase.

Contrary to our initial expectation, H2BS10ph was not induced in response to the formation of the DSBs that initiate meiotic recombination. The WT profile of H2B phosphorylation was observed in a mutant lacking Spo11, the protein that forms meiotic DSBs (Figure 57B; Keeney, 2001). These results demonstrate that H2BS10ph correlates with progression through meiotic prophase and perhaps with meiotic chromosome condensation, rather than other events associated with meiotic DSB repair.

**Figure 58. Anti-H2BS10ph stains pachytene stage of meiotic prophase**

Chromosomes from a time course through meiotic prophase of WT diploid SK1 strains were spread onto glass slides and examined for Zip1 and H2B Ser10 phosphorylation signal by double immunostaining. At pachytene, anti-H2BS10ph brightly stains nucleoids that contain extended Zip1 structures. This H2B signal is competed away with the H2BS10ph (amino acids 4-14) peptide. These data were provided by Kiersten Henderson in Dr. Scott Keeny's laboratory at Cornell Medical Center, NY.



## Discussion

In this Chapter, we first provided evidence for meiotic histone H2B phosphorylation in budding yeast. Similar to histone H3S10ph, H2BS10ph is induced at pachytene stage of meiotic prophase when chromosomes are maximally condensed. In addition, H2BS10ph correlates with meiotic chromosome condensation rather than meiotic DSB repair during prophase. Although H2BS10ph is also present during apoptosis, the reduction of this modification correlates with the end of meiotic division when chromosomes are decondensed. Therefore, these results point to H2BS10ph as a meiotic chromosome condensation marker.

### *H2BS10ph in apoptosis and meiosis*

Our findings indicate that H2BS10ph is a common feature of both apoptosis and meiosis, and is thus a mark used more broadly in biological pathways that involve large-scale changes in chromatin structure. Is there a common theme linking these different physiological processes? One possible link may be through effects of histone phosphorylation on chromatin condensation. In the case of apoptosis, chromatin becomes compacted and this compaction is associated with processes that ultimately lead to permanent elimination of the genome through cell death. In meiosis, in contrast, there is a constant interplay between the condensed and decondensed states of chromatin demanded by the multiple cycles of chromosome segregation that lead to the production of haploid gametic cells. In particular, in prophase I of meiosis, the cyclical changes in chromatin compaction coordinate and/or promote chromosome dynamics

(e.g. recombination; higher-order chromosome structures such as the synaptonemal complex and axial elements (specialized meiotic chromosome axes); and chiasmata (Kleckner et al., 2004)).

Another possible link may involve the enzymes responsible for adding and/or removing the H2BS10ph mark during apoptosis and meiosis. Although Ste20 has no known role in meiosis, it could be a candidate kinase for meiotic H2BS10ph. Another possible kinase candidate is Ipl1/aurora kinase, which governs histone H3 phosphorylation at S10 during mitosis and meiosis in several organisms (de la Barre et al., 2000; De Souza et al., 2000; Hsu et al., 2000; Giet and Glover, 2001). The action of this particular kinase is required for the proper recruitment of the condensin complex, and assembly of the mitotic spindle in a phosphorylated histone H3-dependent manner (Giet and Glover, 2001). Considering that Ipl1 can phosphorylate both H3 and H2B *in vitro* (Hsu et al., 2000), H2BS10ph mediated by Ipl1 and/or Ste20, may be functionally redundant with meiotic H3S10ph, a possibility that remains to be addressed.

Even though the H2BS10ph mark correlates with chromatin condensation in yeast apoptosis and meiosis, the enzymes responsible for these modifications and the biological context of each condensation event may be different. During meiosis, chromatin condensation is thought to be required to minimize the entanglement of chromosomes with one another while being moved by the meiotic apparatus. Reversibility of this condensed state after chromosome separation is critical. In contrast, chromatin condensation in apoptosis leads to degradation of DNA, a final commitment step beyond which effective repair is impossible and cell death becomes inevitable. Hence, the precise role of this phosphorylation mark, whether inducing “cis” structural effects on chromatin



folding alone, or allowing the binding of different “trans” effectors that in turn bring about different downstream effects, remains an open area of considerable interest (see Chapter 5-6). Following the paradigm established for histone acetylation and methylation, I predict that a focused attack on H2B phosphorylation, the enzyme systems responsible for its steady-state balance, and the “effectors” that “read” this mark, if they exist, will lead to valuable insights into how the genome is condensed during meiosis, and apoptosis.

### ***Role of H2BS10ph during meiosis***

Since the pattern of H3S10ph correlates with H2BS10ph (Figure 57 and 58), H2BS10ph might involve regulating chromatin condensation during meiotic prophase. Previously, SPO76 of *Sordaria* has shown to be essential for sister chromatid cohesion, and chromatin condensation in meiosis (van Heemst et al., 1999). Pds5, the SPO76 homologue in *S. cerevisiae*, is a cohesin-related gene and failure in function of Pds5 causes premature separation of chromosomes. Pds5 is required for meiotic prophase chromosome condensation (Yu and Koshland, 2003; Zhang et al., 2005), ensuring the correct chromosome folding by condensins (Lavoie et al, 2002). Condensin is an evolutionarily conserved protein complex and mediates mitotic and meiotic chromosome condensation through axial length compaction (Yu and Koshland, 2003). Since the loading of Pds5 onto chromosome requires the function of a cohesin, Scc1/Mcd1 and Rec8 (Zhang et al., 2005), and cohesin binding to chromatin is dependent on a specific site of histone modifications (Guacci et al., 1997; Nonaka et al., 2002; Sonoda et al., 2001; Bernard et al., 2001), H2BS10ph may play an active role in establishment of cohesin and Pds5 onto chromosome to regulate meiosis.

## Materials and Methods

### *Yeast Strains, and Culture Conditions*

Diploid strains in SK1 background include: SKY165 (*MATa/MAT $\alpha$  ho::LYS2/ho::LYS2 lys2/lys2 ura3/ura3 leu2::hisG/leu2::hisG*). SKY169 (*ndt80 $\Delta$ ::URA3*) and SKY10 (*spo11 $\Delta$ ::URA3*) were derived from SKY165. For the induction of meiosis, log phase cultures in SPS medium (0.5% yeast extract, 1.0% peptone, 0.17% yeast nitrogen base, 1.0% potassium acetate, 0.5% ammonium sulfate, 0.05 M potassium bipthalate, pH 5.5) were diluted to about  $1 \times 10^5$  cells/ml in fresh SPS and were grown for 16 hr to about  $5 \times 10^7$  cells/ml (OD600 1.5-2.0). Cells were then washed with water and resuspended in an equal volume of prewarmed SPM-1/5COM sporulation medium (0.2% potassium acetate, 0.02% raffinose, and 0.015% complete amino acid powder as described in media and reagents in Chapter 2 Materials and Methods).

### *Yeast Nuclei and Histone Extraction, Western Blot, and Immunofluorescence Staining*

Yeast nuclei and histones were extracted, and used for Western analysis as described Chapter 2 Materials and Methods. Antibodies were diluted as follows: anti-H2BS10ph: 1:5000, anti-H4: 1:5000, anti-H3S10ph: 1:1000, anti-H3: 1:1000.

For synaptonemal complex and anti-H2BS10ph immunofluorescence analysis, chromosomes were surface spread and stained as described (Henderson and Keeney, 2004). Guinea pig anti-Zip1 antibody was used at 1:1,000 dilution and anti-guinea pig-Alexa 546 at 1:1,000 (Molecular Probes). Rabbit anti-H2BS10ph was used at 1:100, and anti-Rabbit Alexa 488 at 1: 1,000 (Molecular Probes). For

peptide competition, H2BS10ph 1-20 peptide was added to the diluted anti-H2BS10ph antibody (1.4  $\mu$ g/ $\mu$ l final concentration). Slides were mounted with cover slips in Prolong antifade (Molecular Probes). Images were captured on a Zeiss Axiophot microscope with a 100x objective using a Cooke Sensicam cooled CCD camera. Data capture and image processing were performed using the Slidebook software package (Intelligent Imaging Innovations).

## CHAPTER 7

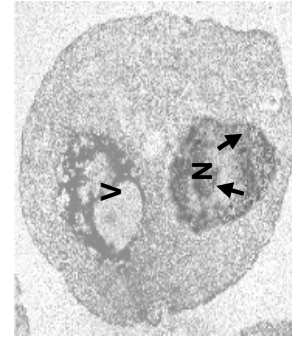
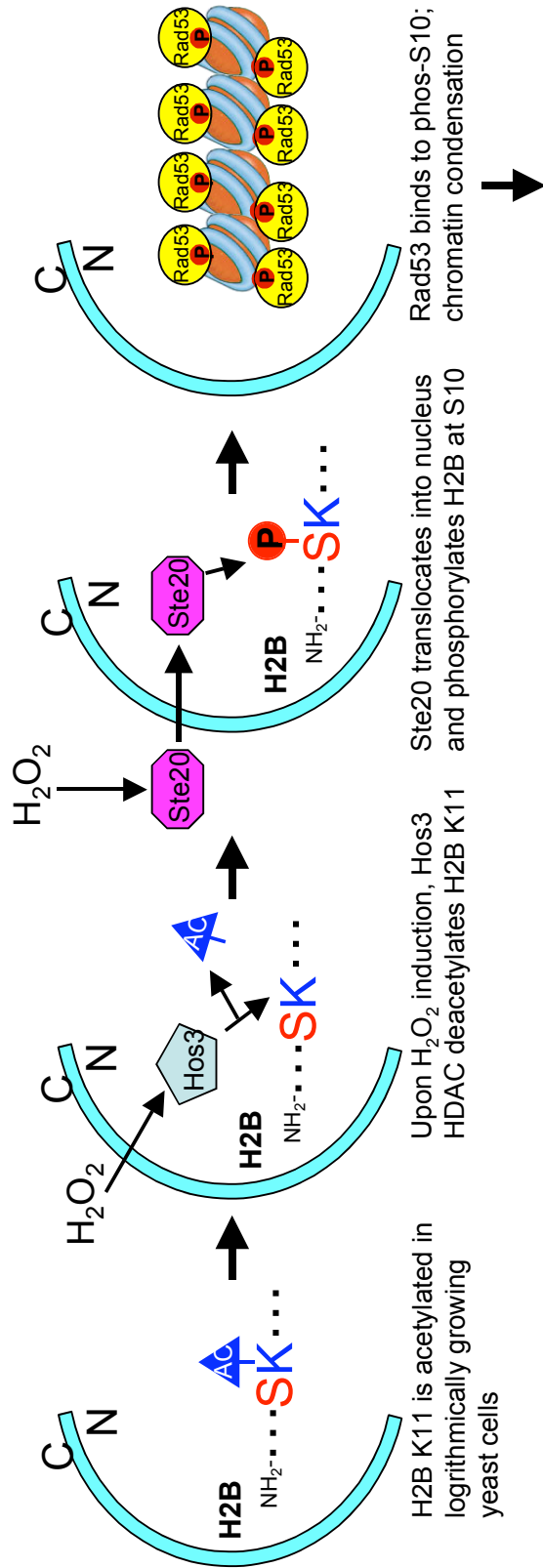
### GENERAL DISCUSSION

#### *Yeast apoptotic cascade*

In this thesis, I have identified and characterized a pair of interacting histone modification marks that regulate chromatin condensation and/or alter chromatin structure during yeast apoptosis. My data supports a model presented in Figure 59. I envision that, upon H<sub>2</sub>O<sub>2</sub> induction, Hos3 HDAC directly catalyzes the deacetylation of H2BK11 and, in turn, allows H2BS10ph by Ste20 kinase in a caspase-independent fashion. H2BS10ph can then either directly affect internucleosomal contacts and histone DNA interactions (“cis” mechanism; Figure 6A) and may also indirectly affect downstream functions (“trans” mechanism; Figure 6B) by recruiting a phospho-specific binding protein. In support of the “cis” mechanism, H2BS10ph is essential for the condensation of chromatin fiber *in vitro*. In support of the “trans” mechanism, I have identified Rad53 as the H2BS10ph binding partner. The latter interaction leads to the inactivation of the DNA damage checkpoint, thereby promoting the apoptotic cascade. Whether chromatin condensation, a hallmark of apoptosis, is mediated by cis, trans, or both mechanisms remains to be explored.

**Figure 59. Model for regulation of Histone H2B in yeast apoptosis**

1) K11 in H2B is acetylated in exponentially growing yeast cells. 2) Upon  $H_2O_2$  treatment, Hos3 HDAC directly catalyzes the deacetylation of H2BK11 (“cross-talk”). 3) Ste20 kinase translocates into the nucleus in a caspase-independent fashion. Once in the nucleus, Ste20 kinase directly phosphorylates H2B at S10. 4) H2BS10ph elicits apoptotic chromatin condensation either by directly affecting the internucleosomal contact (“cis” mechanism) and/or by recruiting Rad53 to H2BS10ph (“trans” mechanism). 5) These events ultimately lead to cell death. N denotes nucleus and V refers to the vacuole. Arrows denote chromatin condensation. (see Figure 21 for the detail).



Cell Death

### ***Function of H2B serine 10 phosphorylation***

Formation of condensed pycnotic chromatin is a hallmark of apoptosis, but the mechanisms underlying these large-scale chromatin changes are unknown. A previous study suggested that the H2B tail could play an essential role in promoting chromatin condensation in *Xenopus* cell-free extracts (de la Barre et al., 2001). However, no specific residue was identified as being responsible for this effect. In 2003, Cheung et al. suggested that H2BS14ph might facilitate chromatin compaction during mammalian apoptosis (Cheung et al., 2003). However this study was unable to address, due to lack of genetic tools in mammalian cells, whether or not this event is required for apoptosis, nor did it address the function of H2BS10ph. By utilizing the well-established genetic and biochemical tools developed for the yeast system, I have identified yeast H2BS10 as a yeast apoptotic phosphorylation mark. Unlike H2BS14, H2BS10ph is essential for yeast apoptosis *in vivo*, as indicated by the resistance of H<sub>2</sub>O<sub>2</sub>-induced cell death by the H2B S10A mutant (Figure 14). Condensed chromatin is not observed in the H2B S10A mutant, suggesting that H2BS10ph is required for these dramatic changes in chromatin structure (Figure 21). In support, a phospho-mimic of H2BS10, S10E, is able to induce 'constitutive' properties of apoptosis including widespread chromatin condensation *in vivo* (Figure 21). *In vitro*, H2B S10E displays an intrinsic ability to form unusual peptide "aggregates" (Figure 39) and is critical for the condensation of chromatin fibers (Figure 44). It is unknown whether there is a direct correlation between peptide aggregation and the chromatin condensation *in vivo*. However, my peptide data correlates precisely with the chromatin compaction *in vitro* and *in vivo* so far. Therefore, I

hypothesize that H2BS10ph plays a direct role in mediating chromatin compaction.

Additional support for the role of H2BS10ph in chromatin compaction comes from studies in meiosis. As discussed earlier, H2BS10ph is a common feature of both apoptosis and meiosis. Though seemingly different, both biological processes involve large-scale changes in chromatin structure. However, the chromatin compaction in these processes lead to different cell fates. In the case of apoptosis, compacted chromatin is associated with processes that ultimately lead to cell death, whereas in meiosis, a constant interplay between the condensed and decondensed states of chromatin leads to the production of haploid gametic cells. Interestingly, chromatin is maximally compacted during prophase I of meiosis and a sharp peak of H2BS10ph is present at a time point corresponding to prophase I (Figure 57). Since the level of H2BS10ph declines rapidly around the time that meiotic divisions occur (Figure 57), when the chromatin is decondensed, H2BS10ph appears to be tightly regulated during meiosis, which further supports its role in chromatin condensation.

There are two models for yeast apoptotic signaling: 1) caspase-dependent, 2) caspase-independent pathways. In the caspase-dependent pathway, caspases such as Yca1 regulate cell death (Madeo et al., 2000). H2BS10ph seems to fall into the caspase-independent pathway since Yca1 is not involved in its cascade (Figure 28C). Although chromatin compaction is a hallmark of apoptosis, only the caspase-independent pathway seems to require H2BS10ph for this apoptotic characteristic. Since H2BS10ph is also present during meiotic prophase when



chromatin is mostly compacted, this invokes an interesting possibility that the caspase-independent apoptotic pathway and meiosis may be conserved.

### ***Why the H2B tail for a potential apoptotic “histone code”?***

As discussed in Chapter 2, I have found a highly conserved phosphorylation mark in the yeast H2B N-terminal tail that plays a role in apoptosis. My genetic experiments in yeast suggest that this “death” function is unique to the H2B N-terminal tail, as no other histone tail (H2A, H3 or H4) has the capacity to influence the cell survival and death properties in my assays. In support, earlier studies, using the *Xenopus* cell-free system, have implicated the H2B tail in chromatin condensation (de la Barre et al., 2001). This leads to the following question: why would one use H2B tails in cells to mark cell death? Recall that H2B histones do not self associate. Hence, they cannot preferentially form a H2B-variant only nucleosome. Accordingly, there are no H2B variants in somatic cells. To date, no H2B variants are found in yeast. Therefore, all the nucleosomes in the genome would contain a similar, if not identical, H2B molecules. If death signals need to be marked on histones, then it may be easier for apoptotic pathways to modify a histone that is similar in all the nucleosomes.

### ***H3 serine 10 phosphorylation and H2B serine 10 phosphorylation***

Unlike the apoptotic pathway, the regulation of the level of histone H2B phosphorylation might be directly linked to H3S10ph in meiosis. In yeast, the strongest peak in H3S10ph is observed during meiotic pachytene when chromosomes are dramatically compacted (Hsu et al., 2000). However, H3 S10A mutations do not result in a major defect in meiotic chromosome transmission in

yeast (Hsu et al., 2000). One potential explanation is that other histone modifications may compensate for the loss of H3S10ph and allow proper chromosome dynamics. Because the pattern of H2BS10ph coincides with that of H3S10ph (Figure 57 and 58), H2BS10 might compensate for the mutation of H3S10 and promote proper chromosomal condensation and segregation during meiosis. Future yeast genetic experiments may provide more insights into the functional redundancy of meiotic phospho-marks.

The functional redundancy between H3 and H2B in meiosis is further supported by the fact that Ipl1 kinase can phosphorylate both H3 and H2B *in vitro* (Hsu et al., 2000). Considering that Ste20 kinase has no known role in meiosis, this raises the possibility that Ipl1 kinase is the enzyme responsible for H2BS10ph during meiosis. If this hypothesis is correct, then the differences between the effect of H2BS10ph in apoptosis versus meiosis may be dictated by the kinase that mediates it. During apoptosis, Ste20 kinase directly phosphorylates H2BS10 but not H3S10 (Figure 22B). This is supported by the observation that H3S10ph is absent during apoptosis (Figure 22B). On the other hand, a kinase other than Ste20, for example Ipl1 kinase, may directly facilitate the onset of both H3S10 and H2BS10 phosphorylation and mediate proper chromatin condensation during meiosis. In support, the action of Ipl1 kinase phosphorylating the H3S10 is thought to be required for proper recruitment of the condensin complex and assembly of the mitotic spindle leading to chromatin condensation (Giet and Glover, 2001). Since Ipl1 kinase is not involved in yeast apoptosis or H2BS10ph during that process (Figure 22B), the identification and characterization of the enzyme responsible for adding phosphate groups to

H2BS10 during meiosis should help to address how one modification may lead to different cell fates.

Another difference between apoptosis and meiosis is that the reduction of H2BS10ph level is present only during meiotic division when chromatin is decondensed. On the other hand, apoptotic cells are characterized by the presence of condensed chromatin. Therefore, the dephosphorylation of H2BS10 might be another key to promoting the production of haploid gametic cells, hence, cell proliferation rather than cell death. If correct, this brings up the intriguing possibility that the reversal of the H2BS10ph event by unknown phosphatase may rescue the apoptotic cells. As for the phosphatase, assuming that Ipl1 kinase directly phosphorylates H2BS10 during meiosis, the phosphorylation can be removed by phosphatase PP1, which is known to counterbalance the activity of Ipl1 kinase (Hsu et al., 2000; Murnion et al., 2001). Although this interplay between these two enzymes needs to be investigated in the near future, the phosphatase may play a role in mediating the chromatin decondensation by recruiting the machinery that blocks the cleavage of structural proteins such as lamins (reviewed in Moir and Goldman, 1993). It should also be noted that H3S10ph might contribute to the dephosphorylation of H2BS10 and vice versa. In other words, the regulation of H3 and H2B (de)phosphorylation may be reciprocal; specifically, the absence of H3S10ph may inhibit the dephosphorylation of H2BS10 during yeast apoptosis. In support, there is no H3S10ph during apoptosis when H2BS10ph is maintained (Figure 23). However, H3S10ph and H2BS10ph are both present during a specific stage of meiosis before H2BS10ph is removed (Figure 57). Therefore, I predict that H3S10

is important for the regulation of H2BS10ph and somehow separates its function in apoptosis versus meiosis.

### *Role of H2B lysine 11*

As discussed in Chapter 3, I have found a covalent histone modification “cross-talk” between H2BS10ph and K11ac during H<sub>2</sub>O<sub>2</sub>- induced yeast apoptosis. In particular, histone H2BK11ac inhibits the phosphorylation of its adjacent site, Ser10, by Ste20 kinase (Figures 32, 34 and 37). Therefore, I propose a model for regulated cross-talk in H2B wherein Hos3 directly catalyzes the deacetylation of H2BK11 that, in turn, mediates H2BS10ph by Ste20 kinase during H<sub>2</sub>O<sub>2</sub>-induced yeast cell death (see Figures 38 and 59). If this model is correct, what upstream role does Hos3 serve leading to S10ph in H2B? The simplest explanation for my results is likely to involve an altered substrate recognition site for Ste20 kinase. In support, K11ac inhibits S10ph by Ste20, whereas deacetylation of pre-acetylated (K11) peptides by the addition of Hos3 promotes S10ph (Figure 37B and 37C). Other more indirect roles are also possible. For example, Hos3 may regulate Ste20 translocation into the nucleus, and in turn, mediate S10ph. I have observed that the translocation of Ste20 into the nucleus precedes the onset of S10ph (Figures 29). K11 deacetylation and Ste20 translocation occur before H2BS10ph (Figure 34). Lastly, Hos3 may play a role in the activation of Ste20 catalytic activity, although little, if anything is known about the acetylation status of Ste20 kinase.

### *Functional mechanism of H2B serine 10 phosphorylation during yeast apoptosis*

One of the aims of my thesis has been to understand the mechanism by which H2BS10ph causes chromatin condensation. As discussed earlier, there are two general mechanisms that are thought to mediate the function of histone modifications (Figure 6): modifications could modulate chromatin structure in cis by directly affecting the nucleosomal contacts and histone DNA interactions, or it could act in trans by recruiting binding partners that then induce and direct downstream functions. Although thought to be mutually exclusive, I have found evidence supporting the existence of both mechanisms in concert during apoptosis.

In support of the cis mechanism, the addition of a single phosphate group is thought to cause changes in chromatin structure and thereby induce condensation. However, a mechanism that works merely through a conformation change of the histone tails itself is difficult to imagine, as it is commonly accepted that the tails do not have any specific secondary structure but instead are relatively disordered. It is also difficult to imagine that the modification could directly cause a stronger interaction with DNA leading to compaction in a mechanism reverse to histone acetylation: adding a phosphate group means increasing the negative charge of the tail, which should weaken or disrupt electrostatic interactions between the histone tails and result in a more accessible chromatin structure rather than a highly condensed form. Despite these paradoxes (reasons that oppose the existence of cis mechanism for H2BS10ph), I have found that a nucleosome array containing the phospho-mimic of H2BS10, S10E, yields a structure more highly compacted than even 30-nm chromatin fibers seen during mitosis (Figure 44). While it is unclear what type of

structure this nucleosome represents, I suspect that H2B N-terminal tails are interacting with themselves in a way that is similar to the aggregation of the peptides carrying H2BS10ph or H2B S10E. Because the effect of the H2B S10E mutant on compaction is more pronounced when looking at a 36-mer array compared to a 12-mer (Dr. Thomas Schalch, personal communication), I speculate that the H2B N-terminal tails somehow reach from one nucleosome to the next across the gyres of the higher order structure. This structure would then theoretically be more compacted than a mitotic 30-nm chromatin fiber, and may be representative of an apoptotic chromatin fiber. It is plausible that apoptotic chromatin fibers are more compacted than even mitotic fibers since apoptosis features the massive cleavage of structural components including chromatin. Detailed structural analysis should determine the influence of H2BS10ph on the site of the chromatin fiber.

A mechanism by which phosphorylation of the H2B N-terminal tail is a platform for interactions with other proteins (e.g. trans mechanism) has gained much interest since it is reminiscent of the heterochromatinization mediated by the chromodomain protein HP1 interaction with the H3 tail. This could either lead to an alteration in histone-histone interactions between neighboring nucleosomes or result in the recruitment of additional effector molecules that in turn mediate chromatin condensation. For example, one or more protein complexes could bridge different nucleosomes and thus cause chromatin to condense. Since apoptosis features the formation of pycnotic and condensed chromatin bodies typical of apoptotic chromatin condensation (Clifford et al., 1996; Kerr et al., 1972), it is possible that the function of H2BS10ph is to mediate chromatin condensation in a trans fashion by the induction of such protein-

protein interactions. In support, I have identified Rad53 as a H2BS10ph binding partner. Rad53 is the DNA damage checkpoint and its activation by Rad9 leads to the activation of the DNA repair pathway (Sanchez et al., 1996; Sun et al., 1996). Considering that an inactive Rad53 inhibits the DNA repair cascade (Pike et al., 2003; Hammet et al., 2000), a Rad53-H2BS10ph interaction might lead to the disruption of the DNA repair pathway. As a consequence, the DNA damage would accumulate and cells would become damaged beyond repair, promoting an apoptotic cascade to eliminate damaged cells. This model is consistent with the observation that the inactivated form of Rad53 is the H2BS10ph binding partner (Figure 53 and 54), although the direct relationship between the H2BS10ph and the accumulation of DNA damage is unknown. It should be also noted that the interaction between H2BS10ph and Rad53 might also promote chromatin condensation, although Rad53 has no known role in altering chromatin structure. Despite these uncertainties, it could be argued that their interaction may serve both purposes: 1) DNA repair disruption and 2) chromatin condensation. If correct, this “trans” mechanism via a phospho-binding partner may be the functional mechanism of H2BS10ph in promoting yeast apoptosis.

The uncertainty of the existence of a cis mechanism of chromatin condensation occurring *in vivo* makes the above hypothesis attractive. However, the nucleosome array system, which best represents histones in their proper and native setting, indicates that H2BS10ph can cause chromatin condensation in a cis fashion. Therefore, I described several possible models that include both trans and cis mechanisms mediating the function of H2BS10ph in the apoptotic cascade. In the first model, H2BS10ph interacts with Rad53 and disrupts repair of the damaged cells (trans). As the heavily damaged cells accumulate, Rad53

dissociates from H2B and H2BS10ph directly mediates the chromatin condensation (cis). This hypothesis assumes that interaction between H2BS10ph and Rad53 occurs before chromatin condensation, which is still unknown at this time. It also suggests that H2BS10ph triggers apoptosis itself in that it prevents repair, if so, S10ph should precede apoptotic DNA fragmentation. Since the onset of S10ph coincides with the apoptotic DNA fragmentation (Figure 18), I suspect this model is an unlikely mechanism for H2BS10ph. The second model consists of cis then trans mechanisms. Chromatin condenses as a result of H2BS10ph and facilitates the binding of Rad53. These events downregulate the DNA repair pathway and consequently promote the apoptotic pathway. Therefore, S10ph should occur before its interaction with Rad53. Although this model is consistent with the association between Rad53 and H2BS10ph, it is inconsistent with the onset of H2BS10ph and its interaction with Rad53. As shown in Figure 54A, the appearance of H2BS10ph and its interaction with Rad53 coincide; 90 minutes post H<sub>2</sub>O<sub>2</sub> induction. Therefore, this model is unlikely to occur. In the third model, H2BS10ph can simultaneously mediate chromatin condensation and the apoptosis of damaged cells through both cis and trans mechanisms. This model is consistent with my results, but based on a high abundance of H2BS10ph compared to Rad53 in the cell. Therefore, it could efficiently compete for Rad53 from other phosphorylated proteins, such as Rad9, and regulate chromatin condensation. Since their abundance has not been addressed at this time, a model that explains the mechanism of H2B Ser10 phosphorylation in yeast apoptosis still remains to be fully elucidated. Nevertheless, my studies support the possibility that both cis and trans mechanisms exist to effect chromatin alterations.



### *Conservation of yeast and mammalian apoptotic cascade*

Phosphorylation of S10 in yeast H2B serves a comparable role to phosphorylation of mammalian H2B at S14 and is catalyzed by Ste20 kinase, a yeast homolog of mammalian Mst1 kinase (Chapter 2; Cheung et al., 2003). Therefore, the conservation of these targeted H2B phosphorylation sites and the enzyme systems responsible for bringing it about point to an ancient apoptotic mechanism that is conserved from yeast to humans. This mechanism might consist of regulated phos/acetyl interplay between mammalian H2BS14 and its neighboring lysine residues. As shown in Figure 31A, numerous lysines are found around the mammalian H2BS14. In particular, K14, located adjacent to S14, is acetylated in asynchronously-growing HeLa cells (Throne et al., 1990) reminiscent of H2BK11ac in growing yeast (Suka et al., 2001). I suggest the intriguing possibility that phos/acetyl cross-talk also exist in mammalian cell H2B between S14 and K15.

In addition, this conserved apoptotic mechanism might include a “trans” mechanism in which Rad53 binding to phosphorylated H2BS10 in yeast or H2BS14 in mammalian cells regulates apoptosis. A Rad53 homolog, Chk2, exists in mammalian cells and functions downstream of ATM (ataxia telangiectasia mutated) and ATR (ATM related) proteins during the DNA damage response pathway (reviewed in Rouse and Jackson, 2002; Rhind and Russell, 2000). Chk2 also participates in apoptosis via phosphorylation of the pro-apoptotic protein PML (Yang et al., 2002), E2F1 (Stevens et al., 2003), and the tumor suppressor protein p53 (Hirao et al., 2002). Unlike Rad53, Chk2 has one FHA domain and it is similar to FHA1 of Rad53 (Hofmann et al., 1995). Since my data suggest that the FHA1 domain of Rad53 binds to H2BS10ph, I hypothesize Chk2 as a binding

protein for mammalian H2BS14ph. Using mammalian apoptotic nuclear extracts and employing similar peptide pull-down and immunoprecipitation experiments should determine their interactions.

### *Perspective*

Finally, my thesis work sheds light on a pair of histone modifications mediating, in particular, yeast apoptosis. In addition, my work presented here has led to the formulation of “cross-talk”, “cis” and “trans” mechanisms. Since H2B phosphorylation and the enzyme system responsible for this process are conserved between higher and lower eukaryotes, the mammalian apoptotic cascade may mirror the yeast apoptotic mechanism.

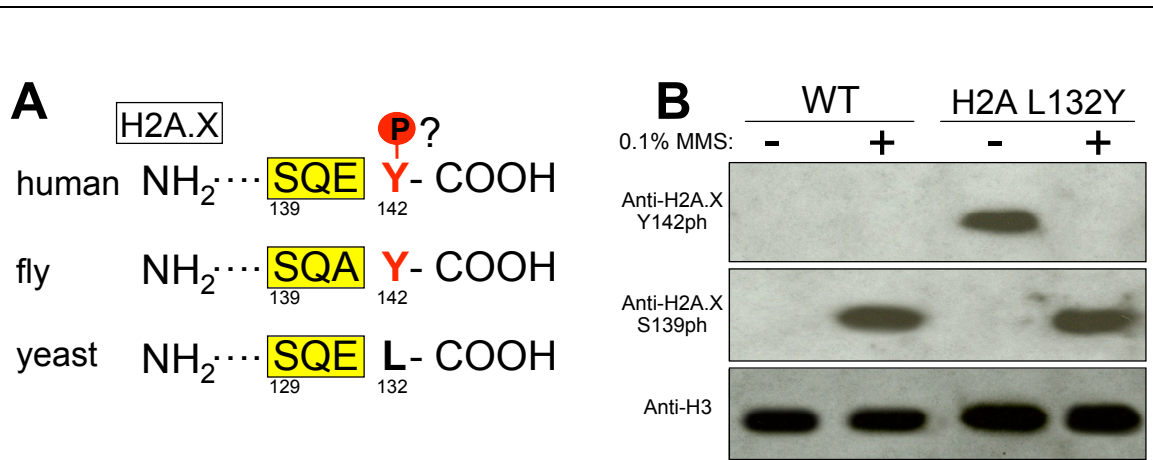
Although both the upstream deacetylation event and binding factor for H2BS14ph has to be worked out in detail, my results may elucidate the mechanism of HDAC inhibitors used in cancer therapy. Considerable evidence has suggested that HDAC inhibitors can trigger cell death in cancer cells (Medina et al., 1997; Qui et al., 2000; Zhang et al., 2004; Shao et al., 2004; Ungerstedt et al., 2005). However, the exact mechanisms of how HDAC inhibitors regulate cell death remain to be elucidated. Some studies have shown that HDAC inhibitors can induce caspase-dependent apoptosis via upregulation of tumor suppressor genes including p21 (Sawa et al., 2004; Archer et al., 2005; Komata et al., 2005; Zhao et al., 2006) or upregulation of pro-apoptotic genes including Bax, Bid, tBid (Ogawa et al., 2004; Choi, 2006). Interestingly, others have shown that HDACi not only upregulates gene expression, but also downregulates a significant number of anti-apoptotic genes, such Bcl-2 (Ogawa et al., 2004; Sawa et al., 2004; Choi, 2006). Moreover, it has been shown that there is a differential regulation of

HDAC mRNA levels by HDACi (TSA or sodium butyrate) in both neurons and lymphocytes (Dangond and Gullans, 1998; Ajamian et al., 2004). It has been shown that with HDACi treatment, the mRNA levels of HDAC1, 3, 5, and 6 are increased, but the mRNA levels of HDAC2 remain unchanged (Ajamian et al., 2004). Perhaps, these HDAC inhibitors might also upregulate the expression of Hos3 like HDAC, HDAC11 in mammalian cells. Based on my findings regarding the cross-talk between H2BS10 and K11 in yeast apoptosis (Chapter 3), it is conceivable that upregulation of Hos3 or its mammalian homologue with HDACi treatment may facilitate apoptosis. Further, if similar mechanism is proven in mammalian cells, it will provide insight in the design of clinical trials involving HDACi, especially when it is combined with cytoreductive chemotherapy.

Similar to yeast apoptosis, the deacetylation of lysines in histones mediated by HDAC11 may be necessary for the Mst1 mediated H2BS14ph. Moreover, the Rad53 counterpart Chk2 is a tumor suppressor and the list of Chk2 mutations in cancer cells is continuously expanding (reviewed in Damia and Broggin. 2004). Since Chk2 is activated mainly by ATM in response to DSBs, if unrepaired results in apoptosis, the interaction between Chk2 H2BS14ph may facilitate the apoptosis via dephosphorylation of Chk2. The same principle might follow in killing cancer cells, because the inhibition of Chk2 sensitizes cancer cells to genotoxic agents (Bartek et al., 2001; McGowan 2002; Bartek and Lukas, 2003). Many questions still need to be answered including the exact molecular mechanisms involved in mammalian apoptosis. Once these components are identified, their regulation and roles in apoptosis, and/or meiosis should be addressed. It is hoped that in the coming years, answers to

this and other questions will provide many more exciting insights into the apoptosis and histone modification in general, which could be of great relevance for potential medical applications including cancer.

## APPENDIX



Appendix Figure A1. Substitution of yeast H2A leucine 132 with tyrosine strongly react with antibodies to mammalian H2A.X tyrosine 142 phosphorylation

(A) Primary sequence alignment of H2A carboxy-terminus from a select group of organisms shows that Tyr142 is conserved in “higher” (mammals and flies) but not in “lower” eukaryotes (yeast). With the help of Andrew Xiao, yeast strain was generated expressing H2A in which L132 was mutated to tyrosine, hereafter referred to as H2A L132Y mutant. (courtesy of Dr. Andrew Xiao ).

(B) Exponentially growing WT, and H2A L132Y strains were treated with the DNA-damaging agent 0.1% MMS for 2 hr. Total nuclear protein was then prepared from these cells before being resolved on SDS-PAGE gel for Western analysis; blots were then probed with anti-H2A.XY142ph, and anti-H2A.XS139ph antibodies. Anti-H2A.XS139ph reacted strongly with WT and H2A L132Y cells following DNA damage. As expected, WT cells did not have affinity for anti-H2A.XY142ph. In contrast, anti-H2A.XY142ph only reacted with nuclear extracts from untreated H2A L132Y cultures, but did not react with extracts from MMS-treated cells. The equal loading of histone proteins were judged by anti-H3. Together, these results demonstrate that Y132 is dephosphorylated upon DNA damage in H2A L132Y mutant background.

## REFERENCES

- Agalioti, T., Lomvardas, S., Parekh, B., Yie, J., Maniatis, T., and Thanos, D. 2000. Ordered recruitment of chromatin modifying and general transcription factors to the IFN-beta promoter. *Cell*. 103(4), 667-678.
- Agalioti, T., Chen, G., and Thanos, D. 2002. Deciphering the transcriptional histone acetylation code for a human gene. *Cell*. 111(3), 381-392.
- Ahmad, K., and Henikoff, S. 2002. Epigenetic consequences of nucleosome dynamics. *Cell*. 111(3), 281-284.
- Ahn, S. H., Cheung, W. L., Hsu, J. Y., Diaz, R.L., Smith, M.M., and Allis, C.D. 2005. Sterile 20 kinase phosphorylates histone H2B at serine 10 during hydrogen peroxide-induced apoptosis in *S. cerevisiae*. *Cell*. 120(1):25-36.
- Aihara, H., Nakagawa, T., Yasui, K., Ohta, T., Hirose, S., Dhoma, N., Takio, K., Kaneko, M., Takeshima, Y., Muramatsu, M., and Ito, T. 2004. Nucleosomal histone kinase-1 phosphorylates H2A Thr 119 during mitosis in the early *Drosophila* embryo. *Genes Dev*. 18(8), 877-888.
- Ajamian, F., Salminen, A., and Reeben, M. 2004. Selective regulation of class I and class II histone deacetylases expression by inhibitors of histone deacetylases in cultured mouse neural cells. *Neurosci Lett*. 365(1), 64-68.
- Ajiro, K., Yasuda, H., and Tsuji, H. 1996. Vanadate triggers the transition from chromosome condensation to decondensation in a mitotic mutant (tsTM13) inactivation of p34cdc2/H1 kinase and dephosphorylation of mitosis-specific histone H3. *Eur J Biochem*. 241(3), 923-930
- Ajiro, K. 2000. Histone H2B phosphorylation in mammalian apoptotic cells. An association with DNA fragmentation. *J Biol Chem*. 275(1), 439-443.
- Allan, J., Hartman, P. G., Crane-Robinson, C., and Aviles, F. X. (1980). The structure of histone H1 and its location in chromatin. *Nature*. 288(5792), 675-679.

Allan, J., Harborne, N., Rau, D. C., and Gould, H. 1982. Participation of core histone "tails" in the stabilization of the chromatin solenoid. *J Cell Biol.* 93(2), 285-297.

Allan, J., Mitchell, T., Harborne, N., Bohm, L., and Crane-Robinson, C. 1986. Roles of H1 domains in determining higher order chromatin structure and H1 location. *J Mol Biol.* 187(4), 591-601.

Allfrey, V. G., Faulkner, R., and Mirsky, A. E. 1964. Acetylation and methylation of histones and their possible role in the regulation of RNA synthesis. *Proc Natl Acad Sci U S A.* 51, 786-794.

Alvarez, M., Rhodes, S. J., and Bidwell, J. P. 2003. Context-dependent transcription: all politics is local. *Gene.* 313, 43-57.

Annunziato, A. T., and Hansen, J. C. 2000. Role of histone acetylation in the assembly and modulation of chromatin structures. *Gene Expr.* 9(1-2), 37-61.

Archer, S. Y., Johnson, J., Kim, H. J., Ma, Q., Mou, H., Daesety, V., Meng, S., and Hodin, R. A. 2005. The histone deacetylase inhibitor butyrate downregulates cyclin B1 gene expression via a p21/WAF-1-dependent mechanism in human colon cancer cells. *Am J Physiol Gastrointest Liver Physiol.* 289(4), G696-703.

Arents, G., Burlingame, R. W., Wang, B. C., Love, W. E., and Moudrianakis, E. N. 1991. The nucleosomal core histone octamer at 3.1 Å resolution: a tripartite protein assembly and a left-handed superhelix. *Proc Natl Acad Sci U S A.* 88(22), 10148-10152.

Arents, G., and Moudrianakis, E. N. 1993. Topography of the histone octamer surface: repeating structural motifs utilized in the docking of nucleosomal DNA. *Proc Natl Acad Sci U S A.* 90(22), 10489-10493.

Armstrong, J. S. 2006. Mitochondrial membrane permeabilization: the sine qua non for cell death. *Bioessays.* 28(3), 253-260.

Arnoult, D., Gaume, B., Karbowski, M., Sharpe, J. C., Cecconi, F., and Youle, R. J. 2003. Mitochondrial release of AIF and EndoG requires caspase activation downstream of Bax/Bak-mediated permeabilization. *EMBO J.* 22(17), 4385-4399.

Ashkenazi, A., and Dixit, V. M. 1998. Death receptors: signaling and modulation. *Science*. 281(5381), 1305-1308.

Ausio, J. 2000. Are linker histones (histone H1) dispensable for survival? *Bioessays*. 22(10), 873-877.

Ausio, J., and Abbott, D.W. 2002. The many tales of a tail: Carboxyl-terminal tail heterogeneity specializes histone H2A variants for defined chromatin function. *Biochemistry* 41(19), 5945-5949.

Avery, O. T., LacLeod, C. M., and McCarty, M. 1944. Studies on the chemical nature of the substance inducing transformation of pneumococcal types. Induction of transformation by a desoxyribonucleic acid fraction isolated from *Pneumococcus* type III. Oswald Theodore Avery (1877-1955). *J. Exp. Med.*, (79), 137-159.

Axton, J. M., Dombradi, V., Cohen, P. T., and Glover, D. M. 1990. One of the protein phosphatase 1 isoenzymes in *Drosophila* is essential for mitosis. *Cell*. 63(1), 33-46.

Bannister, A. J., Zegerman, P., Partridge, J. F., Miska, E. A., Thomas, J. O., Allshire, R. C., and Kouzarides, T. 2001. Selective recognition of methylated lysine 9 on histone H3 by the HP1 chromo domain. *Nature*. 410(6824), 120-124.

Bannister, A. J., Schneider, R., and Kouzarides, T. 2002. Histone methylation: dynamic or static? *Cell*. 109(7), 801-806.

Bannerman, D. D., Sathymoorthy, M., and Goldblum, S. E. 1998. Bacterial lipopolysaccharide disrupts endothelial monolayer integrity and survival signaling events through caspase cleavage of adherens junction proteins. *J Biol Chem*. 273(52), 35371-35380.

Bao, Y., Konesky, K., Park, Y. J., Rosu, S., Dyer, P. N., Rangasamy, D., Tremethick, D. J., Laybourn, P. J., and Luger, K. 2004. Nucleosomes containing the histone variant H2A.Bbd organize only 118 base pairs of DNA. *EMBO J*. 23(16), 3314-3324.

Barber, C. M., Turner, F. B., Wang, Y., Hagstrom, K., Taverna, S. D., Mollah, S., Ueberheide, B., Meyer, B. J., Hunt, D. F., Cheung, P., and Allis, C. D. 2004. The



enhancement of histone H4 and H2A serine 1 phosphorylation during mitosis and S-phase is evolutionarily conserved. *Chromosoma*. 112(7), 360-371.

Barratt, M. J., Hazzalin, C. A., Cano, E., and Mahadevan, L. C. 1994. Mitogen-stimulated phosphorylation of histone H3 is targeted to a small hyperacetylation-sensitive fraction. *Proc Natl Acad Sci U S A*. 91(11), 4781-4785.

Bartek, J., Falck, J., and Lukas, J. 2001. CHK2 kinase--a busy messenger. *Nat Rev Mol Cell Biol*. 2(12), 877-886.

Bartek, J., and Lukas, J. 2003. Chk1 and Chk2 kinases in checkpoint control and cancer. *Cancer Cell*. 3(5), 421-429.

Bashkirov, V. I., Bashkirova, E. V., Haghnazari, E., and Heyer, W. D. 2003. Direct kinase-to-kinase signaling mediated by the FHA phosphoprotein recognition domain of the Dun1 DNA damage checkpoint kinase. *Mol Cell Biol*. 23(4), 1441-1452.

Bassing, C. H., Chua, K. F., Sekiguchi, J., Suh, H., Whitlow, S. R., Fleming, J. C., Monroe, B. C., Ciccone, D. N., Yan, C., Vlasakova, K., Livingston, D. M., Ferguson, D. O., Scully, R., and Alt, F. W. 2002. Increased ionizing radiation sensitivity and genomic instability in the absence of histone H2AX. *Proc Natl Acad Sci U S A*. 99(12), 8173-8178.

Bedford, M. T., and Richard, S. 2005. Arginine methylation an emerging regulator of protein function. *Mol Cell*. 18(3), 263-272. Review.

Belmont, A. S., and Bruce, K. 1994. Visualization of G1 chromosomes: a folded, twisted, supercoiled chromonema model of interphase chromatid structure. *J Cell Biol*. 127(2), 287-302.

Belmont, A. S., Dietzel, S., Nye, A. C., Strukov, Y. G., and Tumber, T. 1999. Large-scale chromatin structure and function. *Curr Opin Cell Biol*. 11(3), 307-311.

Berger, M., Stahl, N., Del Sal, G., and Haupt, Y. 2005. Mutations in proline 82 of p53 impair its activation by Pin1 and Chk2 in response to DNA damage. *Mol Cell Biol*. 25(13), 5380-8.

Berger, S. L. 1999. Gene activation by histone and factor acetyltransferases. *Curr Opin Cell Biol.* 11(3), 336-341.

Bernard, P., Maure, J. F., Partridge, J. F., Genier, S., Javerzat, J. P., and Allshire, R. C. 2001. Requirement of heterochromatin for cohesion at centromeres. *Science.* 294(5551), 2539-2542.

Bernstein, B. E., Humphrey, E. L., Erlich, R. L., Schneider, R., Bouman, P., Liu, J. S., Kouzarides, T., and Schreiber, S. L. 2002. Methylation of histone H3 Lys 4 in coding regions of active genes. *Proc Natl Acad Sci U S A.* 99(13), 8695-8700.

Bishop, D. K. 1994. RecA homologs Dmc1 and Rad51 interact to form multiple nuclear complexes prior to meiotic chromosome synapsis. *Cell* 79, 1081-1092.

Blanchard, H., Fontes, M. R., Hammet, A., Pike, B. L., The, T., Gleichmann, T., Gooley, P. R., Kobe, B., and Heierhorst, J. 2001. Crystallization and preliminary X-ray diffraction studies of FHA domains of Dun1 and Rad53 protein kinases. *Acta Crystallogr D Biol Crystallogr.* 57(Pt 3), 459-461.

Blaschke, U. K., Silberstein, J., and Muir, T. W. 2000. Protein engineering by expressed protein ligation. *Methods Enzymol.* 328, 478-496.

Bloecher, A., and Tatchell, K. 1999. Defects in *Saccharomyces cerevisiae* protein phosphatase type I activate the spindle/kinetochore checkpoint. *Genes Dev.* 13(5), 517-522.

Bone, J. R., Lavender, J., Richman, R., Palmer, M. J., Turner, B. M., Kuroda, M. I. 1994. Acetylated histone H4 on the male X chromosome is associated with dosage compensation in *Drosophila*. *Genes Dev.* 8(1), 96-104.

Bosch, A., and Suau, P. 1995. Changes in core histone variant composition in differentiating neurons: The roles of differential turnover and synthesis rates. *Eur. J. Cell Biol.* 68(3), 220-225.

Bottomley, M. J. 2004. Structures of protein domains that create or recognize histone modifications. *EMBO Rep.* 5(5), 464-469.

Boyce, M., Degterev, A., and Yuan, J. 2004. Caspases: an ancient cellular sword of Damocles. *Cell Death Differ.* 11(1), 29-37.

Bradbury, E. M., Inglis, R. J., and Matthews, H. R. 1974. Control of cell division by very lysine rich histone (F1) phosphorylation. *Nature*. 247(439), 257-261.

Bram, S., and Ris, H. (1971). On the structure of nucleohistone. *J Mol Biol*. 55(3), 325-336.

Brandt, W.F., Strickland, W.N., Strickland, M., Carlisle, L., Woods, D., and von Holt, C. (1979). A histone programme during the life cycle of the sea urchin. *Eur. J. BioChem*. 94(1), 1-10.

Braunstein, M., Rose, A. B., Holmes, S. G., Allis, C. D., and Broach, J. R. 1993. Transcriptional silencing in yeast is associated with reduced nucleosome acetylation. *Genes Dev*. 7(4), 592-604.

Braunstein, M., Sobel, R. E., Allis, C. D., Turner, B. M., and Broach, J. R. 1996. Efficient transcriptional silencing in *Saccharomyces cerevisiae* requires a heterochromatin histone acetylation pattern. *Mol Cell Biol*. 16(8), 4349-4356.

Briggs, S. D., Xiao, T., Sun, Z. W., Caldwell, J. A., Shabanowitz, J., Hunt, D. F., Allis, C. D., and Strahl, B. D. 2002. Gene silencing: trans-histone regulatory pathway in chromatin. *Nature*. 418(6897), 498.

Brownell, J. E., Zhou, J., Ranalli, T., Kobayashi, R., Edmondson, D. G., Roth, S. Y., and Allis, C. D. 1996. Tetrahymena histone acetyltransferase A: a homolog to yeast Gcn5p linking histone acetylation to gene activation. *Cell*. 84(6), 843-851.

Budihardjo, I., Oliver, H., Lutter, M., Luo, X., and Wang, X. 1999. Biochemical pathways of caspase activation during apoptosis. *Annu Rev Cell Dev Biol*. 15, 269-290.

Buendia, B., Courvalin, J. C., and Collas, P. 2001. Dynamics of the nuclear envelope at mitosis and during apoptosis. *Cell Mol Life Sci*. 58(12-13), 1781-1789.

Burbelo, P. D., Drechsel, D., and Hall, A. 1995. A conserved binding motif defines numerous candidate target proteins for both Cdc42 and Rac GTPases. *J Biol Chem*. 270(49), 29071-29074.

Byeon, I. J., Yongkiettrakul, S., and Tsai, M. D. 2001. Solution structure of the yeast Rad53 FHA2 complexed with a phosphothreonine peptide pTXXL:

comparison with the structures of FHA2-pYXL and FHA1-pTXXD complexes. *J Mol Biol.* 314(3), 577-588.

Camerini-Otero, R. D., Sollner-Webb, B., and Felsenfeld, G. (1976). The organization of histones and DNA in chromatin: evidence for an arginine-rich histone kernel. *Cell.* 8(3), 333-347.

Cao, R., Wang, L., Wang, H., Xia, L., Erdjument-Bromage, H., Tempst, P., Jones, R. S., and Zhang, 2002. Role of histone H3 lysine 27 methylation in Polycomb-group silencing. *Science.* 298(5595), 1039-1043.

Carmen, A. A., Griffin, P. R., Calaycay, J. R., Rundlett, S. E., Suka, Y., and Grunstein, M. 1999. Yeast HOS3 forms a novel trichostatin A-insensitive homodimer with intrinsic histone deacetylase activity. *Proc Natl Acad Sci U S A.* 96(22), 12356-12361.

Carney, J. P., Maser, R. S., Olivares, H., Davis, E. M., Le Beau, M., Yates, J. R. 3rd, Hays, L., Morgan, W. F., and Petrini, J. H. 1998. The hMre11/hRad50 protein complex and Nijmegen breakage syndrome: linkage of double-strand break repair to the cellular DNA damage response. *Cell* 93(3),477-486.

Carruthers, L. M., Bednar, J., Woodcock, C. L., and Hansen, J. C. 1998. Linker histones stabilize the intrinsic salt-dependent folding of nucleosomal arrays: mechanistic ramifications for higher-order chromatin folding. *Biochemistry.* 37(42), 14776-14787.

Carruthers, L.M. and Hansen, J.C. 2000. The core histone N termini function independently of linker histones during chromatin condensation. *J. Biol. Chem.* 275(47), 37285-37290.

Cary, P. D., Crane-Robinson, C., Bradbury, E. M., and Dixon, G. H. (1982). Effect of acetylation on the binding of N-terminal peptides of histone H4 to DNA. *Eur J Biochem.* 127(1), 137-143.

Celeste, A., Petersen, S., Romanienko, P. J., Fernandez-Capetillo, O., Chen, H. T., Sedelnikova, O. A., Reina-San-Martin, B., Coppola, V., Meffre, E., Difilippantonio, M. J., Redon, C., Pilch, D. R., Olaru, A., Eckhaus, M., Camerini-Otero, R. D., Tessarollo, L., Livak, F., Manova, K., Bonner, W. M., Nussenzweig, M. C., and Nussenzweig, A. 2002. Genomic instability in mice lacking histone H2AX. *Science.* 296(5569), 922-927.

Celeste, A., Fernandez-Capetillo, O., Kruhlak, M. J., Pilch, D. R., Staudt, D. W., Lee, A., Bonner, R. F., Bonner, W. M., and Nussenzweig, A. 2003. Histone H2AX phosphorylation is dispensable for the initial recognition of DNA breaks. *Nature Cell Biol.* 5(7), 675–679.

Cerf, C., Lippens, G., Ramakrishnan, V., Muyldermans, S., Segers, A., Wyns, L., Wodak, S. J., and Hallenga, K. 1994. Homo- and heteronuclear two-dimensional NMR studies of the globular domain of histone H1: full assignment, tertiary structure, and comparison with the globular domain of histone H5. *Biochemistry.* 33(37), 11079-11086.

Cerretti, D. P., Kozlosky, C. J., Mosley, B., Nelson, N., Van Ness, K., Greenstreet, T. A., March, C. J., Kronheim, S. R., Druck, T., and Cannizzaro, L. A., et al. 1992. Molecular cloning of the interleukin-1 beta converting enzyme. *Science.* 256(5053), 97-100.

Chan, C. S., and Botstein, D. 1993. Isolation and characterization of chromosome-gain and increase-in-ploidy mutants in yeast. *Genetics.* 135(3), 677-691.

Chen, D., Ma, H., Hong, H., Koh, S. S., Huang, S. M., Schurter, B. T., Aswad, D. W., and Stallcup, M. R. 1999. Regulation of transcription by a protein methyltransferase. *Science* 284(5423), 2174-2177.

Cheng, E. H., Wei, M. C., Weiler, S., Flavell, R. A., Mak, T. W., Lindsten, T., and Korsmeyer, S. J. 2001. BCL-2, BCL-X(L) sequester BH3 domain-only molecules preventing BAX- and BAK-mediated mitochondrial apoptosis. *Mol. Cell.* 8(3), 705–711.

Cheung, P., Tanner, K. G., Cheung, W. L., Sassone-Corsi, P., Denu, J. M., and Allis, C. D. 2000. Synergistic coupling of histone H3 phosphorylation and acetylation in response to epidermal growth factor stimulation. *Mol Cell.* 5(6), 905-915.

Cheung, W. L., Ajiro, K., Samejima, K., Kloc, M., Cheung, P., Mizzen, C. A., Beeser, A., Etkin, L. D., Chernoff, J., Earnshaw, W. C., and Allis, C. D. 2003. Apoptotic phosphorylation of histone H2B is mediated by mammalian sterile twenty kinase. *Cell.* 113(4), 507-517.

Cheung, W. L., Turner, F. B., Krishnamoorthy, T., Wolner, B., Ahn, S. H., Foley, M., Dorsey, J. A., Peterson, C. L., Berger, S. L., and Allis, C. D. 2005.

Phosphorylation of histone H4 serine 1 during DNA damage requires casein kinase II in *S. cerevisiae*. *Curr Biol.* 15(7), 656-660.

Chinnaiyan, A. M., O'Rourke, K., Tewari, M., and Dixit, V. M. 1995. FADD, a novel death domain-containing protein, interacts with the death domain of Fas and initiates apoptosis. *Cell.* 81(4), 505-512.

Choi, Y. C, and Chae, C. B. 1991. DNA hypomethylation and germ cell-specific expression of testis-specific H2B histone gene. *J Biol Chem.* 266(30), 20504-20511.

Choi, Y. C., Gu, W., Hecht, N. B., Feinberg, A. P., and Chae, C. B. 1996. Molecular cloning of mouse somatic and testis-specific H2B histone genes containing a methylated CpG island. *DNA Cell Biol.* 15(6), 495-504.

Choi, Y. H. 2005. Induction of apoptosis by trichostatin A, a histone deacetylase inhibitor, is associated with inhibition of cyclooxygenase-2 activity in human non-small cell lung cancer cells. *Int J Oncol.* 27(2), 473-479.

Chu, S., and Herskowitz, I. 1998. Gametogenesis in yeast is regulated by a transcriptional cascade dependent on Ndt80. *Mol Cell.* 1, 685-696.

Clarke, D. J., O'Neill, L. P., and Turner, B. M. 1993. Selective use of H4 acetylation sites in the yeast *Saccharomyces cerevisiae*. *Biochem J.* 294(2), 557-561.

Clarke, P. G. and Clarke, S. Nineteenth century research on naturally occurring cell death and related phenomena. *Anat Embryol (Berl)* 193 (2), 81-99. 1996

Clements, A., Poux, A. N., Lo, W. S., Pillus, L., Berger, S. L., Marmorstein, R. 2003. Structural basis for histone and phosphohistone binding by the GCN5 histone acetyltransferase. *Mol Cell.* 12(2), 461-473.

Clifford, J., Chiba, H., Sobieszczuk, D., Metzger, D., and Chambon, P. 1996. RXRalpha-null F9 embryonal carcinoma cells are resistant to the differentiation, anti-proliferative and apoptotic effects of retinoids. *EMBO J.* 15(16), 4142-4155.

Cobb, J., Miyaike, M., Kikuchi, A., and Handel, M. A. 1999. Meiotic events at the centromeric heterochromatin: histone H3 phosphorylation, topoisomerase II alpha localization and chromosome condensation. *Chromosoma.* 108(7), 412-425.

Creasy, C.L., Ambrose, D.M., and Chernoff, J. 1996. The Ste20-like protein kinase, Mst1, dimerizes and contains an inhibitory domain. *J. Biol. Chem.* 271, 21049-21053.

Cryns, V. L., Bergeron, L., Zhu, H., Li, H., and Yuan, J. 1996. Specific cleavage of alpha-fodrin during Fas- and tumor necrosis factor-induced apoptosis is mediated by an interleukin-1beta-converting enzyme/Ced-3 protease distinct from the poly(ADP-ribose) polymerase protease. *J Biol Chem.* 271(49), 31277-31282.

Cuthbert, G. L., Daujat, S., Snowden, A. W., Erdjument-Bromage, H., Hagiwara, T., Yamada, M., Schneider, R., Gregory, P. D., Tempst, P., Bannister, A. J., and Kouzarides, T. 2004. Histone deimination antagonizes arginine methylation. *Cell.* 118(5), 545-553.

Cvrckova, F., De Virgilio, C., Manser, E., Pringle, J. R., and Nasmyth, K. 1995. Ste20-like protein kinases are required for normal localization of cell growth and for cytokinesis in budding yeast. *Genes Dev.* 9(15), 1817-1830.

Czermin, B., Schotta, G., Hulsmann, B. B., Brehm, A., Becker, P. B., Reuter, G., and Imhof, A. 2001. Physical and functional association of SU(VAR)3-9 and HDAC1 in *Drosophila*. *EMBO Rep.* 2(10), 915-919.

Czermin, B., Melfi, R., McCabe, D., Seitz, V., Imhof, A., and Pirrotta, V. 2002. *Drosophila* enhancer of Zeste/ESC complexes have a histone H3 methyltransferase activity that marks chromosomal Polycomb sites. *Cell.* 111(2), 185-196.

Dai, J., Sultan, S., Taylor, S. S., and Higgins, J. M. 2005. The kinase haspin is required for mitotic histone H3 Thr 3 phosphorylation and normal metaphase chromosome alignment. *Genes Dev.* 19(4), 472-488.

Damia, G., and Broggini, M. 2004. Cell cycle checkpoint proteins and cellular response to treatment by anticancer agents. *Cell Cycle.* 3(1), 46-50.

Dangond, F., and Gullans, S. R. 1998. Differential expression of human histone deacetylase mRNAs in response to immune cell apoptosis induction by trichostatin A and butyrate. *Biochem Biophys Res Commun.* 247(3), 833-837.

Daniel, J. A., Torok, M. S., Sun, Z. W., Schieltz, D., Allis, C. D., Yates, J. R. 3rd, and Grant, P. A. 2004. Deubiquitination of histone H2B by a yeast acetyltransferase complex regulates transcription. *J Biol Chem.* 279(3), 1867-1871.

Dasso, M., Dimitrov, S., and Wolffe, A. P. 1994. Nuclear assembly is independent of linker histones. *Proc Natl Acad Sci U S A.* 91(26), 12477-12481.

Davenport, K. R., Sohaskey, M., Kamada, Y., Levin, D. E., Gustin, M. C. 1995. A second osmosensing signal transduction pathway in yeast. Hypotonic shock activates the PKC1 protein kinase-regulated cell integrity pathway. *J Biol Chem.* 270(50), 30157-30161. □

Davey, C. A., Sargent, D. F., Luger, K., Maeder, A. W., and Richmond, T. J. 2002. Solvent mediated interactions in the structure of the nucleosome core particle at 1.9 Å resolution. *J Mol Biol.* 319(5), 1097-1113.

Davey, C. A., and Richmond, T. J. 2002. DNA-dependent divalent cation binding in the nucleosome core particle. *Proc Natl Acad Sci U S A.* 99(17), 11169-11174.

de la Barre, A. E., Gerson, V., Gout, S., Creaven, M., Allis, C. D., and Dimitrov, S. 2000. Core histone N-termini play an essential role in mitotic chromosome condensation. *EMBO J.* 19(3), 379-391.

de la Barre, A. E., Angelov, D., Molla, A., and Dimitrov, S. 2001. The N-terminus of histone H2B, but not that of histone H3 or its phosphorylation, is essential for chromosome condensation. *EMBO J.* 20(22), 6383-6393.

de la Cruz, X., Lois, S., Sanchez-Molina, S., and Martinez-Balbas, M. A. 2005. Do protein motifs read the histone code? *Bioessays.* 27(2), 164-175.

de Ruijter, A. J., van Gennip, A. H., Caron, H. N., Kemp, S., and van Kuilenburg, A. B. 2003. Histone deacetylases (HDACs): characterization of the classical HDAC family. *Biochem J.* 370(3):737-749.

De Souza, C. P., Osmani, A. H., Wu, L. P., Spotts, J. L., and Osmani, S. A. 2000. Mitotic histone H3 phosphorylation by the NIMA kinase in *Aspergillus nidulans*. *Cell.* 102(3), 293-302.



Deckert, J., and Struhl, K. 2002. Targeted recruitment of Rpd3 histone deacetylase represses transcription by inhibiting recruitment of Swi/Snf, SAGA, and TATA binding protein. *Mol Cell Biol.* 22(18), 6458-6470.

Degterev, A., Boyce, M., and Yuan, J. 2003. A decade of caspases. *Oncogene.* 22(53), 8543-8567.

Dehe, P. M., Pamblanco, M., Luciano, P., Lebrun, R., Moinier, D., Sendra, R., Verreault, A., Tordera, V., and Geli, V. 2005. Histone H3 lysine 4 mono-methylation does not require ubiquitination of histone H2B. *J Mol Biol.* 353(3), 477-484.

Del Carratore, R., Della Croce, C., Simili, M., Taccini, E., Scavuzzo, M., and Sbrana, S. 2002. Cell cycle and morphological alterations as indicative of apoptosis promoted by UV irradiation in *S. cerevisiae*. *Mutat Res.* 513(1-2), 183-191.

Denu, J. M. 2005. The Sir 2 family of protein deacetylases. *Curr Opin Chem Biol.* 9(5), 431-440.

Dey, A., Chitsaz, F., Abbasi, A., Misteli, T., and Ozato, K. 2003. The double bromodomain protein Brd4 binds to acetylated chromatin during interphase and mitosis. *Proc Natl Acad Sci U S A.* 100(15), 8758-8763.

Dhalluin, C., Carlson, J. E., Zeng, L., He, C., Aggarwal, A. K., Zhou, M. M. 1999. Structure and ligand of a histone acetyltransferase bromodomain. *Nature.* 399(6735), 491-496.

Ding, H. F., and Fisher, D. E. 2002. Induction of apoptosis in cancer: new therapeutic opportunities. *Ann Med.* 34(6), 451-469.

Dion, M. F., Altschuler, S. J., Wu, L. F., and Rando, O. J. 2005. Genomic characterization reveals a simple histone H4 acetylation code. *Proc Natl Acad Sci U S A.* 102(15), 5501-5506.

Doonan, J. H., and Morris, N. R. 1989. The bimG gene of *Aspergillus nidulans*, required for completion of anaphase, encodes a homolog of mammalian phosphoprotein phosphatase 1. *Cell.* 57(6), 987-996.

Dorigo, B., Schalch, T., Bystricky, K., and Richmond, T. J. 2003. Chromatin fiber folding: requirement for the histone H4 N-terminal tail. *J Mol Biol.* 327(1), 85-96.

Dorigo, B., Schalch, T., Kulangara, A., Duda, S., Schroeder, R. R., and Richmond, T. J. 2004. Nucleosome arrays reveal the two-start organization of the chromatin fiber. *Science.* 306(5701), 1571-1573.

Dover, J., Schneider, J., Tawiah-Boateng, M. A., Wood, A., Dean, K., Johnston, M., and Shilatifard, A. 2002. Methylation of histone H3 by COMPASS requires ubiquitination of histone H2B by Rad6. *J Biol Chem.* 277(32), 28368-28371.

Dou, Y., Mizzen, C. A., Abrams, M., Allis, C. D., Gorovsky, M. A. 1999. Phosphorylation of linker histone H1 regulates gene expression *in vivo* by mimicking H1 removal. *Mol Cell.* 4(4), 641-647.

Downs, J. A., Lowndes, N. F., and Jackson, S. P. 2000. A role for *Saccharomyces cerevisiae* histone H2A in DNA repair. *Nature.* 408(6815), 1001-1004.

Dresser, M. E., and Giroux, C. N. 1988. Meiotic chromosome behavior in spread preparations of yeast. *J Cell Biol.* 106(3), 567-573

Dunn, K. L., and Davie, J. R. Stimulation of the Ras-MAPK pathway leads to independent phosphorylation of histone H3 on serine 10 and 28. *Oncogene.* 24(21), 3492-3502.

Durocher, D., Henckel, J., Fersht, A. R., and Jackson, S. P. 1999. The FHA domain is a modular phosphopeptide recognition motif. *Mol Cell.* 4(3), 387-394.

Durocher, D., Taylor, I. A., Sarbassova, D., Haire, L. F., Westcott, S. L., Jackson, S. P., Smerdon, S. J., and Yaffe, M. B. 2000. The molecular basis of FHA domain:phosphopeptide binding specificity and implications for phospho-dependent signaling mechanisms. *Mol Cell.* 6(5), 1169-1182.

Durocher, D., and Jackson, S. P. 2002. The FHA domain. *FEBS Lett.* 513(1), 58-66.

Dyer, P. N., Edayathumangalam, R. S., White, C. L., Bao, Y., Chakravarthy, S., Muthurajan, U.M., and Luger, K. 2004. Reconstitution of nucleosome core particles from recombinant histones and DNA. *Methods Enzymol.* 375, 23-44.

Earnshaw, W. C., and Rothfield, N. (1985). Identification of a family of human centromere proteins using autoimmune sera from patients with scleroderma. *Chromosoma*. 91(3-4), 313-321.

Earnshaw, W. C., Martins, L. M., and Kaufmann, S. H. 1999. Mammalian caspases: structure, activation, substrates, and functions during apoptosis. *Annu Rev Biochem*. 68, 383-424.

Eberharter, A., Ferreira, R., and Becker, P. 2005. Dynamic chromatin: concerted nucleosome remodelling and acetylation. *Biol Chem*. 386(8), 745-751.

Ekwall, K. 2005. Genome-wide analysis of HDAC function. *Trends Genet*. 21(11), 608-615.

Ellis, H. M., and Horvitz, H. R. 1986. Genetic control of programmed cell death in the nematode *C. elegans*. *Cell*. 44(6), 817-829.

Enari, M., Sakahira, H., Yokoyama, H., Okawa, K., Iwamatsu, A., and Nagata, S. 1998. A caspase-activated DNase that degrades DNA during apoptosis, and its inhibitor ICAD. *Nature*. 391(6662), 43-50.

Fadeel, B., and Orrenius, S. 2005. Apoptosis: a basic biological phenomenon with wide-ranging implications in human disease. *J Intern Med*. 258(6), 479-517.

Falck, J., Coates, J., and Jackson, S. P. 2005. Conserved modes of recruitment of ATM, ATR and DNA-PKcs to sites of DNA damage. *Nature*. 434(7033), 605-611.

Felsenfeld, G., and Groudine, M. 2003. Controlling the double helix. *Nature*. 421(6921), 448-453.

Fernandez-Capetillo, O., Mahadevaiah, S. K., Celeste, A., Romanienko, P. J., Camerini-Otero, R. D., Bonner, W. M., Manova, K., Burgoyne, P., and Nussenzweig, A. 2003. H2AX is required for chromatin remodeling and inactivation of sex chromosomes in male mouse meiosis. *Dev. Cell*. 4(4), 497-508.

Fernandez-Capetillo, O., Allis, C. D., and Nussenzweig, A. 2004a. Phosphorylation of histone H2B at DNA double-strand breaks. *J Exp Med*. 199(12), 1671-1677.

Fernandez-Capetillo, O., Lee, A., Nussenzweig, M., and Nussenzweig, A. 2004b. H2AX: The histone guardian of the genome. *DNA Repair (Amst.)* 3(8-9), 959-967.

Fischle, W., Wang, Y., and Allis, C. D. 2003a. Histone and chromatin cross-talk. *Curr Opin Cell Biol.* 15(2), 172-183.

Fischle, W., Wang, Y., and Allis, C. D. 2003b. Binary switches and modification cassettes in histone biology and beyond. *Nature.* 425(6957), 475-479.

Fischle, W., Wang, Y., Jacobs, S. A., Kim, Y., Allis, C. D., and Khorasanizadeh, S. 2003c. Molecular basis for the discrimination of repressive methyl-lysine marks in histone H3 by Polycomb and HP1 chromodomains. *Genes Dev.* 17(15), 1870-1881.

Fischle, W., Tseng, B. S., Dormann, H. L., Ueberheide, B. M., Garcia, B. A., Shabanowitz, J., Hunt, D. F., Funabiki, H., and Allis, C. D. 2005. Regulation of HP1-chromatin binding by histone H3 methylation and phosphorylation. *Nature.* 438(7071), 1116-1122.

Fletcher, T. M., and Hansen, J. C. 1995. Core histone tail domains mediate oligonucleosome folding and nucleosomal DNA organization through distinct molecular mechanisms. *J Biol Chem.* 270(43), 25359-25362.

Fletcher, T. M., and Hansen, J. C. 1996. The nucleosomal array: structure/function relationships. *Crit Rev Eukaryot Gene Expr.* 6(2-3), 149-188.

Fletcher, C., Heintz, N., and Roeder, R. G. 1987. Purification and characterization of OTF-1, a transcription factor regulating cell cycle expression of a human histone H2b gene. *Cell.* 51(5), 773-781.

Fleury, C., Mignotte, B., and Vayssiere, J. L. 2002. Mitochondrial reactive oxygen species in cell death signaling. *Biochimie.* 84(2-3), 131-141.

Francisco, L., Wang, W., and Chan, C. S. 1994. Type 1 protein phosphatase acts in opposition to IpL1 protein kinase in regulating yeast chromosome segregation. *Mol Cell Biol.* 14(7), 4731-4740.

Franklin, S. G., and Zweidler, A. (1977). Non-allelic variants of histones 2a, 2b and 3 in mammals. *Nature.* 266(5599), 273-275.

Frohlich, K. U., and Madeo, F. 2000. Apoptosis in yeast--a monocellular organism exhibits altruistic behaviour. *FEBS Lett.* 473(1), 6-9.

Fry, C. J., Peterson, C. L. 2001. Chromatin remodeling enzymes: who's on first? *Curr Biol.* 11(5), R185-R197.

Fu, H., Subramanian, R. R., and Masters, S. C. 2000. 14-3-3 proteins: structure, function, and regulation. *Annu. Rev. Pharmacol. Toxicol.* 40, 617-647.

Fuchs, J., Demidov, D., Houben, A., and Schubert, I. 2006. Chromosomal histone modification patterns--from conservation to diversity. *Trends Plant Sci.* 11(4), 199-208.

Fuks, F. 2005. DNA methylation and histone modifications: teaming up to silence genes. *Curr Opin Genet Dev.* 15(5), 490-495.

Garcia-Ramirez, M., Dong, F., and Ausio, J. 1992. Role of the histone "tails" in the folding of oligonucleosomes depleted of histone H1. *J Biol Chem.* 267(27), 19587-19595.

Garcia-Ramirez, M., Rocchini, C., and Ausio, J. 1995. Modulation of chromatin folding by histone acetylation. *J Biol Chem.* 270(30), 17923-17928.

Georgel, P. T., and Hansen, J. C. 2001. Linker histone function in chromatin: dual mechanisms of action. *Biochem Cell Biol.* 79(3), 313-316.

Gerchman, S. E., and Ramakrishnan, V. 1987. Chromatin higher-order structure studied by neutron scattering and scanning transmission electron microscopy. *Proc Natl Acad Sci U S A.* 84(22), 7802-7806.

Giannattasio, M., Lazzaro, F., Plevani, P., and Muzi-Falconi, M. 2005. The DNA damage checkpoint response requires histone H2B ubiquitination by Rad6-Bre1 and H3 methylation by Dot1. *J Biol Chem.* 280(11), 9879-9886.

Giet, R., and Glover, D. M. 2001. Drosophila aurora B kinase is required for histone H3 phosphorylation and condensin recruitment during chromosome condensation and to organize the central spindle during cytokinesis. *J Cell Biol.* 152(4), 669-682.

Gietz, D., St Jean, A., Woods, R.A., and Schiestl, R.H. 1992. Improved method for high efficiency transformation of intact yeast cells. *Nucleic Acids Res.* 20, 1425.

Gilbert, C. S., Green, C. M., and Lowndes, N. F. 2001. Budding yeast Rad9 is an ATP-dependent Rad53 activating machine. *Mol Cell.* 8(1), 129-136.

Gilbert, N., and Allan, J. 2001. Distinctive higher-order chromatin structure at mammalian centromeres. *Proc Natl Acad Sci U S A.* 98(21), 11949-11954.

Gilbert, N., Boyle, S., Sutherland, H., de Las Heras, J., Allan, J., Jenuwein, T., and Bickmore, W. A. 2003. Formation of facultative heterochromatin in the absence of HP1. *EMBO J.* 22(20), 5540-5550.

Glantschnig, H., Rodan, G. A., and Reszka, A. A. 2002. Mapping of MST1 kinase sites of phosphorylation. Activation and autophosphorylation. *J Biol Chem.* 277(45), 42987-42996.

Glover, J. N., Williams, R. S., and Lee, M. S. 2004. Interactions between BRCT repeats and phosphoproteins: tangled up in two. *Trends Biochem Sci.* 29(11), 579-585.

Goehring, A. S., Mitchell, D. A., Tong, A. H., Keniry, M. E., Boone, C., and Sprague, G. F. Jr. 1998. Synthetic lethal analysis implicates Ste20p, a p21-activated protein kinase, in polarisome activation. *Mol Biol Cell.* 14(4), 1501-1516

Goo, Y. H., Sohn, Y. C., Kim, D. H., Kim, S. W., Kang, M. J., Jung, D. J., Kwak, E., Barlev, N. A., Berger, S. L., Chow, V. T., Roeder, R. G., Azorsa, D. O., Meltzer, P. S., Suh, P. G., Song, E. J., Lee, K. J., Lee, Y. C., and Lee, J. W. 2003. Activating signal cointegrator 2 belongs to a novel steady-state complex that contains a subset of trithorax group proteins. *Mol Cell Biol.* 23(1), 140-149.

Goto, H., Tomono, Y., Ajiro, K., Kosako, H., Fujita, M., Sakurai, M., Okawa, K., Iwamatsu, A., Okigaki, T., Takahashi, T., and Inagaki, M. 1999. Identification of a novel phosphorylation site on histone H3 coupled with mitotic chromosome condensation. *J Biol Chem.* 274(36), 25543-25549.

Goto, H., Yasui, Y., Nigg, E. A., and Inagaki, M. 2002. Aurora-B phosphorylates Histone H3 at serine28 with regard to the mitotic chromosome condensation. *Genes Cells.* 7(1), 11-17.

Green, D. R., and Kroemer, G. 2004. The pathophysiology of mitochondrial cell death. *Science*. 305(5684), 626-629.

Green, G.R., Collas, P., Burrell, A., and Poccia, D.L. 1995. Histone phosphorylation during sea urchin development. *Semin. Cell Biol.* 6(4), 219-227.

Greenhalf, W., Stephan, C., and Chaudhuri, B. 1996. Role of mitochondria and C-terminal membrane anchor of Bcl-2 in Bax induced growth arrest and mortality in *Saccharomyces cerevisiae*. *FEBS Lett.* 380(1-2), 169-175.

Grewal, S. I. 2000. Transcriptional silencing in fission yeast. *J Cell Physiol.* 184(3), 311-318.

Grunstein, M. 1997. Histone acetylation in chromatin structure and transcription. *Nature*. 389(6649), 349-352.

Gu, W., Szauter, P., and Lucchesi, J. C. 1998. Targeting of MOF, a putative histone acetyl transferase, to the X chromosome of *Drosophila melanogaster*. *Dev Genet.* 22(1), 56-64.

Guacci, V., Koshland, D., and Strunnikov, A. 1997. A direct link between sister chromatid cohesion and chromosome condensation revealed through the analysis of MCD1 in *S. cerevisiae*. *Cell*. 91(1), 47-57. Gunjan, A., Paik, J., and Verreault, A. 2005. Regulation of histone synthesis and nucleosome assembly. *Biochimie*. 87(7), 625-635.

Guo, Y. L., Kang, B., and Wailliamson, J. R. 1998. Inhibition of the expression of mitogen-activated protein phosphatase-1 potentiates apoptosis induced by tumor necrosis factor-alpha in rat mesangial cells. *J Biol Chem*. 273(17), 10362-10366.

Gurley, L. R., Walters, R. A., and Tobey, R. A. (1973). Histone phosphorylation in late interphase and mitosis. *Biochem Biophys Res Commun*. 50(3), 744-750.

Haber, J.E. 2000. Partners and pathways repairing a double-strand break. *Trends Genet.* 16(6), 259-264.

Hacker, G. 2000. The morphology of apoptosis. *Cell Tissue Res*. 301(1), 5-17.

Hake, S. B., Xiao, A., and Allis, C. D. 2004. Linking the epigenetic 'language' of covalent histone modifications to cancer. *Br J Cancer*. 90(4), 761-769.

Hall, I. M., Shankaranarayana, G. D., Noma, K., Ayoub, N., Cohen, A., and Grewal, S. I. 2002. Establishment and maintenance of a heterochromatin domain. *Science*. 297(5590), 2232-2237.

Hammet, A., Pike, B. L., Mitchelhill, K. I., The, T., Kobe, B., House, C. M., Kemp, B. E., Heierhorst, J. 2000. FHA domain boundaries of the dun1p and rad53p cell cycle checkpoint kinases. *FEBS Lett*. 471(2-3), 141-146.

Hanahan, D., and Weinberg, R. A. 2000. The hallmarks of cancer. *Cell*. 100(1), 57-70.

Hansen, J. C., Ausio, J., Stanik, V. H., and van Holde, K. E. 1989. Homogeneous reconstituted oligonucleosomes, evidence for salt-dependent folding in the absence of histone H1. *Biochemistry*. 28(23), 9129-9136.

Hansen, J. C. 2002. Conformational dynamics of the chromatin fiber in solution: determinants, mechanisms, and functions. *Annu Rev Biophys Biomol Struct*. 31, 361-392.

Harvey, K.F., Pflieger, C.M., and Hariharan, I.K. 2003. The *Drosophila* Mst ortholog, hippo, restricts growth and cell proliferation and promotes apoptosis. *Cell* 114, 457-467.

Hauf, S., Cole, R. W., LaTerra, S., Zimmer, C., Schnapp, G., Walter, R., Heckel, A., van Meel, J., Rieder, C. L., and Peters, J. M. 2003. The small molecule Hesperadin reveals a role for Aurora B in correcting kinetochore-microtubule attachment and in maintaining the spindle assembly checkpoint. *J Cell Biol*. 161(2), 281-294.

Hayashi, K., Hofstaetter, T., and Yakuwa, N. (1978). Asymmetry of chromatin subunits probed with histone H1 in an H1-DNA complex. *Biochemistry*. 17(10), 1880-1883.

Hayes, J. J., Tullius, T. D., and Wolffe AP. 1990. The structure of DNA in a nucleosome. *Proc Natl Acad Sci U S A*. 87(19), 7405-7409.



Hayes, J. J., Bashkin, J., Tullius, T. D., and Wolffe AP. 1991. The histone core exerts a dominant constraint on the structure of DNA in a nucleosome. *Biochemistry*. 30(34), 8434-8440.

Hayes, J. J., Clark, D. J., and Wolffe, A. P. 1991. Histone contributions to the structure of DNA in the nucleosome. *Proc Natl Acad Sci U S A*. 88(15), 6829-6833.

Hebbes, T. R., Clayton, A. L., Thorne, A. W., and Crane-Robinson, C. 1994. Core histone hyperacetylation co-maps with generalized DNase I sensitivity in the chicken beta-globin chromosomal domain. *EMBO J*. 13(8), 1823-1830.

Hebbes, T. R., Thorne, A. W., Clayton, A. L., and Crane-Robinson, C. 1992. Histone acetylation and globin gene switching. *Nucleic Acids Res*. 20(5), 1017-1022.

Hecht, A., Laroche, T., Strahl-Bolsinger, S., Gasser, S. M., and Grunstein, M. 1995. Histone H3 and H4 N-termini interact with SIR3 and SIR4 proteins: a molecular model for the formation of heterochromatin in yeast. *Cell*. 80(4), 583-592.

Henderson, K. A., and Keeney, S. 2004. Tying synaptonemal complex initiation to the formation and programmed repair of DNA double-strand breaks. *Proc Natl Acad Sci U S A*. 101(13), 4519-4524.

Hendzel, M. J., Wei, Y., Mancini, M. A., Van Hooser, A., Ranalli, T., Brinkley, B. R., Bazett-Jones, D. P., and Allis, C. D. 1997. Mitosis-specific phosphorylation of histone H3 initiates primarily within pericentromeric heterochromatin during G2 and spreads in an ordered fashion coincident with mitotic chromosome condensation. *Chromosoma*. 106(6), 348-360.

Hengartner, M. O. 2000. The biochemistry of apoptosis. *Nature*. 407(6805), 770-776.

Henikoff, S. 2004. Visualizing gene expression: an unfolding story. *Cell*. 116(5), 633-634.

Henikoff, S., Furuyama, T., and Ahmad, K. 2004. Histone variants, nucleosome assembly and epigenetic inheritance. *Trends Genet*. 20(7), 320-326.

Henry, K. W., Wyce, A., Lo, W. S., Duggan, L. J., Emre, N. C., Kao, C. F., Pillus, L., Shilatifard, A., Osley, M. A., and Berger, S. L. 2003. Transcriptional activation via sequential histone H2B ubiquitylation and deubiquitylation, mediated by SAGA-associated Ubp8. *Genes Dev.* 17(21), 2648-2663.

Higashiyama, H., Hirose, F., Yamaguchi, M., Inoue, Y. H., Fujikake, N., Matsukage, A., and Kakizuka, A. 2002. Identification of ter94, *Drosophila* VCP, as a modulator of polyglutamine-induced neurodegeneration. *Cell Death Differ.* 9(3), 264-273.

Hilfiker, A., Hilfiker-Kleiner, D., Pannuti, A., and Lucchesi, J. C. 1997. mof, a putative acetyl transferase gene related to the Tip60 and MOZ human genes and to the SAS genes of yeast, is required for dosage compensation in *Drosophila*. *EMBO J.* 16(8), 2054-2060.

Hirao, A., Cheung, A., Duncan, G., Girard, P. M., Elia, A. J., Wakeham, A., Okada, H., Sarkissian, T., Wong, J. A., Sakai, T., De Stanchina, E., Bristow, R. G., Suda, T., Lowe, S. W., Jeggo, P. A., Elledge, S. J., and Mak, T. W. 2002. Chk2 is a tumor suppressor that regulates apoptosis in both an ataxia telangiectasia mutated (ATM)-dependent and an ATM-independent manner. *Mol Cell Biol.* 22(18), 6521-6532.

Hirata, H., Takahashi, A., Kobayashi, S., Yonehara, S., Sawai, H., Okazaki, T., Yamamoto, K., and Sasada, M. 1998. Caspases are activated in a branched protease cascade and control distinct downstream processes in Fas-induced apoptosis. *J Exp Med.* 187(4), 587-600.

Ho, P. K., and Hawkins, C. J. 2005. Mammalian initiator apoptotic caspases. *FEBS J.* 272(21), 5436-5453.

Hofmann, K., and Bucher, P. 1995. The FHA domain: a putative nuclear signalling domain found in protein kinases and transcription factors. *Trends Biochem. Sci.* 20(9), 347-349.

Hofmann, K., Bucher, P., and Tschopp, J. 1997. The CARD domain: a new apoptotic signalling motif. *Trends Biochem Sci.* 22(5), 155-156.

Holbert, M. A., and Marmorstein, R. 2005. Structure and activity of enzymes that remove histone modifications. *Curr Opin Struct Biol.* 15(6), 673-680.

Hong, S. P., Leiper, F. C., Woods, A., Carling, D., and Carlson, M. 2003. Activation of yeast Snf1 and mammalian AMP-activated protein kinase by upstream kinases. *Proc Natl Acad Sci U S A.* 100(15), 8839-8843.

Horn, P. J., and Peterson, C. L. 2001. The bromodomain: a regulator of ATP-dependent chromatin remodeling? *Front Biosci.* 6, D1019-23.

Horn, P. J., Carruthers, L. M., Logie, C., Hill, D. A., Solomon, M. J., Wade, P. A., Imbalzano, A. N., Hansen, J. C., and Peterson, C. L. 2002. Phosphorylation of linker histones regulates ATP-dependent chromatin remodeling enzymes. *Nat Struct Biol.* 9(4), 263-267.

Horowitz, R. A., Agard, D. A., Sedat, J. W., and Woodcock, C. L. 1994. The three-dimensional architecture of chromatin in situ: electron tomography reveals fibers composed of a continuously variable zig-zag nucleosomal ribbon. *J Cell Biol.* 125(1), 1-10.

Horvath, J. E., Bailey, J. A., Locke, D. P., and Eichler, E. E. 2001. Lessons from the human genome: transitions between euchromatin and heterochromatin. *Hum Mol Genet.* 10(20), 2215-2223.

Houben, A., Demidov, D., Rutten, T., and Scheidtmann, K. H. 2005. Novel phosphorylation of histone H3 at threonine 11 that temporally correlates with condensation of mitotic and meiotic chromosomes in plant cells. *Cytogenet Genome Res.* 109(1-3), 148-155.

Hsu, J.Y., Sun, Z.W., Li, X., Reuben, M., Tatchell, K., Bishop, D.K., Grushcow, J.M., Brame, C.J., Caldwell, J.A., Hunt, D.F., Lin, R., Smith, M.M., and Allis, C.D. 2000. Mitotic phosphorylation of histone H3 is governed by Ipl1/aurora kinase and Glc7/PP1 phosphatase in budding yeast and nematodes. *Cell.* 102(3), 279-91.

Hu, Y., Yao, J., Liu, Z., Liu, X., Fu, H., and Ye, K. 2005. Akt phosphorylates acinus and inhibits its proteolytic cleavage, preventing chromatin condensation. *EMBO J.* 24(20), 3543-3554.

Hudson, B. P., Martinez-Yamout, M. A., Dyson, H. J., and Wright, P. E. 2000. Solution structure and acetyl-lysine binding activity of the GCN5 bromodomain. *J Mol Biol.* 304(3), 355-370.

Hughes, C. M., Rozenblatt-Rosen, O., Milne, T. A., Copeland, T. D., Levine, S. S., Lee, J. C., Hayes, D. N., Shanmugam, K. S., Bhattacharjee, A., Biondi, C. A., Kay, G. F., Hayward, N. K., Hess, J. L., and Meyerson, M. 2004. Menin associates with a trithorax family histone methyltransferase complex and with the *hoxc8* locus. *Mol Cell*. 13(4), 587-597.

Iizuka, M., and Smith, M. M. 2003. Functional consequences of histone modifications. *Curr Opin Genet Dev*. 13(2), 154-160.  
acetylation. *Curr Biol*. 8(12), R422-424.

Imai, S., Armstrong, C. M., Kaeberlein, M., and Guarente, L. 2000. Transcriptional silencing and longevity protein Sir2 is an NAD-dependent histone deacetylase. *Nature*. 403(6771), 795-800.

Ito, K., Barnes, P. J., and Adcock, I. M. 2000. Glucocorticoid receptor recruitment of histone deacetylase 2 inhibits interleukin-1 $\beta$ -induced histone H4 acetylation on lysines 8 and 12. *Mol Cell Biol*. 20(18), 6891-6903.

Jacobs, S. A., Taverna, S. D., Zhang, Y., Briggs, S. D., Li, J., Eissenberg, J. C., Allis, C. D., and Khorasanizadeh, S. 2001. Specificity of the HP1 chromo domain for the methylated N-terminus of histone H3. *EMBO J*. 20(18), 5232-5241.

Jacobs, S. A., and Khorasanizadeh, S. 2002. Structure of HP1 chromodomain bound to a lysine 9-methylated histone H3 tail. *Science*. 295(5562), 2080-2083.

Jacobson, R. H., Ladurner, A.G., King, D. S., and Tjian, R. 2000. Structure and function of a human TAFII250 double bromodomain module. *Science*. 288(5470), 1422-1425.

James, C., Gschmeissner, S., Fraser, A., and Evan, G. I. 1997. CED-4 induces chromatin condensation in *Schizosaccharomyces pombe* and is inhibited by direct physical association with CED-9. *Curr Biol*.;7(4), 246-252.

Jason, L. J., Moore, S. C., Ausio, J., and Lindsey, G. 2001. Magnesium-dependent association and folding of oligonucleosomes reconstituted with ubiquitinated H2A. *J Biol Chem*. 276(18), 14597-14601.

Jason, L. J., Moore, S. C., Lewis, J. D., Lindsey, G., and Ausio, J. 2002. Histone ubiquitination: a tagging tail unfolds? *Bioessays*. 24(2), 166-174.

- Jasencakova, Z., Meister, A., and Schubert, I. 2001. Chromatin organization and its relation to replication and histone acetylation during the cell cycle in barley. *Chromosoma*. 110(2), 83-92.
- Jeanmougin, F., Wurtz, J. M., Le Douarin, B., Chambon, P., and Losson, R. 1997. The bromodomain revisited. *Trends Biochem Sci*. 22(5), 151-153.
- Jenuwein, T., and Allis, C. D. 2001. Translating the histone code. *Science*. 293(5532), 1074-1080.
- Jeppesen, P., and Turner, B. M. 1993. The inactive X chromosome in female mammals is distinguished by a lack of histone H4 acetylation, a cytogenetic marker for gene expression. *Cell*. 74(2), 281-289.
- Jin, Y., Wang, Y., Walker, D. L., Dong, H., Conley, C., Johansen, J., Johansen, K. M. 1999. JIL-1: a novel chromosomal tandem kinase implicated in transcriptional regulation in *Drosophila*. *Mol Cell*. 4(1), 129-135.
- Jin, Y., Wang, Y., Johansen, J., and Johansen, K. M. 2000. JIL-1, a chromosomal kinase implicated in regulation of chromatin structure, associates with the male specific lethal (MSL) dosage compensation complex. *J Cell Biol*. 149(5), 1005-1010.
- Jin, Z., and El-Deiry, W. S. 2005. Overview of cell death signaling pathways. *Cancer Biol Ther*. 4(2), 139-163.
- Johns, E. W. (1967). The electrophoresis of histones in polyacrylamide gel and their quantitative determination. *Biochem J*. 104(1), 78-82.
- Johnson, C. N., Adkins, N. L., and Georgel, P. 2005. Chromatin remodeling complexes: ATP-dependent machines in action. *Biochem Cell Biol*. 83(4), 405-417.
- Johnson, L. M., Kayne, P. S., Kahn, E. S., and Grunstein, M. 1990. Genetic evidence for an interaction between SIR3 and histone H4 in the repression of the silent mating loci in *Saccharomyces cerevisiae*. *Proc Natl Acad Sci U S A*. 87(16), 6286-6290.
- Johnson, L. M., Fisher-Adams, G., and Grunstein, M. 1992. Identification of a non-basic domain in the histone H4 N-terminus required for repression of the yeast silent mating loci. *EMBO J*. 11(6), 2201-2209.

Jordan, J. D., Landau, E. M., and Iyengar, R. 2000. Signaling networks: the origins of cellular multitasking. *Cell*. 103(2), 193-200.

Kadosh, D., and Struhl, K. 1997. Repression by Ume6 involves recruitment of a complex containing Sin3 corepressor and Rpd3 histone deacetylase to target promoters. *Cell*. 89(3), 365-371.

Kadosh, D., and Struhl, K. 1998. Targeted recruitment of the Sin3-Rpd3 histone deacetylase complex generates a highly localized domain of repressed chromatin *in vivo*. *Mol Cell Biol*. 18(9), 5121-5127.

Kamada, Y., Jung, U. S., Piotrowski, J., Levin, D. E. 1995. The protein kinase C-activated MAP kinase pathway of *Saccharomyces cerevisiae* mediates a novel aspect of the heat shock response. *Genes Dev*. 9(13), 1559-1571.

Kamakaka, R. T., and Biggins, S. 2005. Histone variants: deviants? *Genes Dev*. 19(3), 295-310.

Kang, J. J., Schaber, M. D., Srinivasula, S. M., Alnemri, E. S., Litwack, G., Hall, D. J., and Bjornsti, M. A. 1999. Cascades of mammalian caspase activation in the yeast *Saccharomyces cerevisiae*. *J Biol Chem*. 274(5), 3189-3198.

Kasten, M. M., Dorland, S., and Stillman, D. J. 1997. A large protein complex containing the yeast Sin3p and Rpd3p transcriptional regulators. *Mol Cell Biol*. 17(8), 4852-4858.

Kasten, M., Szerlong, H., Erdjument-Bromage, H., Tempst, P., Werner, M., and Cairns, B. R. 2004. Tandem bromodomains in the chromatin remodeler RSC recognize acetylated histone H3 Lys14. *EMBO J*. 23(6), 1348-1359.

Kaszas, E., and Cande, W. Z. 2000. Phosphorylation of histone H3 is correlated with changes in the maintenance of sister chromatid cohesion during meiosis in maize, rather than the condensation of the chromatin. *J Cell Sci*. 113(18), 3217-3226.

Kaufmann, S. H. 1989. Induction of endonucleolytic DNA cleavage in human acute myelogenous leukemia cells by etoposide, camptothecin, and other cytotoxic anticancer drugs: a cautionary note. *Cancer Res*. 49(21), 5870-5878.

Kaufmann, S. H., and Hengartner, M. O. 2001. Programmed cell death: alive and well in the new millennium. *Trends Cell Biol.* 11(12), 526-534. □

Kayalar, C., Ord, T., Testa, M. P., Zhong, L. T., and Bredesen, D. E. 1996. Cleavage of actin by interleukin 1 beta-converting enzyme to reverse DNase I inhibition. *Proc Natl Acad Sci U S A.* 93(5), 2234-2238.

Keeney, S. 2001. Mechanism and control of meiotic recombination initiation. *Curr Top Dev Biol.* 52, 1-53.

Keogh, M. C., Kim, J. A., Downey, M., Fillingham, J., Chowdhury, D., Harrison, J. C., Onishi, M., Datta, N., Galicia, S., Emili, A., Lieberman, J., Shen, X., Buratowski, S., Haber, J. E., Durocher, D., Greenblatt, J. F., and Krogan, N. J. 2006. A phosphatase complex that dephosphorylates gammaH2AX regulates DNA damage checkpoint recovery. *Nature.* 439(7075), 497-501.

Kerr, J. F., Wyllie, A. H., and Currie, A. R. 1972. Apoptosis: a basic biological phenomenon with wide-ranging implications in tissue kinetics. *Br J Cancer.* 26(4), 239-257.

Kim, U. J., Han, M., Kayne, P., and Grunstein, M. 1988. Effects of histone H4 depletion on the cell cycle and transcription of *Saccharomyces cerevisiae*. *EMBO J.* 7(7), 2211-2219.

Kim, Y. J., Hwang, I., Tres, L. L., Kierszenbaum, A. L., and Chae, C. B. 1987. Molecular cloning and differential expression of somatic and testis-specific H2B histone genes during rat spermatogenesis. *Dev Biol.* 124(1), 23-34.

Kischkel, F. C., Hellbardt, S., Behrmann, I., Germer, M., Pawlita, M., Krammer, P. H., and Peter, M. E. 1995. Cytotoxicity-dependent APO-1 (Fas/CD95)-associated proteins form a death-inducing signaling complex (DISC) with the receptor. *EMBO J.* 14(22), 5579-5588.

Kitazono, A.A., Tobe, B.T., Kalton, H., Diamant, N., and Kron, S.J. 2002. Marker-fusion PCR for one-step mutagenesis of essential genes in yeast. *Yeast* 19, 141-149.

Kleckner, N., Zickler, D., Jones, G. H., Dekker, J., Padmore, R., Henle, J., and Hutchinson, J. 2004. A mechanical basis for chromosome function. *Proc Natl Acad Sci U S A.* 101, 12592-12597. □

Klug, A., Rhodes, D., Smith, J., Finch, J. T., and Thomas, J. O. 1980. A low resolution structure for the histone core of the nucleosome. *Nature*. 287(5782), 509-516.

Kobayashi, J., Tauchi, H., Sakamoto, S., Nakamura, A., Morishima, K., Matsuura, S., Kobayashi, T., Tamai, K., Tanimoto, K., and Komatsu, K. 2002. NBS1 localizes to gamma-H2AX foci through interaction with the FHA/BRCT domain. *Curr Biol*. 12(21), 1846-1851.

Komata, T., Kanzawa, T., Nashimoto, T., Aoki, H., Endo, S., Kon, T., Takahashi, H., Kondo, S., and Tanaka, R. 2005. Histone deacetylase inhibitors, N-butyric acid and trichostatin A, induce caspase-8- but not caspase-9-dependent apoptosis in human malignant glioma cells. *Int J Oncol*. 26(5), 1345-1352.

Kondo, T., Wakayama, T., Naiki, T., Matsumoto, K., and Sugimoto, K. 2001. Recruitment of Mec1 and Ddc1 checkpoint proteins to double-strand breaks through distinct mechanisms. *Science*. 294(5543), 867-870.

Kondo, Y., Shen, L., and Issa, J. P. 2003. Critical role of histone methylation in tumor suppressor gene silencing in colorectal cancer. *Mol Cell Biol*. 23(1), 206-215.

Koopman, G., Reutelingsperger, C. P., Kuijten, G. A., Keehnen, R. M., Pals, S. T., and van Oers, M. H. 1994. Annexin V for flow cytometric detection of phosphatidylserine expression on B cells undergoing apoptosis. *Blood*. 84(5), 1415-1420.

Kornberg, R. D. (1974). Chromatin structure: a repeating unit of histones and DNA. *Science*. 184(139), 868-871.

Kornberg, R. D. and Lorch, Y. 1999. Twenty-five years of the nucleosome, fundamental particle of the eukaryote chromosome. *Cell*. 98, 285-294

Kossel, A. Ueber einen peptoartigen bestandheil des zellkerns. 1884. *Z Physiol Chem* 8, 511-515.

Kothakota, S., Azuma, T., Reinhard, C., Klippel, A., Tang, J., Chu, K., McGarry, T. J., Kirschner, M. W., Koths, K., Kwiatkowski, D. J., and Williams, L. T. 1997. Caspase-3-generated fragment of gelsolin: effector of morphological change in apoptosis. *Science*. 278(5336), 294-298.



Krajewski, W. A., and Ausio, J. 1996. Modulation of the higher-order folding of chromatin by deletion of histone H3 and H4 terminal domains. *Biochem J.* 316(2), 395-400.

Kroemer, G., and Martin, S. J. 2005. Caspase-independent cell death. *Nat Med.* 11(7), 725-730.

Kuo, M. H., Brownell, J. E., Sobel, R. E., Ranalli, T. A., Cook, R. G., Edmondson, D. G., Roth, S. Y., and Allis, C. D. 1996. Transcription-linked acetylation by Gcn5p of histones H3 and H4 at specific lysines. *Nature.* 383(6597), 269-272.

Kuo, M. H., Zhou, J., Jambeck, P., Churchill, M. E., and Allis, C. D. 1998. Histone acetyltransferase activity of yeast Gcn5p is required for the activation of target genes in vivo. *Genes Dev.* 12(5), 627-639.

Kurdistani, S. K., Robyr, D. , Tavazoie, S., and Grunstein, M. 2002. Genome-wide binding map of the histone deacetylase Rpd3 in yeast. *Nat Genet.* 31(3), 248-254.

Kurdistani, S. K., and Grunstein, M. 2003. Histone acetylation and deacetylation in yeast. *Nat Rev Mol Cell Biol.* 4(4), 276-284.

Kuzmichev, A., Nishioka, K., Erdjument-Bromage, H., Tempst, P., and Reinberg, D. 2002. Histone methyltransferase activity associated with a human multiprotein complex containing the Enhancer of Zeste protein. *Genes Dev.* 16(22), 2893-2905.

Lachner, M., O'Carroll, D., Rea, S., Mechtler, K., and Jenuwein, T. 2001. Methylation of histone H3 lysine 9 creates a binding site for HP1 proteins. *Nature.* 410(6824), 116-120.

Lachner, M., and Jenuwein, T. 2002. The many faces of histone lysine methylation. *Curr Opin Cell Biol.* 14(3), 286-298.

Lamond, A. I., and Earnshaw, W. C. 1998. Structure and function in the nucleus. *Science.* 280(5363), 547-553.

Latterich, M., Frohlich, K. U., and Schekman, R. 1995. Membrane fusion and the cell cycle: Cdc48p participates in the fusion of ER membranes. *Cell.* 82(6), 885-893.

Launay, S., Hermine, O., Fontenay, M., Kroemer, G., Solary, E., and Garrido, C. 2005. Vital functions for lethal caspases. *Oncogene* 2005, 24(33), 5137–5148.

Lavoie, B. D., Hogan, E., and Koshland, D. *In vivo* dissection of the chromosome condensation machinery: reversibility of condensation distinguishes contributions of condensin and cohesin. *J Cell Biol.* 156(5), 805-815.

Lazebnik, Y. A., Kaufmann, S. H., Desnoyers, S., Poirier, G. G., and Earnshaw, W. C. 1994. Cleavage of poly(ADP-ribose) polymerase by a proteinase with properties like ICE. *Nature.* 371(6495), 346-347.

Lazebnik, Y. A., Takahashi, A., Moir, R. D., Goldman, R. D., Poirier, G. G., Kaufmann, S. H., and Earnshaw, W. C. 1995. Studies of the lamin proteinase reveal multiple parallel biochemical pathways during apoptotic execution. *Proc Natl Acad Sci U S A.* 92(20), 9042-9046.

Leberer, E., Wu, C., Leeuw, T., Fourest-Lieuvin, A., Segall, J.E., and Thomas, D.Y. 1997. Functional characterization of the Cdc42p binding domain of yeast Ste20p protein kinase. *EMBO. J.* 16, 83-97.

Lee, K.K., Ohyama, T., Yajima, N., Tsubuki, S., and Yonehara, S. 2001. MST, a physiological caspase substrate, highly sensitizes apoptosis both upstream and downstream of caspase activation. *J. Biol. Chem.* 276, 19276-19285.

Lee, K. M., and Hayes, J. J. 1997. The N-terminal tail of histone H2A binds to two distinct sites within the nucleosome core. *Proc Natl Acad Sci U S A.* 94(17), 8959-8964.

Lee, M. G., Wynder, C., Cooch, N., and Shiekhata, R. 2005. An essential role for CoREST in nucleosomal histone 3 lysine 4 demethylation. *Nature.* 437(7057), 432–435.

Lee, N., MacDonald, H., Reinhard, C., Halenbeck, R., Roulston, A., Shi, T., and Williams, L. T. 1997. Activation of hPAK65 by caspase cleavage induces some of the morphological and biochemical changes of apoptosis. *Proc Natl Acad Sci U S A.* 94(25), 13642-13647.

Lee, S. J., Duong, J. K., and Stern, D. F. 2004. A Ddc2-Rad53 fusion protein can bypass the requirements for RAD9 and MRC1 in Rad53 activation. *Mol Biol Cell.* 15(12), 5443-5455.

Leist, M., and Jaattela, M. 2001. Triggering of apoptosis by cathepsins. *Cell Death Differ.* 8(4), 324-326.

Lever, M. A., Th'ng, J. P., Sun, X., and Hendzel, M. J. 2000. Rapid exchange of histone H1.1 on chromatin in living human cells. *Nature.* 408(6814), 873-876.

Levine, A., Belenghi, B., Damari-Weisler, H., Granot, D. 2001. Vesicle-associated membrane protein of Arabidopsis suppresses Bax-induced apoptosis in yeast downstream of oxidative burst. *J Biol Chem.* 276(49), 46284-46289.

Levkau, B., Herren, B., Koyama, H., Ross, R., and Raines, E. W. 1998. Caspase-mediated cleavage of focal adhesion kinase pp125FAK and disassembly of focal adhesions in human endothelial cell apoptosis. *J Exp Med.* 187(4), 579-586.

Li, J., Smith, G. P., and Walker, J. C. 1999. Kinase interaction domain of kinase-associated protein phosphatase, a phosphoprotein-binding domain. *Proc. Natl. Acad. Sci. USA* 96(14), 7821-7826.

Li, P., Nijhawan, D., Budihardjo, I., Srinivasula, S. M., Ahmad, M., Alnemri, E. S., and Wang, X. 1997. Cytochrome c and dATP-dependent formation of Apaf-1/caspase-9 complex initiates an apoptotic protease cascade. *Cell.* 91(4), 479-489.

Liao, H., Byeon, I. J., and Tsai, M. D. 1999. Structure and function of a new phosphopeptide-binding domain containing the FHA2 of Rad53. *J Mol Biol.* 294(4), 1041-1049.

Liao, H., Yuan, C., Su, M. I., Yongkiettrakul, S., Qin, D., Li, H., Byeon, I. J., Pei, D., and Tsai, M. D. 2000. Structure of the FHA1 domain of yeast Rad53 and identification of binding sites for both FHA1 and its target protein Rad9. *J Mol Biol.* 304(5), 941-951.

Ligr, M., Madeo, F., Frohlich, E., Hilt, W., Frohlich, K. U., and Wolf, D. H. 1998. Mammalian Bax triggers apoptotic changes in yeast. *FEBS Lett.* 438(1-2), 61-65.

Lim, J. H., Catez, F., Birger, Y., West, K. L., Prymakowska-Bosak, M., Postnikov, Y. V., and Bustin, M. 2004. Chromosomal protein HMGN1 modulates histone H3 phosphorylation. *Mol Cell.* 15(4), 573-584.

Lim, J., and Ping Lu, K. 2005. Pinning down phosphorylated tau and tauopathies. *Biochim Biophys Acta*. 1739, 311-22.

Lin, R., Cook, R. G., and Allis, C. D. 1991. Proteolytic removal of core histone amino termini and dephosphorylation of histone H1 correlate with the formation of condensed chromatin and transcriptional silencing during *Tetrahymena* macronuclear development. *Genes Dev*. 5(9), 1601-1610.

Lindroth, A. M., Shultis, D., Jasencakova, Z., Fuchs, J., Johnson, L., Schubert, D., Patnaik, D., Pradhan, S., Goodrich, J., Schubert, I., Jenuwein, T., Khorasanizadeh, S., and Jacobsen, S. E. 2004. Dual histone H3 methylation marks at lysines 9 and 27 required for interaction with CHROMOMETHYLASE3. *EMBO J*. 23(21), 4286-4296.

Ling, X., Harkness, T. A., Schultz, M. C., Fisher-Adams, G., and Grunstein, M. 1996. Yeast histone H3 and H4 amino termini are important for nucleosome assembly *in vivo* and *in vitro*: redundant and position-independent functions in assembly but not in gene regulation. *Genes Dev*. 10(6), 686-699.

Litt, M. D., Simpson, M., Gaszner, M., Allis, C. D., and Felsenfeld, G. 2001. Correlation between histone lysine methylation and developmental changes at the chicken beta-globin locus. *Science*. 293(5539), 2453-2455.

Liu, H. , Styles, C. A., and Fink, G. R. 1993. Elements of the yeast pheromone response pathway required for filamentous growth of diploids. *Science*. 262(5140), 1741-1744.

Liu, X., Zou, H., Slaughter, C., and Wang, X. 1997. DFF, a heterodimeric protein that functions downstream of caspase-3 to trigger DNA fragmentation during apoptosis. *Cell*. 89(2), 175-184.

Lo, W. S., Trievel, R. C., Rojas, J. R., Duggan, L., Hsu, J. Y., Allis, C.D., Marmorstein, R., and Berger, S. L. 2000. Phosphorylation of serine 10 in histone H3 is functionally linked *in vitro* and *in vivo* to Gcn5-mediated acetylation at lysine 14. *Mol Cell*. 5(6), 917-926.

Lo, W. S., Duggan, L., Emre, N. C., Belotserkovskya, R., Lane, W. S., Shiekhhattar, R., and Berger, S. L. 2001. Snf1--a histone kinase that works in concert with the histone acetyltransferase Gcn5 to regulate transcription. *Science*. 293(5532), 1142-1146.

Lo, W. S., Gamache, E. R., Henry, K. W., Yang, D., Pillus, L., and Berger, S. L. 2005. Histone H3 phosphorylation can promote TBP recruitment through distinct promoter-specific mechanisms. *EMBO J.* 24(5), 997-1008.

Longtine, M.S., McKenzie, A., 3rd, Demarini, D.J., Shah, N.G., Wach, A., Brachat, A., Philippsen, P., and Pringle, J.R. 1998. Additional modules for versatile and economical PCR-based gene deletion and modification in *Saccharomyces cerevisiae*. *Yeast* 14, 953-961.

Lowary, P. T., and Widom, J. 1998. New DNA sequence rules for high affinity binding to histone octamer and sequence-directed nucleosome positioning. *J Mol Biol.* 276(1), 19-42.

Ludovico, P., Sousa, M. J., Silva, M. T., Leao, C., and Corte-Real, M. 2001. *Saccharomyces cerevisiae* commits to a programmed cell death process in response to acetic acid. *Microbiology.* 147(Pt 9), 2409-2415.

Luger, K., Mader, A. W., Richmond, R. K., Sargent, D. F., and Richmond, T. J. 1997. Crystal structure of the nucleosome core particle at 2.8 Å resolution. *Nature.* 389(6648), 251-260.

Luger, K., and Richmond, T. J. 1998. DNA binding within the nucleosome core. *Curr Opin Struct Biol.* 8(1), 33-40.

Luger, K., and Richmond, T. J. 1998. The histone tails of the nucleosome. *Curr Opin Genet Dev.* 8(2), 140-146.

Luger, K. 2003. Structure and dynamic behavior of nucleosomes. *Curr Opin Genet Dev.* 13(2), 127-135.

Luo, R. X., and Dean, D. C. 1999. Chromatin remodeling and transcriptional regulation. *J Natl Cancer Inst.* 91(15), 1288-1294.

Macdonald, N., Welburn, J. P., Noble, M. E., Nguyen, A., Yaffe, M. B., Clynes, D., Moggs, J. G., Orphanides, G., Thomson, S., Edmunds, J. W., Clayton, A. L., Endicott, J. A., and Mahadevan, L. C. 2005. Molecular Basis for the Recognition of Phosphorylated and Phosphoacetylated Histone H3 by 14-3-3. *Molecular Cell.* 20(2), 199-211. □

Madeo, F., Frohlich, E., and Frohlich, K. U. 1997. A yeast mutant showing diagnostic markers of early and late apoptosis. *J Cell Biol.* 139(3), 729-734.

Madeo, F., Frohlich, E., Ligr, M., Grey, M., Sigrist, S. J., Wolf, D. H., and Frohlich, K. U. 1999. Oxygen stress: a regulator of apoptosis in yeast. *J Cell Biol.* 145(4), 757-767.

Madeo, F., Engelhardt, S., Herker, E., Lehmann, N., Maldener, C., Proksch, A., Wissing, S., and Frohlich, K. U. (2002a). Apoptosis in yeast: a new model system with applications in cell biology and medicine. *Curr Genet.* 41(4), 208-216.

Madeo, F., Herker, E., Maldener, C., Wissing, S., Lachelt, S., Herlan, M., Fehr, M., Lauber, K., Sigrist, S. J., Wesselborg, S., and Frohlich, K. U. (2002b). A caspase-related protease regulates apoptosis in yeast. *Mol Cell.* 9(4), 911-917.

Mahadevaiah, S. K., Turner, J. M., Baudat, F., Rogakou, E. P., de Boer, P., Blanco-Rodriguez, J., Jasin, M., Keeney, S., Bonner, W. M., and Burgoyne, P. S. 2001. Recombinational DNA double-strand breaks in mice precede synapsis. *Nat Genet.* 27(3), 271-276.

Mahadevan, L. C., Willis, A. C., and Barratt, M. J. 1991. Rapid histone H3 phosphorylation in response to growth factors, phorbol esters, okadaic acid, and protein synthesis inhibitors. *Cell.* 65(5), 775-783.

Martin, C., and Zhang, Y. 2005. The diverse functions of histone lysine methylation. *Nat Rev Mol Cell Biol.* 6(11), 838-849.

Martin, G. A., Bollag, G., McCormick, F., and Abo, A. (1995) A novel serine kinase activated by rac1/CDC42Hs-dependent autophosphorylation is related to PAK65 and STE20. *EMBO J.* 14(9), 1970-1978.

Martin, S. J., Newmeyer, D. D., Mathias, S., Farschon, D. M., Wang, H. G., Reed, J. C., Kolesnick, R. N., and Green, D. R. 1995. Cell-free reconstitution of Fas-, UV radiation- and ceramide-induced apoptosis. *EMBO J.* 14(21), 5191-5200.

Marushige, Y., and Marushige, K. 1995. Disappearance of ubiquitinated histone H2A during chromatin condensation in TGF beta 1-induced apoptosis. *Anticancer Res.* 15(2), 267-272.

Marvin, K. W., Yau, P., and Bradbury, E. M. 1990. Isolation and characterization of acetylated histones H3 and H4 and their assembly into nucleosomes. *J Biol Chem.* 265(32), 19839-19847.

Mashima, T., Naito, M., Fujita, N., Noguchi, K., and Tsuruo, T. 1995. Identification of actin as a substrate of ICE and an ICE-like protease and involvement of an ICE-like protease but not ICE in VP-16-induced U937 apoptosis. *Biochem Biophys Res Commun.* 217(3), 1185-1192

Matsuoka, S., Huang, M., and Elledge, S. J. 1998. Linkage of ATM to cell cycle regulation by the Chk2 protein kinase. *Science.* 282(5395), 1893-1897.

Matsuura, S., Tauchi, H., Nakamura, A., Kondo, N., Sakamoto, S., Endo, S., Smeets, D., Solder, B., Belohradsky, B. H., Der Kaloustian, V. M., Oshimura, M., Isomura, M., Nakamura, Y., Komatsu, K. 1998. Positional cloning of the gene for Nijmegen breakage syndrome. *Nat. Genet.* 19(2), 179-181.

McBride, A. E., and Silver, P. A. 2001. State of the arg: protein methylation at arginine comes of age, *Cell.* 106(1), 5-8.

Medina, V., Edmonds, B., Young, G. P., James, R., Appleton, S., Zalewski, P. D. 1997. Induction of caspase-3 protease activity and apoptosis by butyrate and trichostatin A (inhibitors of histone deacetylase): dependence on protein synthesis and synergy with a mitochondrial / cytochrome c-dependent pathway. : *Cancer Res.* 57(17), 3697-3707.

Megee, P. C., Morgan, B. A., Mittman, B. A., and Smith, M. M. 1990. Genetic analysis of histone H4: essential role of lysines subject to reversible acetylation. *Science.* 247(4944), 841-845.

Megee, P. C., Morgan, B. A., and Smith, M. M. 1995. Histone H4 and the maintenance of genome integrity. *Genes Dev.* 9(14), 1716-1727.

Meistrich, M. L., Bucci, L. R., Trostle-Weige, P. K., and Brock, W. A. (1985). Histone variants in rat spermatogonia and primary spermatocytes. *Dev Biol.* 112(1), 230-240.

Mello, J. A., and Almouzni, G. 2001. The ins and outs of nucleosome assembly. *Curr Opin Genet Dev.* 11(2), 136-141.

Metzger, E., Wissmann, M., Yin, N., Muller, J. M., Schneider, R., Peters, A. H., Gunther, T., Buettner, R., and Schule, R. 2005. LSD1 demethylates repressive histone marks to promote androgen-receptor-dependent transcription. *Nature*. 437(7057), 436-439.

Miller, T., Krogan, N. J., Dover, J., Erdjument-Bromage, H., Tempst, P., Johnston, M., Greenblatt, J. F., and Shilatifard, A. 2001. COMPASS: a complex of proteins associated with a trithorax-related SET domain protein. *Proc Natl Acad Sci U S A*. 98(23), 12902-12907.

Mills, K., Daish, T., Harvey, K. F., Pfleger, C. M., Hariharan, I. K., and Kumar, S. 2006. The *Drosophila melanogaster* Apaf-1 homologue ARK is required for most, but not all, programmed cell death. *J Cell Biol*. 172(6), 809-815.

Milne, T. A., Briggs, S. D., Brock, H. W., Martin, M. E., Gibbs, D., Allis, C. D., and Hess, J. L. 2002. MLL targets SET domain methyltransferase activity to Hox gene promoters. *Mol Cell*. 10(5), 1107-1117.

Mimnaugh, E. G., Chen, H. Y., Davie, J. R., Celis, J. E., and Neckers, L. 1997. Rapid deubiquitination of nucleosomal histones in human tumor cells caused by proteasome inhibitors and stress response inducers: effects on replication, transcription, translation, and the cellular stress response. *Biochemistry*. 36(47), 14418-14429.

Mimnaugh, E. G., Kayastha, G., McGovern, N. B., Hwang, S. G., Marcu, M. G., Trepel, J., Cai, S. Y., Marchesi, V. T., and Neckers, L. 2001. Caspase-dependent deubiquitination of monoubiquitinated nucleosomal histone H2A induced by diverse apoptogenic stimuli. *Cell Death Differ*. 8(12), 1182-1196.

Mizzen, C. A., Yang, X. J., Kokubo, T., Brownell, J. E., Bannister, A. J., Owen-Hughes, T., Workman, J., Wang, L., Berger, S. L., Kouzarides, T., Nakatani, Y., and Allis, C. D. 1996. The TAF(II)250 subunit of TFIID has histone acetyltransferase activity. *Cell* 87(7), 1261-1270.

Modrich P. 1997. Strand-specific mismatch repair in mammalian cells. *J Biol Chem*. 272(40), 24727-24730.

Moir, R. D., and Goldman, R. D. 1993. Lamin dynamics. *Curr Opin Cell Biol*. 5(3), 408-411.



Moore, S. C., and Ausio, J. 1997. Major role of the histones H3-H4 in the folding of the chromatin fiber. *Biochem Biophys Res Commun.* 230(1), 136-139.

Morillon, A., Karabetsou, N., O'Sullivan, J., Kent, N., Proudfoot, N., and Mellor, J. 2003. Isw1 chromatin remodeling ATPase coordinates transcription elongation and termination by RNA polymerase II. *Cell.* 115(4), 425-435.

Murnion, M. E., Adams, R. R., Callister, D. M., Allis, C. D., Earnshaw, W. C., and Swedlow, J. R. 2001. Chromatin-associated protein phosphatase 1 regulates aurora-B and histone H3 phosphorylation. *J Biol Chem.* 276(28), 26656-26665.

Murray, K. 1964. The occurrence of epsilon-N-methyl lysine in histones. *Biochemistry.* 3, 10-15.

Nakashima, K., Hagiwara, T., and Yamada, M. 2002. Nuclear localization of peptidylarginine deiminase V and histone deimination in granulocytes. *J Biol Chem.* 277(51), 49562-49568.

Nakamura, T., Mori, T., Tada, S., Krajewski, W., Rozovskaia, T., Wassell, R., Dubois, G., Mazo, A., Croce, C. M., and Canaani, E. 2002. ALL-1 is a histone methyltransferase that assembles a supercomplex of proteins involved in transcriptional regulation. *Mol Cell.* 10(5), 1119-1128.

Nakamura, T. M., Du, L. L., Redon, C., and Russell, P. 2004. Histone H2A phosphorylation controls Crb2 recruitment at DNA breaks, maintains checkpoint arrest, and influences DNA repair in fission yeast. *Mol Cell Biol.* 24(14), 6215-6230.

Nakayama, J., Rice, J. C., Strahl, B. D., Allis, C. D., and Grewal, S. I. 2001. Role of histone H3 lysine 9 methylation in epigenetic control of heterochromatin assembly. *Science.* 292(5514), 110-113.

Nagy, P. L., Griesenbeck, J., Kornberg, R. D., and Cleary, M. L. 2002. A trithorax-group complex purified from *Saccharomyces cerevisiae* is required for methylation of histone H3. *Proc Natl Acad Sci U S A.* 99(1), 90-94.

Neamati, N., Fernandez, A., Wright, S., Kiefer, J., and McConkey, D. J. 1995. Degradation of lamin B1 precedes oligonucleosomal DNA fragmentation in apoptotic thymocytes and isolated thymocyte nuclei. *J Immunol.* 154(8), 3788-3795.

Newmeyer, D. D., and Ferguson-Miller, S. 2003. Mitochondria: releasing power for life and unleashing the machineries of death. *Cell*. 112(4), 481-490.

Ng, H. H., Xu, R. M., Zhang, Y., and Struhl, K. 2002. Ubiquitination of histone H2B by Rad6 is required for efficient Dot1-mediated methylation of histone H3 lysine 79. *J Biol Chem*. 277(38), 34655-34657.

Ng, H. H., Robert, F., Young, R. A., and Struhl, K. 2003. Targeted recruitment of Set1 histone methylase by elongating Pol II provides a localized mark and memory of recent transcriptional activity. *Mol Cell*. 11(3), 709-719.

Nielsen, P. R., Nietlispach, D., Mott, H. R., Callaghan, J., Bannister, A., Kouzarides, T., Murzin, A. G., Murzina, N. V., and Laue, E. D. 2002. Structure of the HP1 chromodomain bound to histone H3 methylated at lysine 9. *Nature*. 416(6876), 103-107.

Nonaka, N., Kitajima, T., Yokobayashi, S., Xiao, G., Yamamoto, M., Grewal, S. I., Watanabe, Y. 2002. Recruitment of cohesin to heterochromatic regions by Swi6/HP1 in fission yeast. *Nat Cell Biol*. 4(1), 89-93.□

Nowak, S. J., and Corces, V. G. 2000. Phosphorylation of histone H3 correlates with transcriptionally active loci. *Genes Dev*. 14(23), 3003-3013.

Nowak, S. J., Pai, C. Y., and Corces, V. G. 2003. Protein phosphatase 2A activity affects histone H3 phosphorylation and transcription in *Drosophila melanogaster*. *Mol Cell Biol*. 23(17), 6129-6138.

Nowak, S. J., and Corces, V. G. 2004. Phosphorylation of histone H3: a balancing act between chromosome condensation and transcriptional activation. *Trends Genet*. 20(4), 214-220.

Ogawa, K., Yasumura, S., Atarashi, Y., Minemura, M., Miyazaki, T., Iwamoto, M., Higuchi, K., and Watanabe, A. 2004. Sodium butyrate enhances Fas-mediated apoptosis of human hepatoma cells. *J Hepatol*. 40(2), 278-284.

Ohkura, H., Kinoshita, N., Miyatani, S., Toda, T., and Yanagida, M. 1989. The fission yeast *dis2+* gene required for chromosome disjoining encodes one of two putative type 1 protein phosphatases. *Cell*. 57(6), 997-1007.

Ohsumi, K., Katagiri, C., and Kishimoto, T. 1993. Chromosome condensation in *Xenopus* mitotic extracts without histone H1. *Science*. 262(5142), 2033-2035.

Old, R.W., and Woodland, H.R. 1984. . Histone genes: Not so simple after all. *Cell* 38(3), 624-626.

Olins, D. E., and Olins, A. L. (1972). Physical studies of isolated eucaryotic nuclei. *J Cell Biol*. 53(3), 715-736.

O'Rourke, S. M., and Herskowitz, I. 1998. The Hog1 MAPK prevents cross talk between the HOG and pheromone response MAPK pathways in *Saccharomyces cerevisiae*. *Genes Dev*. 12(18), 2874-2886. □

Orth, K., Chinnaiyan, A. M., Garg, M., Froelich, C. J., and Dixit, V. M. 1996. The CED-3/ICE-like protease Mch2 is activated during apoptosis and cleaves the death substrate lamin A. *J Biol Chem*. 271(28), 16443-16446.

Osborne, B.A. 1996. Cell death in vertebrates: lessons from the worm. *Trends Genet*. 12(12), 489-491.

Owen, D. J., Ornaghi, P., Yang, J. C., Lowe, N., Evans, P. R., Ballario, P., Neuhaus, D., Filetici, P., and Travers, A. A. 2000. The structural basis for the recognition of acetylated histone H4 by the bromodomain of histone acetyltransferase gcn5p. *EMBO J*. 19(22), 6141-6149.

Owen-Hughes, T., Utey, R. T., Cote, J., Peterson, C. L., and Workman, J. L. 1996. Persistent site-specific remodeling of a nucleosome array by transient action of the SWI/SNF complex. *Science*. 273(5274), 513-516.

Paciotti, V., Clerici, M., Lucchini, G., and Longhese, M. P. 2000. The checkpoint protein Ddc2, functionally related to *S. pombe* Rad26, interacts with Mec1 and is regulated by Mec1-dependent phosphorylation in budding yeast. *Genes Dev*. 14(16), 2046-2059.

Palmer, D. K., O'Day, K., Trong, H. L., Charbonneau, H., and Margolis, R. L. 1991. Purification of the centromere-specific protein CENP-A and demonstration that it is a distinctive histone. *Proc Natl Acad Sci U S A*. 88(9), 3734-3738.

Pardue, M. L., and Hennig, W. 1990. Heterochromatin: junk or collectors item? *Chromosoma*. 100(1), 3-7.

Paro, R., and Hogness, D. S. 1991. The Polycomb protein shares a homologous domain with a heterochromatin-associated protein of *Drosophila*. *Proc Natl Acad Sci U S A*. 88(1), 263-267.

Paull, T. T., Rogakou, E. P., Yamazaki, V., Kirchgessner, C. U., Gellert, M., and Bonner, W. M. 2000. A critical role for histone H2AX in recruitment of repair factors to nuclear foci after DNA damage. *Curr Biol*. 10(15), 886-895.

Paulson, J. R., and Taylor, S. S. 1982. Phosphorylation of histones 1 and 3 and nonhistone high mobility group 14 by an endogenous kinase in HeLa metaphase chromosomes. *J Biol Chem*. 257(11), 6064-6072.

Pawson, T., and Nash, P. 2000. Protein-protein interactions define specificity in signal transduction. *Genes Dev*. 14(9), 1027-1047.

Peter, M., Neiman, A. M., Park, H. O., van Lohuizen, M., and Herskowitz, I. 1996. Functional analysis of the interaction between the small GTP binding protein Cdc42 and the Ste20 protein kinase in yeast. *EMBO J*. 15(24), 7046-7059.

Peters, A. H., Mermoud, J. E., O'Carroll, D., Pagani, M., Schweizer, D., Brockdorff, N., and Jenuwein, T. 2002. Histone H3 lysine 9 methylation is an epigenetic imprint of facultative heterochromatin. *Nat Genet*. 30(1), 77-80.

Peters, A. H., Kubicek, S., Mechtler, K., O'Sullivan, R. J., Derijck, A. A., Perez-Burgos, L., Kohlmaier, A., Opravil, S., Tachibana, M., Shinkai, Y., Martens, J. H., and Jenuwein, T. 2003. Partitioning and plasticity of repressive histone methylation states in mammalian chromatin. *Mol Cell*. 12(6), 1577-1589.

Peter, H., and Krammer, I. 2000. CD95's deadly mission in the immune system. *Nature* 407, 789-795.

Peter, M. E., Scaffidi, C., Medema, J. P., Kischkel, F. C., and Krammer, P. H. In *Apoptosis, Problems and Diseases* (ed. Kumar, S.) 25-63 (Springer, Heidelberg, 1998).

Peterson, C. L., and Laniel, M. A. 2004. Histones and histone modifications. *Curr Biol.* 14(14), R546-R551.

Petersen, J., Paris, J., Willer, M., Philippe, M., and Hagan, I. M. 2001. The *S. pombe* aurora-related kinase Ark1 associates with mitotic structures in a stage dependent manner and is required for chromosome segregation. *J Cell Sci.* 114(Pt 24), 4371-4384.

Pike, B. L., Yongkiettrakul, S., Tsai, M. D., and Heierhorst, J. 2003. Diverse but overlapping functions of the two forkhead-associated (FHA) domains in Rad53 checkpoint kinase activation. *J Biol Chem.* 278(33), 30421-30424.

Pilch, D. R., Sedelnikova, O. A., Redon, C., Celeste, A., Nussenzweig, A., and Bonner, W. M. 2003. Characteristics of gamma-H2AX foci at DNA double-strand breaks sites. *Biochem Cell Biol.* 81(3), 123-129.

Poccia, D. L., and Green, G. R. 1992. Packaging and unpackaging the sea urchin sperm genome. *Trends Biochem Sci.* 17(6), 223-227.

Polioudaki, H., Markaki, Y., Kourmouli, N., Dialynas, G., Theodoropoulos, P. A., Singh, P. B., and Georgatos, S. D. 2004. Mitotic phosphorylation of histone H3 at threonine 3. *FEBS Lett.* 560(1-3), 39-44.

Pray-Grant, M. G., Daniel, J. A., Schieltz, D., Yates, J. R. 3rd, and Grant, P. A. 2005. Chd1 chromodomain links histone H3 methylation with SAGA- and SLIK-dependent acetylation. *Nature.* 433(7024), 434-438.

Preuss, U., Landsberg, G., and Scheidtmann, K. H. 2003. Novel mitosis-specific phosphorylation of histone H3 at Thr11 mediated by Dlk/ZIP kinase. *Nucleic Acids Res.* 31(3), 878-885.

Prior, C. P., Cantor, C. R., Johnson, E. M., Littau, V. C., and Allfrey, V. G. 1983. Reversible changes in nucleosome structure and histone H3 accessibility in transcriptionally active and inactive states of rDNA chromatin. *Cell.* 34(3), 1033-1042.

Prunell, A. 1982. Nucleosome reconstitution on plasmid-inserted poly(dA) . poly(dT). *EMBO J.* 1(2), 173-179.

Qiu, L., Burgess, A., Fairlie, D. P., Leonard, H., Parsons, P. G., Gabrielli, B. G. 2000. Histone deacetylase inhibitors trigger a G2 checkpoint in normal cells that is defective in tumor cells. *Mol Biol Cell*. 11(6), 2069-2083.□  
McGowan, C. H. 2002. CHK2: a tumor suppressor or not? *Cell Cycle*. 1(6), 401-403..

Ramakrishnan, V., Finch, J. T., Graziano, V., Lee, P. L., and Sweet, R. M. 1993. Crystal structure of globular domain of histone H5 and its implications for nucleosome binding. *Nature*. 362(6417), 219-223.

Ramakrishnan, V. 1997. Histone H1 and chromatin higher-order structure. *Crit Rev Eukaryot Gene Expr*. 7(3), 215-230.

Rao, B. J, and Rao, M. R. 1987. DNase I site mapping and micrococcal nuclease digestion of pachytene chromatin reveal novel structural features. *J Biol Chem*. 262(10), 4472-4476.

Rao, L., Perez, D., and White, E. 1996. Lamin proteolysis facilitates nuclear events during apoptosis. *J Cell Biol*. 135(6 Pt 1), 1441-1455.

Rea, S., Eisenhaber, F., O'Carroll, D., Strahl, B. D., Sun, Z. W., Schmid, M., Opravil, S., Mechtler, K., Ponting, C. P., Allis, C. D., and Jenuwein, T. 2000. Regulation of chromatin structure by site-specific histone H3 methyltransferases. *Nature*. 406(6796), 593-599.

Rechsteiner, M. 1988. Ubiquitin. New York, Plenum Press.

Redon, C., Pilch, D., Rogakou, E., Sedelnikova, O., Newrock, K., and Bonner, W. 2002. Histone H2A variants H2AX and H2AZ. *Curr. Opin. Genet. Dev*. 12(2), 162-169.

Redon, C., Pilch, D. R., Rogakou, E. P., Orr, A. H., Lowndes, N. F, and Bonner, W. M. 2003. Yeast histone 2A serine 129 is essential for the efficient repair of checkpoint-blind DNA damage. *EMBO Rep*. 4(7), 678-684.

Ren, Q. ,and Gorovsky, M. A . 2001. Histone H2A.Z acetylation modulates an essential charge patch. *Mol Cell*. 7(6), 1329-1335.

Rhind, N., and Russell, P. 2000. Checkpoints: it takes more than time to heal some wounds. *Curr Biol.* 10(24), R908-911.

Rhind, N., and Russell, P. 2000. Chk1 and Cds1: linchpins of the DNA damage and replication checkpoint pathways. *J Cell Sci.* 113 (Pt 22), 3889-3896.

Rice, J. C., and Allis, C. D. 2001. Histone methylation versus histone acetylation: new insights into epigenetic regulation. *Curr Opin Cell Biol.* 13(3), 263-273.

Rice, J. C., Briggs, S. D., Ueberheide, B., Barber, C. M., Shabanowitz, J., Hunt, D. F., Shinkai, Y., Allis, C. D. 2003. Histone methyltransferases direct different degrees of methylation to define distinct chromatin domains. *Mol Cell.* 12(6), 1591-1598.

Richmond, T. J., Finch, J. T., Rushton, B., Rhodes, D., and Klug, A. 1984. . Structure of the nucleosome core particle at 7 Å resolution. *Nature.* 311(5986), 532-537.

Richmond, T. J., and Widom, J. 2000. Nucleosome and Chromatin structure. In Elgin, S. C. R. and Workman, J. L. (eds.), *Chromatin Structure and Gene Expression*. Oxford University Press, Oxford, pp. 1-23.

Richmond, T. J., and Davey, C. A. 2003. The structure of DNA in the nucleosome core. *Nature.* 423(6936), 145-150.

Ris, H. and Mirsky, A. E. 1949. Quantitative cytochemical determination of deoxyribonucleic acid with the Feulgen nucleal reaction. *J Gen Physiol.* 33(2), 125-146.

Ris, H., and Kubai, D. F. 1970. Chromosome structure. *Annu Rev Genet.* 4, 263-294.

Rittinger, K., Budman, J., Xu, J., Volinia, S., Cantley, L. C., Smerdon, S. J., Gamblin, S. J., and Yaffe, M. B. 1999. Structural analysis of 14-3-3 phosphopeptide complexes identifies a dual role for the nuclear export signal of 14-3-3 in ligand binding. *Mol. Cell.* 4(2), 153-166.

Roberts, R. L., and Fink, G. R. 1994. Elements of a single MAP kinase cascade in *Saccharomyces cerevisiae* mediate two developmental programs in the same cell type: mating and invasive growth. *Genes Dev.* 8(24), 2974-2985.

Robyr, D., Suka, Y., Xenarios, I., Kurdistani, S. K., Wang, A., Suka, N., and Grunstein, M. 2002. Microarray deacetylation maps determine genome-wide functions for yeast histone deacetylases. *Cell.* 109(4), 437-446.

Robzyk, K., Recht, J., and Osley, M. A. 2000. Rad6-dependent ubiquitination of histone H2B in yeast. *Science.* 287(5452), 501-504.

Rodriguez, J., and Lazebnik, Y. 1999. Caspase-9 and APAF-1 form an active holoenzyme. *Genes Dev.* 13(24), 3179-3184.

Rogakou, E. P., Pilch, D. R., Orr, A. H., Ivanova, V. S., and Bonner, W. M. 1998. DNA double-stranded breaks induce histone H2AX phosphorylation on serine 139. *J. Biol. Chem.* 273(10), 5858-5868.

Rogakou, E. P., Boon, C., Redon, C., and Bonner, W. M. 1999. Megabase chromatin domains involved in DNA double-strand breaks *in vivo*. *J Cell Biol.* 146(5), 905-916.

Rogakou, E. P., Nieves-Neira, W., Boon, C., Pommier, Y., and Bonner, W. M. 2000. Initiation of DNA fragmentation during apoptosis induces phosphorylation of H2AX histone at serine 139. *J Biol Chem.* 275(13), 9390-9395.

Roghi, C., Giet, R., Uzbekov, R., Morin, N., Chartrain, I., Le Guellec, R., Couturier, A., Doree, M., Philippe, M., and Prigent, C. 1998. The *Xenopus* protein kinase pEg2 associates with the centrosome in a cell cycle-dependent manner, binds to the spindle microtubules and is involved in bipolar mitotic spindle assembly. *J Cell Sci.* 111 ( Pt 5), 557-572. □

Roguev, A., Schaft, D., Shevchenko, A., Pijnappel, W. W., Wilm, M., Aasland, R., and Stewart, A. F. 2001. The *Saccharomyces cerevisiae* Set1 complex includes an Ash2 homologue and methylates histone 3 lysine 4. *EMBO J.* 20(24), 7137-7148.

Rose, M.D., Winston, F., and Hieter, P. 1990. *Methods in Yeast Genetics: A Laboratory Course Manual.* (Cold Spring Harbor, New York: Cold Spring Harbor Laboratory Press).



Rossignol, M., Keriél, A., Staub A., and Egly, J. M. 1999. Kinase activity and phosphorylation of the largest subunit of TFIIF transcription factor. *J. Biol. Chem.* 274(32), 22387–22392.

Roth, S. Y., Schulman, I. G., Richman, R., Cook, R. G., and Allis, C. D. 1988. Characterization of phosphorylation sites in histone H1 in the amitotic macronucleus of *Tetrahymena* during different physiological states. *J Cell Biol.* 107(2), 2473-2482.

Roth, S. Y., and Allis, C. D. 1992. Chromatin condensation: does histone H1 dephosphorylation play a role? *Trends Biochem Sci.* 17(3), 93-98.

Roth, S. Y., Denu, J. M., and Allis, C. D. 2001. Histone acetyltransferases. *Annu Rev Biochem.* 70, 81-120.

Rouse, J., and Jackson, S. P. 2002. Interfaces between the detection, signaling, and repair of DNA damage. *Science.* 297(5581), 547-551.

Rudel, T., and Bokoch, G. M. 1997. Membrane and morphological changes in apoptotic cells regulated by caspase-mediated activation of PAK2. *Science.* 276(5318), 1571-1574.

Ruiz-Carrillo, A., Wangh, L. J., and Allfrey, V. G. 1975. Processing of newly synthesized histone molecules. *Science.* 190(4210), 117-128.

Rundlett, S. E., Carmen, A. A., Kobayashi, R., Bavykin, S., Turner, B. M., and Grunstein, M. 1996. HDA1 and RPD3 are members of distinct yeast histone deacetylase complexes that regulate silencing and transcription. *Proc Natl Acad Sci U S A.* 93(25), 14503-14508.

Rundlett, S. E., Carmen, A. A., Suka, N., Turner, B. M., and Grunstein, M. 1998. Transcriptional repression by UME6 involves deacetylation of lysine 5 of histone H4 by RPD3. *Nature.* 392(6678), 831-835.

Ruppert, S., Wang, E. H., and Tjian, R. 1993. Cloning and expression of human TAFII250: a TBP-associated factor implicated in cell-cycle regulation. *Nature.* 362(6416), 175-179.

Rusche, L. N., Kirchmaier, A. L., and Rine, J. 2003. The establishment, inheritance, and function of silenced chromatin in *Saccharomyces cerevisiae*. *Annu. Rev. Biochem.* 72, 481–516.

Ryser, S., Vial, E., Magnenat, E., Schlegel, W., and Maundrell, K. 1999. Reconstitution of caspase-mediated cell-death signalling in *Schizosaccharomyces pombe*. *Curr Genet.* 36(1-2), 21-28.

Sahara, S., Aoto, M., Eguchi, Y., Imamoto, N., Yoneda, Y., and Tsujimoto, Y. (1999) Acinus is a caspase-3-activated protein required for apoptotic chromatin condensation. *Nature* 401(6749), 168–173.□

Sancar, A., Lindsey-Boltz, L. A., Unsal-Kacmaz, K., and Linn, S. 2004. Molecular mechanisms of mammalian DNA repair and the DNA damage checkpoints. *Annu Rev Biochem.* 73, 39-85.

Sanchez, Y., Desany, B. A., Jones, W. J., Liu, Q., Wang, B., and Elledge, S. J. 1996. Regulation of RAD53 by the ATM-like kinases MEC1 and TEL1 in yeast cell cycle checkpoint pathways. *Science.* 271(5247), 357-360.

Santos-Rosa, H., Schneider, R., Bannister, A. J., Sherriff, J., Bernstein, B. E., Emre, N. C., Schreiber, S. L., Mellor, J., and Kouzarides, T. 2002. Active genes are trimethylated at K4 of histone H3. *Nature.* 419(6905), 407-411.

Sarma, K., and Reinberg, D. 2005. Histone variants meet their match. *Nat Rev Mol Cell Biol.* 6(2), 139-149.

Sassone-Corsi, P., Mizzen, C. A., Cheung, P., Crosio, C., Monaco, L., Jacquot, S., Hanauer, A., and Allis, C. D. 1999. Requirement of Rsk-2 for epidermal growth factor-activated phosphorylation of histone H3. *Science.* 285(5429), 886-891.

Sassoon, I., Severin, F. F., Andrews, P. D., Taba, M. R., Kaplan, K. B., Ashford, A. J., Stark, M. J., Sorger, P. K., and Hyman, A. A. 1999. Regulation of *Saccharomyces cerevisiae* kinetochores by the type 1 phosphatase Glc7p. *Genes Dev.* 13(5), 545-555.

Savill, J., and Fadok, V. 2000. Corpse clearance defines the meaning of cell death. *Nature* 407(6805), 784-788. Review.

Sawa, H., Murakami, H., Kumagai, M., Nakasato, M., Yamauchi, S., Matsuyama, N., Tamura, Y., Satone, A., Ide, W., Hashimoto, I., and Kamada, H. 2004. Histone deacetylase inhibitor, FK228, induces apoptosis and suppresses cell proliferation of human glioblastoma cells *in vitro* and *in vivo*. *Acta Neuropathol (Berl)*. 107(6), 523-31.

Schneider, R., Bannister, A. J., Myers, F. A., Thorne, A. W., Crane-Robinson, C., and Kouzarides, T. 2004. Histone H3 lysine 4 methylation patterns in higher eukaryotic genes. *Nat Cell Biol*. 6(1), 73-77.

Schotta, G., Ebert, A., Krauss, V., Fischer, A., Hoffmann, J., Rea, S., Jenuwein, T., Dorn, R., and Reuter, G. 2002. Central role of Drosophila SU(VAR)3-9 in histone H3-K9 methylation and heterochromatic gene silencing. *EMBO J*. 21(5), 1121-1131.

Schotta, G., Lachner, M., Sarma, K., Ebert, A., Sengupta, R., Reuter, G., Reinberg, D., and Jenuwein, T. 2004. A silencing pathway to induce H3-K9 and H4-K20 trimethylation at constitutive heterochromatin. *Genes Dev*. 18(11), 1251-1262.

Schuck, P. 2000. Size-distribution analysis of macromolecules by sedimentation velocity ultracentrifugation and lamm equation modeling. *Biophys J*. 78(3), 1606-1619.

Schultz, D. R., and Harrington, W. J. Jr. 2003. Apoptosis: programmed cell death at a molecular level. *Semin Arthritis Rheum*. 32(6), 345-369.

Schumperli, D. 1988. Multilevel regulation of replication-dependent histone genes. *Trends Genet*. 4(7), 187-191.

Schurter, B. T., Koh, S. S., Chen, D., Bunick, G. J., Harp, J. M., Hanson, B. L., Henschen-Edman, A., Mackay, D. R., Stallcup, M. R., and Aswad, D. W. 2001. Methylation of histone H3 by coactivator-associated arginine methyltransferase. *Biochemistry*. 40(19), 5747-5756.

Schutkowski, M., Bernhardt, A., Zhou, X. Z., Shen, M., Reimer, U., Rahfeld, J. U., Lu, K. P., and Fischer, G. 1998. Role of phosphorylation in determining the backbone dynamics of the serine/threonine-proline motif and Pin1 substrate recognition. *Biochemistry*. 37(16), 5566-5575.

Schwartz, M. F., Duong, J. K., Sun, Z., Morrow, J. S., Pradhan, D., and Stern, D. F. 2002. Rad9 phosphorylation sites couple Rad53 to the *Saccharomyces cerevisiae* DNA damage checkpoint. *Mol Cell*. 9(5), 1055-1065.

Schwartz, M. F., Lee, S. J., Duong, J. K., Eminaga, S., and Stern, D. F. 2003. FHA domain-mediated DNA checkpoint regulation of Rad53. *Cell Cycle*. 2(4), 384-396.

Schwarz, P. M., and Hansen, J. C. 1994. Formation and stability of higher order chromatin structures. Contributions of the histone octamer. *J Biol Chem*. 269(23), 16284-16289.

Schwarz, P. M., Felthouser, A., Fletcher, T. M., and Hansen, J. C. 1996. Reversible oligonucleosome self-association: dependence on divalent cations and core histone tail domains. *Biochemistry*. 35(13), 4009-4015.

Seale, R. L. 1981. Rapid turnover of the histone-ubiquitin conjugate, protein A24. *Nucleic Acids Res*. 9(13), 3151-3158.

Seet, B. T., Dikic, I., Zhou, M. M., Pawson, T. 2006. Reading protein modifications with interaction domains. *Nat Rev Mol Cell Biol*. 7(7), 473-483.□

Severin, F.F., and Hyman, A.A. 2002. Pheromone induces programmed cell death in *S. cerevisiae*. *Curr. Biol*. 12, R233-R235.

Shaham, S., and Horvitz, H. R. 1996. Developing *Caenorhabditis elegans* neurons may contain both cell-death protective and killer activities. *Genes Dev*. 10(5), 578-591.

Shaham, S., and Horvitz, H. R. 1996. An alternatively spliced *C. elegans* ced-4 RNA encodes a novel cell death inhibitor. *Cell*. 86(2), 201-208.

Shaham, S., Reddien, P. W., Davies, B., and Horvitz, H. R. 1999. Mutational analysis of the *Caenorhabditis elegans* cell-death gene *ced-3*. *Genetics*. 153(4), 1655-1671.

Shahbazian, M. D., Zhang, K., and Grunstein, M. 2005. Histone H2B ubiquitylation controls processive methylation but not monomethylation by Dot1 and Set1. *Mol Cell*. 19(2), 271-277.

Shao, Y., Gao, Z., Marks, P. A., and Jiang, X. 2004. Apoptotic and autophagic cell death induced by histone deacetylase inhibitors. *Proc Natl Acad Sci U S A*. 101(52), 18030-18035.

Shen, X., and Gorovsky, M. A. 1996. Linker histone H1 regulates specific gene expression but not global transcription *in vivo*. *Cell*. 86(3), 475-483.

Shi, Y., Lan, F., Matson, C., Mulligan, P., Whetstine, J. R., Cole, P. A., Casero, R. A., and Shi, Y. 2004. Histone demethylation mediated by the nuclear amine oxidase homolog LSD1. *Cell*. 119(7), 941-953.

Shilatifard, A. 2006. Chromatin Modifications by Methylation and Ubiquitination: Implications in the Regulation of Gene Expression. *Annu Rev Biochem*. 75, 243-269.

Shimizu, S., Matsuoka, Y., Shinohara, Y., Yoneda, Y., and Tsujimoto, Y. 2001. Essential role of voltage-dependent anion channel in various forms of apoptosis in mammalian cells. *J Cell Biol*. 152(2), 237-250.

Shirogane, T., Fukada, T., Muller, J. M., Shima, D. T., Hibi, M., Hirano, T. 1999. Synergistic roles for Pim-1 and c-Myc in STAT3-mediated cell cycle progression and antiapoptosis. *Immunity*. 11(6), 709-719.

Shogren-Knaak, M. A., Fry, C. J., and Peterson, C. L. 2003. A native peptide ligation strategy for deciphering nucleosomal histone modifications. *J Biol Chem*. 278(18), 15744-15748.

Shogren-Knaak, M., Ishii, H., Sun, J. M., Pazin, M. J., Davie, J. R., and Peterson, C. L. 2006. Histone H4-K16 acetylation controls chromatin structure and protein interactions. *Science*. 311(5762), 844-847.

Shroff, R., Arbel-Eden, A., Pilch, D., Ira, G., Bonner, W. M., Petrini, J. H., Haber, J. E., and Lichten, M. 2004. Distribution and dynamics of chromatin modification induced by a defined DNA double-strand break. *Curr Biol*. 14(19), 1703-1711.

Sims, R. J. 3rd, Nishioka, K., and Reinberg, D. 2003. Histone lysine methylation: a signature for chromatin function. *Trends Genet*. 19(11), 629-639.

Smet, C., Sambo, A. V., Wieruszeski, J. M., Leroy, A., Landrieu, I., Buee, L., and Lippens, G. 2004. The peptidyl prolyl cis/trans-isomerase Pin1 recognizes the phospho-Thr212-Pro213 site on Tau. *Biochemistry*. 43(7), 2032-2040.

Sonoda, E., Matsusaka, T., Morrison, C., Vagnarelli, P., Hoshi, O., Ushiki, T., Nojima, K., Fukagawa, T., Waizenegger, I. C., Peters, J. M., Earnshaw, W. C., Takeda, S. 2001. Scc1/Rad21/Mcd1 is required for sister chromatid cohesion and kinetochore function in vertebrate cells. *Dev Cell*. 1(6), 759-770. □

Sterner, D. E., and Berger, S. L. 2000. Acetylation of histones and transcription-related factors. *Microbiol Mol Biol Rev*. 64(2), 435-459

Stevens, C., Smith, L., and La Thangue, N. B. 2003. Chk2 activates E2F-1 in response to DNA damage. *Nat Cell Biol*. 5(5), 401-409.

Stewart, G. S., Wang, B., Bignell, C. R., Taylor, A. M., and Elledge, S. J. 2003. MDC1 is a mediator of the mammalian DNA damage checkpoint. *Nature*. 421(6926), 961-966.

Stiff, T., O'Driscoll, M., Rief, N., Iwabuchi, K., Lobrich, M., and Jeggo, P. A. 2004. ATM and DNA-PK function redundantly to phosphorylate H2AX after exposure to ionizing radiation. *Cancer Res*. 64(7). 2390-2396.

Strahl, B. D., Ohba, R., Cook, R. G., and Allis, C. D. 1999. Methylation of histone H3 at lysine 4 is highly conserved and correlates with transcriptionally active nuclei in Tetrahymena. *Proc Natl Acad Sci U S A*. 96(26), 14967-14972. □

Strahl, B. D., and Allis, C. D. 2000. The language of covalent histone modifications. *Nature*. 403(6765), 41-45.

Strahl, B. D., Briggs, S. D., Brame, C. J., Caldwell, J. A., Koh, S. S., Ma, H., Cook, R. G., Shabanowitz, J., Hunt, D. F., Stallcup, M. R., and Allis, C. D. 2001. Methylation of histone H4 at arginine 3 occurs *in vivo* and is mediated by the nuclear receptor coactivator PRMT1. *Curr Biol*. 11(12), 996-1000.

Strasser, A., O'Connor, L., and Dixit, V. M. 2000. Apoptosis signaling. *Annu Rev Biochem*. 69, 217-245.

Struhl, K. 1998. Histone acetylation and transcriptional regulatory mechanisms. *Genes Dev.* 12(5), 599-606.

Struhl, K. 2005. Transcriptional activation: mediator can act after preinitiation complex formation. *Mol Cell.* 17(6), 752-754.

Strukov, Y. G., Wang, Y., and Belmont, A. S. 2003. Engineered chromosome regions with altered sequence composition demonstrate hierarchical large-scale folding within metaphase chromosomes. *J Cell Biol.* 162(1), 23-35.

Stucki, M., Clapperton, J. A., Mohammad, D., Yaffe, M. B., Smerdon, S. J., and Jackson, S. P. 2005. MDC1 directly binds phosphorylated histone H2AX to regulate cellular responses to DNA double-strand breaks. *Cell.* 123(7), 1213-1226.

Suka, N., Carmen, A. A., Rundlett, S. E., and Grunstein M. 1998. The regulation of gene activity by histones and the histone deacetylase RPD3. *Cold Spring Harb Symp Quant Biol.* 63, 391-399.

Suka, N., Suka, Y., Carmen, A. A., Wu, J., and Grunstein, M. 2001. Highly specific antibodies determine histone acetylation site usage in yeast heterochromatin and euchromatin. *Mol Cell.* 8(2), 473-479.

Suka, N., Luo, K., and Grunstein, M. 2002. Sir2p and Sas2p opposingly regulate acetylation of yeast histone H4 lysine16 and spreading of heterochromatin. *Nat Genet.* 32(3), 378-383.

Sun, Z., Fay, D. S., Marini, F., Foiani, M., and Stern, D. F. 1996. Spk1/Rad53 is regulated by Mec1-dependent protein phosphorylation in DNA replication and damage checkpoint pathways. *Genes Dev.* 10(4), 395-406.

Sun, Z., Hsiao, J., Fay, D. S., and Stern, D. F. 1998. Rad53 FHA domain associated with phosphorylated Rad9 in the DNA damage checkpoint. *Science.* 281(5374), 272-274.

Sun, Z. W., and Allis, C. D. 2002. Ubiquitination of histone H2B regulates H3 methylation and gene silencing in yeast. *Nature.* 418(6893), 104-108.

Suto, R. K., Clarkson, M. J., Trmemthick, D. J., and Luger, K. 2000. Crystal structure of a nucleosome core particle containing the variant histone H2A.Z. *Nature Struct. Biol.* 7(12), 1121-1124.

Sweet, M. T., Carlson, G., Cook, R. G., Nelson, D., and Allis, C. D. 1997. Phosphorylation of linker histones by a protein kinase A-like activity in mitotic nuclei. *J Biol Chem.* 272(2), 916-923.

Sym, M., Engebrecht, J. A., and Roeder, G. S. 1993. ZIP1 is a synaptonemal complex protein required for meiotic chromosome synapsis. *Cell.* 72(3), 365-378.

Takahashi, A., Alnemri, E. S., Lazebnik, Y. A., Fernandes-Alnemri, T., Litwack, G., Moir, R. D., Goldman, R. D., Poirier, G. G., Kaufmann, S. H., and Earnshaw, W. C. 1996. Cleavage of lamin A by Mch2 alpha but not CPP32: multiple interleukin 1 beta-converting enzyme-related proteases with distinct substrate recognition properties are active in apoptosis. *Proc Natl Acad Sci U S A.* 93(16), 8395-8400.

Takahashi, A., Musy, P. Y., Martins, L. M., Poirier, G. G., Moyer, R. W., and Earnshaw, W. C. 1996. CrmA/SPI-2 inhibition of an endogenous ICE-related protease responsible for lamin A cleavage and apoptotic nuclear fragmentation. *J Biol Chem.* 271(51), 32487-32490.

Tauchi, H., Kobayashi, J., Morishima, K., Matsuura, S., Nakamura, A. Shiraishi, T., Ito, E., Masnada, D., Delia, D., and Komatsu, K. 2001. The forkhead-associated domain of NBS1 is essential for nuclear foci formation after irradiation but not essential for hRAD50/hMRE11/NBS1 complex DNA repair activity. *J. Biol. Chem.* 276(1), 12-15.

Taunton, J., Hassig, C. A., and Schreiber, S. L. 1996. A mammalian histone deacetylase related to the yeast transcriptional regulator Rpd3p. *Science.* 272(5260), 408-411.

Terada, Y., Simerly, C. R., Hewitson, L., and Schatten, G. 2000. Sperm aster formation and pronuclear decondensation during rabbit fertilization and development of a functional assay for human sperm. *Biol Reprod.* 62(3), 557-563.

Th'ng, J. P., Guo, X. W., Swank, R. A., Crissman, H. A., and Bradbury, E. M. 1994. Inhibition of histone phosphorylation by staurosporine leads to chromosome decondensation. *J Biol Chem.* 269(13), 9568-9573.



Thoma, F., Koller, T., and Klug A. (1979). Involvement of histone H1 in the organization of the nucleosome and of the salt-dependent superstructures of chromatin. *J Cell Biol.* 83(2 Pt 1), 403-427.

Thoma, F. 1992. Nucleosome positioning. *Biochim Biophys Acta.* 1130(1), 1-19.

Thomas, J. O. 1984. . The higher order structure of chromatin and histone H1. *J Cell Sci Suppl.* 1-20.

Thomas, J. O. 1999. Histone H1: location and role. *Curr Opin Cell Biol.* 11(3), 312-317.

Thompson, C. B. 1995. Apoptosis in the pathogenesis and treatment of disease. *Science.* 267(5203),1456-1462.

Thomson, S., Clayton, A. L., Hazzalin, C. A., Rose, S., Barratt, M. J., and Mahadevan, L. C. 1999. The nucleosomal response associated with immediate-early gene induction is mediated via alternative MAP kinase cascades: MSK1 as a potential histone H3/HMG-14 kinase. *EMBO J.* 18(17), 4779-4793.

Thornberry, N. A., Rano, T. A., Peterson, E. P., Rasper, D. M., Timkey, T., Garcia-Calvo, M., Houtzager, V. M., Nordstrom, P. A., Roy, S., Vaillancourt, J. P., Chapman, K. T., and Nicholson, D. W. 1997. A combinatorial approach defines specificities of members of the caspase family and granzyme B. Functional relationships established for key mediators of apoptosis. *J Biol Chem.* 272(29), 17907-17911.

Thorne, A. W., Sautiere, P., Briand, G., and Crane-Robinson, C. 1987. The structure of ubiquitinated histone H2B. *EMBO J.* 6(4), 1005-1010.

Thorne, A. W., Kmiecik, D., Mitchelson, K., Sautiere, P., and Crane-Robinson, C. 1990. Patterns of histone acetylation. *Eur J Biochem.* 193(3), 701-713.

Trojer, P., Brandtner, E. M., Brosch, G., Loidl, P., Galehr, J., Linzmaier, R., Haas, H., Mair, K., Tribus, M., and Graessle, S. 2003. Histone deacetylases in fungi: novel members, new facts. *Nucleic Acids Res.* 31(14), 3971-3981.

Tse, C., and Hansen, J. C. 1997. Hybrid trypsinized nucleosomal arrays: identification of multiple functional roles of the H2A/H2B and H3/H4 N-termini in chromatin fiber compaction. *Biochemistry*. 36(38), 11381-11388.

Tse, C., Fletcher, T. M., and Hansen, J. C. 1998. Enhanced transcription factor access to arrays of histone H3/H4 tetramer-DNA complexes *in vitro*: implications for replication and transcription. *Proc Natl Acad Sci U S A*. 95(21), 12169-12173.

Tsukada, Y., Fang, J., Erdjument-Bromage, H., Warren, M. E., Borchers, C. H., Tempst, P., and Zhang, Y. 2006. Histone demethylation by a family of JmjC domain-containing proteins. *Nature*. 439(7078), 811-816.

Turner, B. M. 2000. Histone acetylation and an epigenetic code. *Bioessays*. 22(9), 836-845.

Turner, B. M. 2002. Cellular memory and the histone code. *Cell*. 111(3), 285-291.

Unal, E., Arbel-Eden, A., Sattler, U., Shroff, R., Lichten, M., Haber, J. E., and Koshland, D. 2004. DNA damage response pathway uses histone modification to assemble a double-strand break-specific cohesin domain. *Mol Cell*. 16(6), 991-1002.

Ungerstedt, J. S., Sowa, Y., Xu, W. S., Shao, Y., Dokmanovic, M., Perez, G., Ngo, L., Holmgren, A., Jiang, X., and Marks, P. A. 2005. Role of thioredoxin in the response of normal and transformed cells to histone deacetylase inhibitors. *Proc Natl Acad Sci U S A*. 102(3), 673-678.

Uren, A. G., O'Rourke, K., Aravind, L. A., Pisabarro, M. T., Seshagiri, S., Koonin, E. V., and Dixit, V. M. 2000. Identification of paracaspases and metacaspases: two ancient families of caspase-like proteins, one of which plays a key role in MALT lymphoma. *Mol Cell*. 6(4), 961-967.

Utlei, R. T., Lacoste, N., Jobin-Robitaille, O., Allard, S., and Cote, J. 2005. Regulation of NuA4 histone acetyltransferase activity in transcription and DNA repair by phosphorylation of histone H4. *Mol Cell Biol*. 25(18), 8179-8190.

van Heemst, D., James, F., Poggeler, S., Berteaux-Lecellier, V., and Zickler, D. Spo76p is a conserved chromosome morphogenesis protein that links the mitotic and meiotic programs. *Cell*. 98(2), 261-271.□

van Holde, K. E. 1988. Chromatin. Springer-Verlag, New York.

Van Hooser, A., Goodrich, D. W., Allis, C. D., Brinkley, B. R., and Mancini, M. A. 1998. Histone H3 phosphorylation is required for the initiation, but not maintenance, of mammalian chromosome condensation. *J Cell Sci.* 111(23), 3497-3506.

Van Hooser, A. A., Mancini, M. A., Allis, C. D., Sullivan, K. F., and Brinkley, B. R. 1999. The mammalian centromere: structural domains and the attenuation of chromatin modeling. *FASEB J.* 13 (Suppl. 2), S216-S220.

Van Hooser, A. A., Ouspenski, I. I., Gregson, H. C., Starr, D. A., Yen, T. J., Goldberg, M. L., Yokomori, K., Earnshaw, W. C., Sullivan, K. F., and Brinkley, B. R. 2001. Specification of kinetochore-forming chromatin by the histone H3 variant CENP-A. *J. Cell Sci* 114(19), 3529-3542.

van Leeuwen, F., Gafken, P. R., and Gottschling, D. E. 2002. Dot1p modulates silencing in yeast by methylation of the nucleosome core. *Cell.* 109(6), 745-756.

van Roijen, H. J., Ooms, M. P., Spaargaren, M. C., Baarends, W. M., Weber, R. F., Grootegeed, J. A., and Vreeburg, J. T. 1998. Immunoexpression of testis-specific histone 2B in human spermatozoa and testis tissue. *Hum Reprod.* 13(6), 1559-1566.

Varon, R., Vissinga, C., Platzer, M., Cerosaletti, K. M., Chrzanowska, K. H., Saar, K., Beckmann, G., Seemanova, E., Cooper, P. R., Nowak, N. J., Stumm, M., Weemaes, C. M., Gatti, R. A., Wilson, R. K., Digweed, M., Rosenthal, A., Sperling, K., Concannon, P., and Reis, A. 1998. Nibrin, a novel DNA double-strand break repair protein, is mutated in Nijmegen breakage syndrome. *Cell* 93(3), 467-476.

Vavra, K. J., Allis, C. D., and Gorovsky, M. A. 1982. Regulation of histone acetylation in *Tetrahymena* macro- and micronuclei. *J Biol Chem.* 257(5), 2591-2598.

Vavra, K. J., Colavito-Shepanski, M., and Gorovsky, M. A. 1982. Histone acetylation and the deoxyribonuclease I sensitivity of the *Tetrahymena* ribosomal gene. *Biochemistry.* 21(8), 1772-1781.

Villunger, A., Marsden, V. S., Zhan, Y., Erlacher, M., Lew, A. M., Bouillet, P., Berzins, S., Godfrey, D. I., Heath, W. R., and Strasser, A. 2004. Negative selection of semimature CD4(+)8(-)HSA+ thymocytes requires the BH3-only

protein Bim but is independent of death receptor signaling. *Proc Natl Acad Sci U S A*. 101(18), 7052-7057.

Walczak, H., and Krammer, P. H. 2000. The CD95 (APO-1/Fas) and the TRAIL (APO-2L) apoptosis systems. *Exp Cell Res*. 256(1), 58-66.

Wang, H., Huang, Z. Q., Xia, L., Feng, Q., Erdjument-Bromage, H., Strahl, B. D., Briggs, S. D., Allis, C. D., Wong, J., Tempst, P., and Zhang, Y. 2001a. Methylation of histone H4 at arginine 3 facilitating transcriptional activation by nuclear hormone receptor. *Science*. 293(5531), 853-857.

Wang, H., Cao, R., Xia, L., Erdjument-Bromage, H., Borchers, C., Tempst, P., and Zang, Y. 2001b. Purification and functional characterization of a histone H3-lysine 4-specific methyltransferase. *Mol Cell*. 8(6), 1207-1217.

Wang, L., Chen, L., Benincosa, J., Fortney, J., and Gibson, L. F. 2005. VEGF-induced phosphorylation of Bcl-2 influences B lineage leukemic cell response to apoptotic stimuli. *Leukemia*. 19(3), 344-353.

Wang, Y., Wysocka, J., Sayegh, J., Lee, Y. H., Perlin, J. R., Leonelli, L., Sonbuchner, L. S., McDonald, C. H., Cook, R. G., Dou, Y., Roeder, R. G., Clarke, S., Stallcup, M. R., Allis, C. D., and Coonrod, S. A. 2004. Human PAD4 regulates histone arginine methylation levels via demethylation. *Science*. 306(5694), 279-283.

Wang, Z., He, Q., Liang, Y., Wang, D., Li, Y.Y., and Li, D. 2003. Non-caspase-mediated apoptosis contributes to the potent cytotoxicity of the enediyne antibiotic idamycin toward human tumor cells. *Biochem. Pharmacol.* 65, 1767-1775.

Wang, Z. B., Liu, Y. Q., and Cui, Y. F. 2005. Pathways to caspase activation. *Cell Biol Int* 2005, 29(7), 489-496.

Waterborg, J. H. 2000. Steady-state levels of histone acetylation in *Saccharomyces cerevisiae*. *J Biol Chem*, 275(17), 13007-13011.

Watson, J. D., and Crick, F. H. (1953). A structure for deoxyribose nucleic acid. *Nature* 171, 737-773

Wei, Y., Mizzen, C. A., Cook, R. G., Gorovsky, M. A., and Allis, C. D. 1998. Phosphorylation of histone H3 at serine 10 is correlated with chromosome condensation during mitosis and meiosis in *Tetrahymena*. *Proc Natl Acad Sci U S A*. 95(13), 7480-7484.

Wei, Y., Yu, L., Bowen, J., Gorovsky, M. A., and Allis, C. D. 1999. Phosphorylation of histone H3 is required for proper chromosome condensation and segregation. *Cell*. 97(1), 99-109.

Weinberger, M., Ramachandran, L., Feng, L., Sharma, K., Sun, X., Marchetti, M., Huberman, J. A., and Burhans, W. C. 2005. Apoptosis in budding yeast caused by defects in initiation of DNA replication. *J Cell Sci*. 2005 118(15), 3543-3553.

Weinert, T. 1998. DNA damage and checkpoint pathways: molecular anatomy and interactions with repair. *Cell*. 94(5), 555-558.

Weinzierl, R. O., Dynlacht, B. D., and Tjian, R. 1993. Largest subunit of *Drosophila* transcription factor IID directs assembly of a complex containing TBP and a coactivator. *Nature*. 362(6420), 511-517.

Wen, L. P., Fahrni, J. A., Troie, S., Guan, J. L., Orth, K., and Rosen, G. D. 1997. Cleavage of focal adhesion kinase by caspases during apoptosis. *J Biol Chem*. 272(41), 26056-26061.

White, C. L., Suto, R. K., and Luger, K. 2001. Structure of the yeast nucleosome core particle reveals fundamental changes in internucleosome interactions. *EMBO J*. 20(18), 5207-5218.

Widom, J. 1992. A relationship between the helical twist of DNA and the ordered positioning of nucleosomes in all eukaryotic cells. *Proc Natl Acad Sci U S A*. 89(3), 1095-1099.

Widom, J. 1998. Structure, dynamics, and function of chromatin *in vitro*. *Annu Rev Biophys Biomol Struct*. 27, 285-327.

Williams, R. S., Lee, M. S., Hau, D. D., and Glover, J. N. 2004. Structural basis of phosphopeptide recognition by the BRCT domain of BRCA1. *Nat Struct Mol Biol*. 11(6), 519-525.

Winoto, A. 1997. Cell death in the regulation of immune responses. *Curr Opin Immunol.* 9(3), 365-370.

Winston, F., and Allis, C. D. 1999. The bromodomain: a chromatin-targeting module? *Nat Struct Biol.* 6(7), 601-604.

Wissing, S., Ludovico, P., Herker, E., Buttner, S., Engelhardt, S. M., Decker, T., Link, A., Proksch, A., Rodrigues, F., Corte-Real, M., Frohlich, K. U., Manns, J., Cande, C., Sigrist, S. J., Kroemer, G., and Madeo, F. 2004. An AIF orthologue regulates apoptosis in yeast. *J Cell Biol.* 166(7), 969-974.

Wu, C., Whiteway, M., Thomas, D.Y., and Leberer, E. 1995. Molecular characterization of Ste20p, a potential mitogen-activated protein or extracellular signal-regulated kinase kinase (MEK) kinase kinase from *Saccharomyces cerevisiae*. *J. Biol. Chem.* 270, 15984-15992.

Wu, D., Chen, P. J., Chen, S., Hu, Y., Nunez, G., and Ellis, R. E. 1999. *C. elegans* MAC-1, an essential member of the AAA family of ATPases, can bind CED-4 and prevent cell death. *Development.* 126(9), 2021-2031.

Wu, J., Carmen, A. A., Kobayashi, R., Suka, N., and Grunstein, M. 2001. HDA2 and HDA3 are related proteins that interact with and are essential for the activity of the yeast histone deacetylase HDA1. *Proc Natl Acad Sci U S A.* 98(8), 4391-4396.

Wu, J., Suka, N., Carlson, M., and Grunstein, M. 2001. TUP1 utilizes histone H3/H2B-specific HDA1 deacetylase to repress gene activity in yeast. *Mol Cell.* 7(1), 117-126.

Wu, R. S., Kohn, K. W., and Bonner, W. M. (1981). Metabolism of ubiquitinated histones. *J Biol Chem.* 256(11), 5916-5920.

Wu, S., Huang, J., Dong, J., and Pan, D. 2003. Hippo encodes a Ste-20 family protein kinase that restricts cell proliferation and promotes apoptosis in conjunction with salvador and warts. *Cell* 114, 445-456.

Wulf, G., Greg, F., Suizu, F., and Lu, K. P. 2005. Phosphorylation-specific prolyl isomerization: is there an underlying theme?. *Nature Cell Biology* 7(5), 435 – 441.

Wunsch, A.M., Reinhardt, K., and Lough, J. 1991. Normal transitions in synthesis of replacement histones H2A.Z and H3.3 during differentiation of dystrophic myotube cells. *Mech. Ageing Dev.* 59(3), 299-305.

Wurtele, H., and Verreault, A. 2006. Histone post-translational modifications and the response to DNA double-strand breaks. *Curr Opin Cell Biol.* 18(2), 137-144.

Wysocka, J., Myers, M. P., Laherty, C. D., Eisenman, R. N., and Herr, W. 2003. Human Sin3 deacetylase and trithorax-related Set1/Ash2 histone H3-K4 methyltransferase are tethered together selectively by the cell-proliferation factor HCF-1. *Genes Dev.* 17(7), 896-911.

Wysocka, J., Swigut, T., Milne, T. A., Dou, Y., Zhang, X., Burlingame, A.L., Roeder, R. G., Brivanlou, A. H., and Allis, C.D. 2005. WDR5 associates with histone H3 methylated at K4 and is essential for H3 K4 methylation and vertebrate development. *Cell.* 121(6), 859-872.

Wysocka, J., Allis, C. D., and Coonrod, S. 2006. Histone arginine methylation and its dynamic regulation. *Front Biosci.* 11:344-355.

Xue, D., Shaham, S., and Horvitz, H. R. 1996. The *Caenorhabditis elegans* cell-death protein CED-3 is a cysteine protease with substrate specificities similar to those of the human CPP32 protease. *Genes Dev.* 10(9), 1073-1083.

Yaffe, M. B., Rittinger, K., Volinia, S., Caron, P. R, Aitken, A., Leffers, H., Gamblin, S. J., Smerdon, S. J., and Cantley L. C. (1997a). The structural basis for 14-3-3:phosphopeptide binding specificity. *Cell* 91(7), 961-971.

Yaffe, M.B., Schutkowski, M., Shen, M., Zhou, X.Z., Stukenberg, P.T., Rahfeld, J.U., Xu, J., Kuang, J., Kirschner, M.W., Fischer, G., Cantley, L.C., and Lu, K.P. 1997. Sequence-specific and phosphorylation-dependent proline isomerization: a potential mitotic regulatory mechanism. *Science.* 278, 1957-60.

Yaffe, M. B., and Elia, A. E. 2001. Phosphoserine/threonine-binding domains. *Curr Opin Cell Biol.* 13(2), 131-138.

Yamane, K., Toumazou, C., Tsukada, Y., Erdjument-Bromage, H., Tempst, P., Wong, J., and Zhang, Y. JHDM2A, a JmJc-containing H3K9 demethylase, facilitates transcription activation by androgen receptor. *Cell.* 125(3), 483-495.

Yang, S., Kuo, C., Bisi, J. E., and Kim, M. K. 2002. PML-dependent apoptosis after DNA damage is regulated by the checkpoint kinase hCds1/Chk2. *Nat Cell Biol.* 4(11), 865-870.

Yang, Y., Fang, S., Jensen, J. P., Weissman, A. M., and Ashwell, J. D. 2000. Ubiquitin protein ligase activity of IAPs and their degradation in proteasomes in response to apoptotic stimuli. *Science.* 288(5467), 874-877.

Yokoyama, A., Wang, Z., Wysocka, J., Sanyal, M., Aufiero, D. J., Kitabayashi, I., Herr, W., and Cleary, M. L. 2004. Leukemia proto-oncoprotein MLL forms a SET1-like histone methyltransferase complex with menin to regulate Hox gene expression. *Mol Cell Biol.* 24(13), 5639-5649.

Yongkiettrakul, S., Byeon, I. J., and Tsai, M. D. 2004. The ligand specificity of yeast Rad53 FHA domains at the +3 position is determined by nonconserved residues. *Biochemistry.* 43(13), 3862-3869.

Yoshida, K., Komatsu, K., Wang, H. G., and Kufe, D. 2002. c-Abl tyrosine kinase regulates the human Rad9 checkpoint protein in response to DNA damage. *Mol Cell Biol.* 22(10), 3292-3300.

Yu, H. G., and Koshland, D. E. 2003. Meiotic condensin is required for proper chromosome compaction, SC assembly, and resolution of recombination-dependent chromosome linkages. *J Cell Biol.* 163(5), 937-947.□

Yuan, J., Shaham, S., Ledoux, S., Ellis, H. M., and Horvitz, H. R. 1993. The *C. elegans* cell death gene *ced-3* encodes a protein similar to mammalian interleukin-1 beta-converting enzyme. *Cell.* 75(4), 641-652.

Zalensky, A. O., Siino, J. S., Gineitis, A. A., Zalenskaya, I. A., Tomilin, N. V., Yau, P., and Bradbury, E. M. 2002. Human testis/sperm-specific histone H2B (hTSH2B). Molecular cloning and characterization. *J Biol Chem.* 277(45), 43474-43480.

Zeitlin, S. G., Shelby, R. D., and Sullivan, K. F. 2001. CENP-A is phosphorylated by Aurora B kinase and plays an unexpected role in completion of cytokinesis. *J. Cell Biol.* 155(7), 1147-1157.

Zeng, L., and Zhou, M. M. 2002. Bromodomain: an acetyl-lysine binding domain. *FEBS Lett.* 513(1), 124-128.



Zhang, C. L., McKinsey, T.A., and Olson, E.N. 2002. Association of class II histone deacetylases with heterochromatin protein 1: potential role for histone methylation in control of muscle differentiation. *Mol. Cell. Biol.* 22(20), 7302–7312.

Zhang, K., Williams, K. E., Huang, L., Yau, P., Siino, J. S., Bradbury, E. M., Jones, P. R., Minch, M. J., and Burlingame, A. L. 2002. Histone acetylation and deacetylation: identification of acetylation and methylation sites of HeLa histone H4 by mass spectrometry. *Mol Cell Proteomics.* 1(7), 500-508.

Zhang, Q., Chieu, H.K., Low, C.P., Zhang, S., Heng, C.K., and Yang, H. 2003. *Schizosaccharomyces pombe* cells deficient in triacylglycerols synthesis undergo apoptosis upon entry into the stationary phase. *J. Biol. Chem.* 278, 47145-47155.

Zhang, Y., and Reinberg, D. 2001. Transcription regulation by histone methylation: interplay between different covalent modifications of the core histone tails. *Genes Dev.* 15(18), 2343-2360.

Zhang, Y., Griffin, K., Mondal, N., and Parvin, J. D. 2004. Phosphorylation of histone H2A inhibits transcription on chromatin templates. *J Biol Chem.* 279(21), 21866-21872.

Zhang, X. D., Gillespie, S. K., Borrow, J. M., and Hersey, P. 2004. The histone deacetylase inhibitor suberic bishydroxamate regulates the expression of multiple apoptotic mediators and induces mitochondria-dependent apoptosis of melanoma cells. *Mol Cancer Ther.* 3(4), 425-435.

Zhao, X., Muller, E. G., and Rothstein, R. 1998. A suppressor of two essential checkpoint genes identifies a novel protein that negatively affects dNTP pools. *Mol Cell.* 2(3), 329-340.

Zhao, X., Chabes, A., Domkin, V., Thelander, L., and Rothstein, R. 2001. The ribonucleotide reductase inhibitor Sml1 is a new target of the Mec1/Rad53 kinase cascade during growth and in response to DNA damage. *EMBO J.* 20(13), 3544-3553.

Zhao, Y., Lu, S., Wu, L., Chai, G., Wang, H., Chen, Y., Sun, J., Yu, Y., Zhou, W., Zheng, Q., Wu, M., Otterson, G. A., and Zhu, W. G. 2006. Acetylation of p53 at lysine 373/382 by the histone deacetylase inhibitor depsipeptide induces expression of p21(Waf1/Cip1). *Mol Cell Biol.* 26(7), 2782-2790. □

Zhang, Z., Ren, Q., Yang, H., Conrad, M. N., Guacci, V., Kateneva, A., and Dresser, M. E. 2005. Budding yeast PDS5 plays an important role in meiosis and is required for sister chromatid cohesion. *Mol Microbiol.* 56(3), 670-680.

Zhou, B. B., and Elledge, S. J. 2000. The DNA damage response: putting checkpoints in perspective. *Nature.* 408(6811): 433-439.

Zhou, Z., and Elledge, S. J. 1993. *DUN1* encodes a protein kinase that controls the DNA damage response in yeast. *Cell.* 75:1119-1127.

Zhou, Y. B., Gerchman, S. E., Ramakrishnan, V., Travers, A., and Muylldermans, S. 1998. Position and orientation of the globular domain of linker histone H5 on the nucleosome. *Nature.* 395(6700): 402-405.

Zimmermann, K. C., Bonzon, C., and Green, D. R. 2001. The machinery of programmed cell death. *Pharmacol Ther.* 92(1): 57-70.

Zou, H., Henzel, W. J., Liu, X., Lutschg, A., and Wang, X. 1997. Apaf-1, a human protein homologous to *C. elegans* CED-4, participates in cytochrome c-dependent activation of caspase-3. *Cell.* 90(3):405-413.

Zou, H., Li, Y., Liu, X., and Wang, X. 1999. An APAF-1.cytochrome c multimeric complex is a functional apoptosome that activates procaspase-9. *J Biol Chem.* 274(17):11549-11556.